The Role of *S. cerevisiae*Yta7p in DNA Replication

Rebecca Curley

A Thesis Submitted for the Degree of
PhD

University of Edinburgh
2010

This thesis has been composed by Rebecca Curley for submission for the degree of PhD. The work presented is that of Rebecca Curley and has not been submitted for any other degree or professional qualification.

Abstract

In *S. cerevisiae* initiation of replication occurs from discrete sites in the genome, known as origins and these display a characteristic temporal profile of activation during S phase of the cell cycle. The genomic context of origins has been demonstrated to be important to determine the time of firing, more specifically histone acetylation levels surrounding origins can influence their activation time. How increased acetylation is translated into earlier firing of specific origins is currently unknown.

Bromodomains are known to bind acetylated histones *in vivo*. The bromodomain-containing Yta7p has been identified in a complex with various remodelers of chromatin and subunits of DNA polymerase ϵ. It is also a target of cell cycle and checkpoint kinases. Therefore, Yta7p makes an excellent candidate to bind acetylated histones surrounding replication origins and affect an alteration in the chromatin structure that could influence time of firing.

Deletion of the histone deacetylase *RPD3* results in a rapid S phase phenotype due to increased histone acetylation at "late-firing" origins. Increased acetylation at "late" origins leads to an advance in the time of firing of those specific origins. The aim of this study was to investigate the hypothesis that the bromodomain-containing protein Yta7p binds to histones with increased acetylation near to replication origins and subsequently influences origin firing. Hence, deletion of *YTA7* would abolish the rapid S phase of a Δ*rpd3* strain. Indeed the S phase of the Δ*rpd3*Δ*yta7* strain was reverted to WT duration. A role for Yta7p in DNA replication is also inferred by two additional lines of evidence presented in this thesis. Synthetic growth defects are evident when *YTA7* and *RPD3* deletion is combined with mutation of a third replication protein. In addition, Δ*rpd3*Δ*yta7* mutants are sensitive to HU, which is a phenotype shared by many strains with deletions in genes that encode proteins involved in DNA replication.

Evidence to support a direct role of Yta7p in DNA replication events is provided by identification of an S phase specific binding of Yta7p to replication origins. Moreover, levels of Yta7p bound to early-firing origins are increased compared with their later-firing counterparts. Levels of Yta7p that are bound to "late-firing" origins are only increased in conditions of *RPD3* deletion, where the resulting increase in histone acetylation at the "late-firing" origins is associated with advanced time of firing. Time of Yta7p binding at these "late" origins is also advanced concomitantly. This data supports the hypothesis that Yta7p provides a functional link between histone acetylation and time of origin activation.

In searching for a specific replication linked function of Yta7p it was observed that recruitment of the FACT subunit Spt16p to replication origins was increased in conditions of *YTA7* deletion. A second function for Yta7p in the S phase checkpoint was also demonstrated and the two roles of Yta7p, in DNA replication and S phase checkpoint, were separated depending upon their requirement for the bromodomain.

The data produced in this thesis adds to our knowledge of DNA replication events and highlights the importance of histone modifications and chromatin remodeling to the replication field. This thesis describes the direct involvement of a protein, which was previously unassociated, with DNA replication and S phase checkpoint function and provides good ground work for future investigation.

Contents

List of Figures

List of Tables

Acknowledgements

I would like to thank the Stancheva, Hardwick, Beggs, Allshire, Makovets and Schirmer labs for the kind provision of materials. For useful advice throughout the three years I would like to thank my committee members, including Adrian Bird and Irina Stancheva for their advice beyond the assessments. For practical input I am very grateful to Katrina Gordon for general advice, Steve Innocente on matters of QPCR and Dave Kelly for his unending patience every time I used the FACS machine.

A big thank you to my adopted supervisor Lea Harrington for kindly allowing me to continue my project in her lab and all the support and brilliant "pep talks". In extension I would like to thank all the members of my adopted lab, in particular: Jennifer Dorrens, Laura Gardano, Sveta Makovets and Elisa Wong, for being so welcoming and making the transfer as smooth and friendly as possible.

I owe a huge thank you to my supervisor Maria Vogelauer for teaching, guidance and advice in every aspect of the work, providing me a lab and project and offering to take me under her wing. I guess I can no longer say "I don't know anything about yeast".

Finally for Fiona Pryde, Francesca Romana Mariotti and Simone Schatlowski I have a huge hug and a major debt of gratitude. Thanks for your advice, support, practical help and most importantly friendship these past few years. For Fiona and Francesca thanks for the tea and chats, for the 17 hour timecourses, for picking me off the floor and drying my tears and for sharing this rollercoaster without killing me. I certainly would not have finished this thesis without you both. I hope we will meet again many times for a good cup of tea and natter and as good a team as we were in the end, may we never have to do a timecourse again!

Outside of the university I would also like to acknowledge the input of my previous co-

workers. Thanks to Wendy Cooper, my first ever supervisor, for giving me the encouragement to try a life in Biology and for making my first lab experience so much fun. Further thanks to Nigel Carter and all members of team 70/80 at the Sanger Institute for nurturing my enthusiasm and teaching me what a great environment research can be.

Finally thanks to my mom and dad for believing in me all these years and to Becky G for her amazing friendship and always providing a safe haven for escape. To my little sister - if you choose this life I wish you all the luck and success, but most of all happiness in the world. A massive thanks to Luca for bringing light and laughter and beauty to my life in the wind and rain of Edinburgh and beyond.

Abbreviations

5-FOA- 5-Fluoroorotic Acid

°C- degrees Celsius

%- percent

ACS- ARS consensus sequence

ARS- autonomously replicating sequence

ASMS- American Society for Mass Spectrometry

BD- bromodomain

bp- base pair

BrdU- bromodeoxyuridine

C. elegans- *Caenorhabditis elegans*

CDK- cyclin dependant kinase

ChIP- chromatin immunoprecipitation

ChIP-Chip- chromatin immunoprecipitation plus microarray analysis

Chr. - chromosome

DDK- Dbf4p dependant kinase

DMA- dimethyl adipimidate

DNA- deoxyribonucleic acid

dNTP- deoxyribonucleotide triphosphate

DSB- double strand break

FACS- fluorescence assisted cell sorting

Fig.- Figure

H2A- histone two A

H2AK123- the lysine in amino acid position 123 of the histone two A protein sequence

H2Aser129P- phosphorylation of serine 129 of histone two A

H2B- histone two B

H3- histone three

H3K4, K9, K14, K36, K56, K79- histone three lysines 4, 9, 14, 36, 56 and 79 respectively

H3K4me- methylation of lysine 4 of histone three

H3K4me2- dimethylation of lysine 4 of histone three

H3K4me3- trimethylation of lysine 4 of histone three

H3K36me- methylation of lysine 36 of histone three

H3K36me3- trimethylation of lysine 36 of histone three

H3K56ac- acetylation of lysine 56 of histone three

H4- histone four

H4K5, K8, K12 and K16- histone four lysines 5, 8, 12 and 16 respectively

H4ser1- histone four serine 1

HAT- histone acetyltransferase

HDAC- histone deacetylase complex

HU- hydroxyurea

INP- input

IP- immunoprecipitate

Kb- kilobase

L- litre

LR-PCR- long range polymerase chain reaction

M- molar

MCM- mini chromosome maintenance

mg- milligrams

μg- micrograms

MgCl2- magnesium chloride

min(s)- minute(s)

ml- millilitres

μl- microlitres

mm- millimetre

mM- millimolar

mRNA- messenger RNA

NAT- nourseothricin

ng- nanograms

ORC- origin recognition complex

ORF- open reading frame

PCR- polymerase chain reaction

PK- protein kinase

PreRC- pre-replication complex

PTM - post translational modification

QPCR- quantitative polymerase chain reaction

RC- replication complex

rDNA- ribosomal DNA

RFA- replication factor A

RFB- replication fork barrier

RFC- replication factor C

RNA- ribonucleic acid

RT- room temperature

ser129- serine in amino acid position 129

S. cerevisiae- Saccharomyces cerevisiae

secs- seconds

S phase- synthesis phase

Tbud- time at which 50 percent cells are budded

TEL- telomere

TEL VI- telomere six

T. thermophila- Tetrahymena thermophila

ts - temperature sensitive

WT- wild type

Chapter 1

Introduction

1.1 DNA Replication

Duplication of the genome is one of the most fundamental and vital processes for any organism. From single cell prokaryotes to multi cellular mammals, the process has to be performed with both exceptional accuracy and within the time constraints imposed by S phase length. In bacteria, duplication begins at one single point: the replication origin. This efficient system allows the entire genome to be copied only once, in a temporally linear fashion, by two diverging replication forks that terminate upon contact with a specific sequence [Messer, 1987]. Owing to the larger size and complex packaging of its genome, DNA replication in eukaryotes is adapted to perform the same function on a much larger scale. Replication in eukaryotes is achieved via the use of multiple origins of replication spread throughout the genome.

The eukaryotic cell cycle is composed of four stages: G1, S, G2 and M phase. DNA replication occurs during S (synthesis) phase, but control of replication is not limited to this phase (as reviewed in [Toone et al., 1997]). Each replication origin has to be regulated so that it fires only once per cell cycle. This regulation prevents over replication of the genome and regulation is accomplished by events in various stages of the cell cycle. In addition, replication origins are exposed to extra layers of control that act within S phase to regulate the temporal programme of origin firing, reviewed in [Weinreich et al., 2004]. Only a subset of replication origins are active during any given S phase [Santocanale and Diffley, 1996]. In fact, it is possible to characterise origins as efficient or inefficient; the characterisation will depend upon the percentage of cell cycles in which the origins are active. Origins that do not activate are known as dormant. In addition, only a subset of origins activate at a given time in S phase and, subsequently, only a subset of replication forks are present at a particular moment. Origins can also be characterised as "early" or "late-firing" depending upon the time within S phase that they become active. Replication progression and DNA damage are also monitored by the cell, and S phase checkpoint activation affects the activation of some replication origins and the stability of stalled replication forks, reviewed in [Branzei and Foiani, 2005]. Many of the proteins and complexes involved in

DNA replication have been well characterised, and the pathways in which they are involved have been intensely investigated; refer to [Bell and Dutta, 2002] for review. However, there is still a lot to be understood; specifically, within the topic of temporal regulation of replication origins there have been recent advances, but much remains unexplained.

1.2 DNA Replication in *S. cerevisiae*

Most of what we know about the actual mechanism of DNA replication in eukaryotes we have learned via the use of the budding yeast *Saccharomyces cerevisiae* (*S. cerevisiae*). This model system has proven to be an exceptionally useful tool. It is more easily manipulated than most available experimental systems, with the deletion of non lethal genes a relatively simple process. Also, most of the replication protein complexes and their mechanisms of action are conserved from yeast to mammals. Therefore, *S. cerevisiae* can function to provide a simplistic model, with which we hope to decipher more complex mechanisms of higher eukaryotes in the future. An excellent aspect of using *S. cerevisiae* is that we can take advantage of the wealth of information already available to enable the study of how the mechanisms of DNA replication are controlled.

1.2.1 Pre-replication Complex

In *S. cerevisiae* replication origins were identified originally as specific sequences that possessed the ability to replicate a plasmid inside a cell [Stinchcomb et al., 1979], hence the name Autonomously Replicating Sequence (ARS). Within the ARS there is a highly conserved sequence known as the ARS Consensus Sequence (ACS), which consists of 11 base pairs that act as the binding site of the Origin Recognition Complex (ORC) [Bell and Stillman, 1992]. ORC is a complex of six proteins that remains bound to the ACS throughout the cell cycle [Donaldson and Blow, 1999] and represents the "building block" for formation of the Pre replicative complex [Bell and Dutta, 2002].

During G1 phase of the cell cycle the recruitment of Cdt1p and Cdc6p to ORC bound origins enables the MCM2-7 complex to be loaded (reviewed in [Takeda and Dutta, 2005]). Cdt1p is required for localization of MCM2-7 to the nucleus in G1 [Diffley, 2004]. Cdc6p, an AAA+ ATPase, stabilizes ORC binding to origins and is responsible for the ATP dependent loading of MCM2-7 [Harvey and Newport, 2003], [Tye, 1999]. The heterohexameric MCM2-7 complex is the putative DNA helicase, which will facilitate DNA unwinding to allow replication to begin [Kanter et al., 2008], [Bochman and Schwacha, 2008]. The PreRC (Pre-replication complex) defines sites of potential replication activation. The process of origin firing and DNA unwinding, however, requires a subsequent set of proteins that bind in a regulated manner at each individual origin; refer to Fig. 1.1. Only once these additional proteins are bound can an origin that is "licensed" for replication by the presence of the PreRC become an active origin.

1.2.2 Replication Complex - Initiation

In order to initiate, an origin requires the binding of multiple proteins after the PreRC is formed. The main functions of these replication complex proteins are to uncouple MCM2-7 from the PreRC, to promote unwinding of the DNA and to load the replicative polymerases. These three functions allow replication to begin and facilitate the progression of the replicative machinery along the fork. The proteins identified thus far, which are required for these functions, include: Mcm10p, Cdc45p, Sld2p, Sld3p, Dpb11p, RPA and the GINS complex. The known functions of these proteins are summarised in Table 1.1. Only once all of these factors are assembled can an origin initiate. Although the exact order of loading and absolute functions of these proteins remain unknown, it has been demonstrated that time of binding of Cdc45p has a direct correlation with time of origin firing [Aparicio et al., 1999].

All of these proteins assemble at origins in S phase in an inter-dependent manner. For instance, Cdc45p is required for the binding of polymerases α and ϵ, whilst loading and function of Cdc45p requires interaction with RPA, MCM2-7 complex and CDK phosphorylated Sld3p. Dbp11p physically interacts with phosphorylated Sld2p and phosphorylated Sld3p [Zegerman and Diffley, 2007], in addition to DNA polymerase ϵ. Association of Dpb11p with the origin is co-dependent with all three of these proteins, in addition to RPA. Co-operation between Cdc45p and Dpb11p is also dependent on GINS. GINS, Cdc45p and MCM2-7 have been identified as a complex in a variety of organisms and formation of this complex in humans is dependent on Mcm10p [Im et al., 2009]. GINS has also been shown to complex with, and enhance the activity of, DNA polymerase ϵ *in vitro* [Seki et al., 2006].

1.2.3 Regulation of Initiation by CDK and DDK Activity

CDK is composed of the catalytic subunit Cdk1p and its regulatory cyclins. The phosphorylation activity and substrate specificity of Cdk1p is regulated throughout the cell cycle by controlling transcription levels of its cyclins. The G1 phase cyclins are Cln1p, Cln2p and Cln3p, while the main S phase cyclins are Clb5p and Clb6p and the mitotic cyclins are Clbs1p-4p. The cyclins promote different functions for CDK. The G1 cyclins are responsible for progress through START (the point at which a cell is committed to entering a new cell cycle), transcription of the Clb5p and Clb6p genes and degradation of the CyclinB(Clb)-CDK inhibitor Sic1p, as reviewed in [Cross, 1995]. Following START many processes begin; these processes include activation of G1 transcription machinery, spindle pole body duplication, bud emergence [Lew and Reed, 1993], DNA replication and growth (reviewed in [Toone et al., 1997]). The S phase cyclins are responsible for replication origin activation [Early et al., 2004].

Regulation of the assembly of the initiation proteins by CLB-CDK phosphorylation of Sld2p and Sld3p, as per Fig. 1.1, limits replication to S phase when CLB-CDK levels are high and the PreRC has been previously formed. At the same time, high levels of CLB-CDK prevent PreRC assembly and, therefore, guarantee that a replication origin is activated only once per cell cycle. CLB-CDK uses several redundant pathways to prevent PreRC formation, demon-

Protein/complex	Known Functions
Mcm10p	Required for replication initiation, potentially through anchoring and then subsequent release of MCM2-7 from origins [Homesley et al., 2000]. Involved in replication elongation through origins. Required for DNA polymerase α stability and co-ordination of DNA polymerase α and MCM2-7 association [Ricke and Bielinsky, 2004] [Warren et al., 2009].
Cdc45p	Time of assembly at origins coincides with time of firing. Required for loading of DNA polymerases at origins [Aparicio et al., 1999]. Possible role in replication elongation as Cdc45p moves with the replication fork [Aparicio et al., 1997].
GINS	Complex of subunits: Sld5p, Psf1p, Psf2p and Psf3p. Genetic interaction with *DPB11* and *SLD3*. Required for replication initiation [Takayama et al., 2003]. Complexes with Cdc45p and MCM2-7 and is required for their interaction [Gambus et al., 2006] [Labib and Gambus, 2007].
Sld2p	Target of CDK. Phosphorylation induces binding to Dpb11p BRCT (3 & 4) domain and this is required for initiation to occur [Masumoto et al., 2002] [Zegerman and Diffley, 2007].
Sld3p	Target of CDK. Forms complex with Cdc45p when phosphorylated and both associate with origins in a mutually dependent manner. Interacts with Dpb11p BRCT (1 & 2) domain when phosphorylated [Kamimura et al., 2001] [Zegerman and Diffley, 2007].
RPA	Coats and stabilises single stranded DNA and promotes unwinding of DNA helix (reviewed in [Takeda and Dutta, 2005]).
Dpb11p	Complexes with DNA Polymerase ϵ at origins and is required for DNA polymerase α association [Masumoto et al., 2000].
DNA polymerase α	Synthesises primer required for both leading and lagging strand DNA replication, reviewed in [Burgers, 1998].
DNA polymerases δ and ϵ	Leading and lagging strand DNA synthesis, reviewed in [Burgers, 1998].

Table 1.1: Known components of the replication complex.

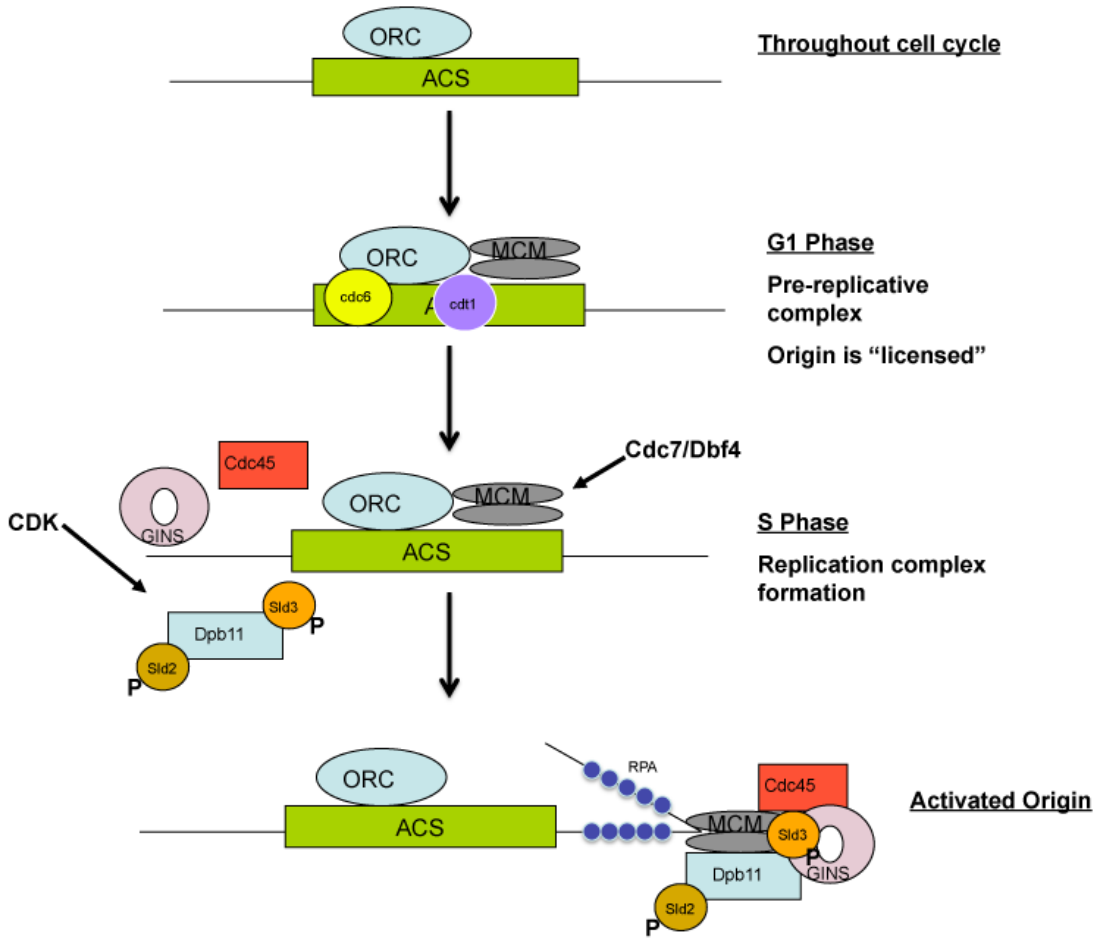

Figure 1.1: Transition from PreRC assembly to initiation; the major players. Adapted from [Takeda and Dutta, 2005]. Line 1 - Black line is DNA, green box is the ACS and blue oval is ORC. Line 2 - Proteins that bind in G1 phase - double grey oval is MCM2-7 complex, yellow circle is Cdc6p and purple circle is Cdt1p. Line 3 - Proteins that bind in S phase - pink oval is GINS complex, red rectangle is Cdc45p, blue rectangle is Dpb11p orange circles are Sld2p and Sld3p and P is phosphorylation. CDK and Cdc7p/Dbf4p are kinases that are required for S phase progression. Line 4 - Active origin - small blue circles are RPA. All other proteins as per line 3. Some of the proteins will remain bound and will be the basis of the replicative fork.

strating the importance of this mechanism to the cell. CLB-CDK promotes degradation of Cdc6p, relocalisation of Cdt1p and unbound MCM2-7 outside of the nucleus and phosphorylates ORC, all to prevent further PreRC formation until CLB-CDK is degraded in the M/G1 transition [Mimura et al., 2004], [Nguyen et al., 2001], [Tanaka and Diffley, 2002]. Additional levels of control of PreRC formation have been identified in *Xenopus laevis* and mammalian cells. Geminin was identified to inhibit loading of the MCM2-7 complex in higher eukaryotes [McGarry and Kirschner, 1998]. ORC also behaves differently in mammalian cells as it does not remain bound to replication origins that have fired, as is suggested for *S. cerevisiae*. ORC1 in mammals is released after its affinity for chromatin is decreased and then the free ORC1 is targeted for ubiquitination [DePamphilis, 2003].

A second regulator that acts at the level of the individual origin is the Dbf4p dependent kinase (DDK), Cdc7p, reviewed in [Duncker and Brown, 2003]. Cdc7p activity is regulated by Dbf4p, whose levels peak during S phase. Once bound and activated at an origin, it has been shown that Cdc7p phosphorylates MCM2-7 and is likely to promote the helicase activity of MCM2-7 and allow DNA unwinding [Lei et al., 1997]. It is also possible that DDK allows the association of Cdc45p with MCM2-7 at the time of initiation, reviewed in [Takeda and Dutta, 2005].

1.2.4 The Replication Fork

The replicative complex includes the DNA polymerases, which function in co- operation with a number of different proteins at the replication fork to duplicate both strands of DNA. Some additional components of the replicative complex such as MCM2-7 and Cdc45p have been shown to migrate with the fork [Aparicio et al., 1997], but the replisome (entire complex of proteins required for replication) consists of many more proteins.

Much of the original information that is available about the replication fork came from studies that used an *in vitro* SV40 system in mammalian cells [Li and Kelly, 1984]. Many of the eukaryotic proteins involved were subsequently confirmed through continued use of the SV40 system and yeast genetic studies [Waga and Stillman, 1994]. The main proteins identified so far are summarized in Table 1.2.

As reviewed in [Waga and Stillman, 1998], a simplistic model requires loading of the DNA polymerase clamp PCNA by the ATPase RFC. PCNA allows greater processivity of the polymerases by stabilizing their presence at the fork. DNA polymerase α is the primase that generates the RNA:DNA primer to initate replication, however its limited processivity and proof reading ability make it necessary to switch the polymerase once the primer is in place. For the leading strand it is suggested DNA polymerase ϵ could be the main DNA polymerase in yeast [Burgers, 2009]. Polymerase switching allows replication of the leading strand in a processive fashion.

Owing to the sole $5'$ to $3'$ polymerase activity, replication of the lagging strand is a more complicated process and this strand has to be duplicated in small Okazaki fragments. Resolution of these fragments requires the additional action of Fen1p and DNA ligase I. DNA polymerase δ is the polymerase suggested to function in lagging strand synthesis [Burgers, 2009]. As DNA

Protein/complex	Known Functions
MCM2-7	Unwinds DNA at replication fork.
DNA polymerase α /primase	Synthesis of RNA:DNA primer at leading and lagging strands.
DNA polymerase δ and DNA polymerase ϵ	Elongation of primers at the leading and lagging strands.
PCNA	Processivity factor for DNA polymerase δ and DNA polymerase ϵ.
Replication Factor C	Loading of PCNA, polymerase switching.
Replication Protein A	Protection of single stranded DNA, fidelity clamp for DNA polymerase α/primase.
Fen1p	Cleavage of RNA:DNA flap structures at the lagging strand.
DNA ligase I	Ligation of DNA pieces.
DNA topoisomerases	Removal of DNA topological constraints during replication.

Table 1.2: Replication fork proteins. Adapted from [Toueille and Hubscher, 2004].

polymerase δ proceeds along the DNA at the fork it displaces the RNA:DNA primer left by the previous Okazaki fragment. The resulting flap is cleaved by Fen1p, the gap processed by DNA polymerase δ and the DNA ligated by DNA ligase I, resulting in a single long DNA molecule; Fig. 1.2.

1.2.5 The Intra S phase Checkpoint

A checkpoint is a monitoring/control mechanism that prevents an event in the cell cycle from occurring if a pre-required event has not completed successfully. The term checkpoint was originally defined by [Hartwell and Weinert, 1989] as "control mechanisms enforcing dependency in the cell cycle" and the function of checkpoints is "to ensure the completion of early events before late events begin". The experiment that supported this original concept of a checkpoint came from studies of *rad9* mutant cells. WT cells that are irradiated in S or G2 phase of the cell cycle arrest in G2 to allow for DNA repair. However, *rad9* mutant cells fail to arrest and continue through consecutive cell cycles until cell death occurs. This result indicates that *RAD9* behaves as a checkpoint signal [Weinert and Hartwell, 1988]. This role for *RAD9* as a checkpoint gene rather than a gene involved in DNA repair was further supported by an experiment where the G2 checkpoint was mimicked in a *rad9* strain, by using a microtubule poison. Allowing the cell to delay G2 increased cell viability in this strain [Weinert and Hartwell, 1988].

There are several different checkpoints active throughout the cell cycle in addition to the G2 checkpoint. One such checkpoint is active during S phase. The intra-S phase checkpoint

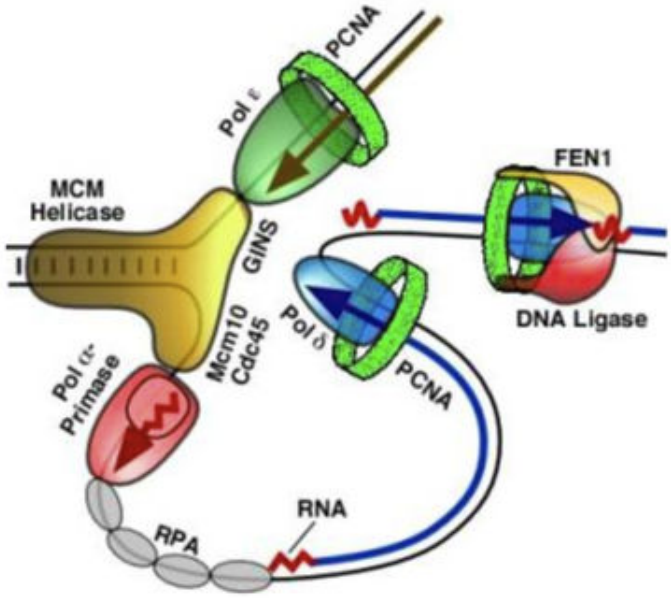

Figure 1.2: Eukaryotic replication fork machinery. Figure taken from `www.biochem.wustl.edu/~burgersw3/Replication.html` (December 2009). Black line is DNA, brown triangle is MCM2-7 complex plus Cdc45p plus GINS complex plus Mcm10p, green loop is PCNA, red egg shape is polymerase α, blue egg shape is polymerase δ, green egg shape is polymerase ϵ, grey circles are RPA, red wave is RNA primer, yellow spoon shape is Fen1p and red spoon is DNA ligase.

monitors replication and acts to stall the cell cycle and allow time for repair when damage is detected or under conditions of replicative stress. One particular pathway of the checkpoint responds when cells are treated with hydroxyurea (HU); refer to Fig. 1.3. As reviewed in [Branzei and Foiani, 2005], HU depletes the cellular dNTP pool and causes replication fork stalling. Fork stalling results in RPA coated single stranded DNA, which is the proposed signal for recruitment of the effector kinase Mec1p. The increased RPA levels cause binding of Ddc2p, which brings Mec1p to the site of stalling. Mec1p allows stable association of Cdc45p and the polymerases at the fork [Cobb et al., 2003]. Mec1p also phosphorylates Mrc1p, which, in turn, binds to Rad53p and reveals a phosphorylation site to Mec1p. Initial phosphorylation of Rad53p by Mec1p allows subsequent autophosphorylation by Rad53p to amplify the signal.

Phosphorylation of Rad53p results in four major outcomes. Through downstream effectors Rad53p acts to stabilise the forks, arrest the cell cycle (preventing entry into mitosis), prevent recombination events at the stalled fork and severely delay firing of late-activating origins, reviewed in [Branzei and Foiani, 2006]. Additional roles in regulating histone protein levels and chromatin structure have also been inferred for Rad53p [Dohrmann and Sclafani, 2006], [Gunjan and Verreault, 2003].

One of the effects of Rad53p phosphorylation is to delay late-firing origin activation via the dissociation from chromatin and binding of Dbf4p so that Cdc7p is no longer recruited to these origins. The binding of Rad53p to Dbf4p could act to alter Dbf4p, or simply sequester it. It has been demonstrated that the same N terminal domain of Dbf4p binds either Rad53p or ORC alternatively and that over expression of *DBF4* abates the prevention of late origin firing by Rad53p when cells are treated with HU [Duncker et al., 2002]. The role of Cdc7p-Dbf4p is also conserved in mammalian cells in the S phase checkpoint [Kim et al., 2003].

Another effect of checkpoint activation is fork stabilisation. Mrc1p, in addition to Tof1p, is already localised at the replication fork and, once activated, these proteins may stabilise the MCM2-7 complex and Cdc45p to prevent collapse. This will eventually allow replication to continue once the block to replication is inactivated [Katou et al., 2003], [Nedelcheva et al., 2005]. Mrc1p, Csm3p and Tof1p are presumed to act as a bridge to regulate the progression of DNA unwinding with DNA synthesis. When treated with HU, *mrc1* and *tof1* mutant cells display a mis-localisation of the replication fork proteins away from sites of DNA replication. If the sites of DNA synthesis are monitored by BrdU incorporation, the replication fork proteins can be monitored by ChIP-chip in HU to be a number of kbp away from the regions of synthesis [Katou et al., 2003]. This result suggests that the replisome is not paused correctly at the site where synthesis was arrested. The result is that *mrc1* mutants are unable to recover from checkpoint activation. *tof1* mutants, however, possess a better recovery when compared with *mrc1*, attributed to the fact that they maintain the ability to activate some late-firing origins [Tourriere et al., 2005]. Therefore, for cells that are unable to restart stalled replication forks, the use of late-firing origins becomes essential to enable complete replication [Tourriere and Pasero, 2007]. A requirement to activate additional origins has been noted in human cells, where in response to continued exposure to HU dormant origins activate to

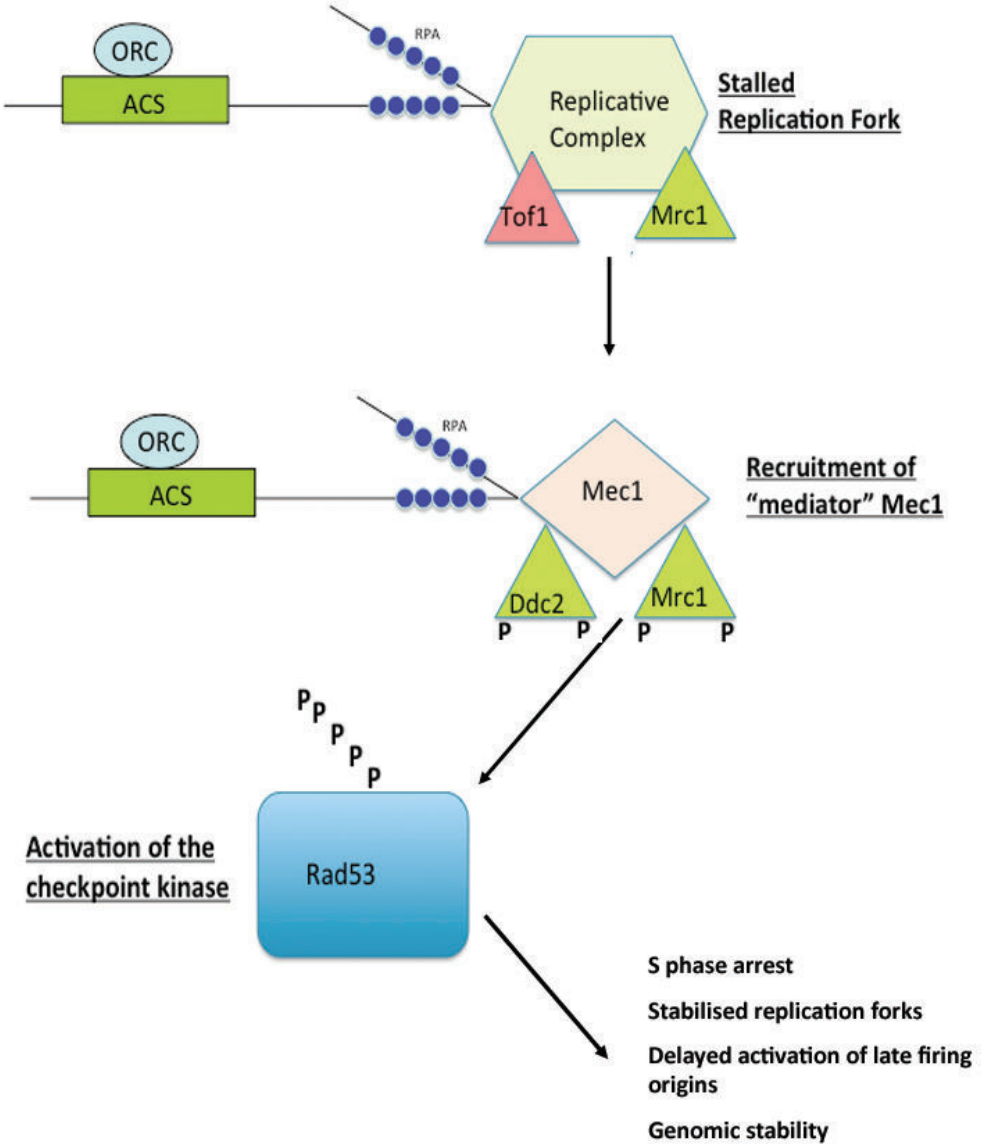

Figure 1.3: S phase response to stalled replication forks. This response is initiated when cells are treated with the ribonucleotide reductase inhibitor HU. Adapted from [Longhese et al., 2003]. Line 1 - green rectangle is ACS, blue circle is ORC, black line is DNA, small blue circles are RPA. Stalled replication forks should maintain association of replicative complex (hexagon) and both Tof1p (pink triangle) and Mrc1p (green triangle). Line 2 - pink diamond is Mec1p, green triangles are Ddc2p and Mrc1p, black P is phosphorylation. Line 3 - blue rectangle is checkpoint kinase Rad53p, black P is phosphorylation.

compensate for stalled forks. Decreasing the amount of MCM2-7 complex available for loading at dormant origins results in slower replication rates and decreased viability [Ge et al., 2007].

A further protein that is proposed to have a role in both efficient activation of the S phase checkpoint and stabilisation of the resulting stalled replication forks is the Sgs1p helicase. Sgs1p binds to and stimulates phosphorylation of Rad53p and is required for stabilisation of DNA polymerase ϵ at stalled replication forks [Bjergbaek et al., 2005].

1.2.6 Fork Pausing, Replication Termination and Replication of Telomeres

In addition to their role in the S phase checkpoint, it is suggested that Mrc1p and Tof1p have an independent role in replication fork progression in an unchallenged S phase. Both proteins were found to co-purify with members of the MCM2-7 complex in cells that were not exposed to HU and were identified by ChIP-Chip at sites of active DNA replication [Nedelcheva et al., 2005], [Katou et al., 2003]. Deletion of *MRC1* also resulted in slower replication fork progression through chromatin in an unchallenged S phase [Szyjka et al., 2005].

In addition to the fork stalling that is induced by checkpoint activation, replication forks also pause at specific sites in the genome even when not subject to DNA damage or dNTP depletion. Examples include forks that encounter bound proteins or chromatin or transcriptional machinery. One such site of highly active transcription is the rDNA cluster, where a specialised mechanism of replication control is employed. In this region of rDNA repeats, replication proceeds in a largely unidirectional manner due to the presence of the Replication Fork Barrier (RFB), which is the binding site of Fob1p; refer to Fig. 1.4. Replication initiates from the replication origin present in each repeat unit. The fork travelling to the left replicates the small 5S subunit of the rRNA gene in the same direction as transcription until it reaches the barrier. The fork travelling to the right replicates the much larger 35S subunit, also in the same direction as transcription, until it reaches the subsequent barrier, reviewed in [Labib and Hodgson, 2007]. The Tof1p-Csm3p complex is required for correct function of the barriers, which are thought to be essential for homologous recombination and sustainability of the rDNA locus [Tourriere and Pasero, 2007]. Whilst deletion of *TOF1* does not affect replication fork rates, as is the case for *mrc1*Δ, it does result in loss of replication fork barrier function [Hodgson et al., 2007].

Deletion of *SGS1* results in an increased accumulation of replication forks at the barrier when compared to WT [Weitao et al., 2003]. Hence, the Sgs1p helicase also acts at the RFB to resolve or stabilise paused replication forks. An additional helicase Rrm3p is required for replication through all pause sites and for replication at the telomeres [Azvolinsky et al., 2006].

When there are no RFBs present, as is the case for most of the genome, replication of a specific region terminates when two opposing forks collide. This mechanism serves as a check that all of the DNA between two active replication origins has been replicated completely [Santamaria et al., 2000]. However, one notable exception would be replication at

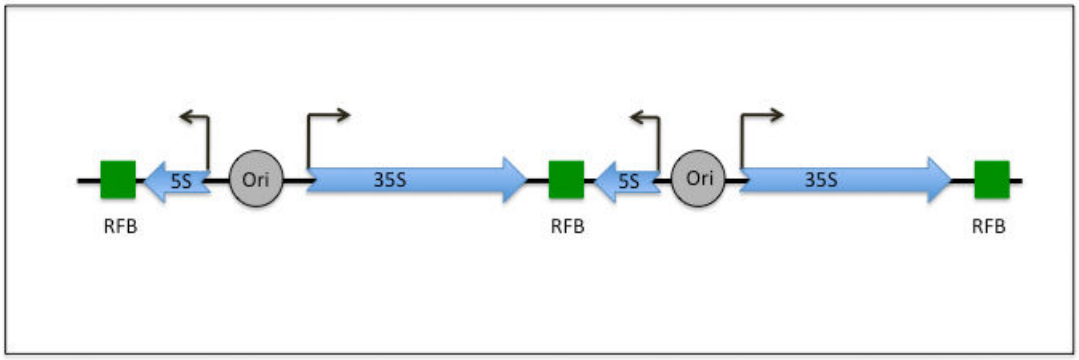

Figure 1.4: DNA replication at the specialised rDNA repeat locus. Direction of replication is indicated by blue arrows, direction of transcription by brown arrows, replication origins are represented by grey circles and RFB by green squares. Black line is DNA. DNA replication forks proceed in both directions from the replication origin but the forks are stalled at the RFB, so that replication proceeds largely in the direction of transcription of the 35S subunit gene. Adapted from [Labib and Hodgson, 2007].

the telomeres where the fork would replicate DNA until it reached the TG telomere tract. Replication of the telomeres is thought to be a passive event because although replication origins are found within the subtelomeric regions, they are rarely activated or they activate very late in S phase [Stevenson and Gottschling, 1996], [Stevenson and Gottschling, 1999]. The TG tract is maintained separately through the action of telomerase, but it has been suggested that maintenance of telomeres by telomerase is dependent upon DNA replication. [Dionne and Wellinger, 1998].

1.3 Mapping Replication Origins in *S. cerevisiae*

Since the initial identification of certain sequences that were capable of sustaining plasmids in yeast ([Stinchcomb et al., 1979]), and the further identification of the ACS, experiments to map the precise locations of all the *S. cerevisiae* replication origins have been undertaken. Replication origins are much harder to detect in other eukaryotes as the sequence specificity of the *S. cerevisiae* ACS has not been identified outside of this system. Even in *S. cerevisiae*, not all regions that contain an ACS or bind ORC will function as active replication origins in their chromosomal context [Santocanale and Diffley, 1996]. Further experiments to characterize replication origins *in vivo* have greatly increased our current knowledge regarding active replication origin location.

Original experiments relied on the use of 2D gel electrophoresis [Huberman et al., 1987], [Brewer and Fangman, 1987] to detect physical structures corresponding to replication intermediates. This technique had the advantage of detecting both structures resulting from an active origin and also structures corresponding to elongating replication forks [Fangman and Brewer, 1991]. However, 2D gel electrophoresis is limited by having to test individually small regions of the genome, corresponding to multiple restriction fragments. In addition, not all regions that contain an ACS function as origins, hence to choose a region with an active origin based on ACS sequence is difficult. The active origin also requires additional sequence elements known as the B and C elements (A being the ACS and its immediate flanking sequence) [Toone et al., 1997].

More recent studies have used whole genome approaches to identify replication origins. Micro array based assays [Raghuraman et al., 2001], [Yabuki et al., 2002] or Chromatin Immunoprecipitation (ChIP) of MCM2-7 and ORC [Wyrick et al., 2001] led to the acquirement of huge amounts of data that culminated in the computationally led identification of 228 replication origins [Nieduszynski et al., 2006]. The location of these origins can be found on the SGD and oriDB [Nieduszynski et al., 2007] databases at `www.yeastgenome.org` and `www.oridb.org` respectively.

These studies led not only to the mapping of replication origins, but also provided information on the efficiency and time of activation of origins.

1.4 Factors that Determine Time of Replication Origin Firing

The ARS sequence is present in abundance throughout the *S. cerevisiae* genome, but only a subset of origins that assemble a PreRC will fire during a cell cycle. Not only will some (inefficient) origins not fire every cell cycle, but there is a temporal program controlling the order of initiation for the ones that do fire [Raghuraman et al., 2001]; refer to Fig. 1.5 for an example of time of replication across a chromosome. There are two proposals to explain this temporal programme, as reviewed in [Rhind, 2006]. The first proposal is based upon the concept that each origin has a pre-determined time of firing in S phase and that a certain origin will always fire at a given time in relation to the others. There would be a mechanism that "marks out" origins for activation prior to S phase and their order of activation will be strictly guided by this mechanism. The second proposal offers a more probabilistic model and suggests that each origin has a certain efficiency (that is, a high or low probability to fire) based upon some intrinsic value (for example it has a location that favours access of the replication machinery). Each origin activates randomly and those with a low probability to fire will either be late to activate, or never will. For example, if there were two neighbouring origins but owing to some intrinsic property one was more efficient than the other, the low probability origin would have a higher chance to be passively replicated by the fork of its neighbour. As the fork replicates

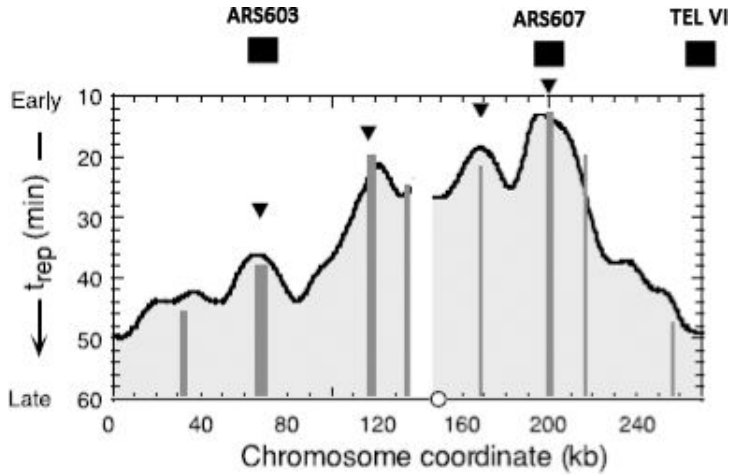

Figure 1.5: Replication profile of chromosome six as an example of regulated timing. Figure taken from [Raghuraman et al., 2001]. X axis is the co-ordinate along *S. cerevisiae* chromosome six in kilobase pairs and the circle is the centromere. Y axis is the time of half maximal replication in minutes. Grey bars represent known ARS's and the four with black triangles above them are used in more than 50 percent of cell cycles. Black boxes are origins used later in this study and show the locations of ARS603, ARS607 and the TELVI region referred to in the results chapters. ARS603 is a late firing efficient origin (small peak, black triangle). ARS607 is an early firing efficient origin (large peak, black triangle). TELVI is one of the latest regions to replicate on this chromosome.

the origin the PreRC would be removed and the origin would lose its ability to fire. The main problem of this model is that origins would fire randomly and this could lead to potential large non-replicated gaps. A solution to the gap problem would be if one of the proteins involved in either the RC or DDK were rate-limiting. The amount of active origins at any time would be finite. As S phase progresses the amount of licensed origins would decrease, due to activation or passive replication, therefore increasing the probability that those origins that remain would activate. Therefore, even less efficient origins would eventually activate if they were in a gap region.

Why the origins fire in a repeatable temporal pattern is currently unknown. It should be identified whether the temporal pattern is a matter of probability, if it is pre-determined or if it is a combination of the two. Further investigation is required to understand which factors can influence origin efficiency, whether there is a rate limiting factor in origin activation and to examine the effects of deregulation of the temporal pattern. The ability to initiate replication from multiple sites allows the cell to replicate the genome within the time limit of S phase. Removing that ability by deletion or inactivation of origins leads to incomplete DNA synthesis and genome instability [van Brabant et al., 2001].

Two proteins that affect the time of origin firing are Clb5p and Rad53p. It has been suggested that Rad53p has a positive effect on replication initiation, independent from its ability to delay firing of late origins during an S phase checkpoint response. There is no

direct evidence of delayed replication initiation in *RAD53* mutated strains and deletion of *RAD53* is lethal. However, one allele of *RAD53*, that does not possess a checkpoint defect, displays a synthetic interaction with *cdc7-1*. This synthetic interaction is exerted through direct interaction with and/or by controlling the levels of Dbf4p (the Cdc7p associated kinase) [Sun et al., 1996] [Dohrmann et al., 1999]. Decreased Dbf4p resulting from reduced Rad53p function could affect origin activation levels.

Perturbations in the S phase cyclins can specifically affect timing of DNA replication. The functions of Clb5p-CDK and Clb6p-CDK have been separated and it has been shown that Clb6p-CDK is sufficient for activation of early origins, where as Clb5p-CDK is necessary for activation of origins that fire later in S phase. *CLB5* deletion strains rely on forks of the early origins to complete replication. Deletion of both S phase cyclins delays replication even further until the mitotic cyclins are expressed. The mitotic cyclins can then activate replication without disturbing the temporal programme (i.e. in a mitotic cyclin controlled S phase all events are delayed but the early origins still fire early in comparison with the late origins, with the same time difference between the two events) [Donaldson et al., 1998]. A further investigation of whole genome replication timing in $\Delta clb5$ cells reinforced the dependence on Clb5p-CDK for activating late origins, but suggested that this dependence was due to instability of Clb6p later in S phase. Replacing Clb6p with a stable protein in late S phase restored late origin firing in $\Delta clb5$ cells. This whole genome approach demonstrated that early-firing origins display no loss of efficiency in $\Delta clb5$ with reduced efficiency restricted to regions of approximately half the genome that contain the identified late origins. The authors argue that this result implies that the time of origin firing cannot be entirely probabilistic and that some temporal order applies [McCune et al., 2008].

Other factors also act on the time of replication of the telomeric regions. The Ku complex consists of two proteins Ku70p and Ku80p that are involved in DNA damage repair, localisation of telomeres and transcriptional silencing at telomeres [Laroche et al., 1998]. The usually late-firing telomeric or subtelomeric regions are replicated much earlier in *ku* mutants. This earlier replication was attributed to the particular Ku function of localisation of telomeres to the nuclear periphery [Cosgrove et al., 2002]. In addition, it was suggested that telomere length can influence time of replication. Those telomeres that replicate earlier, relative to the other telomeres, within a single S phase are more likely to be elongated by telomerase [Bianchi and Shore, 2007].

It was recognised many years ago, in *S. cerevisiae*, that there is a position effect regulating time of origin firing [Ferguson and Fangman, 1992]. The silent mating locus and subtelomeric sequences tend to fire very late in S phase or not at all. It was demonstrated that a late-firing origin requires its flanking region to remain late-firing when expressed on a circular plasmid. Removal of that flanking region results in earlier origin firing and, in fact placing a usually early-firing origin in that same flanking region causes the origin to fire much later [Friedman et al., 1996].

A direct effect of chromatin structure on time of origin firing was witnessed when

mutations in *SIR3* (the *SIR* genes encode for proteins involved in the generation of transcriptionally silent chromatin) resulted in activation of an otherwise silent origin [Stevenson and Gottschling, 1999]. Three components of the SIR complex are Sir2p, Sir3p and Sir4p. Sir4p is required for establishment and maintenance of the complex, Sir3p and Sir2p are involved in spreading of the complex throughout regions of heterochromatin and Sir2p is the catalytically active deacetylase component, as reviewed in [Kurdistani and Grunstein, 2003a]. In addition to its role in silencing at the mating-type loci and the telomere, Sir2p also functions at the rDNA repeat region and has been implicated as a negative regulator of DNA replication. Deletion of *SIR2* suppresses the temperature sensitivity of a *cdc6-4* strain [Pappas et al., 2004], which is defective for preRC formation. This suppression was demonstrated to be due to increased PreRC formation at a subset of origins in a *cdc6-4* Δ*sir2* strain when compared to *cdc6-4* alone; shown by detection of Mcm2p at specific origins in either strain. The catalytic activity of Sir2p was important for the suppression of *cdc6-4*, but it was not shown directly that a loss of catalytic activity leads to increased acetylation of histones at replication origins. Direct targeting of Sir4p or a silencing sequence (HMR-E) is also sufficient to delay the time of firing of an early origin [Zappulla et al., 2002]. While it was not investigated if the Δ*sir4* effect was *SIR2* dependant, it is presumed that deletion of *SIR4* would result in reduction of establishment and maintenance of the entire SIR complex. Direct targeting of the silencing sequence (HMR-E) also relied upon the presence of Sir4p to confer the late-firing effect on the early origin, but it was shown that the presence of Sir4p was not required to maintain HMR-E as a late replicating region in its native location. There is likely to be a secondary mechanism that can influence the time of replication of the HMR-E region [Zappulla et al., 2002].

While it was not shown conclusively that Sir2p deacetylation of histones is responsible for the negative effect of Sir2p on DNA replication, there is compelling evidence that the acetylation level of histone residues surrounding an origin affects the time at which that origin fires during S phase. Deletion of the histone deacetylase *RPD3* results in a global increase in histone H3 acetylation [Vogelauer et al., 2000]. A strain with the Δ*rpd3* mutation completes S phase faster than WT. This faster S phase was attributed to earlier firing of late origins [Vogelauer et al., 2002], [Aparicio et al., 2004]. Histone acetylation was also shown to have a direct effect when targeting of the H3/H2B histone acetyltransferase (HAT) Gcn5p caused earlier firing of a usually late origin [Vogelauer et al., 2002]. This effect is also supported by experiments conducted in human HeLa cells. Increased global H4 acetylation resulted in faster S phase progression and firing of less efficient replication origins [Kemp et al., 2005]. *RPD3* deletion has a global effect on histone acetylation and Δ*rpd3* was shown to affect the time of firing of multiple (especially late- firing) origins with the exception of HMR-E [Vogelauer et al., 2002]. The effect of Δ*sir2* on DNA replication in a *cdc6-4* strain was more specific; influencing only a subset of origins [Pappas et al., 2004]. The influence of *SIR2* deletion on replication origins is interesting, but the use of this strain is complicated by the effects of *SIR2* deletion on the "silent regions". Use of this strain would require further confirmation that any DNA replication observations were not a result of effects at these "silent regions", as was performed in [Pappas et al., 2004].

Since Δ*sir4* did not alter the time of replication of the HMR-E [Zappulla et al., 2002] there could be an additional mechanism, alternative to chromatin structure, that can affect time of replication in this region (also recall in [Vogelauer et al., 2002] there was a lack of effect of Δ*rpd3* on replication in this region). Due to the chance that DNA replication at the telomeric and mating type loci are possibly influenced by alternative mechanisms than histone acetylation, investigations into the effect of histone acetylation on replication timing would be better served by focusing at regions that replicate late, but are not located within these specialised regions.

Histone hyperacetylation could provide a binding site for proteins that bind to chromatin. In addition, acetylation neutralises the positive charge of lysine residues, therefore decreasing the affinity of histones for the negatively charged DNA. This decreased affinity may result in a less compact chromatin structure, reviewed in [Shahbazian and Grunstein, 2007].

Acetylation of certain histone residues along with other modifications have been observed as markers of transcriptionally active chromatin. In humans it has been noted that transcriptional activity has a positive correlation with earlier replication [Woodfine et al., 2004]. It should be pointed out that this correlation is not observed in *S. cerevisiae*, but owing to the size of the genomes these systems are not comparable in this respect. The *S. cerevisiae* genome is much smaller and does not possess the large domains of transcriptional activation and silencing of the human genome (with the exception of the telomeric and mating type loci). Therefore, most of the *S. cerevisiae* genome could be described as transcriptionally active. The active replication origins identified thus far in *S. cerevisiae* are all within intergenic regions with the notable exception of ARS605. ARS605 is located inside a gene only expressed during meiosis, but the origin is only active during pre-meiotic S phase[1].

What remains unknown is how hyperacetylation functions to alter the temporal program of DNA replication. One possibility is that there is a direct effect at individual origins whereby histone acetylation recruits a replication factor to allow initiation of the origin. A second possibility is that the effect is indirect and histone acetylation is simply associated with a more "open" chromatin context, which allows increased access of replication factors to origins. A third possibility is that histone acetylation causes localisation of regions into early or late replicating nuclear compartments during S phase [Zink, 2006].

1.5 DNA Replication and Chromatin Modifications/Remodeling

All of the processes (PreRC formation, replication initiation, replication fork movement and stalling) that contribute to replication of the genome have to take place in the context of chromatin. DNA in the nucleus is packaged into chromatin by nucleosomes, which are composed of the histone proteins H2A, H2B, H3 and H4. Histones can be chemically modified,

[1]Refer to `www.yeastgenome.org/cgi-bin/locus.fpl?locus=ARS605` (February 2010)

usually (but not exclusively) on their N terminal tails, and identification of differences in the pattern of modifications present on nucleosomes has led to the proposition of a "histone code" [Strahl and Allis, 2000] and Fig. 1.6.

In addition to targeted effects of HATs and HDACs on histone tails, such as those involved in transcription and DNA repair, there is a global turnover of histone acetylation and deacetylation [Vogelauer et al., 2000]. Specifically, in regard to replication, there is a constant turnover of histones at the replication fork that requires removal of histones in front of the fork and replacement of twice the number of removed histones behind the fork. Those histones with newly added modification marks need to be altered, to reflect and "remember" the previous chromatin state [Corpet and Almouzni, 2009]; refer to Fig. 1.7.

In addition to chemical modification, histones can also be affected physically, which leads to either "shifting" of nucleosomes along DNA, or "loosening", or complete disassembly of nucleosomes.

1.5.1 Regulation of DNA Replication by Chromatin

The regulation of transcription by remodeling or modification of chromatin is well characterized, but how chromatin affects DNA replication is not as clear. However, there are many circumstances during the replication process where chromatin remodeling/modification would seem necessary. In simple terms, chromatin represents a barrier to efficient DNA replication and therefore would have to be modified or remodelled for increased access of replication proteins, to both origins and forks, during PreRC assembly, origin initiation, fork elongation and S phase checkpoint activation. One example of how chromatin can influence replication is illustrated by the fact that ORC bound DNA has a nucleosome positioning pattern that has to be maintained for effective origin firing. When ORC is bound the ACS is a nucleosome free region, which suggests a "free" DNA fibre is the required substrate for PreRC complex formation [Lipford and Bell, 2001]. However, at least for ARS1, the positioning of nucleosomes immediately adjacent to the origin is equally important to origin efficiency. Shifting of nucleosomes over ARS1 results in decreased activation of that origin [Simpson, 1990]. Similarly, shifting the adjacent nucleosomes away from ARS1 results in decreased MCM2-7 complex binding, and, therefore, decreased origin activation, which suggests that nucleosomes can also have a positive influence on DNA replication [Lipford and Bell, 2001]. Therefore, it is not just a simple case of removal of nucleosomes to activate origins. Whilst an open chromatin conformation would seem conducive to activation, it is also important to recognize that this chromatin conformation needs to be differentially controlled through out the cell cycle. It is as important to "tighten" the chromatin as it is to "open" it. For example, it has been suggested that acetylation of H3 could be decreased from the G1 to S transition and then reacetylated for individual origins at different stages in S phase. This regulation of histone acetylation still remains to be identified in the *S. cerevisiae* model, but was observed for a viral replication origin active in various cell lines [Zhou et al., 2005]. A similar regulation of chromatin may be required at replication forks where the chromatin should be relaxed for access of the replication proteins and unwinding of

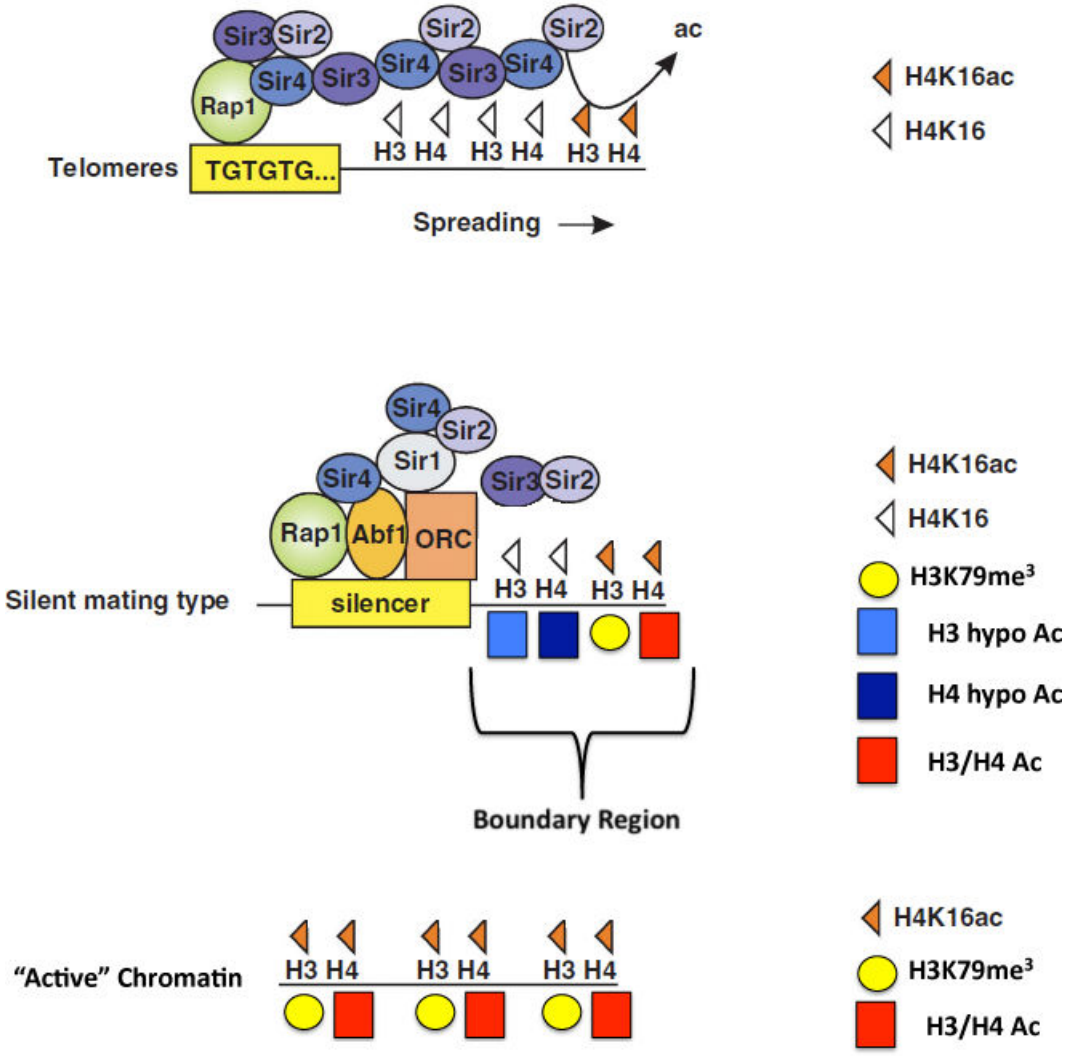

Figure 1.6: Active and silent chromatin in *S. cerevisiae*. Histone tail residues can be modified in a number of ways. Identification of some of those modifications as "active" or "repressive" marks has led to the proposal of a histone code. In *S. cerevisiae* most of the genome can be considered "active" with only a few specialised regions of "heterochromatin", such as the telomere and mating type loci. Boundary regions can contain both types of modification as they mark the region that separates the two chromatin states. At the telomere and mating type loci repressive modifications allow the propagation of the SIR complex, and the H4K16ac modification prevents the complex from spreading into "active" regions. Generally histone acetylation and H3K79me3 are markers of "active" chromatin, whilst histone hypoacetylation is a marker of "silent" chromatin. Legend key describes content of figure. Figure adapted from [Buhler and Gasser, 2009] and [Tackett et al., 2005].

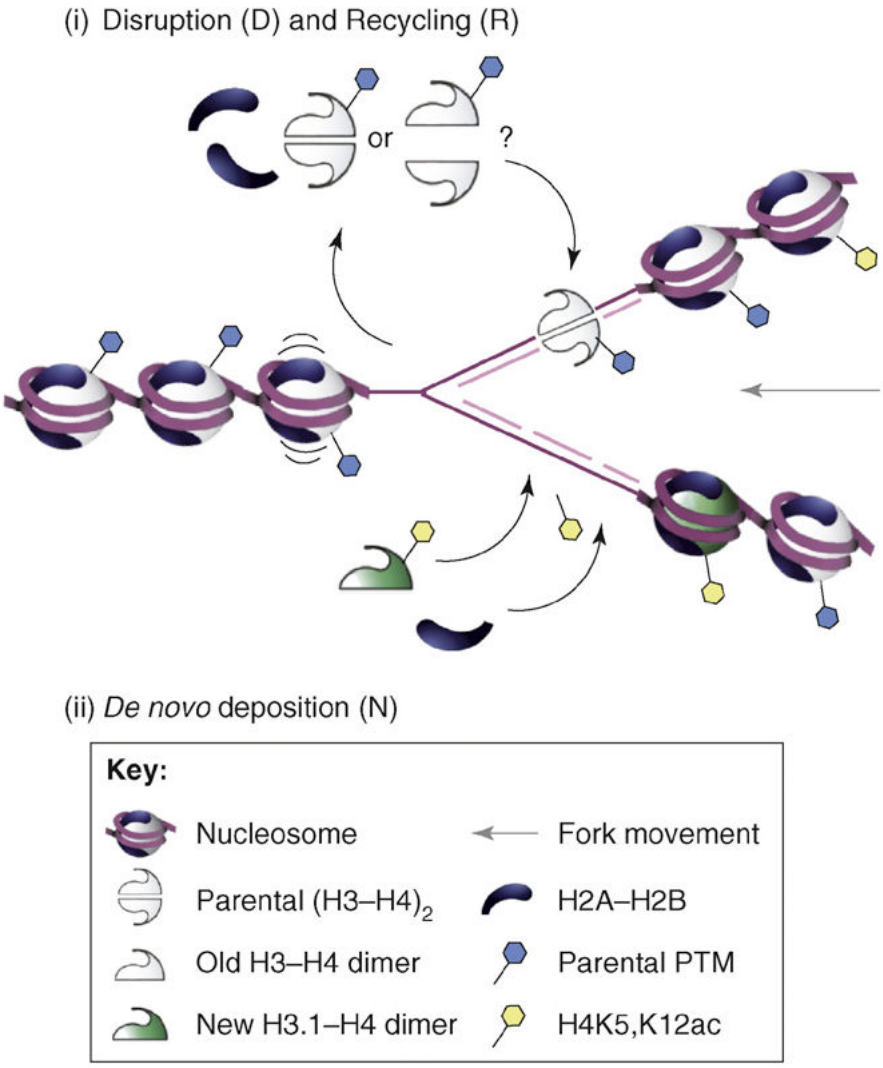

Figure 1.7: Histone Dynamics. Nucleosomes are removed in front of replication forks and need to be reassembled behind the fork with relevant modifications intact. Legend key describes content of figure. Figure taken from [Corpet and Almouzni, 2009].

the DNA, but be re-packaged both behind the fork and in conditions of checkpoint activation. It could be imagined that during S phase checkpoint activation a tighter packaging would aid stabilization of the fork structure and replication complexes. Again, this would be competing with the requirement of access to the DNA by the checkpoint/DNA repair proteins.

In *S. cerevisiae* there are only a few chromosomal regions where a specialised form of heterochromatin is found. These regions are also termed "silent chromatin" since expression of genes is repressed in these areas. These chromosomal regions are the highly regulated telomeric regions, the mating type switching loci and the rDNA repeat tract. Origin activation and progression of replication in these three regions may require an additional complement of remodelers. Indeed, in human cells where heterochromatin is far more abundant, complexes containing the nucleosome dependent ATPase ISWI family are required for replication of these heterochromatic regions [Collins et al., 2002], [Poot et al., 2005]. In yeast, there is a requirement for both the ISW and INO80 remodeling complexes for timely fork progression through late replicating regions, especially under conditions of replicative stress [Vincent et al., 2008]. In fact, Ino80p has been identified in numerous studies to be required for replication fork stability and retention of replication proteins at the fork in DNA damaging conditions [Papamichos-Chronakis and Peterson, 2008], [Shimada et al., 2008]. A separate chromatin remodeling complex, NoRC, affects replication timing of the specialised rDNA locus [Li et al., 2005]. Hence, for the specialised chromatin regions that rely upon chromatin remodeling for timely activation, physical shifting of the nucleosomes seems relevant. It could be speculated that other late replicating regions, that are not "heterochromatic", might also contain a nucleosome positioning pattern that does not favour DNA replication and that these regions might also benefit from the action of nucleosome remodelers.

In addition to physical remodeling, chromatin can also be altered through modification of the histone tails. It remains possible that acetylation of the histone tails leads to a general relaxation of the chromatin by decreasing the affinity of the histones for DNA. However, the effect of acetylation, methylation and phosphorylation of histone tail residues could be to recruit directly proteins that are involved in replication to origins/forks. In addition to acetylation, methylation of histone residues has also been shown to affect replication events. In different ways methylation of H3K4, K36 and K79 have been linked to replication. Replication origins tend to be found in regions of low H3K79 trimethylation but higher levels of H3K4 monomethylation [Nieduszynski et al., 2006], however caution must be taken when interpreting genome wide tendencies. H3K36 methylation seems to have a far more complex effect. H3K36 dimethylation was originally observed to be enriched along active open reading frames (ORFs), where it recruits the Eaf3p containing RPD3S deacetylase complex, which acts to prevent spurious transcription [Rao et al., 2005], [Carrozza et al., 2005]. Recent evidence also suggests a role for the H3K36me mark in replication, but in this case it is the balance between mono and tri methylated forms of H3K36 that is important [Pryde et al., 2009]. H3K36 methylation is required for the earlier firing of "late-replicating" origins in conditions of increased histone acetylation, indicating that it has a positive role in replication. However, trimethylation is enriched at

later-firing origins suggesting that this has a negative effect on time of replication.

Numerous modifications can be applied to histones and these modifications themselves can lead to different effects depending on how many moieties are added. As demonstrated, the effect of mono and tri methylation can be very different. One particular modification can signal a single function or multiple modifications can signal the same function. In addition, there can be an interdependency between modifications, for example the methylation of H3K4 and K79 is dependent on H2BK123 ubiquitination [Kurdistani and Grunstein, 2003a]. Sometimes the alteration of one single residue is enough to have a profound effect. For example, acetylation of H4K16 in subtelomeric regions is one mechanism of preventing the spread of SIR mediated heterochromatin formation, reviewed in [Shahbazian and Grunstein, 2007]. One modification can signal multiple complexes that would seem to have opposing roles to perform one common function; refer to Section 1.7 for an example involving the HAT complex NuA4 and the HDAC complex RPD3S. In this case the end response depends upon which complex is recruited at a particular time. The temporal order of complex recruitment in the completion of a single function can be influenced by additional neighbouring modifications, expression of/available levels of the proteins to be recruited, differing affinities of the complexes for the modification or post translational modification of the complexes.

As previously stated, a role for histone acetylation has been indicated in determining the time of replication origin firing. A partially redundant range of HATs and HDACs exists in *S. cerevisiae* and specific roles related to replication have been assigned to a number of them. Hat1p and Hat2p in association with Hif1p, for example, are most likely responsible for the H4K5 and K12 acetylation marks that signify newly synthesised histones [Parthun et al., 1996], [Ai and Parthun, 2004]. Recently a Hif1p independent role for Hat1p and Hat2p directly at replication origins through association with ORC has been inferred [Suter et al., 2007]. However, defects in replication were subtle and only observed in combination with ORC mutation, which indicates redundancy for these proteins. The levels of this HAT/ORC complex were not very high and were not regulated; the complex was found constitutively throughout the cell cycle. This result, whilst preliminary, highlights the possibility that a direct role of HAT and HDAC complexes exists in DNA replication.

Global histone acetylation and deacetylation patterns are maintained by a combination of HATs and HDACs. The HATs Gcn5p (catalytic subunit of SAGA) and Esa1p (catalytic subunit of the NuA4 and piccolo NuA4 complexes) are responsible for both targeted and global acetylation of H3 and H2A/H4 respectively. Deletion of *ESA1* is lethal, resulting in cell cycle arrest in the G2/M phase of the cell cycle [Clarke et al., 1999]. An experiment to investigate if over expression of *ESA1* could cause earlier firing of late origins prior to HU induced arrest, therefore implicating the protein in a replication related function, resulted in no advance in time of origin firing [Early et al., 2004]. However, the presence of Esa1p was necessary to exit from G1 arrest. Sas3p, the catalytic component of NuA3 is partially redundant with GCN5p and also acetylates H3 tail residues. Neither *GCN5* nor *SAS3* deletion is singularly lethal, but a combination of these two deletions results in the same inviability and G2/M arrest phenotype of an *ESA1*

deletion. This phenotype suggests that Sas3p and Gcn5p have overlapping functions. Whilst no evidence for a direct role in replication initiation exists for either protein, targeting of Gcn5p to a late-firing origin resulted in earlier firing, as mentioned in Section 1.4. Gcn5p has also been implicated in H3K9 acetylation associated with "new" histones [Corpet and Almouzni, 2009].

Evidence of a role for HATs in DNA replication is currently highlighted by studies in human cells. In humans the NuA4 homologue does not appear to be involved in replication. The two complexes implicated in DNA replication functions are the HBO1 H4 HAT complex and possibly the MOZ/MORF H3 HAT complex, which are more homologous to the yeast NuA3 complex [Doyon et al., 2006]; Fig. 1.8. In human cells HBO1 was identified as the H4 HAT essential to PreRC formation. Knockdown of HBO1 levels resulted in loss of MCM2-7 recruitment to chromatin in G1 phase of the cell cycle [Iizuka et al., 2006]. In addition, a catalytically inactive form of HBO1 can associate with origins, but is unable to load the MCM2-7 complex efficiently [Miotto and Struhl, 2010]. HBO1 is also required throughout S phase for efficient DNA replication, which indicates it may be important for replication elongation in addition to initiation [Doyon et al., 2006].

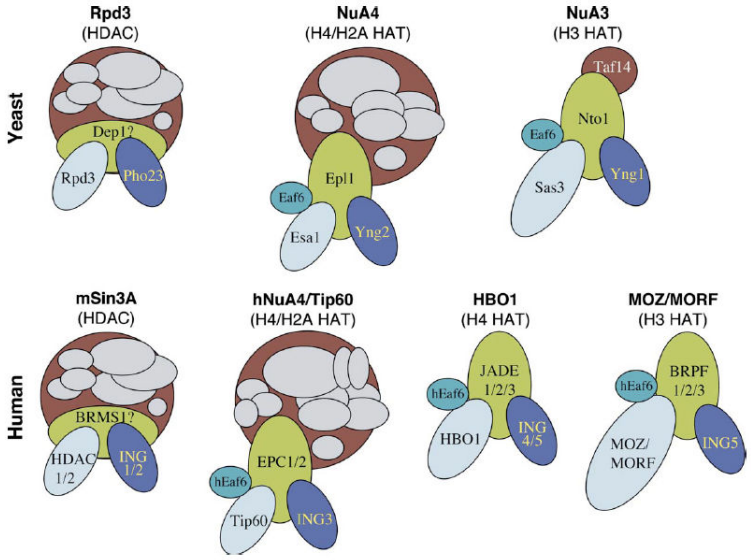

Figure 1.8: Yeast HAT complexes and their human homologues. In humans only those HAT complexes that contain the ING5 subunit are assumed to have a role in replication, but in yeast there may be potential roles for all of the complexes in replication processes. Figure taken from [Doyon et al., 2006]. Top row are the three HAT complexes found in yeast. Bottom row are the four HAT complexes found in humans. Subunits are colour coded to show corresponding homologues, or subunits that perform a similar task. For example, the catalytic subunit of each complex is shown as the oval shape on the bottom left hand side of each diagram.

A role for HDACs in DNA replication is also indicated. The histone deacetylase Rpd3p exists in two separate complexes, RPD3L and RPD3S. The effect of *RPD3* deletion on DNA

replication in *S. cerevisiae* was previously discussed. This effect on DNA replication was further investigated by the Aparicio lab, using a micro array based approach to locate the specific replication origins whose replication timing was altered in *rpd3*Δ strains. This study revealed many replication origins whose initiation was affected by the RPD3L complex, with a small subset influenced by the RPD3S complex [Knott et al., 2009].

An additional modification, characteristic of newly sythesized H3, has been shown to be required for numerous replication associated processes. H3K56 acetylation is cell cycle regulated. Peak activity for the responsible HAT, Rtt109p, occurs during S phase. In addition, the histone chaperone Asf1p stimulates the HAT activity of Rtt109p [Han et al., 2007a], [Driscoll et al., 2007]. H3K56 acetylation is required for efficient DNA damage response, as loss of this mark results in susceptibility to DNA damaging agents and leads to chromosome breaks [Masumoto et al., 2005], [Driscoll et al., 2007], [Han et al., 2007a]. H3K56ac is also required to stabilise replication proteins RFC, DNA polymerase ϵ and PCNA. In addition, H3K56ac prevents recombination at stalled or paused replication forks and is required for accurate chromosome positioning [Han et al., 2007b], [Hiraga et al., 2008]. However, it is not only the presence of this modification that is important; regulation of the removal of H3K56ac is also required. Cells which lack the H3K56 histone deacetylases, Hst3p and Hst4p, also have high levels of DNA damage [Celic et al., 2006], [Celic et al., 2008].

Hence, regulation of histone modifications by HATs and HDACs, both on newly synthesised histones and to maintain chromatin states, may have a role in DNA replication. This role in DNA replication may be to recruit relevant complexes. In summary, the processes of DNA replication could be regulated by both histone modification and remodeling.

1.5.2 Replicating Chromatin

In addition to the DNA sequence, chromatin also has to be replicated during S phase. Histones have to be removed to allow passage of the replication fork and then reassembled with the addition of newly synthesised histones on both branches of replicated DNA behind the fork. Histone modifications may be used to regulate the chromatin assembly of newly synthesised histones. This process is under the control of histone chaperones, which escort newly made histones and recycle "parental" histones at sites of replication. Newly synthesised histones tend to exhibit high levels of acetylated H4K5 and H4K12. These acetylation marks are redundant for effective incorporation into nucleosomes. In fact, to see defects in chromatin assembly it is necessary to mutate H4K5, K8 and K12, in addition to deletion of the H3 tail [Ma et al., 1998]. These modifications are removed some time after deposition and the original modifications of the particular region are presumably restored by using the parental histones as a template [Probst et al., 2009]. Whether this occurs by creating hybrid nucleosomes, or by randomly placing old and new histones on each daughter strand, or by the new daughter strand using the old strand as a histone template is still to be determined; refer to Fig. 1.9 for schematic.

The histone chaperones include Asf1p, which acts as a donor and has been shown to connect with the MCM2-7 complex via a H3-H4 bridge in human cells [Groth et al., 2007]. The authors

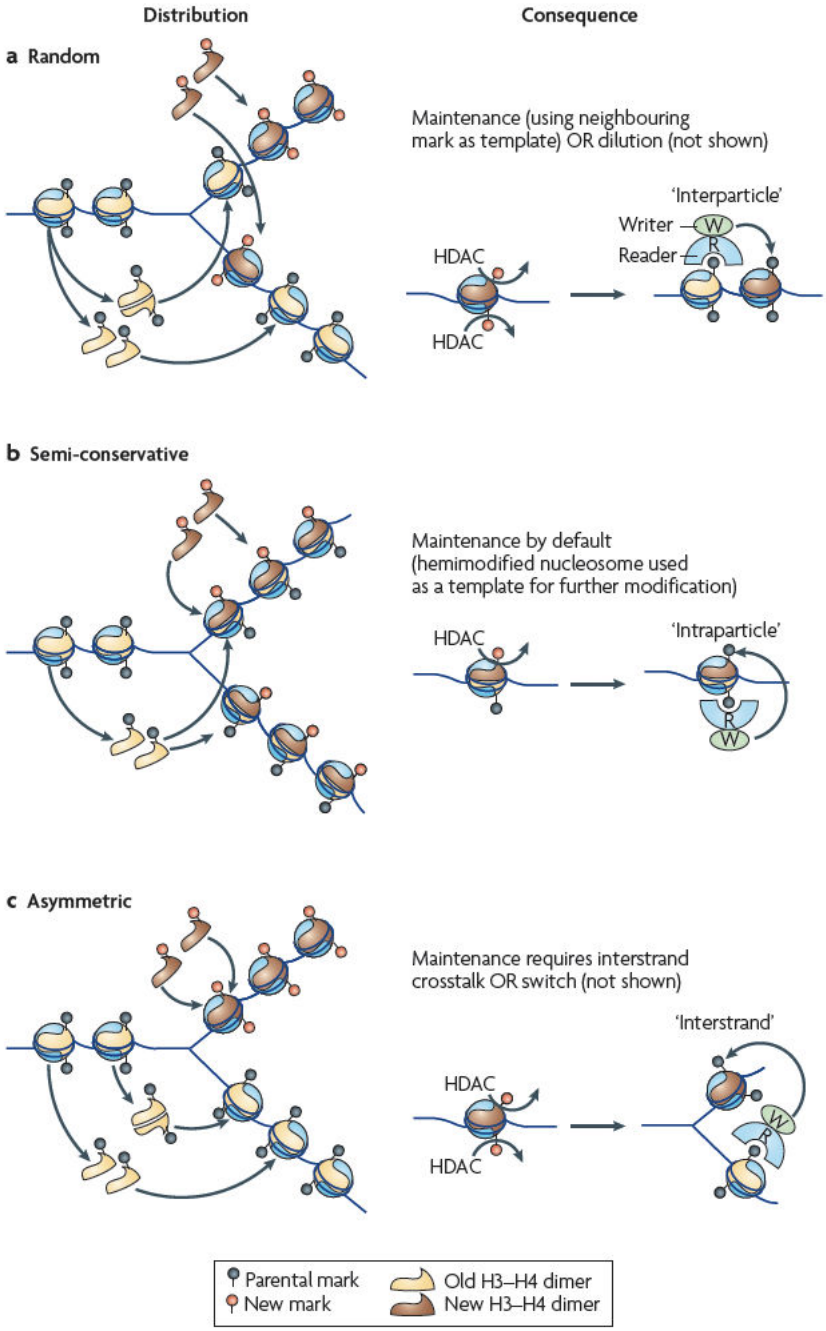

Figure 1.9: Three hypotheses (random, semi-conservative and asymmetric) to describe the pattern of histone redistribution behind the replication fork. In each case the marks on the recycled or newly synthesised histones deposited behind the fork are read by a protein that recruits a chromatin modifier to allow relevant chromatin states to be reproduced. Legend key describes some content of figure. In addition large blue and yellow/orange circles are nucleosomes, blue line is DNA, blue semi circle labelled R is a "reader" of histone modifications and the small green oval labelled W is a "writer" of histone modifications. Figure taken from [Probst et al., 2009].

proposed a model whereby Asf1p functions as a donor of newly synthesised histones and acts at the fork with MCM2-7 to recycle parental histones. An excess of new histones would draw Asf1p away from the fork hence, the MCM2-7/H3-H4/Asf1p partnership functions to regulate the unwinding of DNA with the supply of newly synthesised histones. A second histone chaperone, Caf1p, is placed at the fork via its interaction with PCNA [Shibahara and Stillman, 1999]. Caf1p acts to accept histones as soon as they are displaced from the area in front of the fork (or newly synthesised histones when they are donated by Asf1p) and then deposits them behind the fork. Both of these chaperones act on H3/H4, while the H2A/H2B "chaperone" is proposed to be the FACT complex (made up of Spt16p and Pob3p) with a possible role for Nap1p, reviewed in [Corpet and Almouzni, 2009], [Verreault, 2000].

An additional chaperone, HIRA, is required for replication independent histone turnover in *Xenopus laevis* [Ray-Gallet et al., 2002]. In yeast the Hir proteins can compensate for lack of Caf1p, which suggests a redundant replication deposition role for yeast Hira, reviewed in [Gunjan et al., 2005]. It should be pointed out that both Hira and Asf1p have a role in regulating histone gene transcription [Mousson et al., 2007]. Interestingly Caf1p and Asf1p are thought to act as "buffers" in conditions of excess histones and therefore may have a role in controlling histone levels. However, the main protein identified so far to induce the degradation of excess histones is the checkpoint protein Rad53p, although checkpoint activation is not necessary for this function [Gunjan and Verreault, 2003]. Histone transcription is cell cycle regulated leading to increased levels of histones in S phase [Hereford et al., 1981]. The excess of free histones resulting from checkpoint arrest or the lower replication levels towards the end of S phase are toxic for the cell if not rapidly degraded.

1.6 Protein Complexes that Bind to Modified Histones

As stated in Section 1.5, histone modifications can act to recruit specific complexes to chromatin. These complexes usually contain proteins that can themselves modify or remodel the chromatin, in addition to proteins containing the "recognition" subunit. Proteins that contain bromodomains bind actetylated histones (see next section for details). Proteins containing chromo, tudor, WD40 and PHD domains bind methylated histones; refer to [Lee and Workman, 2007] for a review on HAT complexes that contain these domains. Complexes can contain one or a number of these subunits that presumably direct them to specific regions depending on the affinity of each subunit for its "mark"; refer to Fig. 1.10.

One such multisubunit complex that recognises multiple modifications is the *S. cerevisiae* NuA4 HAT complex. NuA4 acetylates H2A and H4, although its activity can be repressed by H4serine1 phosphorylation [Utley et al., 2005]. NuA4 consists of multiple subunits that include: Arp4p, Eaf1p, Eaf3p, Swc4p, Yaf9p and Yng2p, all of which contain domains that may bind to DNA or chromatin. Eaf1p contains a SANT domain, which is a domain that

binds generally to histone tails [Boyer et al., 2004]. Eaf3p has a chromodomain that binds methylated H3K36 and methylated H3K4 [Xu et al., 2008]. Swc4p also contains a SANT domain in its N terminal region, which is required for an essential function of this protein [Micialkiewicz and Chelstowska, 2008], [Lu et al., 2009]. Yaf9p contains a YEATS domain, which is a domain of unknown function that may also have histone binding properties [Schulze et al., 2009]. Yng2p contains a PHD finger domain, which is a domain known to bind H3K4me2 and H3K4me3 [Shi et al., 2006]. Arp4p is required for binding of phosphorylated H2A as detailed below. These subunits can be common to more than one complex, for example the SWR1 complex shares three of the above subunits: Arp4p, Yaf9p and Swc4p. SWR1 is required for yKu80p binding and NHEJ (non-homologous end joining) during DNA repair [van Attikum et al., 2007]. The Arp4p subunit is also shared by a third complex INO80. INO80 is required for efficient Mec1p dependent checkpoint activation, binding of Mre11p and eviction of H2A variants during DNA repair [van Attikum et al., 2007]. NuA4, SWR1 and the INO80 complex therefore share common subunits and common functions such as histone variant exchange and DNA damage repair.

During DNA damage repair, NuA4 binds to phosphorylated ser129 of H2A through its Arp4p subunit [Downs et al., 2004]. In this case the recruitment of all three complexes (NuA4, SWR and INO80) is dependent on H2A phosphorylation, but the recruitment is temporally regulated with NuA4 recruited first, reviewed in [Clapier and Cairns, 2009]. Despite its requirement for H2A phosphorylation, INO80 complex recruitment is dependent on two of its subunits, Nph10p and Ies3p, that have no known phoshorylation binding properites [Morrison et al., 2004]. This infers that INO80 might be targeted by a second signal, but recruitment may be dependent on a H2A phosphorylation event (possibly even NuA4 binding itself). Both the INO80 and SWR complexes belong to the INO80 family of chromatin remodelers, which along with the SWI/SNF and ISWI family also represent complexes containing multiple modification recognition sites and ATPase domains; see Fig. 1.10.

These complexes are just some of the examples of chromatin remodelers that might be targeted to specific areas of the genome based on histone modifications. One other example is the NuA3 HAT complex which has the TAF14p and Yng1p subunits, which contain a YEATS domain and PHD finger domain respectively.

1.7 Rpd3p-Containing Complexes

The NuA4 HAT complex is required to process DNA double strand breaks. In this same process the Rpd3p-containing HDAC complex, RPD3S, is also involved in accurate repair. Both of these complexes share a common subunit, Eaf3p, that, as stated in Section 1.6, contains a chromodomain and is required for binding to H3K36me. It is possible that competition between these opposing complexes for the same binding substrate allows regulation of their effects [Biswas et al., 2008]. The RPD3S complex may have a higher affinity for the H3K36me3 mark, perhaps due to a stabilising effect of the PHD domain of the Rco1p sub-

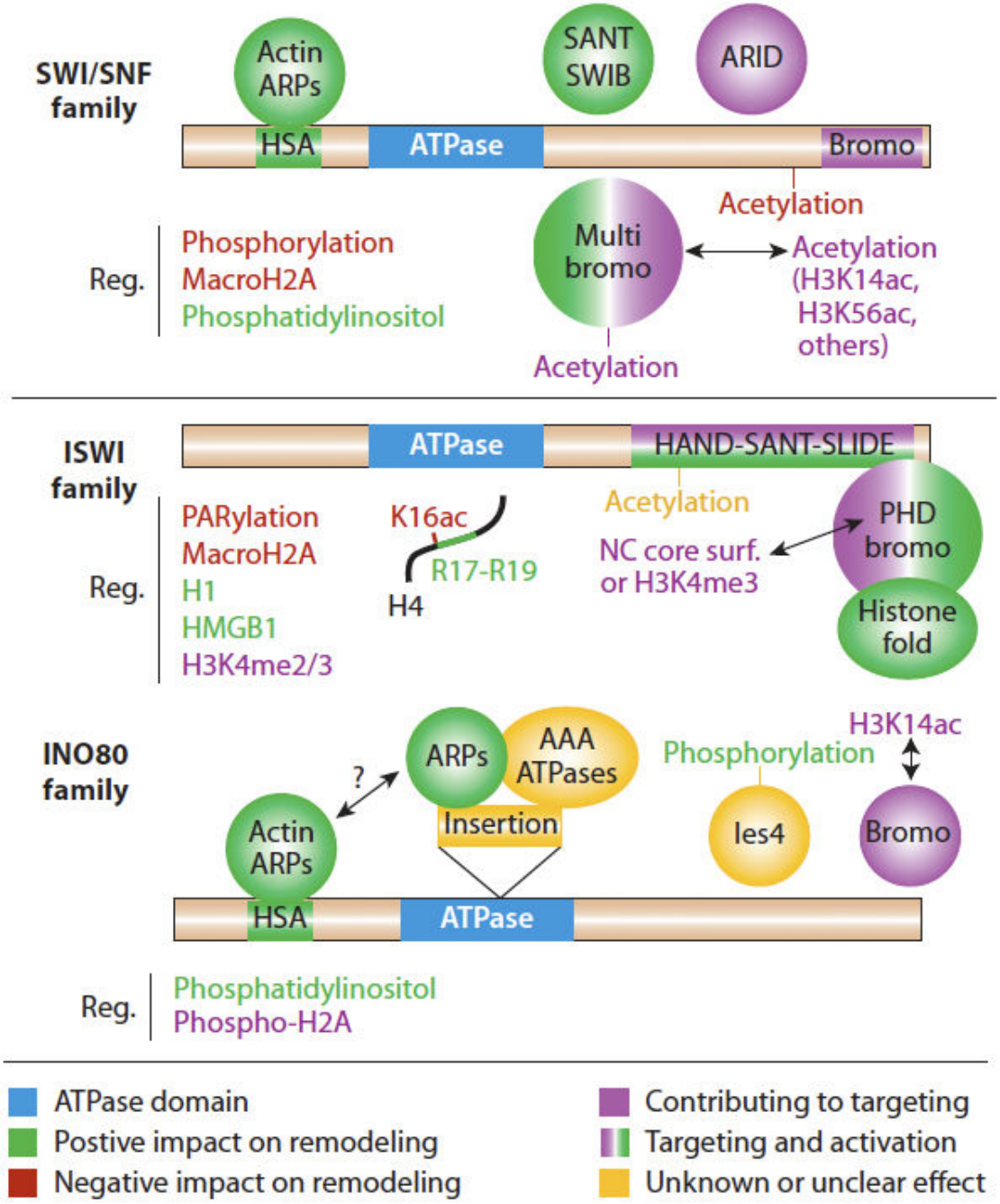

Figure 1.10: Chromatin remodelers and modifiers contain histone modification recognition domains. The figure represents three families of chromatin remodellers; the SWI/SNF family (top), the ISWI family (middle) and the INO80 family (bottom). Legend key describes content of figure, where circles and rectangles describe protein domains present in each family and the writing describes some modifications recognised by these domains. Figure taken from [Clapier and Cairns, 2009].

unit [Li et al., 2007]. When acetylation is required Rpd3p-containing complexes can be sequestered by modulators such as the 14,3,3 proteins [Lottersberger et al., 2007]. NuA4 also has additional subunits that can potentially recognise other modifications, such as H2A phosphorylation and H3K4me (as stated in Section 1.6), and so does not have to rely solely on the H3K36me mark for recruitment. In fact, in DNA DSB repair NuA4 is recruited first through H2Aser129P and leads to increased H4 acetyation, which presumably aids repair by allowing recruitment of the repair and checkpoint proteins [Downs et al., 2004]. A Sin3p/Rpd3p complex is recruited a few hours later and is suggested to compete with NuA4. Sin3/Rpd3 purified complexes were shown to have kinase activity and it is suggested that this activity is supplied by CK2 which phosphorylates H4ser1. This particular mark was linked to decreased NuA4 activity in acetylation of H4 [Utley et al., 2005].

Rpd3p has been implicated in a wide range of functions in addition to its role as a global histone deacetylase and its more targeted role at DSBs. Rpd3p exists in two separate complexes, RPD3L and RPD3S. While they share some subunits, the two complexes have been assigned different roles and a balanced level of each complex is required. For example, mutations affecting just the small or just the large complex are synthetic lethal in combination with *gcn5* mutants, but loss of both complexes restores viability. Mutations of the large complex also show synthetic defects with compromised FACT levels, whilst mutations of the small complex suppress FACT mutants [Biswas et al., 2008]. Again, contradictory to its role in a HDAC, which would suggest a repressive effect on chromatin, deletion of Rpd3p or Sin3p results in enhanced silencing at the "heterochromatic" regions of the *HMR*, telomere and rDNA loci [Sun and Hampsey, 1999]. There is also evidence for a role of Rpd3p in the G2/M checkpoint of the DNA damage response and in response to HU. In checkpoint deficient strains caused by *MEC1* deletion or *RAD9* deletion a further deletion of *RPD3* restores the G2/M checkpoint, increasing survival rates. This increased survival is not due to restoration of the Rad53p dependent checkpoint, but instead relies upon a functioning spindle checkpoint [Scott and Plon, 2003]. Also highlighted in [Scott and Plon, 2003] was a moderate suppression of the lethality of Δ*mec1* strains in HU when *RPD3* was also deleted. However, this suppression only applied at very low levels of HU induction.

Another study also found partial suppression of a HU induced replication defect in *RPD3* deleted strains [Lottersberger et al., 2007]. This time deletion of *RPD3* suppressed the inability to resume replication after HU arrest of a *bmh1/2* (14,3,3 proteins) mutant strain. The authors suggested that the replication defect of the *bmh1/2* mutant strain was caused by a lack of regulation of HAT and HDAC activity. Usually 14,3,3 proteins bind to NuA4 (and presumably act to mediate acetylation) through out the cell cycle, and also bind to Rpd3p (presumably to suppress deacetylation) both during standard S phase and after HU induced replication stalling. Depletion of the Bmh1/2p might therefore lead to mis-targeted NuA4 activity and increased histone deacetylation by Rpd3p in HU. The Bmh1/2p deficient cells showed persistent phosphorylation of the checkpoint protein Rad53p, even after removal of HU. This phospory-lation was restored to an almost WT pattern upon deletion of *RPD3*. Both of the mentioned

studies, [Scott and Plon, 2003] and [Lottersberger et al., 2007], suggest a role for HATs and HDACs, and therefore regulated acetylation, in efficient checkpoint functioning (both S phase and G2/M) through multiple pathways.

The role of Rpd3p that is most interesting for this study, however, is its ability to regulate time of replication origin firing. In addition to the observation that *RPD3* deletion leads to increased acetylation, and subsequent earlier activation of typically late-firing origins [Vogelauer et al., 2002], it was also shown that deletion of *RPD3* suppresses the slower S phase of *CLB5* mutants [Aparicio et al., 2004]. By allowing the late origins to become earlier-firing, the "late" origins no longer require the action of Clb5p-CDK and it is assumed they are now under the control of Clb6p-CDK, as for other earlier firing origins. [Aparicio et al., 2004] also showed that in HU, but not MMS, Δ*rpd3* strains displayed fork structures indicative of activation at both typically early and late-firing origins, this means that the late origins can escape the prolonged inactivation by Rad53p, which is normally identified in the S phase checkpoint. Therefore, the "late" origins that were tested must have fired before the S phase checkpoint is activated, but not before the response activated by MMS treatment. The authors also observed a small, but reproducible, delay in Rad53p phosphorylation in both HU and MMS in the Δ*rpd3* strain compared to WT cells.

Rpd3p-containing complexes can both bind to modifications of certain histone tail residues and deacetylate others, using multiple subunits. It is possible that the increased acetylation observed in a Δ*rpd3* strain is bound by a second complex that, in turn, modifies or remodels the chromatin to allow replication at specific origins in certain stages of S phase.

1.8 Bromodomains

An excellent candidate to read the increased acetylation signal surrounding replication origins and instigate an effect on the replication machinery would be a protein containing a bromodomain. Bromodomains have been shown to bind acetylated histones with increased affinity in both humans and yeast [Dhalluin et al., 1999], [Jacobson et al., 2000], [Owen et al., 2000]. In fact, some bromodomains have been shown to bind specific acetylated residues, such as the preference of the yeast Rsc4p bromodomains to bind acetylated forms of H3K14 [Kasten et al., 2004], and the preference for H4 acetylation of the yeast Bdf1p bromodomain [Matangkasombut and Buratowski, 2003]. Rsc4p contains two tandem bromodomains that are partially redundant, but individually required for viability. A second Bdf protein (Bdf2p) also contains a bromodomain, but while Bdf1p shows preferential binding to acetylated H4, Bdf2p binds equally well to both acetylated and unacetylated H4. The binding efficiency of bromodomains may also be influenced by the amino acid sequence of the histone; the nature of the peptides that surround the acetylated lysine that is bound can be important [Owen et al., 2000]. Proteins that contain bromodomains also tend to function in complexes that are involved in histone modification and remodeling of chromatin, or play a role in transcription [Hassan et al., 2002], [Jacobson et al., 2000].

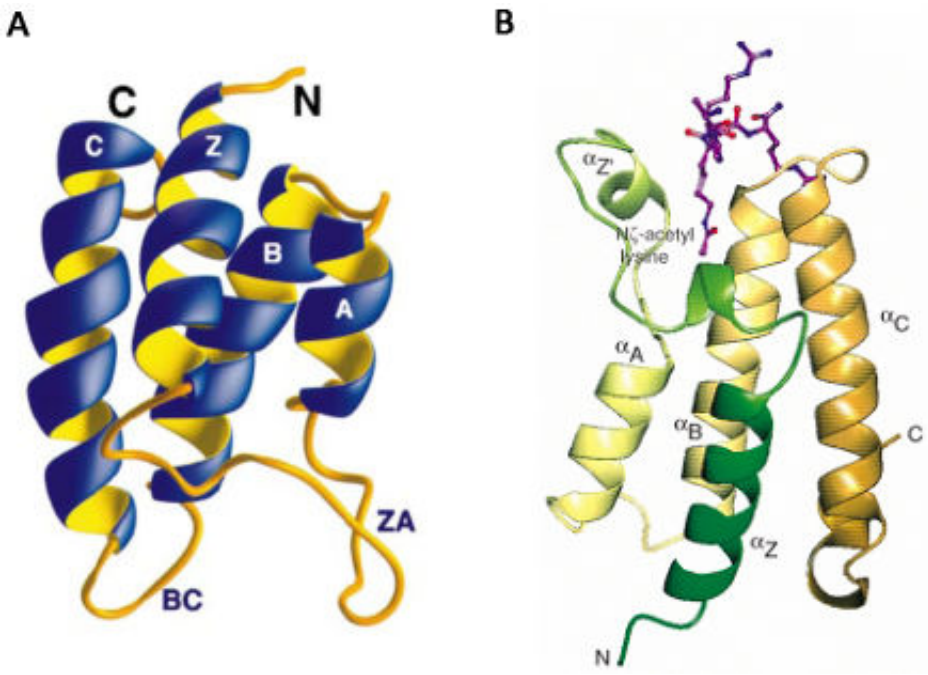

Figure 1.11: Bromodomains. (A): Ribbon structure of the P/CAF bromodomain. C is the carboxyl terminus, N is the amino terminus, C,Z,B and A are helices and BC and ZA are loop structures. The binding pocket of the bromodomain is located between the loop structures. (B): Ribbon structure of the Gcn5p bromodomain binding to Acetyl lysine residue. Description as for (A) except the figure is "upside-down" and the purple structure is a N-acetyl lysine residue binding to the pocket of the bromodomain between the BC and ZA loops. Figures taken from [Dhalluin et al., 1999], [Owen et al., 2000].

The predicted structure of the bromodomain indicates four helices: Z, A, B and C that form a hydrophobic pocket between the ZA and BC loops; refer to Fig. 1.11. The hydrophobic pocket is the N-acetyl lysine binding site and the affinity of N-acetyl lysine binding depends on both conserved residues of the bromodomain, within the hydrophobic pocket, and the residues that follow the acetylated lysine residue on the histone tail [Owen et al., 2000].

In *S. cerevisiae* there are 11 proteins that contain one or more bromodomain. These proteins assemble into five functional complexes. These include: the RSC (remodels the structure of chromatin), SAGA (HAT), and SWI/SNF (chromatin remodeler) complexes, in addition to: Bdf1p, Bdf2p and Yta7p. Yta7p represents a very good candidate to have a role in replication for a number of reasons, which are outlined in the following section.

1.9 Yta7p

The exact functions of Yta7p in *S. cerevisiae* are currently unknown, but Yta7p contains a single bromodomain and two AAA ATPase domains, which, in turn, contain nucleoside triphosphate

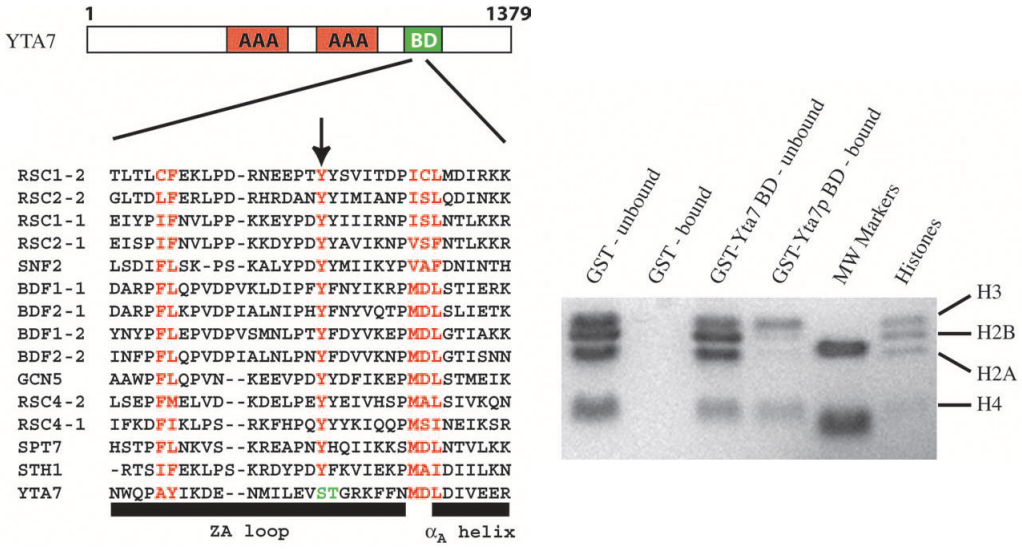

Figure 1.12: Yta7p binds histones. Yta7p contains two AAA ATPase domains and one bromodomain which has a serine/threonine site to replace the highly conserved tyrosine, which is traditionally required for acetlylysine binding. Despite this Yta7p can bind histones H3 and H4 *in vitro*. Left hand side figure: red boxes are ATPase domains, green box is the bromodomain, sequences are the amino acid sequence of the bromodomain for the *S. cerevisiae* protein indicated to the left of each line, red letters are conserved residues. Right hand side figure: IP against histone proteins using a GST-Yta7bromodomain fusion protein. Lanes 1-2 are GST. Lanes 3-4 are GST- Yta7BD. Lane 5 is a molecular marker. Lane 6 is histone proteins as INPUT. Figures taken from [Jambunathan et al., 2005].

hydrolases. The bromodomain of Yta7p is the least conserved among all of the bromodomains present in yeast; refer to Fig. 1.12. However, the bromodomain has been tested for *in vitro* binding of histones and was shown to bind both H3 and H4, [Jambunathan et al., 2005].

Yta7p was purified, *in vivo*, in a complex with the H2A, H2B, H3 and H4 histones, along with several proteins involved in replication and transcription processes; see Fig. 1.13 for a description. These proteins potentially form one large chromatin remodeling complex that prevents spreading of the silent chromatin to surrounding regions. Thus this complex acts as a boundary element to separate active and silent chromatin; see Fig. 1.13. This was the only function attributed to Yta7p at the beginning of this thesis [Jambunathan et al., 2005], [Tackett et al., 2005]. However, Yta7p is also a potential substrate for phosphorylation by Cdk1p [Ubersax et al., 2003], interacts with Rad53p [Smolka et al., 2005] and complexes with an S phase expressed protein (encoded for by *YLR455W*). Added to the fact that it binds histones, Yta7p is an excellent candidate to bind to hyperacetylated histones at replication origins and have a subsequent involvement in replication processes. What little is known about Yta7p ties it to other major replication effectors. There is also evidence, provided by studies in mammalian cells, that ISWI complexes (one component of the "boundary" complex shown in Fig.1.13) are required for replication through

heterochromatin [Collins et al., 2002].

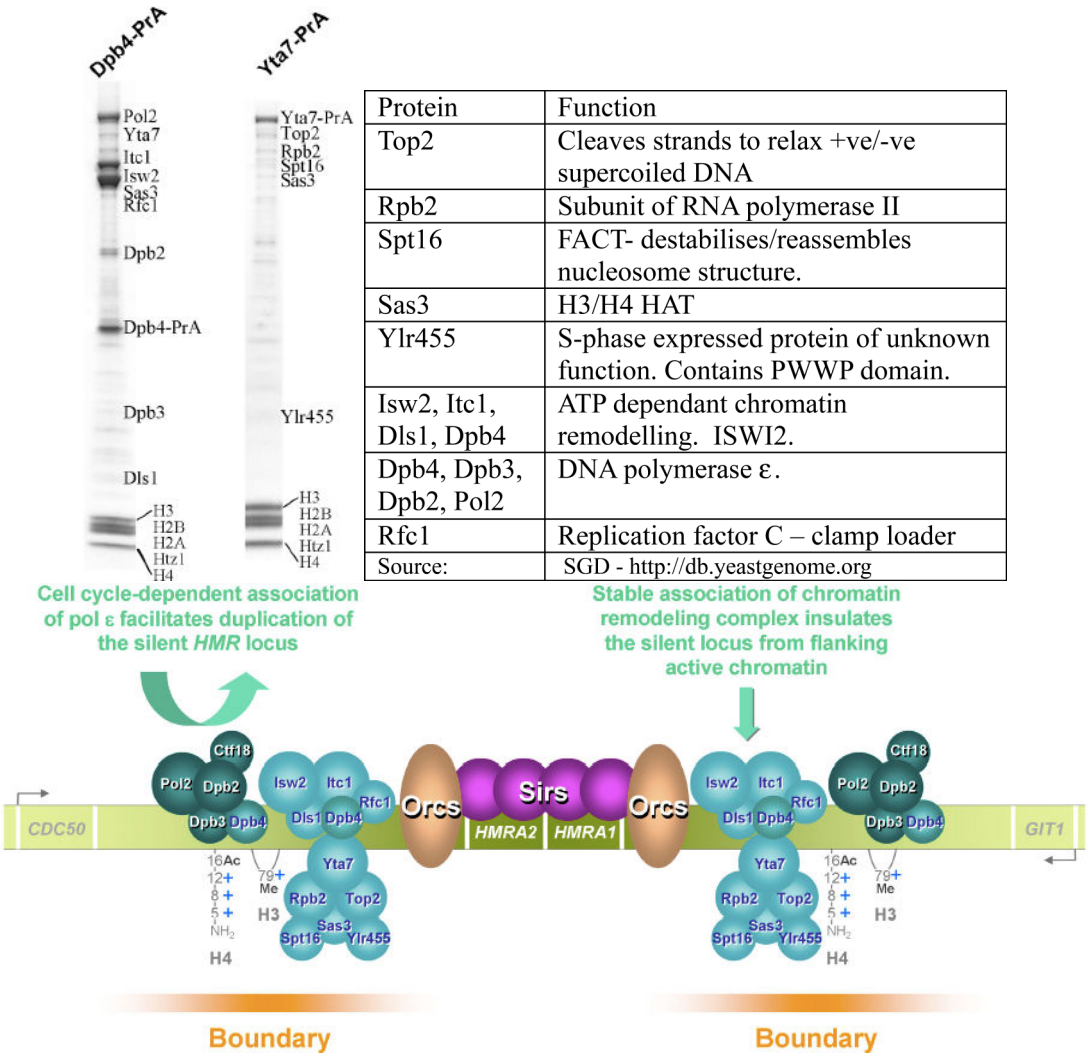

Protein	Function
Top2	Cleaves strands to relax +ve/-ve supercoiled DNA
Rpb2	Subunit of RNA polymerase II
Spt16	FACT- destabilises/reassembles nucleosome structure.
Sas3	H3/H4 HAT
Ylr455	S-phase expressed protein of unknown function. Contains PWWP domain.
Isw2, Itc1, Dls1, Dpb4	ATP dependant chromatin remodelling. ISWI2.
Dpb4, Dpb3, Dpb2, Pol2	DNA polymerase ε.
Rfc1	Replication factor C – clamp loader
Source:	SGD - http://db.yeastgenome.org

Figure 1.13: Yta7p complex. Yta7p can be precipitated in a large potential complex and is proposed to act as a boundary element to separate active and inactive chromatin. Figure includes; mass spectrometry results (left hand side) for proteins precipitated with Dpb4p-Protein A (left) or Yta7p-Protein A (right), a table (right hand side) highlighting functions of proteins that were identified in the boundary complex and a proposed model (bottom) for complex formation and function at the *HMR* boundary. The region of the genome and the proteins that are involved in the model are labelled in the figure. Figure taken/adapted from [Tackett et al., 2005].

1.10 Yta7p Complexes with Proteins Already Known to have a Role in DNA Replication

1.10.1 Spt16p

The *S. cerevisiae* FACT complex consists of two subunits: Spt16p and Pob3p. FACT is required for transcriptional elongation through chromatin by allowing passage of RNA Polymerase II [Orphanides et al., 1998]. In addition, both Spt16p and Pob3p have also been identified to have potential roles in DNA replication processes [Schlesinger and Formosa, 2000], [Wittmeyer et al., 1999]. The function of FACT is suggested to be disruption of nucleosomes through its interaction with the H2A/H2B dimer. It remains to be identified whether FACT acts to remove H2A/H2B from the nucleosome or if there is just a transformation to a looser state. The role for FACT in DNA replication is hypothesised to be to allow access of the replication machinery to replication origins/forks, potentially in both the initiation and elongation steps. Yeast FACT has been purified in a complex with DNA polymerase α and human FACT is associated with the MCM2-7 helicase complex, putting it in a good position to act at replication origins/forks, [Wittmeyer et al., 1999], [Tan et al., 2006]. Recently a "Replisome Progression Complex" has been purified and was shown to contain MCM2-7, Cdc45p and GINS, Mrc1p, Tof1p, Csm3p, Ctf4p and both components of FACT [Aparicio et al., 2006].

The complete role of FACT as a complex may be more complicated than simple disruption of nucleosomes. The two subunits of FACT have shown opposing genetic interactions, some of which are allele specific, which indicates that different mutations affect different functions of the proteins [Formosa et al., 2002]. *spt16* mutant strains show sensitivity to an increased ratio of H3/H4 levels over H2A/H2B, whereas *Pob3* mutants are sensitive to the reverse ratio. *spt16* phenotypes were also enhanced when combined with deletion/mutation of the HATs *SAS3*, *GCN5*, and *ESA1*. Further to this, the authors tested the histone modifications that are produced by Sas3p, Gcn5p and Esa1p; *spt16* mutant strains displayed growth defects when combined with H4K5 and K12 mutations to arginine, which cannot be acetylated. Again, there was a difference observed in *Pob3* mutants as these were more sensitive to changes in H4K8 and K16 mutation.

Directly related to replication, mutations in either subunit of FACT can lead to G1 arrest or delayed G1-S transition, which are followed by a prolonged S phase. Mutations in *SPT16* or *POB3* can be sensitive to HU. The G1 arrest of cells in an *spt16* mutant was accounted for by the fact that these mutants are unable to synthesise appropriate levels of cyclins [Rowley et al., 1991]. However, an effect on transcriptional control was not confirmed for the *Pob3* mutant phenotype [Schlesinger and Formosa, 2000].

1.10.2 Sas3p

Sas3p is the catalytic domain of the *S. cerevisiae* HAT complex NuA3 [John et al., 2000]. Sas3p acetylates mainly H3 tail residues and its role in transcription can be either activating or repressive depending on gene context. Sas3p has been shown to have both a physical and genetic interaction with the Spt16p subunit of FACT and it is proposed that this interaction facilitates the elongation function of FACT in both transcriptional and replication processes [John et al., 2000].

The MOZ/MORF H3 HAT complex shares similar subunits with yeast NuA3 and is suggested to be the human homologue. However, one of the subunits, BRPF1/2/3, contains a bromodomain and PHD finger domain [Ullah et al., 2008]. NuA3 does not have a bromodomain but, as previously stated, Sas3p is present in the complex purified by Tackett and colleagues; shown in Fig. 1.13. In this complex there is a bromodomain provided by Yta7p. As stated in section 1.5, multiple potential roles exist for HATs in different aspects of DNA replication in both humans and yeast. Given its interaction with FACT and the possible role in DNA replication of its human homologue, Sas3p may also be involved in replication processes.

1.10.3 Top2p

Top2p and Top1p are partially overlapping DNA topoisomerases that function to resolve topological constraints present at structures such as the replication fork. Unwinding of the DNA helix causes torsion that is relieved by cleavage of the DNA. Top1p acts on single strands to resolve tension, by allowing one strand to rotate around the other. Top2p has the ability to cleave both strands, which allows the resolution of more complicated structures (reviewed in [Wang, 1996]. *Top1*Δ has no effect on S phase progression. *top2* mutated cells also display WT S phase, but have subsequent problems that lead to G1 arrest caused by activation of the DNA damage checkpoint at the M-G1 transition. Analysis of the combined deletion of *TOP1* and mutation of *TOP2* at different stages of the cell cycle however, led to the observation that the topoisomerases co-operate to allow completion of S phase by facilitating replication fork stability. The topoisomerases also act to prevent DNA damage and the resulting checkpoint activation. Both proteins are located at active replication forks during S phase, whilst Top2p also has a number of non replication related binding regions through out S phase [Bermejo et al., 2007].

1.10.4 Dpb4p

Dpb4p is a subunit of both DNA polymerase ϵ and the ISWI2/yCHRAC chromatin remodeling complex [Iida and Araki, 2004]. DNA polymerase ϵ is the polymerase involved in leading strand DNA synthesis. The other proteins that were pulled down with Yta7p in the Dpb4p-Protein A precipitation, Dpb3p, Dpb2p and Pol2p (the catalytic subunit), are also subunits of DNA polymerase ϵ.

1.11 Summary and Aims

DNA replication is a fundamental process with multiple layers of regulation. This regulation ensures that DNA is replicated once, in an accurate and timely manner, within the constraints of S phase. Mechanisms to cope with DNA damage, replication fork stalling, depletion of histones or dNTPs and incomplete synthesis all function to promote the accuracy of this process. Replication occurs in a step wise manner, from multiple sites across the genome. The replication process begins with PreRC formation and requires the concerted regulation of many proteins and complexes. The whole process has to occur within the context of chromatin, which is itself an additional regulator of the timing of DNA replication. The identified temporal programme of DNA replication allows replication origins to be grouped into those that activate early in S phase and those that activate late in S phase. Specifically, the importance of histone acetylation has been highlighted for its ability to affect the timing profile of the replication program. How increased histone acetylation at replication origins advances their time of firing is an intriguing question. Multiple proteins/complexes have been identified that bind to histone modifications; this binding is implicated in regulating a number of cellular processes, such as DNA damage repair. It is, therefore, possible that histone acetylation at origins acts to recruit a protein that can affect activation of those origins. Given the identification of the bromodomain as a histone binding module that shows preference for the acetylated state, a protein containing such a domain would be a good candidate for recruitment to origins. Histone modifications generally function to recruit specific chromatin remodelers that can alter the structure of chromatin. The role that various chromatin remodelers and modifiers could play in DNA replication is beginning to be appreciated. Any candidate protein could use chromatin remodeling properties to alter the "availability" of the origin for binding by replication proteins. Yta7p represents one such candidate.

The aim of this thesis was therefore to establish which, if any, protein that contains a bromodomain has a role in DNA replication, beginning with Yta7p. Any such role would be further investigated, with the aim to uncover the mechanism that allows increased acetylation at replication origins to translate to earlier firing of that origin.

Chapter 2

Materials and Methods

2.1 Materials

Yeast extract, peptone, yeast nitrogen base and agar were supplied by Becton Dickinson. All other materials (chemicals and media) were supplied by SIGMA unless specified.

2.1.1 Strains

All strains used were *S. cerevisiae*, derived from a W303a background.

Name	**Description**	**Derived from**	**Reference**
YDS2	*MAT***a**, *ade2-1*, *can1-100*, *his3-*Δ*200,leu2-3,112*,*trp1*, and *ura3-52*	W303a	[Laman et al., 1995]
MMY001	*bar1::HIS3*	YDS2	[Vogelauer et al., 2002]
MMY002	*bar1::HIS3, rpd3::LEU*	MMY001	[Vogelauer et al., 2002]
MMY033	*bar1::HIS3, ura3::LEU2*, Cdc45-FLAG(NAT)	MMY001	[Vogelauer et al., 2002]
MVY51	*rpd3::TRP1*	MMY033	[Vogelauer et al., 2002]
MVY63	*yta7::HYG*	MMY033	This study
MVY64	*rpd3::TRP1, yta7::HYG*	MVY51	This study
MMY013	*rpd3::LEU, hda1::KANMX*	MMY001	Unpublished
YB556	WT (*Cdc7*^{ts})		[Zou and Stillman, 2000]
MVY71	*yta7::HYG*	YB556	This study
MVY72	*rpd3::KANMX*	YB556	This study
MVY73	*yta7::HYG, rpd3::KANMX*	YB556	This study
MVY104	Yta7-FLAG(NAT)	MMY001	This study

Name	**Description**	**Derived from**	**Reference**
MVY105	Yta7-FLAG(NAT), *rpd3::LEU*	MMY002	This study
MVY125	Mcm2-FLAG(NAT)	MMY001	This study
KH174	*MAT*α, *bar1*Δ, *mad3::URA3*	W303	Supplied by K.Hardwick
MVY139	Ccd45-13MYC(TRP)	MVY125	This study
MVY155	*MAT*α, *bar1::HIS3*, Cdc45-13MYC(TRP)	KH174/ MVY139 cross	This study
MVY209 (MVY001 replacement)	*bar1::HIS3*	MVY105/ MVY155 cross	This study
MVY210 (MVY104 replacement)	*bar1::HIS3*, Yta7-FLAG(NAT)	MVY105/ MVY155 cross	This study
MVY211 (MVY105 replacement)	*bar1::HIS3*, Yta7-FLAG(NAT), *rpd3::LEU*	MVY105/ MVY155 cross	This study
MVY212	*yta7::URA*	MVY209	This study
MVY213	*ura::yta7*Δ*BD*	MVY212	This study
MVY214	*ura::yta7*Δ*BD*-FLAG(NAT)	MVY213	This study
MVY215	*rpd3::TRP*	MVY209	This study
MVY216	*ura::yta7*Δ*BD, rpd3::TRP*	MVY213	This study
MVY 168	*yta7::HYG*	MMY001	This study
MVY179	Spt16-FLAG(NAT)	MMY001	This study
MVY178	Sas3-FLAG(NAT)	MMY001	This study
MVY182	Top2-FLAG(NAT)	MMY001	This study
MVY180	Spt16-FLAG(NAT), *yta7::HYG*	MVY168	This study
MVY183	Sas3-FLAG(NAT), *yta7::HYG*	MVY168	This study
MVY177	Top2-FLAG(NAT), *yta7::HYG*	MVY168	This study
NK1a	*MAT***a** *ura3-52 trp1-289 leu2-3,112 bar1::LEU2*	A364a	[Makovets et al., 2004]
NK1542α	*MAT*α *sst2::KAN*	S228c	Supplied by S. Makovets

Table 2.1: Strains used in this study.

2.1.2 Primers

Oligo	Sequence	Reference
Building/confirming strains		
YTA7 F1	TGCAGCTGAACTTGTTGAGGCATTAGCCGCTGAGGAA TTTTTTTCTGCCTCGGATCCCCGGGTTAATTAA	This study
YTA7 R1	ATGAACTAACTACATTTAAGAATTATATAAACATTATG GACTCCTGCTTAGAATTCGAGCTCGTTTAAAC	This study
YTA7 C1int	ACACAACGGAACTGATACAGGC	This study
YTA7 C2	ACGTATGCCAGAACAGTGACTG	This study
YTA7 F2	CATGGGATAAAACAGGAACTGTCGATGAAATAATAAA ATTTTTATCTGAACGGATCCCCGGGTTAATTAA	This study
clonNAT intR	ATGTTCGGATGTGATGTGAG	This study
Hygro intR	ACAATTCAACGCGTCTGTGAG	This study
Hyg intF1	TCGTATGTGAATGCTGGTC	This study
Rpd3 F1	ATTTGTAAATATATGTCCCATATTTTGCCTTGAAATTT ATCTTTTTATTTCGGATCCCCGGGTTAATTAA	This study
Rpd3 R1	TTCTTTTGTTTCACATTATTTATATTCGTATATACTTC CAACTCTTTTTTGAATTCGAGCTCGTTTAAAC	This study
Rpd3 C1upF	CTCAGCATAACGAATTGACGGGAG	This study
Rpd3 C2intR	GAACATGTCATGACACGATCCG	This study
TRP1 intR1	TCTTGCCACGACTCATCTCCATGC	This study
TRP1 intF	CTGCAACATACTACTCAGTGCAGC	This study
KanMX intR2	TCAGAAACAACTCTGGCCGATC	This study
MCM2 F2	GTGTTCGCCGCCAACTCCGCAGGTCTTTCGCAATTTA TACCTTGGGTCACCGGATCCCCGGGTTAATTAA	This study
MCM2 R1	AGAATTTTTTATCTTCATATCCAGATATTCGTAGGAAT AACAAAGTTTTAGAATTCGAGCTCGTTTAAAC	This study
Spt16 F2	AATTAGAGAAAAAGGCTGCTAGGGCTGATAGGGGTGC AAACTTTAGAGATCGGATCCCCGGGTTAATTAA	This study
Spt16 R1	TGTCAGATCAAGGTCTTGCTGGTGAAACCCAGTAAGT GTTATAAAGTCTAGAATTCGAGCTCGTTTAAAC	This study
Spt16 C1	AGACGACGTAAGTGATGAAAGCGC	This study
Spt16 C2	ACGCAAACGTCCTATGACCTTGAC	This study
Top2 F2	ATGATGAAGAGGAAAACCAAGGATCAGATGTTTCGTT CAATGAAGAGGATCGGATCCCCGGGTTAATTAA	This study
Top2 R1	GATATAAACATATAAAAAGAATGGCGCTTTCTCTGGAT AAATATTATTCAGAATTCGAGCTCGTTTAAAC	This study
Top2 C1	CGATCAAGGAGACAAAGATCGTCG	This study

Oligo	Sequence	Reference
Top2 C2	CTCGAAGAATTTTCTCGGGCAG	This study
Sas3 F2	TCAGAAAAAGAAGAAAAATAACTCTAATAGAGGATGA CGAAGAACGGATCCCCGGGTTAATTAA	This study
Sas3 R1	TTACATGTATATGCTTATATCCAATATATACCCATCGCC GCTTAGAATTCGAGCTCGTTTAAAC	This study
Sas3 C1	CCCTTGATGATGACATTGAGGATG	This study
Sas3 C2	TAATCGCACCCACACATGTACACAC	This study
yta7 URA3 F2	GTATCACCGCACGAAAACGCCAGAACGAACGAAGAGC TTACTTAATCGGATCCCCGGGTTAAATTAA	This study
yta7 URA3 R2	ATTTTTGCAACGGACGAATGAACATCTTCTAATTGAG AAACCGTAATCGATGAATTCGAGCTCGTTTAAAC	This study
URA3alb Int F	ACATCATCTGCCCAGATGCGAA	This study
Cdc45 F2	GTGAAGATCTTTCACCATTCCTGGAGAAGCTGACCTT GAGTGGATTGTTACGGATCCCCGGGTTAATTA	This study
Cdc45 R1	ATATTCATATGCTGGTATATATGTACGACTAAATAATAT AAATTTGATTAGAATTCGAGCTCGTTTAAAC	This study
Cdc45 CintF	ACTCTTGGATATCGTGGGTC	This study
Cdc45 CdownR	GAAACAACTTGCCTTCGTTC	This study
Radioactive PCR		
HHF2 upF	AGCCATAGCCGTGATTGTGCGT	This study
HHF2 upR	AACTCTCGGTCTAGTACCACT	This study
HTA1C1 Xu	TTTTCGCGGAAGAAAGGGTGCAAC	[Xu et al., 2005]
HTA1C2 Xu	ACGGGCGTTTCTTCAACAACGACG	[Xu et al., 2005]
His2 ORF A	TCTCTGGTGATTGGCTTTCCTC	This study
His2 ORF B	ATACGTCCGCATTAAGAAAGCGCC	This study
TEL1A	GCGTAACAAAGCCATAATGCCTCC	Vogelauer[1]
TEL1B	CTCGTTAGGATCACGTTCGAATCC	Vogelauer[1]
ARS603A	CATAGGTTAAATAGGACGTTCTCC	Vogelauer[1]
ARS603B1	CATTTCTCAATTTCGAGGC	Vogelauer[1]
ARS607A	GTGGTGATATAAACACTACATTCGC	Vogelauer[1]
ARS607B	GCTTTCTAGTACCTACTGTGCCG	Vogelauer[1]
ARS305A	CAGTTTCATGTACTGTCCGGTGTG	Vogelauer[1]
ARS305B	CATCAAACTCCGTTTTTAGCCCCC	Vogelauer[1]
ARS1412A	TTCAGACGTGGAATGGTGGGAAAG	Vogelauer[1]

[1] [Vogelauer et al., 2002]

Oligo	Sequence	Reference
ARS1412B	TCCTCTATAATGGCATCTTCCCCC	Vogelauer[2]
ARS609A	TCTTGTCTGGAGGATCAATCGTCC	Vogelauer[2]
ARS609B	TCCAGCACCAAAAGCTACATCACC	Vogelauer[2]
ARS501A	CTTTTTTAATGAAGATGACATTGCTCC	Vogelauer[2]
ARS501B	GATGATGATGAGGAGCTCCAATC	Vogelauer[2]
Yta7-LR-PCR		
Yta7 Seq1_ALT	ACGGTCTATTTCTCTCTTCTCGC	This study
Yta7 Seq Reverse 2	CTAATGGATCGAGGTCTGCA	This study
Yta7 Seq2	GCGCATGATCCAGAAGAAGATGA	This study
Yta7 Seq Reverse 3	CTACCAGTAGATCTCGCAGATGA	This study
Yta7 Seq5	ATGGCAAGAGCGTTAGCAGCA	This study
Yta7 Seq Reverse 4	TGGAGCTGCGTTTGAAGTTAC	This study
Yta7 Seq8	ATACAGTGGAGAGGAAGAAGA	This study
Yta7 Seq Reverse 5	GTGGTTATCTCTGACGTGCA	This study
Yta7 Seq10	AATGGTGAGCCACTGTCTGA	This study
Yta7 Seq Reverse 6	CGGACGAATGAACATCTTCT	This study
Yta7 Seq13 (yta7 C1 int)	ACACAACGGAACTGATACAGGC	This study
YTA7 C2	ACGTATGCCAGAACAGTGACTG	This study
Yta7-Sequencing		
Yta7 Seq1_ALT	ACGGTCTATTTCTCTCTTCTCGC	This study
Yta7 Seq1	GTGCAGAAAGAACATGGCA	This study
Yta7 Seq2	GCGCATGATCCAGAAGAAGATGA	This study
Yta7 Seq3	CGATGAGAATGATAATAGCAGGA	This study
Yta7 Seq4	GGTGGCAATGACGTAACTACA	This study
Yta7 Seq5	ATGGCAAGAGCGTTAGCAGCA	This study
Yta7 Seq6	TACCTGATGTTAAAGCACGT	This study
Yta7 Seq8	ATACAGTGGAGAGGAAGAAGA	This study
Yta7 Seq9	AGACAGCCCTCAGTTGTATT	This study

[2] [Vogelauer et al., 2002]

Oligo	Sequence	Reference
Yta7 Seq10	AATGGTGAGCCACTGTCTGA	This study
Yta7 Seq12	CTATCAATACAGCCTCTATCGT	This study
Yta7 Seq13 (yta7 C1 int)	ACACAACGGAACTGATACAGGC	This study
Yta7 Seq14	GCTTAATCGAACACTGTCAGA	This study
Q PCR		
ARS607a SP	TTCTCCAAATGTGGTGATATAAACACTACATTCGC	This study
ARS607a ASP	TCCAGATCTAGTTTTTTAAAACTTGATCCCAACGT	This study
ARS1412a SP	TCTCTTTTTTTTTTTTTTTTTTCAGACGTGGAATG	This study
ARS1412a ASP	TCATGTATTTTTTAACTTTTAGCCGCGGTCA	This study
TEL6 SP	ACAACCACTCAAAGAGAAATTTACTGGAAGATTCG	This study
TEL6 ASP	TTATGGCTTTGTTACGCTTGCACTTGAAAA	This study
ASC1(2) SP	CAACGGTTGGGTCACATCTTTG	Supplied by J.Beggs
ASC1(2) ASP	AGACAAAGCGTAAGCACCGTCA	Supplied by J.Beggs
CHR8 NO ORF SP	CATGGTCAAAATAGTCAATAAAAAACGCCCAGAAA	This study
CHR8 NO ORF ASP	CCCCATTTGGAAGGAATTAGGAAATTATTTTGTG	This study

Table 2.2: Primers used in this study.

2.1.3 Plasmids

Plasmid Name	Description	Reference
pAG32	Deletion set: HYG	[Goldstein and McCusker, 1999]
pAG60	Deletion set: URA	[Goldstein et al., 1999]
pFA6a- TRP1	Longtine set: TRP1	[Longtine et al., 1998]
pFA6a- KanMX6	Longtine set: KanMX6	[Longtine et al., 1998]
pFA6a- 13MYC TRP1	Longtine set: 13MYC TRP1	[Longtine et al., 1998]
pBSK	YGR270w minus bromodomain, ordered from ATG Biosynthesis	This study
FLAG-NAT	3xFLAG NAT	Supplied by A. Kagansky

Table 2.3: Plasmids used in this study.

2.1.4 Media

Liquid YPDA

1% (w/v) yeast extract, 2% (w/v) peptone, 2% (w/v) glucose and 0.005% (w/v) adenine.

YPD plates

1% (w/v) yeast extract, 2% (w/v) peptone, 2% (w/v) bactoagar and 2% (w/v) glucose.

Selection Plates

YPD plates plus 100mM Hydroxyurea.
YPD plates plus 0.012% (w/v) Methyl Methanesulfonate (Fluka).
YPD plates plus 100μg/ml ClonNAT (Werner Bioagents).
YPD plates plus 300μg/ml Hygromycin (Roche).
YPD plates plus 200μg/ml G418 (Gibco).

Amino acid drop out plates

0.15% (w/v) yeast nitrogen base, 0.5% (w/v) ammonium sulphate, 2% (w/v) bactoagar, amino acid drop out mixture added according to manufacturers instructions (Formedium) and 2% (w/v) glucose.

5-Fluoroorotic Acid plates (5-FOA)

URA- amino acid drop out plate plus 0.005% (w/v) uracil and 500μg/ml 5-FOA (Melford).

LBamp plates

LB plus 100μg/ml ampicillin, supplied in House.

Sporulation Plates

0.67% (w/v) yeast nitrogen base, 2% (w/v) bactoagar and 2% (w/v) KoAc.

Minimum Plates

0.67% (w/v) yeast nitrogen base, 2% (w/v) bactoagar and 2% (w/v) glucose.

2.2 Methods

2.2.1 Construction of Strains

Amplification of Gene Deletion Fragments/Protein Tagging Fragments

Primers

Primers were designed for gene deletion that contained 50bp homology with the upstream and downstream sequence of the gene of interest; in addition primers contained a 20bp Longtine constant sequence (blue font in Table 2.2) to amplify selection markers from plasmids for transformation. For protein tagging forward primers contained 50bp homology to the 5′ region of the gene of interest, prior to the stop codon, and the 20bp constant sequence. Reverse primers contained 50bp homology to the sequence directly downstream of the gene of interest, including the stop codon, plus the 20bp Longtine constant sequence to amplify a plasmid containing 3xFLAG and a NAT resistance cassette (Plasmid Supplied by A. Kagansky); refer to Table 2.2 for sequences.

Plasmid Isolation

Plasmids, shown in Table 2.3, that contain selective markers or a 3xFLAG tag were transformed into SURE2 competent cells (provided by Stancheva and Schirmer labs). After heat shock the cells were grown at 37°C in LB containing 50mg/ml ampicillin for one hour and then plated to LB amp plates and grown at 37°C overnight. Qiagen midi prep was performed as per the manufacturers instructions.

PCR

All PCR was performed on a PTC100 Peltier Thermal Cycler GRI unless specified. Gene deletion fragments were amplified using 200ng plasmid DNA, 1x PCR buffer (50mM KCl, 10mM Tris pH9 and 0.1% (v/v) Triton X), 50mM MgCl2, 1μM each of forward and reverse primers (Eurofins MWG), 0.8mM dNTPs (Promega), 1x BSA (NEB), 9 U Taq DNA polymerase (contribution of Stancheva lab, made in house), 2 U Vent polymerase (NEB) and sterile water to a total volume of 200μl. PCR programme consisted of an initial denaturing step at 96°C for 30 secs, with the addition of polymerase following a cooling to 10°C. Cycling was performed 32 times with a denaturation step at 95°C for 30 secs, an annealing step at 60°C for 1min and an elongation step at 72 °C for 2 mins and 30 secs. The programme was ended with final elongation at 72°C for 10 mins.

Conditions to generate protein tagging fragments were optimised for each primer pair; refer to Table 2.2 for sequences. The protocol was modified from [Goldstein and McCusker, 1999]. The Yta7-FLAG fragment reactions required 40ng plasmid DNA, 1x PCR buffer (50mM KCl, 10mM Tris pH9 and 0.1% (v/v) Triton X), 10mM Tris pH 8.5, 1x BSA (NEB), 1.5mM MgCl2, 0.8mM dNTPs (Promega), 0.5μM each forward and reverse primer (Eurofins MWG), 5% (v/v) DMSO, 9 U Taq DNA polymerase (Stancheva lab), 6 U Vent DNA polymerase (NEB) and sterile water to a total volume of 200μl. For Top2-FLAG the reactions were as above, but with 2μM of each primer. For both Spt16-FLAG and Sas3-FLAG the reactions were as for Top2-FLAG, but with only 0.75mM MgCl2 and 18 U Taq DNA polymerase. The PCR programme was identical for all 4 fragments and consisted of a 94°C hot start for 2 mins, addition of DNA polymerase at 10°C, then 30 cycles of 94°C for 1 min, 55°C for 1 min and 72°C for 3 mins, with a final elongation step of 72°C for 20 mins.

Extraction and Confirmation of PCR Fragments

Each fragment was extracted using standard phenol chloroform procedure and salt precipitation and re-suspended in 30μl TE 1x pH8. The fragments were visualised for approximate concentration and checked for size on a 1% (w/v) agarose gel in 1x TBE (90mM Tris, 90mM Boric acid and 2.5mM EDTA) with 1kb DNA ladder (Fermentas).

Transformation of Gene Deletion/Tagging Fragments

Transformation

Yeast transformation was via the Li Ac method, adapted from [Gietz and Woods, 2002]. Relevant strains were grown to saturation overnight in YPDA at 30°C, then diluted to OD^{600} 0.2 in 40mls YPDA, as determined by spectrophotometer (Ralston Scientific CE2040). After growth reached log phase, approximately OD^{600} 0.6, cells were harvested by centrifugation (3,500rpm, 4°C, 5 mins) washed in 40mls sterile water, washed in 1ml 1xTE pH8/100mM LiAc and finally re-suspended in 1ml 1xTE pH8/100mM LiAc. 100μl of the re suspended cells were added to 5μl

(10mg/ml stock) heat denatured salmon sperm DNA (Trevigen), 1-3μg relevant DNA fragment and 700μl 1xTE pH8/100mMLiAc/40% (w/v) PEG. After mixing, the cells were incubated at 30°C for 90 mins then heat shocked 42°C for 15 mins. Following centrifugation (2,500rpm, 5 mins, RT), cells were re-suspended in 150μl sterile water and plated to YPD/relevant selection plate with sterile glass beads and incubated at 30°C.

Selection of Colonies with Required Genotype

Those strains grown on YPD overnight were replica plated to a second selection plate and then colonies that were growing well were selected for testing by colony PCR. Primers for both the deleted gene (or untagged gene) were used in parallel with those for the replacement gene/tag with the resistance cassette. Primers were designed to give fragments of different sizes for the original gene and replacement. Cells were picked into eppendorfs and heat shocked for 1 min on full power in a microwave then transferred immediately to ice. Then a 25μl mastermix of 1x PCR buffer(50mM KCl, 10mM Tris pH9 and 0.1% (v/v) Triton X), 50mM MgCl2, 1μM forward and reverse primer (MWG), 20mM dNTP (Promega), 1.5 U Taq polymerase (in house) and sterile water was added, and mixed by pipetting. The PCR consisted of a 94°C denaturing step of 2 mins followed by 30 cycles of 94°C for 30 secs, 55°C for 1 min and 72°C for 2 mins 30 and ending with a 5 min elongation step at 72°C. Fragments were resolved on a 1% (w/v) agarose gel in 1x TBE (90mM Tris, 90mM Boric acid and 2.5mM EDTA) and the correct colonies were identified by size comparison with a 1kb ladder (Fermentas).

2.2.2 Confirmation of Expression Levels of Tagged Proteins

TCA Protein Preparation

Overnight cultures of relevant strains were diluted to OD^{600} 0.1 in 5 mls YPDA then grown to log phase (Approx. OD^{600} 0.4). Equivalent amounts of each culture were centrifuged (3,500rpm, 5 mins, 4°C), then cells were re-suspended in 150μl 1.85M NaOH/7.4% (v/v) 2-mercaptoethanol, vortexed and then incubated on ice for 10 mins. 150μl 50% (w/v) TCA was added, cells vortexed and incubated for 10 mins on ice. Cells were centrifuged full speed for 2 mins at 4°C; the pellet was rinsed with 1ml ice cold acetone and centrifuged full speed for 2 mins at 4°C. The final cell pellet was re-suspended in 100μl sample buffer (4x Laemmli loading buffer, 50mM DTT, 30mM Tris and sterile water), vortexed and boiled at 100°C for 5 mins before it was loaded on a gel.

Western Blot

Identification of tagged proteins was performed by running appropriate samples on a 4.5% (v/v) stacking/7% (v/v) separating polyacrylamide gel (29:1 acrylamide:bis-acrylamide). The

stacking gel was made with 0.1% (w/v) APS, 0.16% (v/v) TEMED and 1x stacking buffer pH8.8 (0.1% (w/v) SDS, 2mM EDTA and 375mM Tris). The separating gel was made with 0.1% APS (w/v), 0.08% (v/v) TEMED and 1x separating buffer pH 6.8 (as per stacking buffer). Relevant amounts of sample were added to achieve an approximate equal loading based on OD^{600} and the gel was run at 150 volts in Laemmli running buffer (0.1% (w/v) SDS, 200mM glycine and 25mM Tris) using a Full Range Rainbow Molecular weight marker (Amersham) for size comparison. The blots were transferred to 0.45μM PVDF membranes (Roche) for 60 mins at 400mA in 25% (v/v) methanol transfer buffer (200mM glycine, 25mM Tris), then washed in PBS/0.1% (v/v) TWEEN. The membranes were then blocked for one hour in 5% (w/v) dried milk (PBS/0.1% (v/v)TWEEN) and incubated for one hour in 3% (w/v) dried milk (PBS/0.1% (v/v) TWEEN) with primary antibody: 1:2500 α FLAG (SIGMA F1804), 1:5000 α Pgk1 (Invitrogen A-6457) or 1:2000 α H3 C terminal (Abcam ab1791). Next the membrane was washed 1x 10 mins, 2x 5 mins in PBS/0.1% (v/v) TWEEN, re-blocked 15 mins in 3% (w/v) dried milk (PBS/0.1% (v/v)TWEEN) and incubated 1 hour with secondary antibody: 1:5000 α mouse (Amersham NA931) or α rabbit (Amersham NA934). Finally the membrane was re-washed 1x 10 mins, 2x 5 mins in PBS/0.1% (v/v) TWEEN and protein was detected with ECL plus (Amersham) as per manufacturer's instructions.

2.2.3 Re-building of Yta7-FLAG Strains

Tetrad Dissection

To rebuild the Yta7-FLAG strains in a new background MVY105 was crossed with MVY155. MVY155 resulted from previously crossing KH174 and MVY139. In both cases cells from both strains were mated on YPD plates overnight then selected for diploids on relevant drop out plates after approximately two days of growth. Finally the selected diploids were sporulated on minimal KAc (sporulation plates) for approximately one week and checked for sporulation under a light microscope. Spores were dissected by incubation on a nutator for one hour (RT) in 1% (v/v) or 2.5% (v/v) glucuronidase, followed by 3 hours on ice. The spores were then spread on to YPD plates and single spores were transferred to gridded YPD plates using a Singer dissecting microscope. Haploid spores were genotyped using a full range of drop out plates and a mating type halo assay using strains NK1a and NK1542 (provided by S. Makovets). Those spores with the required genotype were selected.

2.2.4 Construction of the *yta7ΔBD* Strains

Sequence Design

Plasmid pBSK was designed with the Seqbuilder programme (Laser Gene 6) using [Tackett et al., 2005] as a guide. The plasmid contained YGR270w, minus 309bp of the bromodomain region, and was ordered from ATG biosynthesis; the sequence was confirmed by the company and compared to that ordered upon receipt.

Bacterial Transformation and Restriction Digestion

Plasmid pBSK was transformed into SURE2 competent E.coli (provided by Schirmer and Stancheva labs) as described above, then midi prepped using a Qiagen kit as per manfacturer's instructions. The plasmid was then subjected to restriction digestion in two consecutive reactions. 10μg of pBSK was digested with 30 units of Xba1 (Fermentas) in 1x tango yellow buffer (Fermentas) at 37°C for 2 hours, followed by a second restriction in 30 units each of Xho1 and Bgl1 (Fermentas) in 1x tango yellow buffer for an additional 2 hours at 37°C. Restricted fragments were separated on 0.8% (w/v) agarose gel in 1x TBE (90mM Tris, 90mM Boric acid and 2.5mM EDTA) with 1kb ladder (Fermentas) and the 3941bp fragment, that contained YGR270w minus the bromodomain, was extracted using a Qiagen gel extraction kit as per manufacturer's instructions. This fragment was phenol extracted and transformed into MVY212 using the LiAc method described previously. Colonies were selected and confirmed for the deletion by colony PCR. yta7ΔBD was then FLAG tagged and expression of the protein was confirmed by western blot as described previously. In addition the non-tagged strain was sequenced to confirm correct integration and lack of mutation within the desired sequence.

LR PCR and Sequencing

Genomic DNA was prepared from strain MVY213 using a Qiagen Gentrapuregene kit for yeast and bacteria as per manufacturer's instructions. Following phenol extraction, the DNA was amplified in small fragments across YGR270w (minus the bromodomain) by using relevant oligos (refer to Table 2.2) and the Roche Expand Long Template PCR kit. Reactions required 250ng template DNA, 1x LR PCR buffer 2(kit), 1μM (each) forward and reverse primer (MWG), 2mM dNTPs (Promega) and 3.75 units taq mix(kit). Cycling was performed on a Biorad DNA engine and the programme had 2 mins denaturation at 94°C prior to 10 cycles of 94°C for 10 secs, 55°C for 30 secs and 68°C for 2 mins 30 secs then 25 cycles of 94°C for 15 secs, 55°C for 30 secs and 68°C for 3 mins, finishing with a 7 min elongation step at 68°C. PCR products were checked for size and concentration by resolution on a 1% (w/v) agarose gel in 1x TBE (90mM Tris, 90mM Boric acid and 2.5mM EDTA), then phenol extracted for use as sequencing templates. 80ng DNA template was mixed with 3.2pmol forward primer and sequenced in house, using a BIG dye 3.1 reaction mix and an ABI 3730 48 capillary Sanger Sequencer. The sequence was compared to the YGR270w sequence (minus the bromodomain) using Seqbuilder (Laser Gene 6).

2.2.5 HU Sensitivity Assays

Spot Test Plates

Saturated overnight cultures were diluted to OD^{600} 0.2 and grown to log phase in 5mls YPDA at 30°C. Approximately 3 x10^6 cells per strain were taken and 1:10 serial dilutions created; 5μl were then spotted to both YPDA and 100mM HU plates.

HU Survival Curves

Saturated overnight cultures were diluted to OD^{600} 0.2 and grown to log phase in YPDA at 30°C. 1 ml of culture was taken to make serial dilutions and the amount required for approximately 200 cells was calculated. This amount was plated onto YPD plates. 100 mg/ml HU was added to the remaining cultures and additional samples were taken at 1, 2, 3, 4.5, 6 and 7.5 hours after addition of HU. The YPD plates were incubated at 30°C overnight, then the number of surviving colonies for each strain was counted at all timepoints.

2.2.6 S phase Kinetics Timecourse Experiments

Timecourse Analysis (General Protocol)

Saturated overnight cultures were diluted to OD^{600} 0.1 in YPDA then grown at 30°C to log phase before being arrested in G1 phase by addition of 1.3μg/ml alpha factor (Zymo research). Once more than 95% of cells displayed schmoos (as visualized by light microscope) samples for timepoint 0 were taken (volumes for FACS, budding and ChIP as per later timepoints) and remaining cells were washed x3 in sterile water and released into fresh YPDA plus 100μg/ml pronase. 2.5ml samples for FACS, 100μl for budding and (if required) 50ml for ChIP were taken and stored on ice at relevant time points. FACS samples were fixed in 5mls 70% (v/v) Ethanol at 4°C overnight, budding samples were fixed in 0.45% (w/v) NaCl/1.85% (v/v) formaldehyde and stored at 4°C. ChIP samples were cross-linked for 1 hour (Yta7p), or 20 mins (Spt16p/Mcm2p/Cdc45p) in 1% (v/v) formaldehyde then quenched for 5 mins in 135mM glycine followed by 2x washes in 40mls ice cold PBS, final centrifugation (3,500rpm, 5 mins, 4°C) and removal of all supernatant for storage at -80°C.

FACS

FACS samples were processed by a wash step in 5mls 50mM Na Citrate (all centrifugation 4000rpm, 4 mins, 4°C), a sonication step of 2x 10 secs in a waterbath sonicator at 4°C (Diagenode Bioruptor 300), followed by re-suspension in 1ml 50mM Na Citrate with 1mg/ml RNase and incubation for 5 hours at 37°C. After overnight storage at 4°C the samples were then washed in a further 1ml 50mM Na Citrate and half the cells were re-suspended in 500μl 50mM Na Citrate/1μM Sytox Green (Invitrogen) and stained for 2 hours on a nutator (RT). Once stained, cells were sonicated 2x 20 secs in the waterbath sonicator, then finally added to 1ml 50mM Na Citrate/1μM Sytox green and analysed using a FACSCalibur machine (Becton Dickinson).

HU Arrest FACS Analysis

Overnight cultures of strains MMY033, MVY51, MVY63, MVY64 and MMY013 were diluted to OD^{600} 0.1 and grown to log phase in YPDA at 30°C. At this point a 2.5ml sample was

taken as timepoint 0 then cells were spun down and re-suspended in 50mls pre-warmed YPDA with 200mM HU. 2.5ml samples were taken every hour for 4 hours and fixed in 5mls 70% (v/v) EtOH at 4°C overnight. Samples were stained as stated above and analysed by FACS machine.

HU Release FACS Analysis

As previously described, overnight cultures of strains MMY033, MVY51, MVY63, MVY64 and MMY013 were diluted to OD^{600} 0.1 and grown to log phase. Cells were arrested with alpha factor as above, washed x2 with sterile water, then re-suspended in 50ml pre warmed YPDA, plus 200mM HU and 100μg/ml pronase. After incubation at 30°C for 75 minutes a 2.5ml sample was taken for timepoint 0. The remaining cells were then washed x2 in 50mls sterile water, then released into a second 50mls pre-warmed YPDA at 30°C. 2.5ml samples were taken at timepoints 20, 40 and 60 minutes and fixed in 5mls 70% (v/v) EtOH at 4°C overnight. Staining and analysis were performed as above.

Budding Index

5μl of Budding Index sample were loaded on a haemoytometer (Neubauer). Cells were counted over 10 squares, then the number of budded cells was counted for the same 10 squares and the percentage of buds were calculated for each strain at every timepoint.

Chromatin Immunoprecipitation

Cell pellets, prepared as described previously, were taken from -80°C and re-suspended, on ice, in relevant amount of FA buffer (50mM Hepes pH7.6, 140mM NaCl, 1mM EDTA, 1% (v/v) Triton X and 0.1% (w/v) Na-deoxycholate) with 1x protease inhibitor (Roche) to give equal cell concentrations based on OD^{600} readings. Cells were lysed using 0.5mm glass beads (Bio Spec Products inc.) by mixing in 1.5ml siliconised eppendorfs (Sarstedt) for one hour on an IKA Vibrax VXR Basic at 4°C. Lysates were retrieved and sonicated for 4x 10secs with a Branson Digital Sonifier. Lysates were removed from the cell debris (centrifugation 13,000rpm, 15 mins 4°C) and purified through a Millipore PVDF 0.45μM column. After transfer to clean eppendorfs and final centrifugation as above, equal amounts of lysate and FA buffer (300μl for Yta7p, 100μl for Cdc45p and Mcm2p or 50μl lysate + 150μl FA for Spt16p) were added to 25μl (pre-washed in FA buffer) M2 agarose mouse α FLAG beads. Incubation was at 4°C overnight on a rocking platform. An additional 20μl lysate was stored at 4°C overnight to be processed as INP.

Incubated α FLAG beads were washed, using Millipore PVDF 0.45μM columns, 1x 10 mins, then 2x 5 mins in 500μl FA buffer (recipe as above), 1x 10mins, then 2x 5mins in 500μl FA buffer (500mM NaCl) and 1x 5mins in Deoxycholate Buffer (1mM EDTA, 10mM Tris pH8, 0.25M LiCl, 0.5% (v/v) NP40 alternative (CalbiChem) and 0.5% (w/v) deoxycholate). Bound proteins and DNA were eluted (2x 30 min incubation then 2,000 rpm, 2mins, RT) using deoxycholate buffer with 0.6mg/ml 3xFLAG peptide. Eluates were incubated overnight at 65°C with reverse cross-

linking mix (10mM Tris pH8, 4mM EDTA and 100mM NaCl). INP samples were incubated overnight at 65°C with DNA clean up (1xTE and 1% (w/v) SDS).

Protein was degraded by 3 hour incubation at 56°C in 4μl PK (Roche) and 3μl glycogen (Roche) (for INP samples 94μl 1xTE plus 5μl PK (Roche) and 1μl glycogen (Roche)). DNA was isolated by 2x phenol extraction and salt precipitation and re-suspended in 50μl 1xTE for samples and 700μl 1xTE for INP.

Radioactive PCR and Polyacrylamide Gels

Yta7-FLAG, Mcm2-FLAG and Cdc45-FLAG ChIP samples were quantified by PCR integration of dATPα^{32}P, using the PCR primers in Table 2.2 (under the header radioactive PCR). Samples were then visualised on 6% (v/v) polyacrylamide gels run in 1x TBE (90mM Tris, 90mM Boric acid and 2.5mM EDTA) and analysed using Image Quant (Amersham). 1μl of sample was amplified using Invitrogen Taq DNA Polymerase kit. Each reaction required 1xPCR buffer (kit), 1.5mM MgCl2 (kit), 17.5pmol oligo mix (AS Technology), 0.4mM dNTP (Promega), 5 units Taq polymerase (kit) and 1μCi/μl dATPα^{32}P (Perkin Elmer). Reactions were cycled in a PTC100 GRI for 2 mins at 95°, followed by 25 cycles of 95°C for 30 secs, 55°C for 30 secs and 72°C for 45 secs, with a final step at 72°C for 5 mins. PCR products were resolved through a 6% (v/v) polyacrylamide (29:1 acrylamide:bis-acrylamide) gel made with 1x TBE (90mM Tris, 90mM Boric acid and 2.5mM EDTA), 0.1% (w/v) APS and 0.1% (v/v) TEMED for 45 mins at 150 volts. Gels were dried to blotting paper at 80°C for one hour using a gel dryer (Amersham), then developed onto a phosphor imaging screen (Amersham). The screen was scanned onto an Amersham STORM 860 machine and analysed using Image Quant (Amersham), which assigned a percentage intensity to each band. These assigned intensity figures were input into an excel spreadsheet and percentage figures of ChIP sample bands were divided by their corresponding INP sample band figure. The resulting calculation for each positive region was further divided by the resulting calculation for TEL (used as a negative control region) and plotted for each timepoint.

QPCR

Spt16-FLAG ChIP samples were analysed by using a quantitative PCR approach. 10μl reactions consisted of 5μl Platinum SYBR green qPCR supermix UDG (Invitrogen), 1μl (3μM stock) of relevant oligo pair (refer to Table 2.2) and 4μl DNA (1/10 dilutions except for no tag ChIP samples which were diluted 1/5) were amplified in 96 well plates (AB gene thermoscientific) on a Stratagene MX3500. The programme consisted of denaturation at 95°C for 2 mins followed by 35 cycles of 95°C for 10 secs, 60°C for 10 secs and 72°C for 15 secs plus an additional cycle to create the melting curve of 95°C for 10 secs, 60°C for 5 secs and 95°C for 5 secs. The data was qualified for quality; ct values were extracted using the MXpro analysis programme (Stratagene). The "delta ct" method was then applied to create %INP amounts. Each oligo pair was qualified before use with the samples and a serial dilution of pooled INP samples was

used on every plate to generate a standard curve. A plate was deemed to have passed quality criteria if the standard curve gave an r squared value greater than 0.99 and a percent efficiency of between 90 and 100%.

Chapter 3

Yta7p has a Role in DNA Replication and the S phase Checkpoint

3.1 Statement of Aims

If histone acetylation were to act as a binding site for a protein that could then influence time of activation of DNA replication, deletion of the protein would remove the "activation signal". The bromodomain has been identified as a histone binding module that shows preference for the acetylated lysine residues of the histone tails. Therefore, the original aim of this thesis was to identify if deletion of any *S. cerevisiae* protein that contains a bromodomain could cause a reversion to WT of the faster S phase, which results from increased histone acetylation at replication origins, witnessed in a Δ*rpd3* strain.

Once a protein that has an effect on S phase had been identified, the further aims of this thesis were to gain additional evidence for a direct role in replication and to characterise the function of this protein in regard to replication processes.

3.2 Introduction

The first aim of this study was to identify a protein whose absence could affect the S phase kinetics of a Δ*rpd3* strain. If it is assumed that acetylated histones in the vicinity of a replication origin are bound by a bromodomain-containing protein, which can affect firing of that origin, then deletion of the bromodomain gene (BDG) could result in a slower S phase for both the single Δ*BDG* and the double mutant Δ*rpd3*Δ*BDG*. A slower S phase would indicate that the protein has a dominant and unique, but not essential, role in DNA replication. However, replication

linked processes have a tendency for some level of redundancy, as do histone modifications and chromatin remodelers. Therefore, there is an advantage to using the Δ*rpd3* system. It is probable that the needs of the Δ*rpd3* strain, in firing excess origins at the same time, would highlight a requirement for a BD protein even if redundant processes exist that can compensate under WT circumstances. Those origins that rely on the increased acetylation in a Δ*rpd3* background to fire earlier [Vogelauer et al., 2002] would no longer be able to recruit the protein and would strain the redundant system and, hence, would not be able to reproduce the advanced time of firing. Hence, the S phase would become WT in a double deletion mutant Δ*rpd3*Δ*BDG*, but the single mutant would remain unaffected. To test this hypothesis I chose Yta7p as the first candidate protein that has a bromodomain. Due to the information available, which is highlighted in Section 1.9, Yta7p was the most promising candidate to be involved in DNA replication.

3.3 Results

Both Δ*yta7* and Δ*rpd3*Δ*yta7* strains were created by using WT and Δ*rpd3* strains available in the lab (see Table 2.1). The *YTA7* gene was replaced with a hygromycin (*HYG*) resistance cassette. Deletion of *YTA7* was confirmed via growth on selective media and colony PCR, in which primers to amplify both the WT *YTA7* gene and the *HYG* cassette were used. PCR products were visualised and strains were selected by size of the fragment amplified; as per Fig. 3.1.

To visualise S phase length, FACS analysis of G1 released cells was performed on all four strains. In this assay cells are arrested in G1, then released and allowed to progress through S phase. Samples are taken at pre-determined time points and the DNA content of the cells is analysed. Cells should move from a 1N to 2N DNA content as they complete DNA synthesis.

The faster S phase and extended G2/M that were previously reported for the Δ*rpd3* strain [Vogelauer et al., 2002] were repeatable in the FACS experiment. However, this phenotype was abolished in the Δ*rpd3*Δ*yta7* double mutant. This abolished phenotype can be seen in Fig. 3.2 (compare the second (Δ*rpd3*) and fourth (Δ*rpd3*Δ*yta7*) column), where the blue bar denotes approximate length of S phase. The length of S Phase was measured starting from the moment where a shift of the 1N profile to the right is visible in the FACS analysis. The end of S phase was assigned to the time point where the 1N peak no longer continues to decrease. Therefore, this represents the length of time it takes most of the cells tested to completely replicate their DNA. The fact that the S phase of a Δ*rpd3* strain is longer in a Δ*yta7* background than in a WT background, suggests that Yta7p is required to facilitate the Δ*rpd3* S phase. This requirement could be directly related to the mechanism that allows for a faster S Phase in a Δ*rpd3* strain, which is to activate late firing origins earlier. Yta7p may function to facilitate this earlier activation. Alternatively Yta7p may be required to maintain the speed of replication forks, slower moving forks delay the completion of DNA replication which would also be reflected by a slower progression of cells from 1N to 2N in the FACS analysis. The S phase of

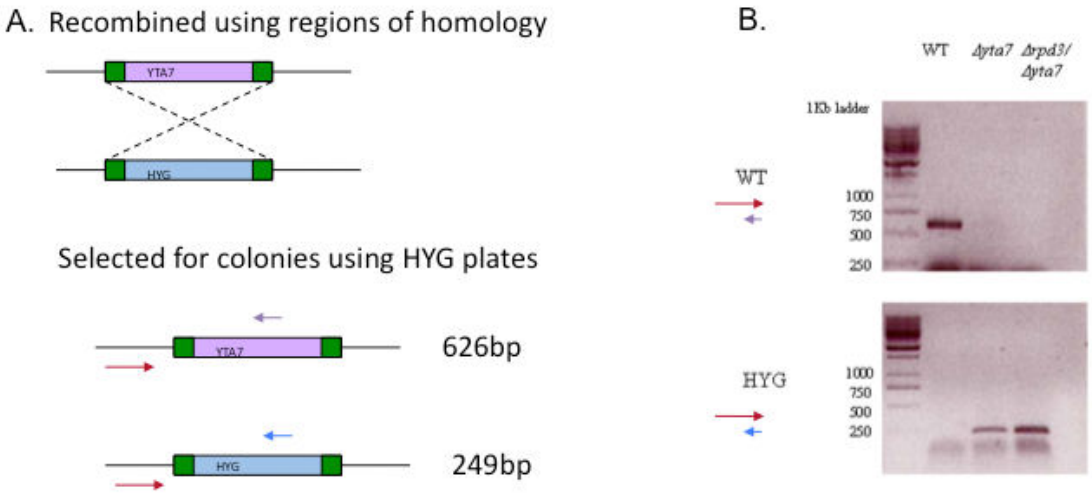

Figure 3.1: Construction of deletion strains. Process for targeted deletion of *YTA7* and replacement with *HYG*. (A): Purple box represents *YTA7* coding region. Light blue box represents hygromycin resistance gene coding region. Dark green box represents regions of shared homology. Coloured arrows indicate primer pairs used for each subsequent PCR reaction. Number represents expected length of PCR product generated. (B): Colony PCR confirmed resistance marker is present and *YTA7* is deleted in relevant strains. Coloured arrows indicate primer pairs used for each reaction as per (A). WT PCR products were run on upper gel. HYG PCR products were run on lower gel.

the single Δ*yta7* mutant had WT kinetics; this indicates potential redundancy for a replication function of Yta7p under "normal" conditions (compare first (WT) and third (Δ*yta7*) columns; Fig. 3.2). All experiments presented in the results section were repeated, unless indicated, and one representative result is shown.

It remained possible that the S phase reversion to WT, which was witnessed in the double mutant, was influenced by asynchronous release of the tested strains from alpha factor induced G1 arrest. To address this issue it was necessary to assess the cell cycle progress in all of the strains and verify that they were synchronised. As stated in Section 1.2.3, G1 transcription, bud emergence, spindle pole body formation, cell growth and DNA replication begin following START. All of these processes can be monitored to reflect progress of the cell cycle. To compare the replication profiles of the strains of this study with another cell cycle event, bud emergence was chosen. As progress of bud emergence is independent from DNA synthesis [Schwob et al., 1994], budding index is routinely used to demonstrate the synchronous release of different mutant strains from G1 arrest [Early et al., 2004]. Moreover, the budding index is a simple process to monitor and does not require an additional manipulation of the cell. Samples used to calculate the Tbud (time at which 50 percent of the cells displayed buds) were taken in parallel with the FACS samples. Cells were fixed and the number of buds present in a subset of cells were counted for each strain at each timepoint. The number of buds should increase at the same rate in all strains if they are progressing synchronously through the cell cycle. All four strains have a Tbud of approximately 55 minutes, which indicates that the release from G1 was synchronous; refer to Fig. 3.3. Hence, the slower S phase profile of the double mutant Δ*rpd3*Δ*yta7* when compared to the single Δ*rpd3*, is not due to asynchronous release of the two strains.

The deletion of the gene of an alternative protein that contains a bromodomain, the HAT *GCN5*, was unable to revert the Δ*rpd3* profile (M. Vogelauer, personal communication); the effect of Yta7p on the S phase length of a Δ*rpd3* strain is not a general feature of bromodomain-containing proteins. Hence, a role for Yta7p in DNA replication is indicated.

Once an effect of a ΔBD gene on the length of a Δ*rpd3* S phase had been identified, the next step was to investigate a role for the protein encoded by this gene in DNA replication. Additional evidence to support the hypothesis that Yta7p is involved in replication is provided by the sensitivity of the Δ*rpd3*Δ*yta7* double mutant to a third mutation that affects the *CDC7* gene. As per Section 1.2.3, Cdc7p is the catalytic subunit of the DDK required to activate individual origins throughout S phase (reviewed in [Duncker and Brown, 2003]). DDK can be regulated by binding of the regulatory subunit, Dbf4p, to the checkpoint kinase Rad53p [Duncker et al., 2002]. Rad53p is also a potential binding partner of Yta7p [Ho et al., 2002], [Smolka et al., 2005], [Smolka et al., 2006].

A strain containing a temperature sensitive (ts) allele of the essential *CDC7* gene was used to create a double Δ*rpd3 cdc7ts* mutant, a double Δ*yta7 cdc7ts* mutant and a triple Δ*rpd3* Δ*yta7 cdc7ts* mutant. These strains were used to investigate the effect of combining the deletion of *RPD3* and *YTA7* with a second impaired gene that is essential to DNA replication.

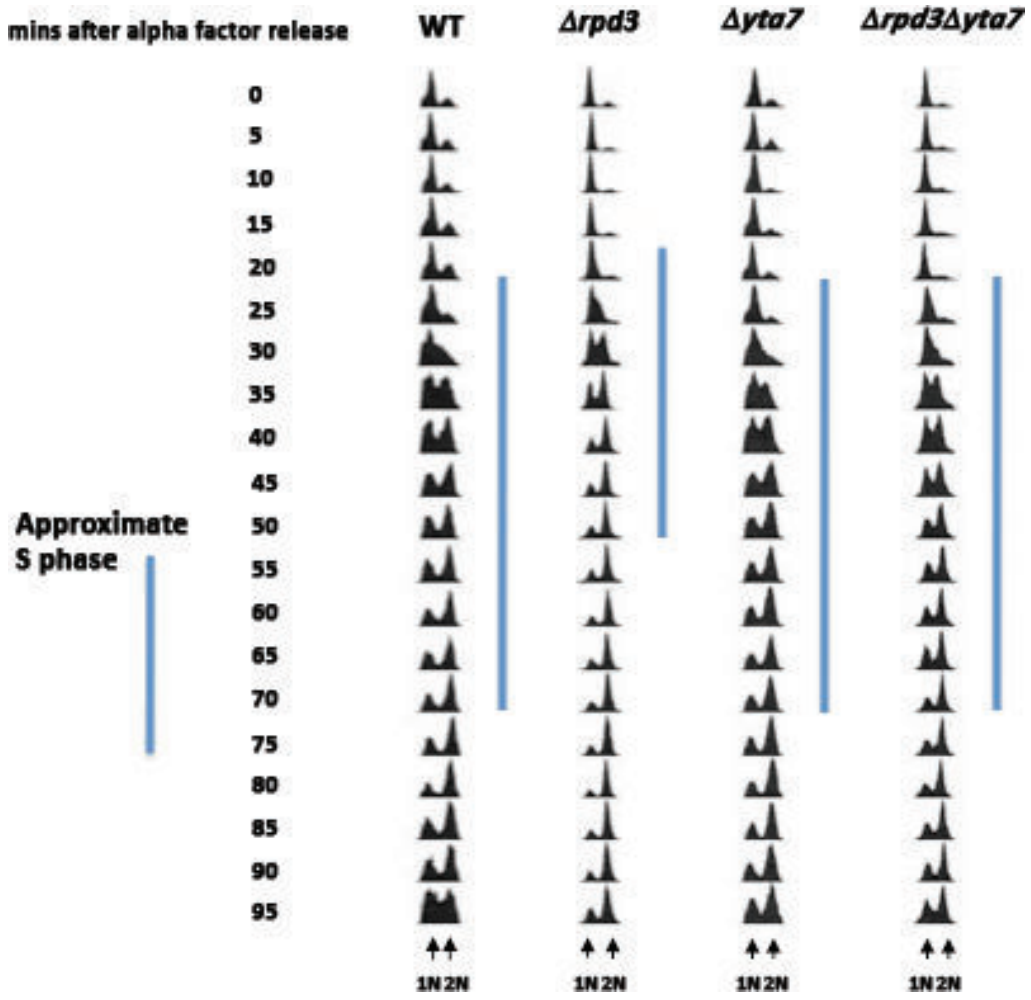

Figure 3.2: Yta7p is required for the faster S phase of Δ*rpd3* - FACS. FACS profile of synchronised G1 release of WT (MMY033) and deletion mutant strains: Δ*rpd3* (MVY51), Δ*yta7* (MVY63) and Δ*rpd3*Δ*yta7* (MVY64). Each time point indicates the minutes following alpha factor release. 1N indicates a haploid DNA content. 2N indicates the cells have replicated the DNA completely. Blue bar indicates approximate S phase length in each case. S phase onset is assigned to the time point where cells are beginning to shift towards a 2N DNA content - represented in the figure by the slope that develops at the bottom right hand side of the 1N peak. The end of S phase is assigned to the time point where the 1N peak displays no large decrease in height at the subsequent time point, indicating that the majority of the cells have replicated their DNA. FACS analysis was performed twice and results were repeatable, one representative result is shown.

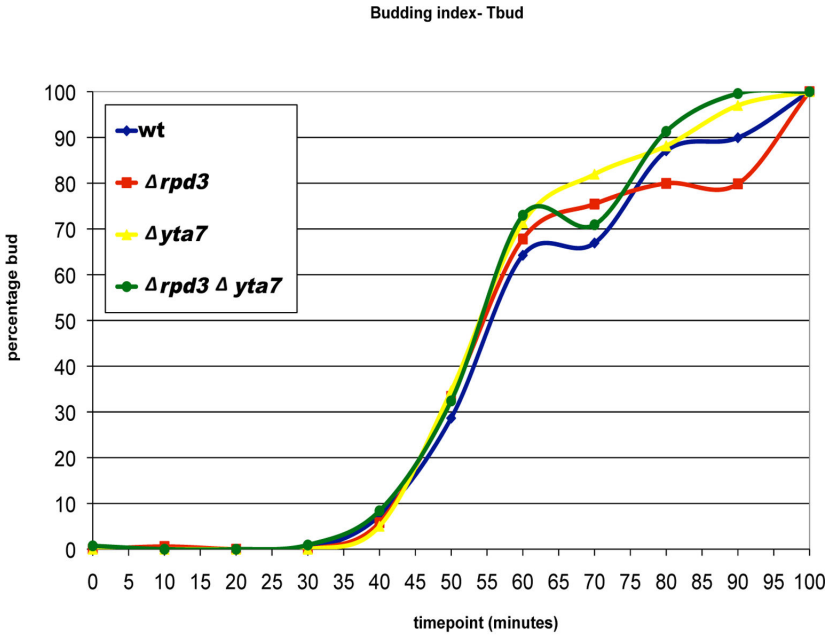

Strain	Tbud (minutes)
WT	55
Δrpd3	54
Δyta7	54
Δrpd3Δyta7	54

Figure 3.3: Yta7p is required for the faster S phase of Δ*rpd3* - budding. Budding Index of WT and deletion mutants indicates synchronous release from G1 of all strains. Number of buds at each indicated time point were counted in the same four strains of the FACS analysis. Y axis represents the number of buds reached as a percentage of total buds for each strain. X axis represents time in minutes. Blue line is strain MMY033 (WT), red line is MVY51 (Δ*rpd3*), yellow line is MVY63 (Δ*yta7*) and green line is MVY64 (Δ*rpd3*Δ*yta7*). The table gives the Tbud value for each strain that is the time at which 50 percent of the cells were budded.

Spotting assays at a variety of temperatures were performed on YPD plates. Refer to Fig. 3.4, where the top two plates contain the temperature sensitive strains spotted onto YPD at two different temperatures and the bottom plate is the equivalent "WT" strains grown at 30°C to demonstrate "normal" growth. Even at the permissive temperature of 23°C there is a synthetic growth defect (a 25 fold effect) in the combined Δ*rpd3* Δ*yta7* *cdc7ts* mutant. This defect is increased to an approximately 125 fold effect for the triple mutant in comparison to any other mutation at 25°C. As anticipated, all strains placed at the non-permissive temperature were unable to grow sufficiently, hence detection of strain dependent defects at these temperatures was not possible (data not shown).

The synthetic growth phenotype of a Δ*rpd3*Δ*yta7* strain containing the temperature sensitive *cdc7* allele suggests that these three proteins share a common function. Once again, the single Δ*rpd3* or Δ*yta7* mutants, in the *cdc7* background, displayed only a minor growth defect when compared to WT (Fig. 3.4). Hence, either both Rpd3p and Yta7p perform a similar function that requires the presence of one of the proteins, or deletion of *RPD3* unmasks a role for Yta7p alone, that is similar to a role of Cdc7p, which is compensated for in conditions with WT levels of Rpd3p.

Deletion of genes that are involved in DNA replication, such as *POL32*, *ASF1*, and subunits of FACT, are often sensitive to the ribonucleotide reductase inhibitor hydroxyurea (HU) [Parsons et al., 2004], [Schlesinger and Formosa, 2000]. HU depletes the available cellular dNTP levels, which stalls replication and causes activation of the S phase checkpoint. A further indicator that Yta7p is involved in DNA replication would be if it were also sensitive to this agent. Therefore, the WT, Δ*rpd3*, Δ*yta7* and Δ*rpd3*Δ*yta7* strains were spotted onto YPD plates containing 100mM HU. The Δ*rpd3*Δ*hda1* mutant strain was also included as a positive control; Hda1p is a member of a second HDAC and this double mutant has previously displayed increased sensitivity to HU (M. Vogelauer, personal communication). As per Fig. 3.5, neither of the single mutants displayed a significant growth defect in HU, but the double deletion strain, Δ*rpd3*Δ*yta7*, was very sensitive to this agent. Compare Fig. 3.5 (A) and (B) where all strains grow equally well on YPD (A), but the double mutant is between 100 to 1000 times more sensitive to 100mM HU than the WT strain or either single mutant (B). In addition, a survival curve assay using the WT and mutant strains clearly shows that the Δ*rpd3*Δ*yta7* double mutation is rapidly lethal after treatment with HU; refer to graph in Fig. 3.6. In this survival curve assay cells were grown in HU for the indicated length of time and then equal amounts were plated to YPD. Surviving colonies were counted and the rapid drop in the number of survivors in the double mutant is represented by the steep downwards curve of the green line.

As previously stated, sensitivity to HU is a characteristic of strains that have mutations of genes that are involved in DNA replication [Parsons et al., 2004]. The primary effect of HU treatment is to activate the S phase checkpoint [Longhese et al., 2003]; hence, sensitivity to this agent could also be caused by a checkpoint defect. In the case of the Δ*rpd3*Δ*yta7* strain this defect could be that the S phase checkpoint is not activated efficiently. This would lead to continued progression of the cell cycle and DNA replication events under conditions

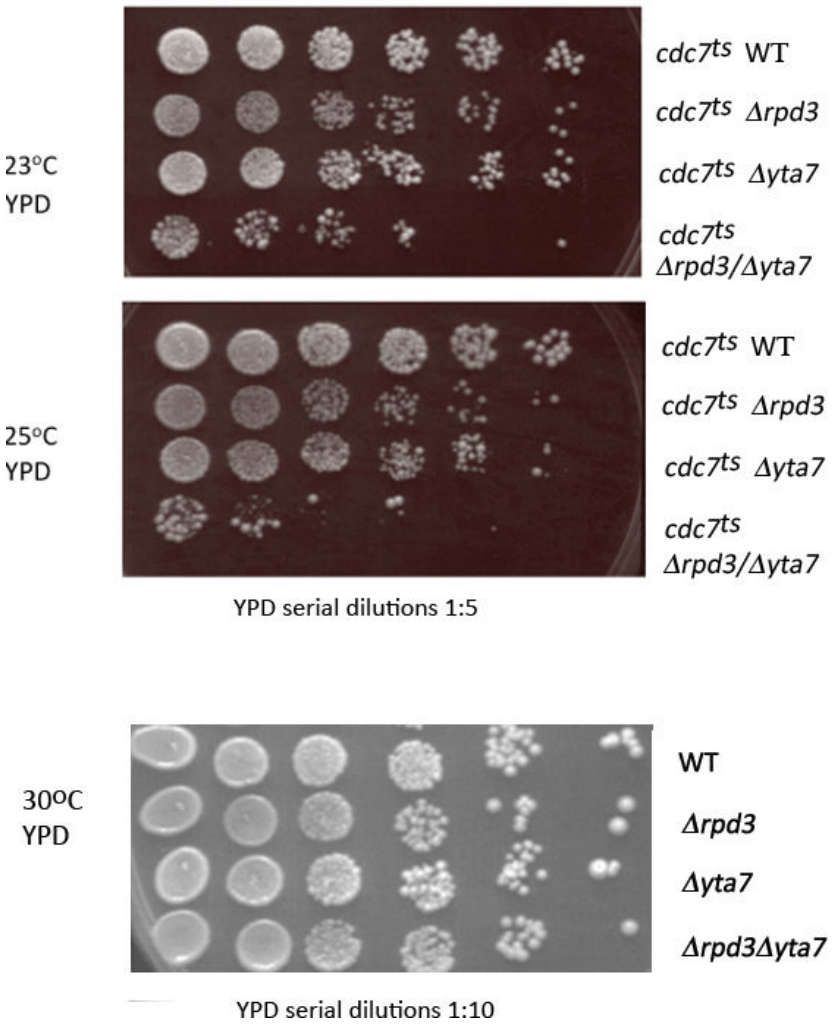

Figure 3.4: Synthetic interaction between Yta7p, Rpd3p and the DDK Cdc7p. Upper two plates are spotting plates with 1:5 serial dilutions of cells, which were grown at 23°C and 25°C on YPD plates. Indicated strains are YB556 (*cdc7ts* WT), MVY72 (*cdc7ts* Δ*rpd3*), MVY71 (*cdc7ts* Δ*yta7*) and MVY73 (*cdc7ts* Δ*rpd3*Δ*yta7*). Left hand lane shows growth of neat samples with each subsequent lane, moving left to right, a 1:5 dilution of the previous lane. Therefore each spot, moving backwards, from right to left represents a 5 fold, 25 fold, 125 fold, 625 and 3125 fold difference in growth, respectively. The spot test was repeated twice and a representative experiment is shown. Bottom plate shows how the Δ*rpd3* and the Δ*yta7* mutations affect growth of a WT strain at 30°C on YPD for comparison. Left hand side lane displays growth of neat sample with each subsequent lane a 1:10 dilution of the lane immediately to the left. Indicated strains are MMY013 (Δ*rpd3*Δ*hda1*), MMY033 (WT), MVY51 (Δ*rpd3*), MVY63 (Δ*yta7*) and MVY64 (Δ*rpd3*Δ*yta7*).

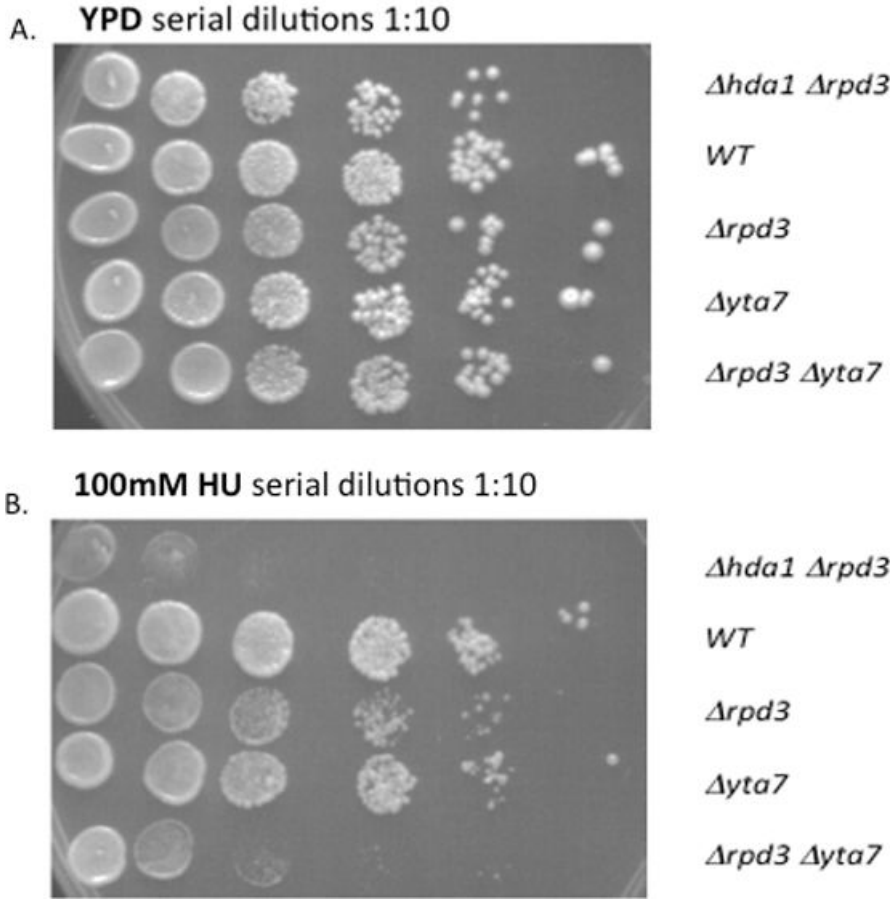

Figure 3.5: Double mutant Δ*rpd3*Δ*yta7* is sensitive to HU. Indicated strains were spotted with 1:10 serial dilutions onto; (A): YPD and (B): 100mM HU plates and grown at 30°C. Strains used are MMY013 (Δ*rpd3*Δ*hda1*), MMY033 (WT), MVY51 (Δ*rpd3*), MVY63 (Δ*yta7*) and MVY64 (Δ*rpd3*Δ*yta7*). Each lane from right to left represents a 10 fold, 100 fold, 1000 fold, 10,000 fold and 100,000 fold growth difference compared to the first lane. The spot test was repeated twice and a representative experiment is shown.

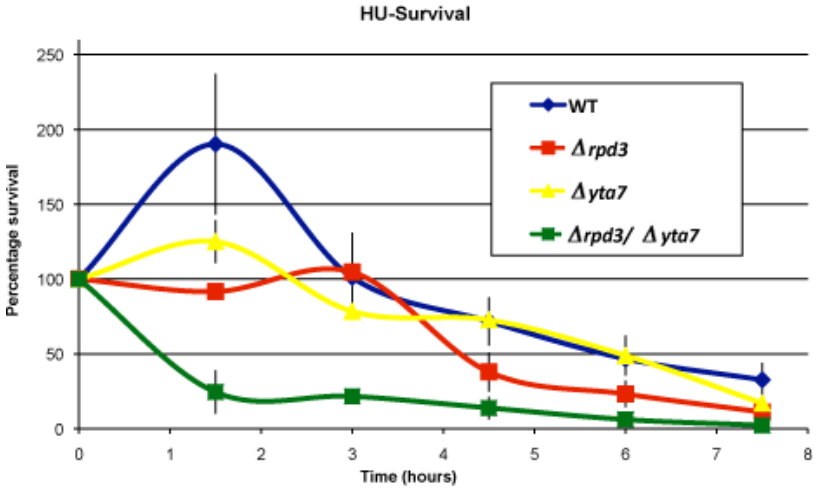

Figure 3.6: HU survival curves. The Δ*rpd3*Δ*yta7* strain is sensitive to the agent HU. The rapid lethality of the double mutant upon HU treatment can be observed using survival curves. Relevant strains were grown in HU for the indicated number of hours (X axis) then spotted to YPD plates and number of colonies formed was counted. Percentage survival (Y axis) is the number of colonies on the plate as a percentage of the number of colonies at time point 0. Blue line is strain MMY033 (WT), red line is MVY51 (Δ*rpd3*), yellow line is MVY63 (Δ*yta7*) and green line is MVY64 (Δ*rpd3*Δ*yta7*). Black vertical lines are error bars generated using the standard error of the mean calculation for the two independent experiments.

that were not sustainable; genomic instability and cell death would ensue. Another possibility is that the checkpoint is activated normally in this strain and that the problem is release from the checkpoint. A problem with release from the checkpoint could be caused by either an inability to deactivate the checkpoint or an inability to resume DNA replication after checkpoint deactivation. In order to test if the phenotype of the Δ*rpd3*Δ*yta7* strain was caused by defects in checkpoint activation or checkpoint release the WT and mutant strains were subjected to two conditions, HU arrest and HU release, with analysis by FACS. The first approach was to determine if the cells could arrest appropriately with a 1N content early in S phase, as would be expected if the checkpoint were activated efficiently. The second approach was to ascertain if the cells could continue to replicate after the block to replication had been removed, which would be indicated by the shift from a 1N to a 2N DNA content of the cells upon release from HU. As is evident in the FACS profiles of Fig. 3.7, all tested strains arrested within two hours with a 1N DNA content in early S phase when treated with 100mM HU. Therefore, the lethality of a Δ*rpd3*Δ*yta7* mutation in HU is not caused by an inability of the cell to activate the S phase checkpoint. All strains maintained the arrest for a further 2 hours (data not shown).

In contrast to this, when challenged with HU and then washed and released into fresh media, the Δ*rpd3*Δ*yta7* strain, alone, is unable to complete synthesis by 60 minutes post release. As shown in Fig. 3.8, the WT strain and both single mutants all had cells that had replicated their DNA and displayed a 2N content by the 60 minute time point. In addition, the Δ*rpd3*Δ*hda1*

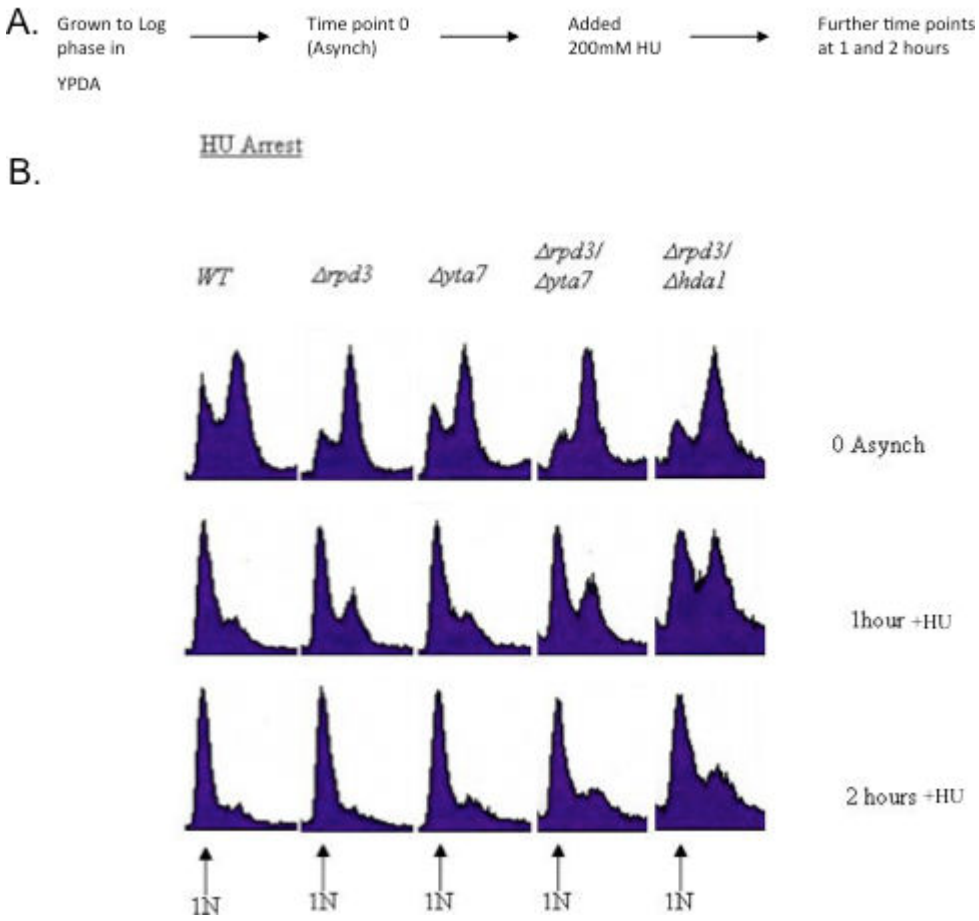

Figure 3.7: All strains are able to induce efficient S phase checkpoint activation upon treatment with HU. (A): Schematic of experiment. (B): FACS analysis produced using schematic in (A). Strains MMY033 (WT), MVY51 (Δ*rpd3*), MVY63 (Δ*yta7*), MVY64 (Δ*rpd3*Δ*yta7*) and MMY013 (Δ*rpd3*Δ*hda1*) were grown to log phase and sample 0 was taken from the asynchronously growing cells. Following HU treatment samples were taken after 1 and 2 hours to check for efficient arrest. 1N indicates haploid DNA content.

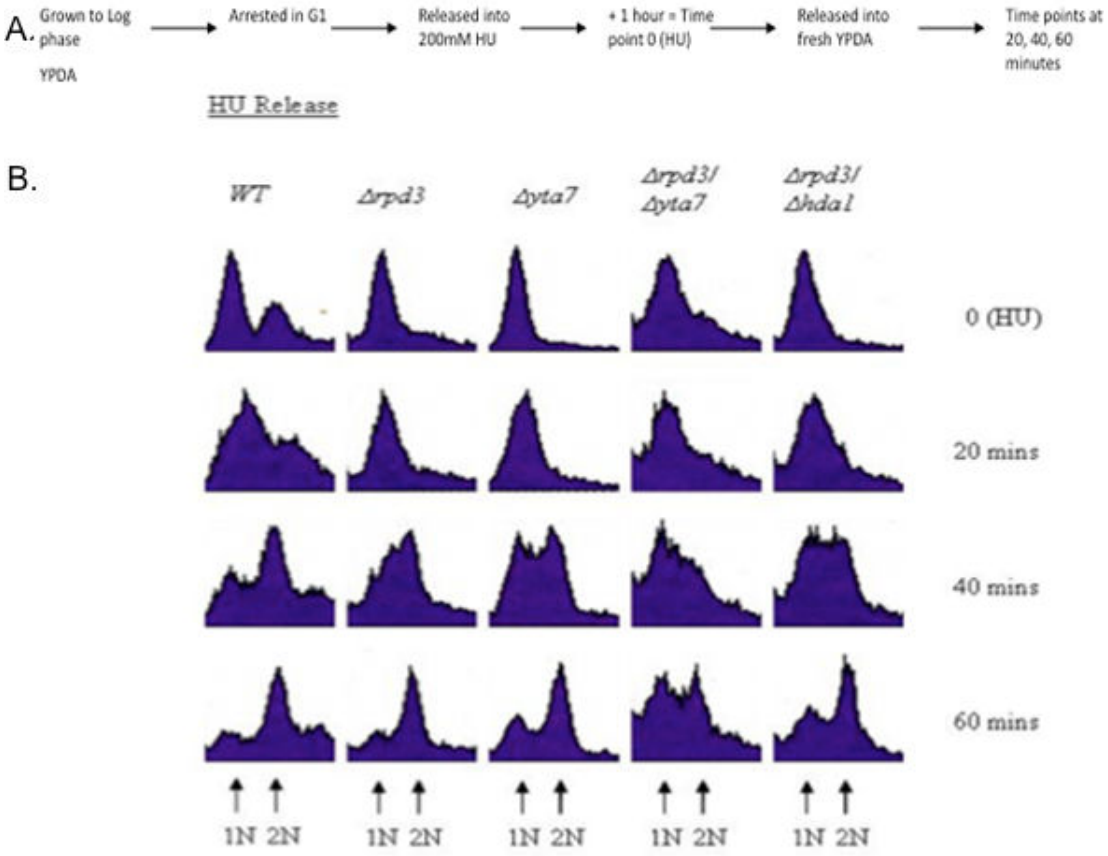

Figure 3.8: Double mutant Δ*rpd3*Δ*yta7* displays inefficient recovery from S phase checkpoint activation. (A): Schematic of experiment. (B): FACS analysis produced using schematic in (A). Strains MMY033 (WT), MVY51 (Δ*rpd3*), MVY63 (Δ*yta7*), MVY64 (Δ*rpd3*Δ*yta7*) and MMY013 (Δ*rpd3*Δ*hda1*) were arrested in alpha factor then released and re-arrested immediately with HU. Cells were washed and released into S phase. 1N represents the haploid genome. 2N represents complete replication of the DNA.

strain also had the majority of cells with a 2N content by the end of the assay. The Δ*rpd3*Δ*yta7* double mutant had a subset of cells that were in the process of being replicated, but had not completed replication by 60 minutes, as shown by the large proportion of cells between 1N and 2N in the FACS profile.

3.4 Discussion

Based on the results it is possible that Yta7p has a role in both DNA replication and the S phase checkpoint. The presence of Yta7p is required to complete a faster S phase in a Δ*rpd3* strain background and the slower S phase in the Δ*rpd3*Δ*yta7* double mutant is not due to experimental design; release from alpha factor arrest was synchronous in all strains based on a budding index. In addition the presence of Yta7p or Rpd3p is also required to resume DNA replication after release from the S phase checkpoint. There are a number of possible explanations for the FACS profile, and the survival curve profile, of the Δ*rpd3*Δ*yta7* double mutant after release from HU. These include the three following options. First, the checkpoint is unable to deactivate. Second, the checkpoint is deactivated but the replication forks were unable to be stabilised, subsequent fork collapse would mean that replication could not be resumed from those origins already activated. Third, following checkpoint deactivation no further origins were able to activate and the cell was relying on those already fired to replicate the entire genome. Any of these three explanations, or in fact a combination of them, could be responsible for the HU sensitivity. Further experiments could be focused to test the three hypotheses. Checkpoint deactivation could be investigated by monitoring the phosphorylation status of the Rad53p checkpoint kinase. Chronic activation would be confirmed if phosphorylation of Rad53p were to continue in the Δ*rpd3*Δ*yta7* strain long after it was removed in WT cells, following HU release. To deduce if the strain has fork stabilisation defects, the fork structures could be monitored in HU arrested cells through the use of 2D gel electrophoresis to look for abnormalities. For confirmation of origin activation following HU release, known late-firing origins could also be monitored by 2D gel electrophoresis to observe replication bubbles.

One observation of the HU sensitivity assays is that only the double Δ*rpd3*Δ*yta7* mutant is sensitive to HU. Hence, it could be that these two proteins share a common function or that Δ*rpd3* unmasks an effect of Δ*yta7*. Deducing this would be the first step before further investigation of the post checkpoint defect. Rpd3p has previously been identified to have a role in multiple checkpoints; refer to Section 1.7. However, deletion of *RPD3* has always been identified to suppress checkpoint defects caused by mutations in other genes. In the case of Δ*yta7*, deletion of *RPD3* causes a synthetic, post S phase checkpoint, defect; therefore, it is probable that the simplest explanation may be true. That is, it is possible that the double mutant is lethal simply because Δ*rpd3* activates more origins prior to S phase checkpoint activation than WT, which was shown by [Aparicio et al., 2004], and the cells require Yta7p to cope with stabilising these extra structures. The effect of Yta7p deletion on S Phase length in a Δ*rpd3* strain could be due to reversion of late firing origins to their correct activation time.

However, the longer S phase length when Δ*yta7* is deleted in a Δ*rpd3* strain might, instead, be due to slower progression of the replication fork and origin firing may remain as it is for a Δ*rpd3* strain. If the late origins have already fired in a Δ*rpd3*Δ*yta7* strain, before checkpoint activation, and the forks have collapsed after checkpoint activation, then it would be impossible to replicate the rest of the genome through activation of a new complement of origins, which is analogous to the situation observed in the Δ*mrc1* strains described in Section 1.2.5. Hence, an experiment to identify if the usually late-firing origins are still activated before checkpoint activation in the double mutant Δ*rpd3*Δ*yta7* would be important. Again 2D gel electrophoresis to check both early and late-firing origins in all four HU treated strains (WT, Δ*rpd3*, Δ*yta7* and Δ*rpd3*Δ*yta7*) would indicate in which strains the late origins had fired prior to checkpoint activation.

In summary, the above results indicate that there is a potential (redundant) role for Yta7p in both DNA replication and recovery from S phase checkpoint activation. This evidence does not point to either a specific direct or indirect role. However, the role in DNA replication is inferred by three lines of evidence: Yta7p is required for the faster S phase of a Δ*rpd3* strain (highlighting a potential role in replication timing), Δ*yta7* has a synthetic growth defect in combination with Δ*rpd3* and *cdc7ts* and, as for many other genes involved in DNA replication, Δ*rpd3*Δ*yta7* is sensitive to HU treatment. In addition, the Δ*rpd3*Δ*yta7* strain displays defects in resumption of DNA replication following release from the S phase checkpoint.

Chapter 4

Yta7p Binds to the Histone Gene Promoters, but Δ*yta7* does not Affect H3 Protein Levels.

4.1 Introduction

As stated, the role in DNA replication of Yta7p suggested by the evidence in the previous chapter does not rule out the possibility that Yta7p and Rpd3p are involved in an indirect function; Yta7p and Rpd3p may be required to regulate the transcription of genes that are necessary for DNA replication. In fact, the role of Rpd3p in transcriptional repression is well documented, in addition Rpd3p has a role in activation of transcription at some regions (although these may be indirect effects) as reviewed in [Kuo and Allis, 1998]. Recent evidence also highlights a role for Yta7p in regulating the *FLO11* gene. In fact, in addition to Yta7p, subunits of both the Rpd3L complex and the SWI/SNF chromatin remodeling complex were identified as activators of the *FLO11* gene [Barrales et al., 2008]. The LEX1 protein of *C. elegans*, which is similar to *S. cerevisiae* Yta7p, is also required for gene expression within repetitive heterochromatin [Tseng et al., 2007].

The most informative way to ascertain if the role of Yta7p in DNA replication is direct was to determine if Yta7p is bound to replication origins and forks. In addition, if the original hypothesis, that Yta7p binds to regions of increased histone acetylation in the vicinity of origins, were correct then Yta7p should be detectable at those origins. If Yta7p were to affect replication events, then it should also be detectable at origins at the time of activation. To test this possibility, optimisation of a ChIP timecourse experiment against Yta7p was required. The ChIP process used in this thesis is outlined in Fig. 4.1.

Briefly the desired protein is used as a target to isolate DNA that is bound either directly to the protein or through a protein-protein complex. The proteins and DNA/chromatin are

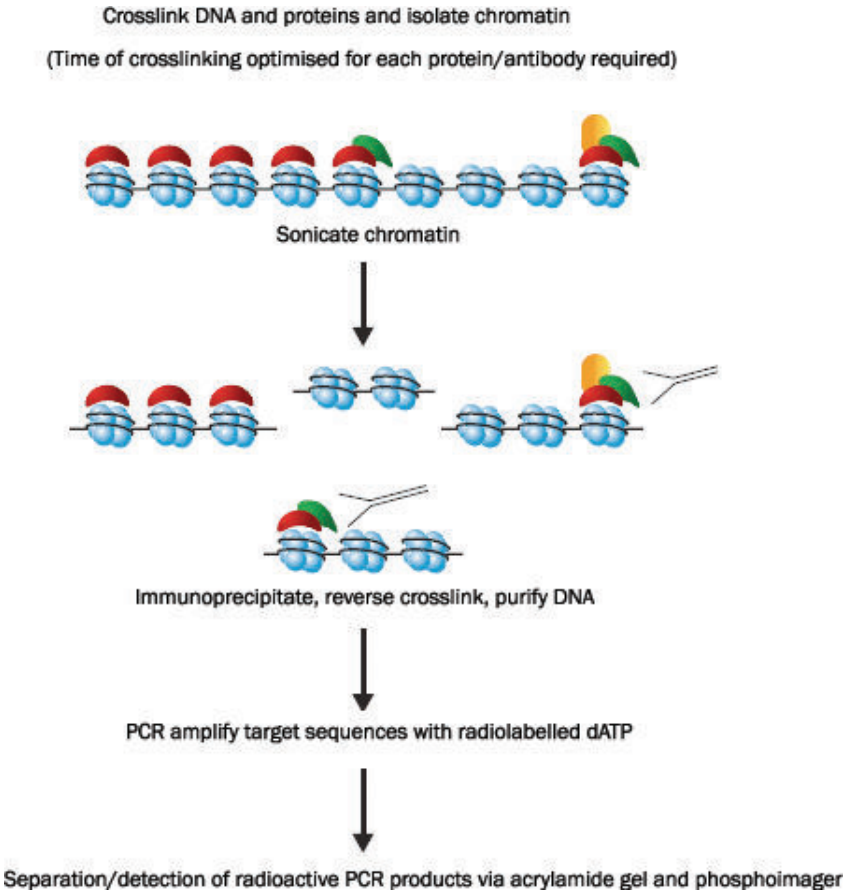

Figure 4.1: Chromatin precipitation - outline of key steps. Figure taken and adapted from `www.abcam.com/index.html?pageconfig=resource&rid=9` (June 2010). Black line (DNA) and blue circles (histones) represent chromatin. Red, yellow and green shapes are proteins; specifically green shape is protein of interest. Black fork shape is antibody.

chemically cross-linked, then the chromatin is sheared into small fragments. An antibody directed against the protein of interest is used to isolate the DNA sequences that are bound only to that protein (complex), followed by reversal of the cross-link and digestion of the proteins. Finally, the DNA is purified and PCR (or more recently micro array hybridisation or next generation sequencing) is used to detect if regions of interest are bound or not by the target protein. Cross-linking can be achieved via the use of various chemicals that have different specificities, for example formaldehyde cross links everything that is in a close proximity to the DNA, but cannot detect all of the less specific binding. Hence, for some proteins the use of DMA is beneficial as this chemical also cross-links proteins so that proteins that are bound to a region via a second protein are also detected more frequently [Kurdistani and Grunstein, 2003b]. The ChIP method is useful as it acts as a snapshot of the interactions of a protein with DNA at a particular moment; ChIP experiments can provide information of the binding profile of a protein and how that changes at different moments of the cell cycle. However, it is more probable to detect an interaction if a protein remains bound to DNA for a longer time and, as such, dynamic interactions are often missed. In addition, the method is limited by the resolution afforded by the fragmentation method used and conditions have to be optimised for individual proteins and antibodies and results will depend on the specificity and efficiency of the antibody used and the dynamics and levels of the protein in the cell. Although, once optimised, this method provides valuable information and can link specific processes of the cell to previously unrelated proteins via the physical presence of the protein at the relevant time and place of activity.

4.2 Results

To test for the binding of Yta7p to replication origins I used the above ChIP method. Since there was no direct antibody against Yta7p available it was necessary to tag the protein. Strains were constructed to contain a C terminal FLAG tagged Yta7p by targeting the 3X FLAG sequence, complemented with the nourseothricin (NAT) resistance marker, to the $5'$ of the *YTA7* STOP codon. The Yta7-FLAG strain was built in both a WT and Δ*rpd3* background and positives were selected based on resistance to CLONAT, colony PCR to identify tagged sequences from non-tagged by length, western blot to confirm expression of the protein and a HU sensitivity test to confirm correct function of the tagged protein.

In the course of the experiment it became necessary to re-build the strains. The original Yta7-FLAG strain in the MMY001 background (MVY104; refer to Table 2.1) began to experience a very slow S phase and became sick when grown. The Yta7-FLAG strain built in the MMY002 background (MVY105; refer to Table 2.1) did not display such problems. The reason for this problem could not be identified and it became prudent to re-build the strains by mating MVY105 with the alpha mating strain MVY155. After sporulation, dissection, growth on relevant media to detect required markers, and a mating type assay, required strains were selected to replace all three previous strains (No Tag, Yta7-FLAG and Yta7-FLAG Δ*rpd3*). Once again a western blot and HU sensitivity assay were performed. Both the timecourses

conducted with the older strains and the re-made strains gave the same result (refer to next chapter). The western blot of the newly-made strains indicates that Yta7p is expressed equally in both WT and Δ*rpd3* strain backgrounds; the signal is similar between both of the strains for both Yta7-FLAG and the loading control Pgk1p; Fig. 4.2(A, lanes 5 and 6). The Yta7-FLAG protein runs at a higher than expected molecular weight (even when taking the FLAG tag into account). This is due to the resolution of the gel as the percentage of the gel had to accommodate both Yta7p and Pgk1p which have a very different size range. Therefore, to fit them both on the same gel there was a loss of resoultion at the highest molecular weight range. There was no signal in the untagged strain for Yta7-FLAG (lane 4). Since I previously identified that the double mutant, Δ*rpd3*Δ*yta7*, is sensitive to HU I would expect that if the FLAG tag had rendered Yta7p non-functional, then the Yta7-FLAG strain built in the Δ*rpd3* background would also show sensitivity. However, the only strain to display sensitivity on the HU plate was the Δ*rpd3*Δ*yta7* positive control; refer to Fig. 4.2(B- middle gel) . All strains grew equally on YPD (top gel). There is a slight effect of Yta7-FLAG Δ*rpd3* compared to WT. However, a slight effect was also evident in the Δ*rpd3* strain spotted onto HU in the previous chapter (refer to Fig. 4.2 bottom). Thus the FLAG tag of Yta7p has no large additional effect on the Δ*rpd3* strain. Hence, all strains used for the timecourse experiments contained an expressed and functional Yta7-FLAG protein.

Next it was necessary to identify positive and negative binding regions of Yta7p to optimise the ChIP conditions. For this purpose primers were designed or taken directly from [Xu et al., 2005]; refer to Fig. 4.3, (this figure was taken directly from the Xu paper). These sites were chosen as positive controls as it was suggested that Yta7p might preferentially bind to H3K56ac at this region, or at least that Yta7p may co-exist with this modification (information taken from a poster by Lavender and Tackett presented at 55th proceeding of the ASMS [1], data later confirmed in [Gradolatto et al., 2008]). The regions of [Xu et al., 2005] are enriched for this H3K56ac modification and so represented good candidates for binding of Yta7p. The *HIS2* ORF was chosen as a candidate negative control region as it was not near a promoter, known boundary region or replication origin. No evidence for binding of Yta7p to these types of regions exist, hence it was chosen to test for lack of signal in the Yta7-FLAG ChIP.

Optimisation of the ChIP experiment was performed on both G1 arrested cells and cells that were arrested in S phase through the use of HU. An Mcm2-FLAG strain was used as a positive control; Mcm2p should localise at origins in G1 arrested cells. Cells were cross-linked in either formaldehyde alone or both formaldehyde and DMA, and a subset of cross-linking times were tested. ChIP analysis was performed by electrophoresis of radioactive PCR products that amplified the chosen regions, followed by assignment of relative signal intensities by Image Quant (Amersham). Signal intensities were normalised to the INP and expressed as enrichment over the negative control region; data is presented as a bar graph for ease of comparison. Results

[1] Poster available at `www.asms.org/tabid/368/type/searchresults/Default.aspx` (April 2007)

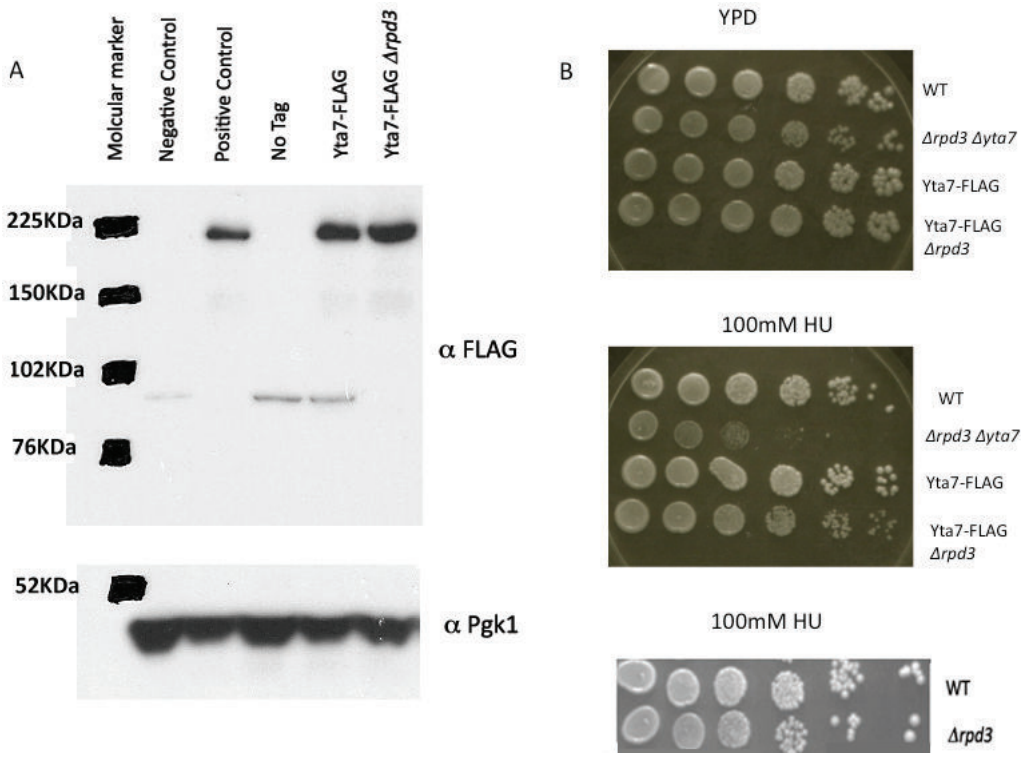

Figure 4.2: Yta7p is stably expressed and functional when tagged. (A): Western blot using αFLAG and αPgk1p. Exposure time of αPgk1p adjusted from that of αFLAG so that signals were not saturated. Lane 1 contains molecular marker. Strains shown are MMY001 (negative control), MVY105 (positive control), MVY209 (No Tag), MVY210 (Yta7-FLAG) and MVY211 (Yta7-FLAG Δ*rpd3*). Approximate molecular weight for untagged protein, as taken from SGD, should be for Yta7p 157.5KDa, and for Pgk1p 45KDa. (B): Spot tests to show HU sensitivity of relevant strains. All plates are spotted in 1:10 dilutions from left (neat) to right. Strains shown in top two figures are MVY209 (WT), MVY210 (Yta7-FLAG) and MVY211 (Yta7-FLAG Δ*rpd3*). Top figure displays growth on YPD of all strains; middle figure displays growth on 100mM HU. Bottom figure contains strains MMY033 (WT) and MVY51(Δ*rpd3*) and is included to demonstrate how the Δ*rpd3* mutation affects growth of a WT strain on 100mM HU.

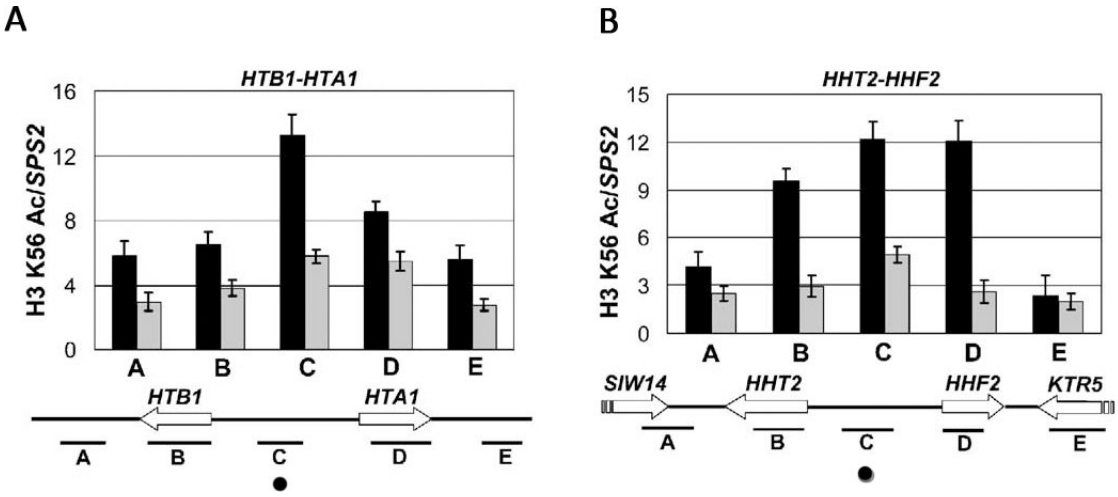

Figure 4.3: Primers for positive control Yta7p binding region. The figure was taken from [Xu et al., 2005] as the primers used in my thesis were designed based on or taken directly from [Xu et al., 2005] and the region they cover corresponds to the black dot in this figure. Both regions chosen have increased H3K56ac. The Y axes of the graphs are the level of H5K56ac enrichment at the histone gene loci indicated above the graph, divided by the enrichment at the *SPS2* control region. The X axes are the indicated regions A, B, C, D and E which are also displayed below the graphs as locations relative to the histone ORFs. The black bars show H3K56ac levels in a WT strain. The grey bars are H3K56ac levels in an *spt10* (HAT) mutant.

figures include the raw gel image in support of the graphs produced by analysis.

As per Fig.4.4, the ChIP gave an enrichment of Mcm2-FLAG that was 9 times greater than that of the untagged protein at the ARS609 replication origin, when compared with the *HHT2-HHF2* locus, in G1 phase (compare No tag with MCM2-FLAG strains in graph). This indicates that the ChIP procedure is accurately detecting the binding of a known member of the preRC to a replication origin in G1 phase, as expected.

The results of the Yta7-FLAG ChIP were more surprising. Yta7p was found to be enriched by approximately 10 and 6 times, respectively, at the *HTA1-HTB1* and *HHT2-HHF2* promoters when compared with the *HIS2* ORF in G1, a time when H3K56ac is not presumed to be present as it is an S phase specific modification; refer to Fig.4.5. However, this corresponds well with later works that suggest that Yta7p and H3K56ac can be co-localised but are not dependent on each other [Gradolatto et al., 2008], [Fillingham et al., 2009]. Optimal enrichment of Yta7-FLAG occurred with 1 hour of formaldehyde cross-linking time; Fig. 4.5 (Yta7-FLAG 60 and Yta7-FLAG Δ*rpd3* 60 in graph).

Formaldehyde alone was the optimal cross-linking agent, as including DMA increased non-specific background (results not shown). Therefore, formaldehyde cross-linking for 1 hour was used in subsequent Yta7-FLAG experiments. Closer examination of the gel images reveals that there is a slight enrichment of Mcm2-FLAG at the *HTA1* promoter (refer to lane 4 in the left hand gel of Fig. 4.5). Upon investigation of this region using SGD there is an origin, ARS428,

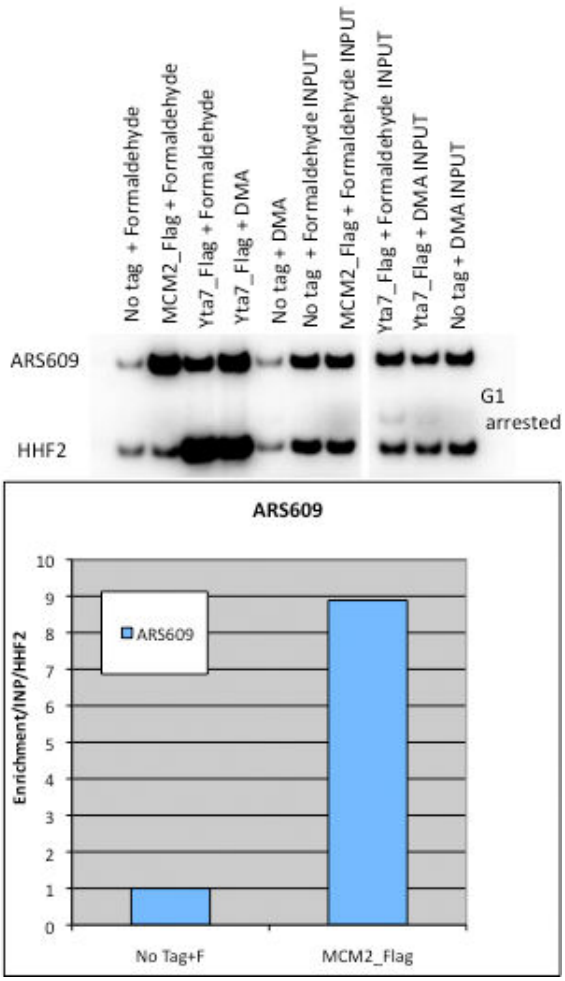

Figure 4.4: Optimisation of ChIP conditions - positive control. Mcm2-FLAG strain showed high enrichment at ARS609 in G1 arrested cells as expected. Top figure is raw gel image for comparison with analysis data. Strains are MMY001 (No Tag), MVY125 (Mcm2-FLAG) and MVY104 (Yta7-FLAG) cross-linked with either formaldehyde (formaldehyde) or formaldehyde and DMA (DMA) as indicated. First 5 lanes from left to right are IPs; second 5 lanes are corresponding INPs. Regions tested for enrichment are ARS609 and the *HHT2-HHF2* promoter region shown in Fig. 4.3. Graph shows enrichment of Mcm2-FLAG (blue bar on right) compared to No Tag (blue bar on left) at the ARS609 region in G1 arrested cells. Y axis is αFLAG signal normalised to INP, and divided by normalised *HHF2*. X axis is the No Tag experiment that was cross-linked in formaldehyde followed by the Mcm2-FLAG experiment that was cross-linked in formaldehyde. Optimisation experiments were performed with variable conditions until good results were achieved. Thus the experiment was repeated with various levels of success, however the experiment shown represents the optimised conditions and was performed once.

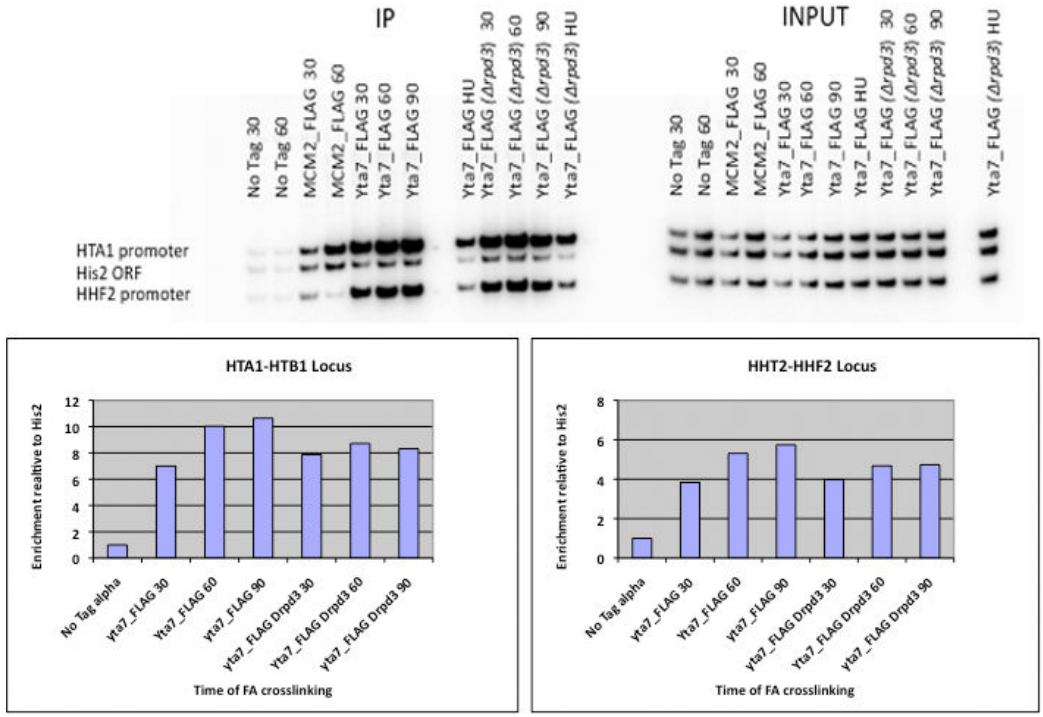

Figure 4.5: Optimisation of ChIP conditions - Yta7p. Formaldehyde cross-linking times of 30, 60 and 90 minutes were compared for the G1 arrested Yta7-FLAG strains in either a WT or a Δ*rpd3* background. No tag strains were cross linked for either 30 or 60 minutes and these strains were arrested in G1. Top figure is raw gel data for comparison with analysis results. Strains used are MMY001 (No tag), MVY125 (Mcm2-FLAG), MVY104 (Yta7-FLAG) and MVY105 (Yta7-FLAG Δ*rpd3*). G1 arrested samples were cross-linked in formaldehyde for 30, 60 and 90 minutes as indicated, or cells were arrested in HU prior to cross-linking (HU). First gel contains IPs, second gel (right hand side) contains INPs. Regions tested for enrichment are those in Fig. 4.3 (*HTB1-HTA1* promoter and *HHT2-HHF2* promoter) and the *HIS2* ORF as a negative binding region. Graphs display analysed results. X axes show no tag strain cross-linked for 60 minutes, followed by the Yta7-FLAG strain cross-linked for 30, 60 or 90 minutes and finally the Yta7-FLAG Δ*rpd3* strain cross-linked for 30, 60 or 90 minutes. Y axes represent enrichment of Yta7-FLAG normalised to INP, and divided by normalised *HIS2* ORF. Left hand side graph represents enrichment at the *HTA1-HTB1* locus and the right hand side graph is for the *HHT2-HHF2* locus. As per previous optimisation experiment, the experiment shown represents the optimised conditions and was performed once.

approximately 300bp away from the *HTB1* gene and therefore, approximately 800bp from the promoter. Therefore the enrichment of Mcm2p witnessed at the *HTA1-HTB1* promoter likely reflects loading of the MCM2-7 complex at ARS428. Mcm2-FLAG enrichment at the *HTA1-HTB1* promoter is lower than at ARS609, which would be expected, as only a subset of DNA fragments produced by sonication would be long enough to have been immunoprecipitated with Mcm2p by the FLAG antibody and also contain the *HTA1-HTB1* region detected with the primers used. There is no enrichment of Mcm2-FLAG at the *HHF2* promoter (gel image Fig. 4.5) and correspondingly on SGD there is no known ARS element in the vicinity of this promoter.

One interesting fact to emerge from these optimisation experiments was that when treated with HU, the level of Yta7p bound to the histone gene promoters in both WT and Δ*rpd3* backgrounds was reduced to approximately half the level observed in G1; refer to Fig. 4.6 (compare columns 3 and 4 plus columns 5 and 6 in each graph). It is not conclusive if this is a real biological effect or a consequence of less than optimal cross-linking in cells treated with HU. However, if there is less Yta7p at histone promoters in HU, then this, in combination with the fact that Yta7p binds at histone promoters when not in HU, could indicate a role for Yta7p in controlling histone levels. Histone levels should be rapidly decreased in HU [Hereford et al., 1981] and Yta7-FLAG shows reduced binding to the histone promoters. In addition, three recent papers all suggest a role for Yta7p in controlling histone gene expression [Gradolatto et al., 2008], [Fillingham et al., 2009], [Gradolatto et al., 2009]. These authors suggest opposing roles for Yta7p, with one group suggesting it acts as a cell cycle dependent repressor at all histone loci, and the other suggesting it acts at all loci except *HTA2-HTB2* as an activator of histone gene transcription. Therefore, there could be an indirect transcriptional role of Yta7p in DNA replication. These indirect transcriptional effects of Yta7p on histone genes could explain the slower S phase of a Δ*rpd3* strain that is lacking Yta7p. Therefore, before continuing with a timecourse experiment to detect Yta7p at replication origins, it was important to understand if Δ*yta7* could affect the histone protein levels in the cell.

The first of the three reports, referred to above, was published shortly after I had completed the optimisation of the ChIP experiment, with the other two published very recently, after I had completed all of the subsequent experiments. The earliest report indicated that Yta7p could be a repressor of histone genes and this made it necessary to confirm if the replication phenotypes I had observed in Chapter 3 were due to misregulation of histone levels. High levels of histones during HU induced arrest, which may result from loss of a histone gene repressor, could divert Asf1p away from replication origins, refer back to Section 1.5.2. According to the proposed model, DNA replication would not resume efficiently without adequate levels of Asf1p available for parental histone recycling at the fork [Groth et al., 2007]. This model was proposed based on experiments in human cells. To test if this could be the cause of the observed DNA replication phenotypes of the Δ*rpd3*Δ*yta7* strain, cells were taken from both an asynchronous population and a HU arrested population (confirmed by FACS profiles; Fig. 4.7(A)) for WT, Δ*rpd3*, Δ*yta7* and Δ*rpd3*Δ*yta7* strains. Then a western blot using an antibody for the H3 C

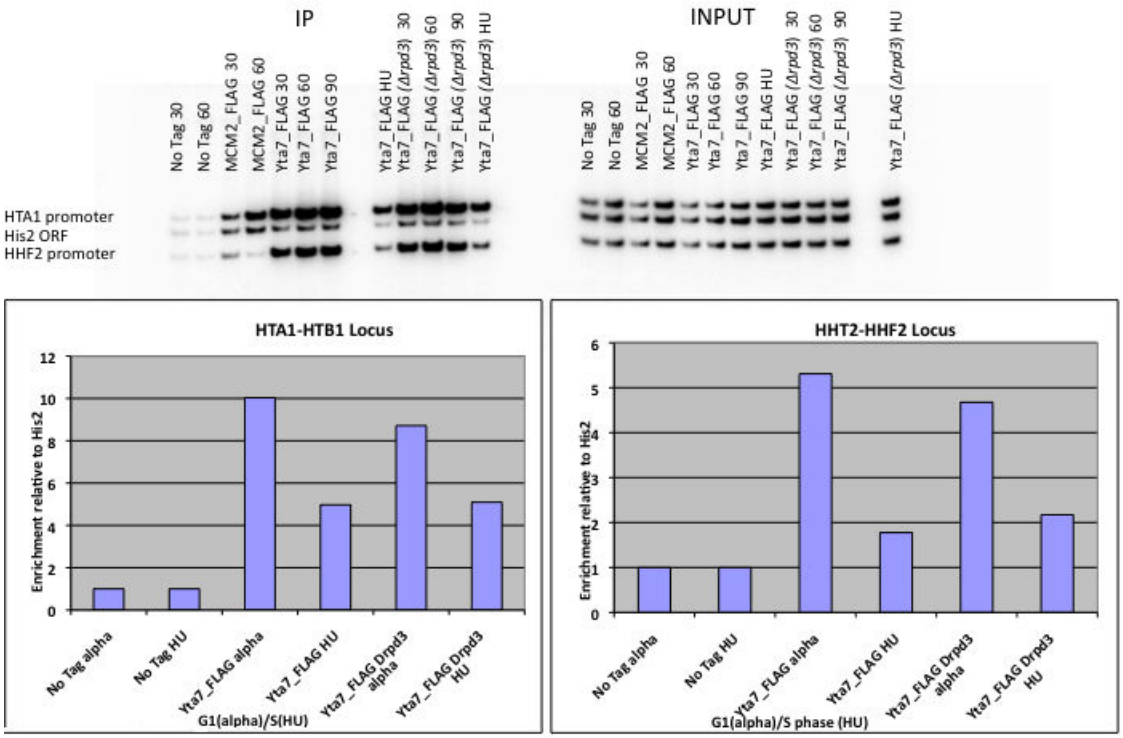

Figure 4.6: Level of Yta7-FLAG bound at histone gene promoters reduces to approximately half that of G1 (alpha) arrested cells upon HU treatment. Top figure is raw gel data for comparison with analysis results. Strains used are MMY001 (No tag), MVY125 (Mcm2-FLAG), MVY104 (Yta7-FLAG) and MVY105 (Yta7-FLAG Δ*rpd3*). Strains were either arrested in G1 (alpha) or Hydroxyurea (HU) and crosslinked for 60 minutes with formaldehyde. Left hand image represents IP experiments, right hand image is INP. Regions tested for enrichment are those in Fig. 4.3 (*HTB1-HTA1* promoter and *HHT2-HHF2* promoter) and the *HIS2* ORF as a negative binding region. Graphs display analysed results. X axes show no tag strain arrested in G1 or HU, followed by the Yta7-FLAG strain arrested in G1 or HU and finally the Yta7-FLAG Δ*rpd3* strain arrested in G1 or HU. Y axes represent enrichment of Yta7-FLAG normalised to INP, and divided by normalised *HIS2* ORF. Left hand side graph represents enrichment at the *HTA1-HTB1* locus and the right hand side graph is for the *HHT2-HHF2* locus. As per previous optimisation experiments, the experiment shown represents the optimised conditions and was performed once.

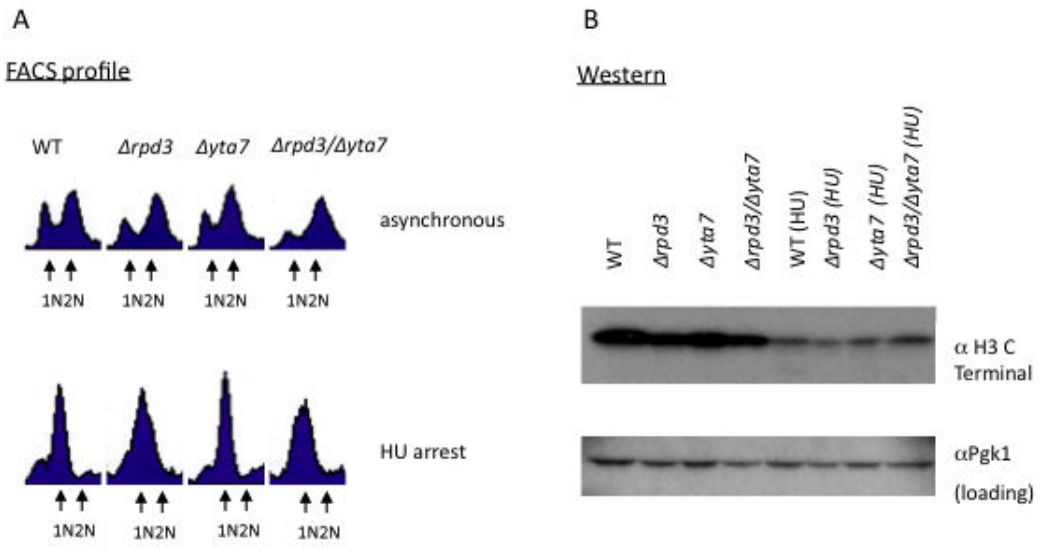

Figure 4.7: H3 levels are similar in WT and deletion strains. (A): FACS analysis was performed on all strains to confirm asynchrony and efficient S phase arrest. Top figure shows the FACS profile of strains MMY033 (WT), MVY51 ($\Delta rpd3$), MVY63 ($\Delta yta7$) and MVY64 ($\Delta rpd3\Delta yta7$) when growing asynchronously. Cells are distributed randomly between 1N and 2N DNA content. Bottom figure confirms that the same strains were arrested in HU in early S phase with a 1N DNA content of cells. (B): Western blot using antibodies for αH3 C Terminal and αPgk1p as a loading control. The same strains that are represented by the FACS profiles in (A) were used to test H3 levels. Top image is the fluorescence signal detected for H3. Bottom image is the fluorescence signal detected for Pgk1p. The four lanes on the left are the asynchronous strains and the four lanes on the right are the HU arrested strains. The experiment was repeated twice and one representative result is shown.

terminal was performed to compare H3 protein levels in these strains; Fig. 4.7(B).

If the phenotypes observed for $\Delta rpd3\Delta yta7$ were due to largely altered levels of histones in this strain, then this alteration could be observed in both the asynchronous and HU arrested conditions. This experiment would allow comparison of histone levels, both for normal replication (asynchronous experiment) and in the S phase checkpoint (HU experiment) and highlight any alterations. As shown in Fig. 4.7(B), an alteration in H3 levels was not the case with total H3 protein levels remaining the same for all strains (compare relative intensity of H3 signal with relative intensity of Pgk1p signal for each strain). In addition, the levels reduced concomitantly in all strains upon HU induced arrest as anticipated. Given the more recent result that Yta7p is an activator of at least some histone genes, as is suggested in [Fillingham et al., 2009], it would have been prudent to check H3 levels in $\Delta rpd3\Delta yta7$ cells that are recovering from HU induced arrest. Histone availability would have to be increased again once the stimulus to activate the checkpoint had been removed. Decreased availability of histones at this time, caused

by deletion of a histone gene activator, could also affect the ability of a cell to resume efficient DNA replication after HU recovery. At the time, however, an activation role was not indicated. Plus, under normal replication conditions the H3 levels of all four strains were not significantly altered, as the asynchronous strains show (compare the first four lanes of Fig. 4.7(B) for both H3 and Pgk1p in each strain). This HU recovery experiment could still be interesting to complete; if the histone protein levels are decreased in a Δ*rpd3*Δ*yta7* strain compared to WT when recovering from S phase checkpoint arrest, this could add to our information regarding the HU sensitivity of this strain.

4.3 Discussion

As a result of optimising the ChIP conditions for Yta7-FLAG so that a time course profile of Yta7p binding to origins could be produced I identified Yta7p binding to the histone gene promoters. This result has been confirmed in subsequent papers of two independent groups [Gradolatto et al., 2008], [Fillingham et al., 2009]. However, while I identified binding of Yta7p to both the *HTB1-HTA1* and the *HHT2-HHF2* promoters, and I witnessed a decrease of binding in conditions of HU treatment, I could not detect any influence of deletion of *YTA7* or *RPD3* on the total levels of the H3 protein. Therefore the probability that the role of Yta7p in DNA replication is due to effects on the histone genes is reduced. Many points highlighted here argue against all of the observed replication phenotypes being caused by Yta7p effects on histone gene transcription alone. Firstly, whilst transcription and mRNA levels might change depending on the absence or presence of Yta7p the protein levels that could directly affect replication do not seem largely altered. Western blot would not detect very subtle changes in protein levels, but any large alteration would have been noticed. Secondly, it is well documented that transcription is not the only form of control of cellular histone levels. Protein degradation through the action of Rad53p, in addition to mRNA processing, can also affect the histone protein levels during S phase [Gunjan and Verreault, 2003], [Xu et al., 1990]. Thirdly, it is possible that the effect of decreased Yta7p binding in HU may be an artefact of HU treatment, but even if the observed decrease were true the same difference is observed in both a WT and Δ*rpd3* background, so an effect would be anticipated in both the single Δ*yta7* and double mutant on histone levels, but the single mutant has no DNA replication phenotype. For the double mutant alone to be affected there would have to be a confirmed effect of Δ*rpd3* on histone levels, which to my knowledge there is not, and the combined effect would have to affect total protein levels.

As described previously, the three reports that suggest that Yta7p has a role in histone gene transcription have contradictory results, with one group noting repression of histone genes and the other activation of histone genes by Yta7p [Gradolatto et al., 2008], [Fillingham et al., 2009], [Gradolatto et al., 2009]. The first report, [Gradolatto et al., 2008], looked specifically at S phase and used RNA extraction followed by reverse transcription and real-time PCR. They noted only a small delay in reaching maximum levels of histone mRNA

levels when Yta7p was present in comparison to when it was absent. Total histone mRNA levels were not different between the WT and $\Delta yta7$ strains in this assay. The experiments relied upon synchronous release from both alpha factor and nocodazole separately. The authors observed large asynchrony in the nocodazole release between strains and so relied on the alpha factor release to draw their main conclusion. However, in the alpha factor released strains the minor increase in mRNA levels observed at earlier timepoints for $\Delta yta7$ was accompanied by a minor asynchrony between the two strains (observable by FACS at the 30 minute time point) and a lower proportion of WT cells in S phase (implied from the Budding Index at the 0 time point).

The second report, [Fillingham et al., 2009], used a Synthetic Genetic Array to test the effect of specific gene deletion on *HTA1* gene expression. The experiment was designed to test specifically for promoter regulation and not mRNA stability. $\Delta yta7$ resulted in an approximate 2 fold decrease in *HTA1* expression. The other histone genes were not investigated for a specific $\Delta yta7$ effect. However, the author's investigation of Yta7-TAP binding showed that Yta7-TAP is located at the promoter of all histone gene pair regions except *HTA2-HTB2*. Furthermore, the binding of Yta7p at *HTA1-HTB1* is dependent on *HIR1*, but is not affected by Rtt109p directed H3K56ac. In turn, Yta7p binding at the promoter and over the ORF restricts Rtt106p binding from spreading through the ORFs of *HTA1* and *HTB1*. Hir1p is a histone chaperone involved in transcriptional repression of the histone loci and Rtt106p is involved in deposition of histones specific for "heterochromatin". Thus, Yta7p acts as a boundary element at the *HTA1-HTB1* locus to prevent heterochromatin spreading and silencing of *HTA1*. This elegant study also demonstrated that the binding of Yta7p to the ORFs of histone genes meant that it occupied the same region as yFACT. They also suggested that *HIR1* dependent recruitment of Yta7p could be due to the post translational histone modifications present on the Asf1p/Hir/Rtt106p deposited H3/H4, although this remains to be tested.

The binding of Yta7-MYC to all of the histone loci except *HTA2-HTB2* was also confirmed by ChIP-Chip in [Gradolatto et al., 2008]. The authors suggest binding at the *HTA2-HTB2* locus also, but enrichment over the promoter region is approximately 1 compared to a range of approximately 2.7 to 4 fold for the other promoter regions. In addition peak enrichment of the *HTA2-HTB2* region occurs over the ORFs. Furthermore the highest level of enrichment (approximately 3) relies on the presence of only two clones of the array, if these were removed the peak of enrichment of the whole region would be approximately 2.4 fold (compared with a range of 3.7 to 4.5 fold for the other regions). However, the fact that Yta7p binds at least at three of the histone promoter regions suggests Yta7p could have an effect on several histone genes. This effect is possibly quite complicated, as the third report [Gradolatto et al., 2009] showed that $\Delta yta7$ led to an increase in *HTB1* transcription through use of RNA extraction, reverse transcription and real-time QPCR of asynchronous cells. It should be noted, however, that the primers used in [Gradolatto et al., 2008] were all tested for specificity except for the primers of this specific region as deletion of the *HTB1* gene was inviable. The other regions were not included in [Gradolatto et al., 2009].

These conflicting results, that Yta7p both activates and represses histone gene transcription, could be explained by the nature of the two experimental approaches. One group found a decrease in transcription of *HTA1*, whilst the other noted increased mRNA levels at an earlier time point in S Phase when *YTA7* is deleted. Perhaps indeed Yta7p acts as a boundary element to prevent the spread of heterochromatin at histone loci, while at the same time it can also affect histone mRNA stability, whereby loss of Yta7p causes an increase in mRNA levels in a shorter time frame. A role as a boundary element, rather than a direct activator or repressor, for Yta7p at the histone gene loci is also supported by the fact that I observed high levels of Yta7p bound in G1 and lower levels of Yta7p, but still present, in HU. Whilst the "co-existence" of Yta7p with H3K56ac [Gradolatto et al., 2008] would suggest that it is also bound throughout S phase. Hence, it does not show the specific binding pattern that would be expected for a role as an "on" or "off" switch.

In terms of the transcription effect of Yta7p on histone genes being responsible for the S phase phenotype of the $\Delta rpd3\Delta yta7$ strain in Chapter 3, if the effect seen in [Gradolatto et al., 2008] of increased levels of histone mRNA at an earlier time point in a $\Delta yta7$ strain were to affect the histone protein levels, then there would be an increase in the available histone pool. According to the Asf1p model of [Groth et al., 2007] this would draw Asf1p away from the fork, but in humans this resulted in a checkpoint activation defect and was dependent on increasing the histone levels by 3 fold. None of the strains used in the previous experiments of this thesis displayed such a checkpoint activation defect and there is not a 3 fold increase in H3 levels in any strain. However, if Yta7p is involved in activating histone gene transcription then this could play a part in its role in DNA replication; if there are less cellular histones available perhaps firing excess origins at an earlier time point, as for $\Delta rpd3$, would no longer be feasible. However, it is improbable that histone activation would be a major part because for histone transcription to be the sole effect it would have to alter the total protein levels, not just the transcription levels.

It has been shown that $\Delta yta7$ has synthetic defects with the histone chaperones [Gradolatto et al., 2008], [Gradolatto et al., 2009]. The authors showed genetic interactions with *SPT16*, *ASF1* and the *HIR1/2* genes either at 34°C or under HU treatment. Spt16p and Asf1p also have a role at the replication fork, refer back to Sections 1.10.1 and 1.5. Therefore, a direct role for Yta7p at replication origins/forks is still possible.

In summary, the ChIP conditions which have been optimised in this chapter could serve to monitor Yta7p at replication origins during S phase. By cross-linking cells with formaldehyde for 60 minutes, then using an anti FLAG antibody to enrich for DNA bound by Yta7p I have managed to detect binding of Yta7-FLAG to the histone gene promoters. The signal was specific to this region as the same ChIP experiment identified no binding of Yta7p to the *HIS2* ORF and showed no enrichment in an untagged strain. This binding of Yta7p to the histone promoter region has since been confirmed by two independent studies [Gradolatto et al., 2008], [Fillingham et al., 2009]. I have ruled out the probability that the S phase phenotypes of the $\Delta rpd3\Delta yta7$ strain are due to the effect of Yta7p on histone gene

transcription. Hence, the most efficient way to understand if the role of Yta7p in DNA replication is to function directly at sites of active replication would be to continue with the time course experiment.

Chapter 5

Yta7p is Localised to Replication Origins at Approximate Time of Activation

5.1 Introduction

Once the ChIP experiment for Yta7p was optimised and the probability that histone transcription was the major effect for Yta7p in DNA replication was ruled out, I continued with the time course experiment. The original hypothesis suggested that Yta7p might bind to replication origins at the time of their activation and also that there would be an increased binding of Yta7p to the late-firing origins in the Δ*rpd3* strain. The increase in acetylation at the late-firing origins that causes them to fire earlier should recruit more Yta7p to those origins specifically in the Δ*rpd3* strain compared to the WT. As stated in Chapter 4, this ChIP experiment was performed in two different strain backgrounds (although both in W303a strains). This made comparison of the two sets of results more difficult, but simultaneously gave an increased confidence in the results attained. For unbiased comparison I provide the results of both of the experiments in this chapter.

5.2 Results

No Tag, Yta7-FLAG and Yta7-FLAG Δ*rpd3* strains were synchronised with α factor then released into S phase and samples were taken every five minutes for FACS analysis, Budding analysis (x1) and ChIP in parallel.

The FACS analysis and Tbud for the first experiment presented indicate that, while each strain displayed a good arrest and synchronous release of cells individually, the release was not

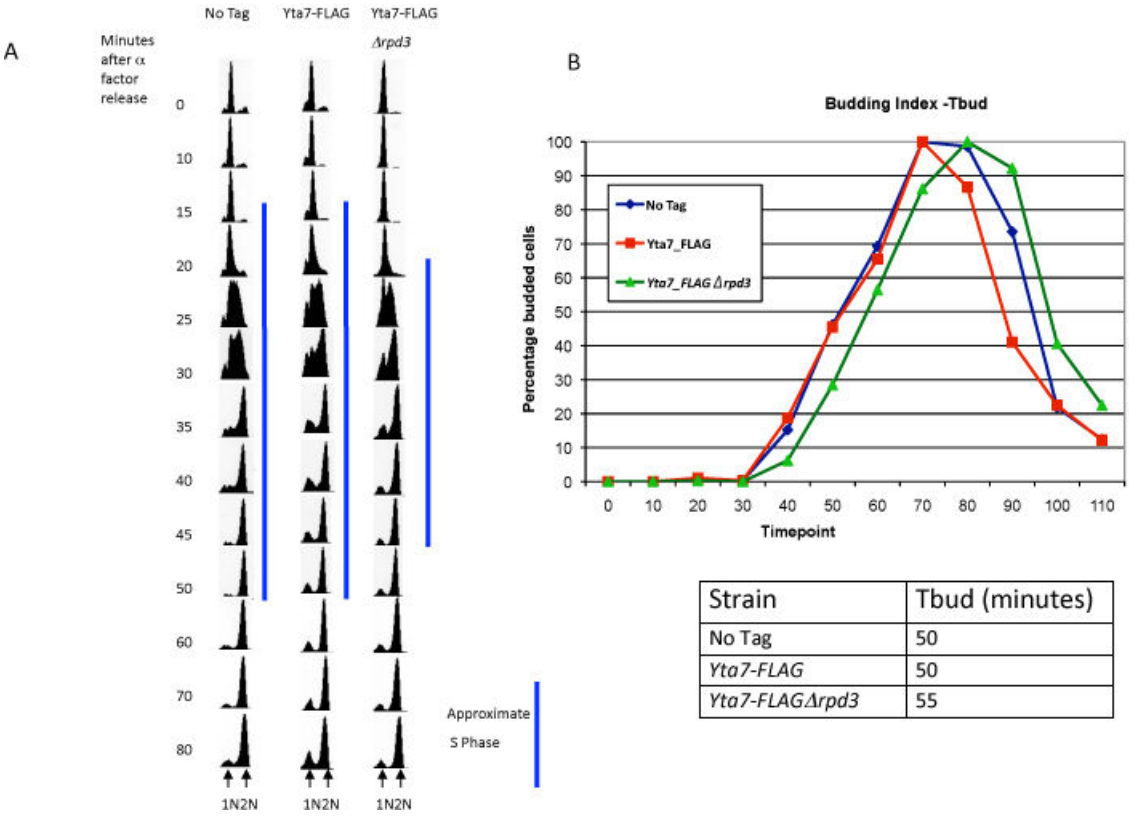

Strain	Tbud (minutes)
No Tag	50
Yta7-FLAG	50
Yta7-FLAGΔrpd3	55

Figure 5.1: Yta7-FLAG ChIP experiments. Release from alpha factor was delayed by approximately 5 minutes in the Yta7-FLAG Δ*rpd3* strain. (A): FACS analysis of strains MVY209 (No Tag), MVY210 (Yta7-FLAG) and MVY211 (Yta7-FLAG Δ*rpd3*). Each time point indicates the minutes following alpha factor release. 1N indicates a haploid DNA content. 2N indicates the cells have replicated the DNA completely. Blue bar indicates approximate S phase length in each case. S phase was assigned as per same parameters of Fig. 3.2. (B): Budding Index confirms the delayed release of Yta7-FLAG Δ*rpd3* from alpha factor of approximately 5 minutes. Y axis of graph represents the number of buds reached as a percentage of total buds for each strain. X axis represents time in minutes. Blue line is strain MVY209 (No Tag), red line is MVY210 (Yta7-FLAG), and green line is MVY211 (Yta7-FLAG Δ*rpd3*). The table gives the Tbud value for each strain, which is the time at which 50 percent of the cells were budded.

completely synchronous between the four strains; Fig. 5.1. The Δ*rpd3* strain release displayed an approximate five minute delay when compared with the No Tag and Yta7-FLAG strains; note that 50 percent of cells were budded at the 50 minute time point for the No Tag and Yta7-FLAG strains while this occurred at approximately 55 minutes for Yta7-FLAG Δ*rpd3*; Fig. 5.1(B). This is most likely a strain dependent effect as it was observed again in the strains re-made by crossing MVY105 and MVY155, that also had Δ*rpd3* (see subsequent Chapter 7). This 5 minute delay should be taken into account for subsequent analyses. In addition, when comparing results, including those of the previous experiments performed using the original strains (refer to Figs. 5.4, 5.6, 5.8 and 5.10), the time of binding should be correlated with the onset of S phase according to each particular FACS analysis. Regardless of the delay, the faster S phase of the strain without Rpd3p was repeatable; approximate length of S phase is between 25 and 30 minutes compared with 35 to 40 minutes for the No Tag and Yta7-FLAG strains (blue bars in Fig. 5.1(A)). Hence, Fig. 5.1 shows that Yta7-FLAG Δ*rpd3* began DNA synthesis approximately 5 minutes later than the other two strains, but then completed S phase in a much faster time frame as expected. With the exception of the 5 minute delay, the release was efficient; all three strains progressed through S phase and reached a 2N DNA content. Therefore, it was possible to continue with the ChIP experiment.

As for the western blot in Fig. 4.2, in the second experiment shown in this present chapter (using the original strains MMY001, MVY104 and MVY105) there was roughly equal expression of Yta7p in both WT and Δ*rpd3* backgrounds; Fig. 5.2(A). There is a slightly lighter signal in the MVY104 strain, but this particular western was performed long after the original ChIP experiments and this may reflect the fact that this strain was becoming sick. As can be observed by the FACS analysis provided, in the time course using the No tag (MMY001) and Yta7-FLAG (MVY104) strains replication began approximately 30 minutes into the experiment in both strains Fig. 5.2(B). In the time course using the Yta7-FLAG (MVY104) and Yta7-FLAG Δ*rpd3* (MVY105) strains replication can be observed from the 20 minute time point in the Δ*rpd3* background, but not until 25 minutes for the WT background Fig. 5.2(C).

All of the ChIP samples were processed using the optimised conditions that were previously presented. However, in contrast to the optimisation experiments, these samples were taken throughout the cell cycle as the point was to monitor S phase. This meant that in order to test the binding of Yta7p to origins I had to choose a new negative control region. Since the cells are undergoing replication there is, in essence, no true negative region for a protein that travels with the replication fork, which could be the case for Yta7p. Therefore, a very late replicating region with no nearby efficient origins, approximately 500bp centromeric to telomere VI-R, was chosen as the best possible "negative" region. This region would not be replicated, and hence display a signal, until after the tested origins had fired and so would not interfere in detection of bound Yta7p at either the early-activating or late-activating origins. To cover a range of activation times primer pairs were chosen that covered the early-firing origins ARS607 and ARS305, the late-firing origins ARS1412 and ARS603 and the subtelomeric ARS501. As stated in Section 1.3, a number of studies have been undertaken to identify replication origins in *S. cerevisiae* and

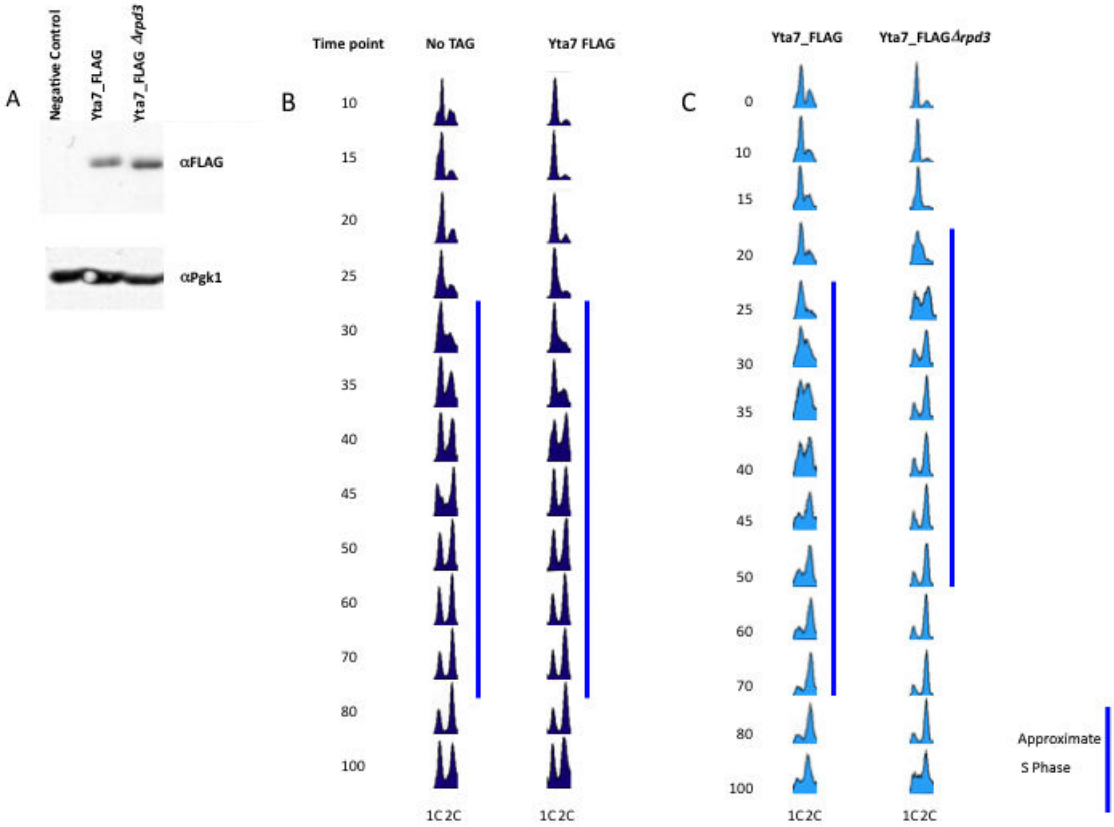

Figure 5.2: Yta7-FLAG strain verification and FACS replicates for original Yta7-FLAG timecourse experiments in MMY001, MVY104 and MVY105. (A): Western blot of strains MMY001 (Negative Control), MVY104 (Yta7-FLAG) and MVY105 (Yta7-FLAG Δ*rpd3*). Top gel is signal of αFLAG and bottom gel is for loading control, αPgk1p. (B): Original FACS analysis of No Tag and Yta7-FLAG strains (MMY001 and MVY104). As per previous FACS, each time point indicates the minutes following alpha factor release. 1C indicates a haploid DNA content. 2C indicates the cells have replicated the DNA completely. Blue bar indicates approximate S phase length in each case. S phase was assigned as per same parameters of Fig. 3.2. (C): Original FACS analysis of strains with Yta7-FLAG in WT and Δ*rpd3* backgrounds (MVY104 and MVY105). Description of figure as per (B).

all of the origins used in this study have been identified as efficient with a calculated time of activation on OriDB[1]. In order to be confident in the amplification signals produced by the radioactive PCR, each primer set was tested for linearity across a range of DNA concentrations (0.5, 1 and 2μl) for a subset of samples (one from the Yta7-FLAG ImmunoPrecipitate (IP) and INPUT (INP) and one from the Yta7-FLAG Δ*rpd3* IP and INP). This was to check that the PCR reaction conditions meant that the amount of DNA was being doubled in every cycle when using a certain amount of starting material. The results can be seen in supplementary data Figs. 9.1, 9.2 and 9.3. For the first ChIP experiment shown, conducted with strains MVY209, MVY210 and MVY211, the primer sets were all in the linear range with the conditions used, the percentage signal approximately doubled between the 0.5μl and 1μl samples and then doubled again between the 1μl and 2μl samples; Figs. 9.1, 9.2. Subsequent amplifications used these same conditions and 1μl of DNA. For the second experiment, using MMY001, MVY104 and MVY105, the primers were not as linear as for the first ChIP time course; Fig. 9.3. The DNA of a lower concentration, 0.5μl, had a slight tendency towards over amplification. However in terms of the time course experiment where 1μl of DNA was used this over amplification might only increase "background" signals, hence any enrichment (which would be divided by background) may be slightly underestimated.

The ChIP results, as previously, include the raw image of the gel to support the graph produced by analysis for the relevant primer combinations. Since these results are produced via time course experiments and each result represents a moment in time, it is not possible to repeat the experiment to generate error bars and one final averaged result. In addition, as stated, these experiments were performed using re-made strains; I, therefore, present the data from both experiments here, with the results from one experiment presented immediately before the same result from the second experiment. Fig. 5.3 contains the results for the No Tag (MVY209) and Yta7-FLAG (MVY210) strains when Primer set 1 (ARS607, ARS1412, ARS501 and TEL VI) was used. The No Tag enrichment is generally low, which indicates that the ChIP procedure produced very little background signal. However, there is a slightly increased background for the ARS1412 region when compared with ARS607. There is a striking increase in Yta7-FLAG binding at ARS607 (refer to right hand side graph Fig. 5.3), which reaches maximal levels at the 15 to 20 minute time points. It is expected that the efficient early origins would activate just prior to the point when synthesis was observed in the FACS profile. Indeed, referring back to Fig. 5.1(A), 15 to 20 minutes into the experiment is the time at which synthesis begins in those cells (note that the shift from 1N to 2N in the Yta7-FLAG strain begins around this time). In addition there is a small but reproducible peak of Yta7p binding at both the late-firing origin, ARS1412, and the subtelomeric origin, ARS501, at the 25 to 30 minute time points. Again, referring back to Fig. 5.1(A), this is the point at which the cells of the Yta7-FLAG strain are mid-replication and so fits with the time that it would be expected that the later firing origins would activate. The much lower level of Yta7p bound at the later origins suggests that Yta7p may be more important for the firing of early origins. This

[1] `www.oridb.org` (January 2007)

supports the hypothesis that Yta7p may bind to histone acetylation in the area surrounding early-firing origins to allow their earlier activation.

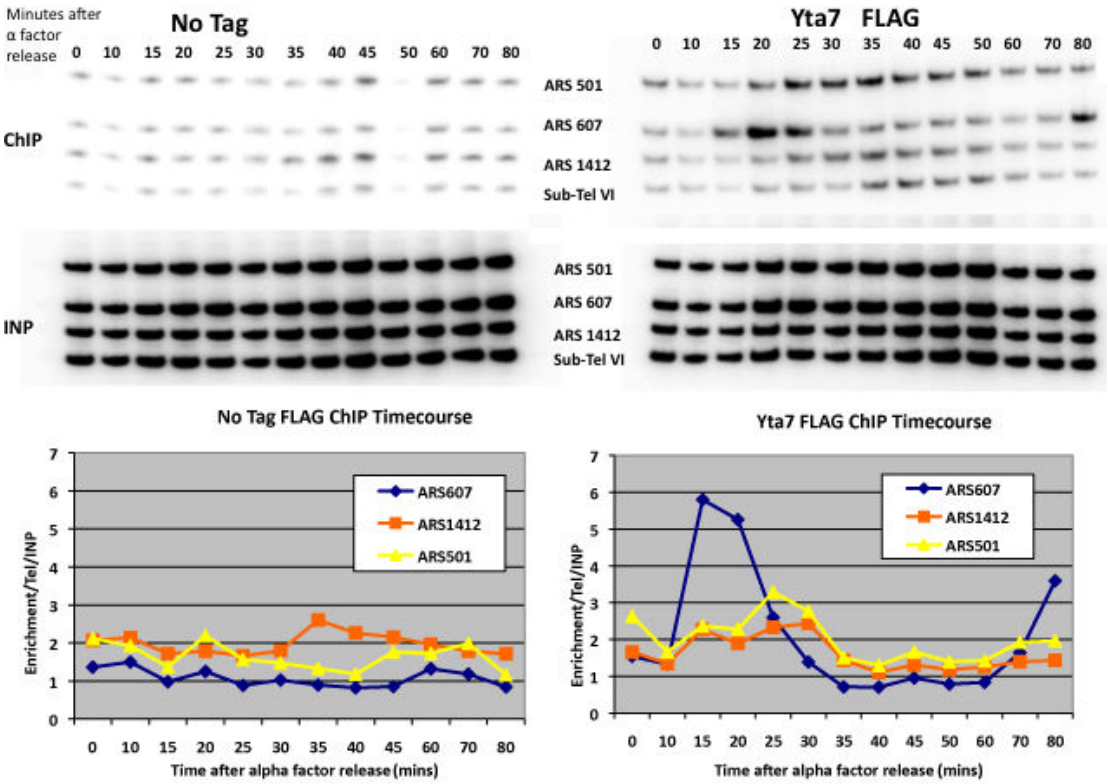

Figure 5.3: Yta7p binds to replication origins at approximate time of activation - 1. Strains used are MVY209 (No Tag) and MVY210 (Yta7-FLAG). Both raw image gels and graphs produced by analysis are shown. Top half are the gels for ChIP (top) and INP (bottom) for the No Tag (left) and Yta7-FLAG (right) strains. Gels from left to right show each time point after alpha factor release. Gels from top to bottom show signal at ARS501, ARS607, ARS1412 and TEL VI. Graphs display analysed results. X axes are time after alpha factor release. Y axes are Yta7-FLAG ChIP signals at origins normalised to INP and divided by normalised TEL VI signal. Left hand side graph is No Tag strain. Right hand side is Yta7-FLAG. Blue line is early origin ARS607, orange line is late origin ARS1412 and yellow line is sub telomeric origin ARS501. Yta7p shows peak binding to ARS607 at 15 minutes, to ARS1412 at 30 minutes and to ARS501 at 25 minutes.

The second ChIP time course experiment displays the same results as the one already presented. For example, in the first graph shown here there is a uniform low signal for the No tag strain, but a defined peak of enrichment for Yta7p at the early-firing ARS607 at the 25-30 minute time point; Fig. 5.4. This mirrors the onset of S phase in this strain, which was approximately 30 minutes; refer back to Fig.5.2(B). Peak enrichment at the late-firing ARS1412 occurred 10-15 minutes later than that for the early origin and was a much lower level, which

repeats the observation of the first experiment; compare Fig. 5.4 with Fig. 5.3 taking into account onset of S phase in both cases.

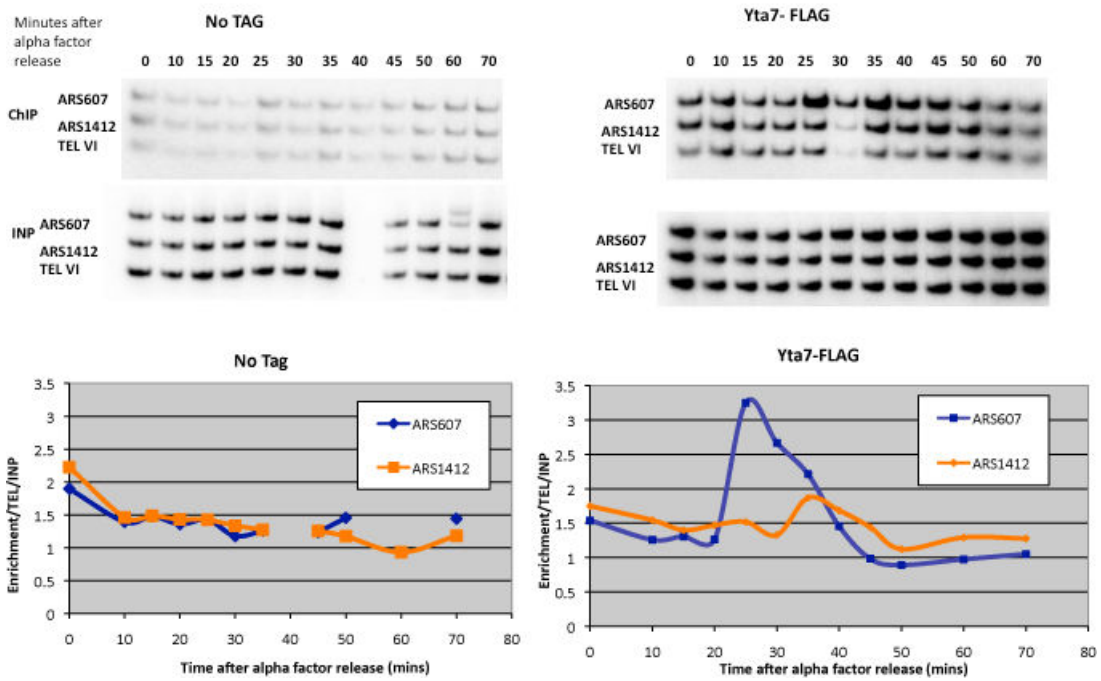

Figure 5.4: Yta7p binds to replication origins at the approximate time of activation - 2. Strains used are MMY001 (No Tag) and MVY104 (Yta7-FLAG). Both raw image gels and graphs produced by analysis are shown. Top half are the gels for ChIP (top) and INP (bottom) for the No Tag (left) and Yta7-FLAG (right) strains. Gels from left to right show each time point after alpha factor release. Gels from top to bottom show signal at ARS607, ARS1412 and TEL VI. Graphs display analysed results. X axes are time after alpha factor release. Y axes are Yta7-FLAG ChIP signals at origins normalised to INP and divided by normalised TEL VI signal. Left hand side graph is No Tag strain. Right hand side is Yta7-FLAG. Blue line is early origin ARS607, orange line is late origin ARS1412. Yta7p shows peak binding to ARS607 at 25-30 minutes and to ARS1412 at 35-40 minutes. Gap regions are due to failed amplification or missing samples.

I next compared the binding profile of Yta7p in the WT and the Δ*rpd3* backgrounds. If the original hypothesis was correct, I could expect to find that the binding of Yta7p to the later firing origins in Δ*rpd3* was at an earlier time point, to coincide with their earlier activation [Vogelauer et al., 2002]. In addition, there would be an increased binding of Yta7p to those "late-firing" origins, which would correlate to the increase in histone acetylation. Fig. 5.5 supports this original hypothesis. The binding of Yta7p to ARS607 in the Δ*rpd3* strain reached maximal levels at the 20 minute time point which, when taking into account the 5 minute delay of this strain, is comparable with the time of binding of Yta7p in the Yta7-FLAG WT strain. Once again, referring to Fig. 5.1(A), twenty minutes post alpha factor release is the point at

which this Δ*rpd3* strain begins DNA synthesis. The striking difference in the Yta7-FLAG Δ*rpd3* binding profile is that the late-firing origin, ARS1412, displays Yta7p (S phase) maximal binding at the 20 minute time point, ten minutes earlier that its WT counterpart (if you take into account the five minute delay). This would correspond well with the conversion of this origin to an "early- activating" origin. The subtelomeric origin, ARS501, also displayed earlier binding of Yta7p in the Δ*rpd3* strain at 25 minutes, but was not as advanced as ARS1412. This result suggests that there might be some secondary effect on subtelomeric regions. In addition, the level of Yta7p bound to these usually late-firing regions is relatively increased; for ARS1412 the increase is to the level observed at the "early" ARS607 in this strain. There is a second difference, noticeable immediately in the Yta7-FLAG Δ*rpd3* binding profile of Fig. 5.5, which is the increased binding of Yta7p in G1 to both ARS1412 and ARS501. However, this G1 signal was not witnessed in the other experiment (Fig. 5.6) and may be an effect of processing in this experiment.

Aside from the G1 signal witnessed in the first experiment the second experiment was again quite comparable with the first even with the different strains used. Fig. 5.6 describes the comparatively increased enrichment of Yta7p at an earlier time point for the late-firing ARS1412 in a Δ*rpd3* strain. Note how the peak enrichment for all origins is between 20 and 25 minutes in the Yta7-FLAG Δ*rpd3* strain (Fig. 5.6) to coincide with an onset of S phase at approximately 20 minutes in this strain (Fig. 5.2(C)). The WT strain has peak enrichment at 30 minutes for ARS607 reflecting the minor delay in release of this strain and once again there is a modest enrichment 10 minutes later at late-firing ARS1412; Fig. 5.6 left hand graph. Compare the binding profiles in Fig. 5.6 with those of Fig. 5.5, again taking into account the onset of S phase as demonstrated by FACS in each case.

The TEL VI region, as previously explained, was chosen as a negative region because it replicates very late in S phase and contains no efficient origins. As can be seen in Fig. 5.5 (refer to the gel image), there is a slight and reproducible (see also Fig. 5.6) enrichment of Yta7p bound to the TEL VI region in both strains at the 35-40 minute time point. However, this slight enrichment occurs after the main enrichment of the late-firing origins and so interferes as little as possible with the ChIP signals. The slight enrichment at the TEL VI region could represent the passing of the replication fork through this region, which would indicate that Yta7p might function at the replication fork. This is a hypothesis that is worth further investigation given the S phase checkpoint recovery defect of the Δ*rpd3*Δ*yta7* strain.

The fact that Yta7p binds to origins at the approximate time that they are expected to activate, and that the level of bound Yta7p increases in conditions when histone acetylation is also increased, supports the original hypothesis, but it was necessary to confirm if these results were repeatable at alternative "early" and "late" firing origins. The ChIP analysis was therefore repeated using the early-firing ARS305 and the late-firing ARS603, with the TEL VI region as a "negative" control. The results are repeatable, with low levels of background for the No Tag strain; refer to graph in Fig. 5.7. The Yta7-FLAG strain has a peak of Yta7p binding at the 15 to 20 minute time points for ARS305, comparable to the results for ARS607, and there is a

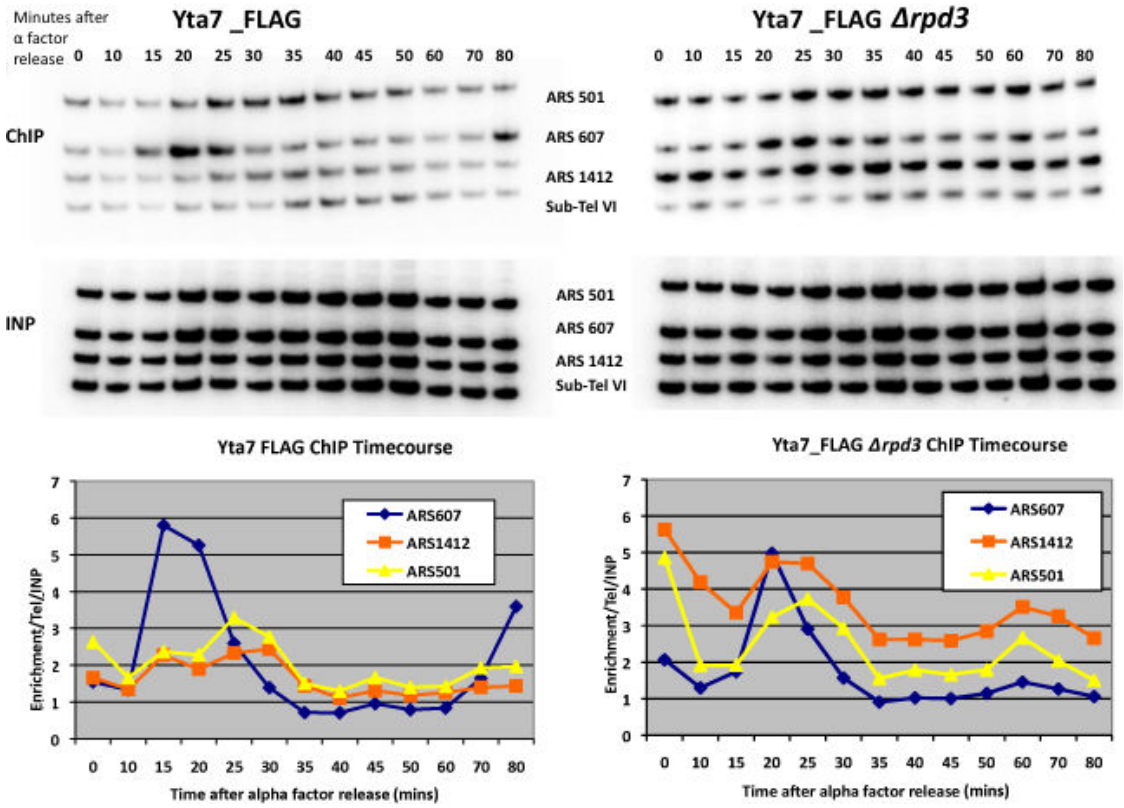

Figure 5.5: Yta7p levels and time of binding of Yta7p to late-firing origins are altered in a Δ*rpd3* strain - 1. Strains used are MVY210 (Yta7-FLAG) and MVY211 (Yta7-FLAG Δ*rpd3*). Both raw image gels and graphs produced by analysis are shown. Top half are the gels for ChIP (top) and INP (bottom) for the Yta7-FLAG (left) and Yta7-FLAG Δ*rpd3* (right) strains. Gels from left to right show each time point after alpha factor release. Gels from top to bottom show signal at ARS501, ARS607, ARS1412 and TEL VI. Graphs display analysed results. X axes are time after alpha factor release. Y axes are Yta7-FLAG ChIP signals at origins normalised to INP and divided by normalised TEL VI signal. Left hand side graph is Yta7-FLAG strain. Right hand side is Yta7-FLAG Δ*rpd3*. Blue line is early origin ARS607, orange line is late origin ARS1412 and yellow line is sub telomeric origin ARS501. Yta7p shows peak binding to ARS607 at 15 minutes, to ARS1412 at 30 minutes and to ARS501 at 25 minutes in MVY210. Yta7p shows peak binding to ARS607 at 15 minutes, to ARS1412 at 15 minutes and to ARS501 at 20 minutes in MVY211, when adjusted for delayed budding.

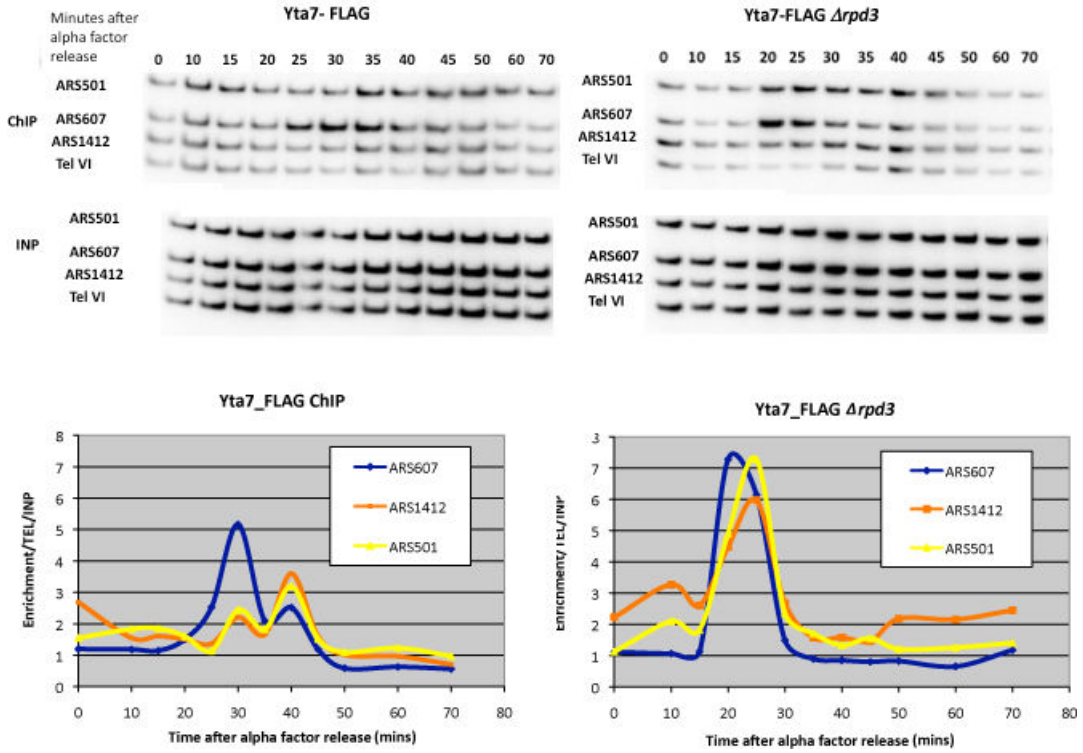

Figure 5.6: Yta7p levels and time of binding of Yta7p to late-firing origins are altered in a Δ*rpd3* strain - 2. Strains used are MVY104 (Yta7-FLAG) and MVY105 (Yta7-FLAG Δ*rpd3*). Both raw image gels and graphs produced by analysis are shown. Top half are the gels for ChIP (top) and INP (bottom) for the Yta7-FLAG (left) and Yta7-FLAG Δ*rpd3* (right) strains. Gels from left to right show each time point after alpha factor release. Gels from top to bottom show signal at ARS501, ARS607, ARS1412 and TEL VI. Graphs display analysed results. X axes are time after alpha factor release. Y axes are Yta7-FLAG ChIP signals at origins normalised to INP and divided by normalised TEL VI signal. Left hand side graph is Yta7-FLAG strain. Right hand side is Yta7-FLAG Δ*rpd3*. Blue line is early origin ARS607, orange line is late origin ARS1412 and yellow line is sub telomeric origin ARS501. Yta7p shows peak binding to ARS607 at 25 minutes, to ARS1412 at 35 minutes and to ARS501 at 35 minutes in MVY104, when adjusted for delayed budding. Yta7p shows peak binding to ARS607 at 20 minutes, to ARS1412 at 25 minutes and to ARS501 at 25 minutes in MVY105.

small peak enrichment at the 25 to 30 minute time point at the late-firing ARS603, comparable to ARS1412.

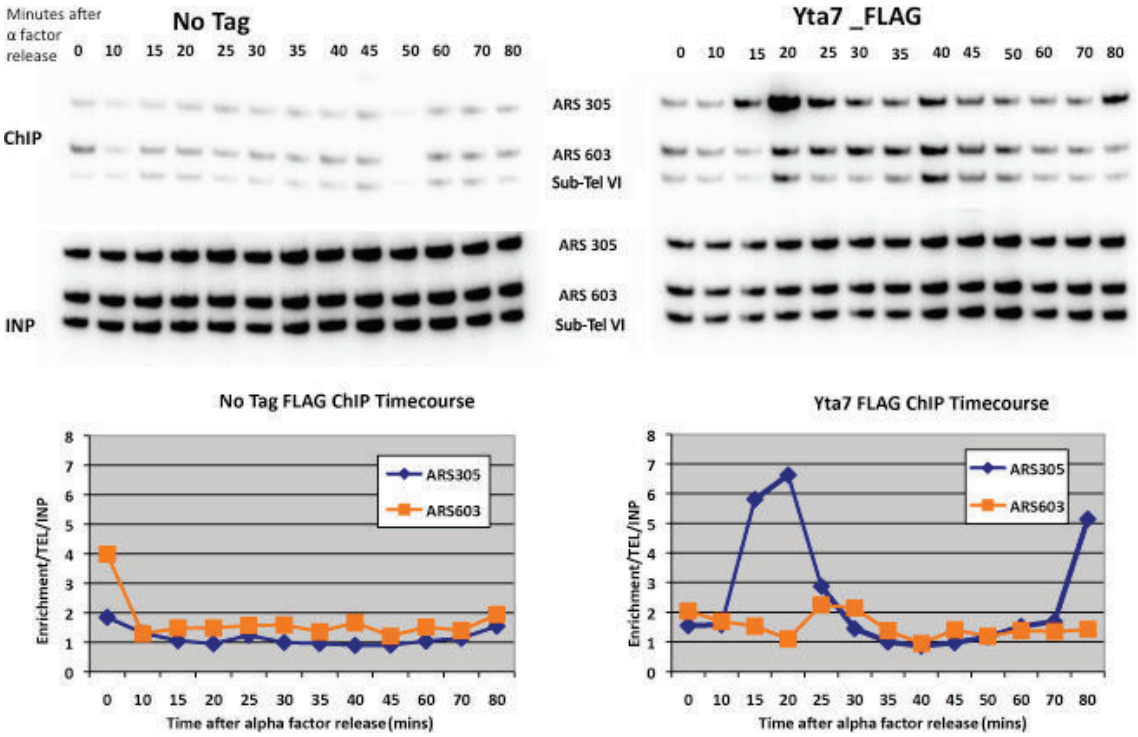

Figure 5.7: The S phase specific binding of Yta7p to replication origins is repeatable at alternative origins - 1. Strains used are MVY209 (No Tag) and MVY210 (Yta7-FLAG). Both raw image gels and graphs produced by analysis are shown. Top half are the gels for ChIP (top) and INP (bottom) for the No Tag (left) and Yta7-FLAG (right) strains. Gels from left to right show each time point after alpha factor release. Gels from top to bottom show signal at ARS305, ARS603 and TEL VI. Graphs display analysed results. X axes are time after alpha factor release. Y axes are Yta7-FLAG ChIP signals at origins normalised to INP and divided by normalised TEL VI signal. Left hand side graph is No Tag strain. Right hand side is Yta7-FLAG. Blue line is early origin ARS305 and orange line is late origin ARS603. Yta7p shows peak binding to ARS305 at 15-20 minutes and to ARS603 at 30 minutes.

The profile of Yta7p binding at an alternative set of origins was also investigated using the MMY001 and MVY104 strains. As for the previous origins, the same low uniform signal can be seen for the No tag strain, while Yta7p peak binding at early-firing ARS305 occurs at 25 minutes in the Yta7-FLAG strain, similar to ARS607 in this strain; Fig. 5.8. Peak enrichment at the late-firing ARS603 is delayed by 15 minutes to the 40 minute time point in this case, and levels of bound Yta7p are, once again, to a much lower level than that seen at "early" origins. A similar profile is witnessed in both Fig. 5.8 and Fig. 5.7.

Fig.5.9 describes the levels of bound Yta7-FLAG in a WT and Δ*rpd3* background at the

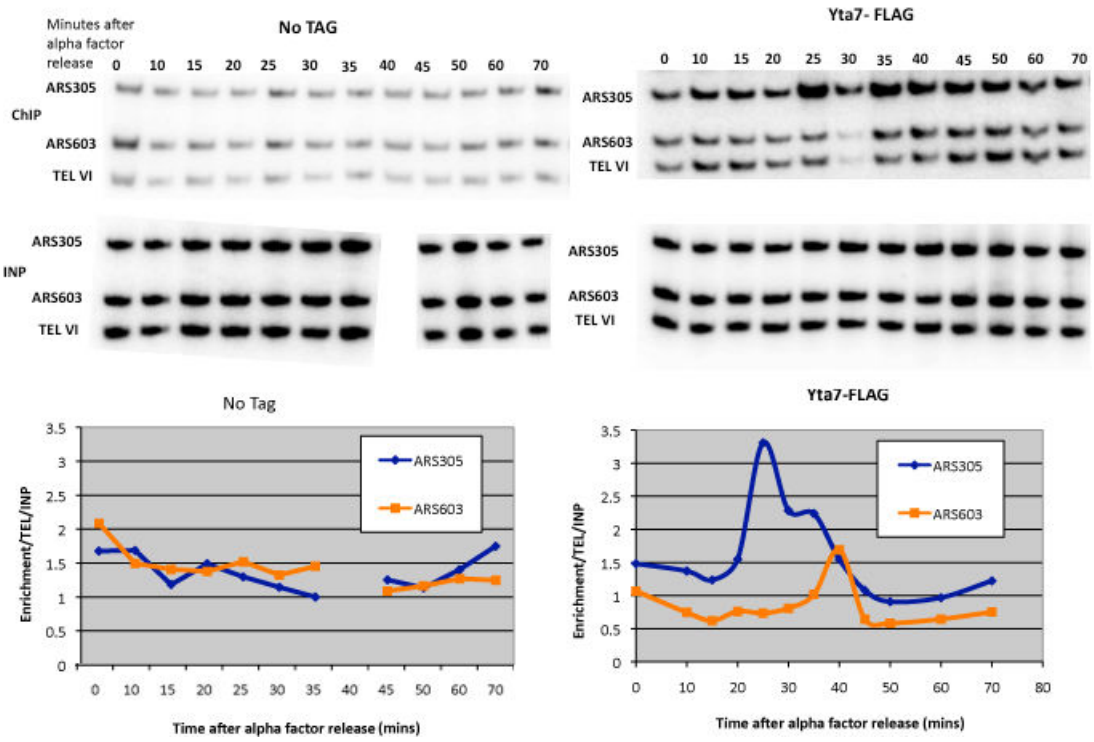

Figure 5.8: The S phase specific binding of Yta7p to replication origins is repeatable at alternative origins - 2. Strains used are MMY001 (No Tag) and MVY104 (Yta7-FLAG). Both raw image gels and graphs produced by analysis are shown. Top half are the gels for ChIP (top) and INP (bottom) for the No Tag (left) and Yta7-FLAG (right) strains. Gels from left to right show each time point after alpha factor release. Gels from top to bottom show signal at ARS305, ARS603 and TEL VI. Graphs display analysed results. X axes are time after alpha factor release. Y axes are Yta7-FLAG ChIP signals at origins normalised to INP and divided by normalised TEL VI signal. Left hand side graph is No Tag strain. Right hand side is Yta7-FLAG. Blue line is early origin ARS305, orange line is late origin ARS603. Yta7p shows peak binding to ARS607 at 25 minutes and to ARS1412 at 40 minutes. Gap regions are due to failed amplification or missing samples.

alternative origins. The earlier binding and increase in Yta7p levels that were identified at ARS1412 in the Δ*rpd3* strain were also observed at the late activating ARS603 when histone acetylation is increased; Fig. 5.9. The maximum binding for both ARS305 and ARS603 is at the 20 minute time point in the Δ*rpd3* strain, and the levels of Yta7p bound to these two origins are much more similar than those in the WT. This result mirrors the situation of ARS607 and ARS1412 in the Δ*rpd3* strain.

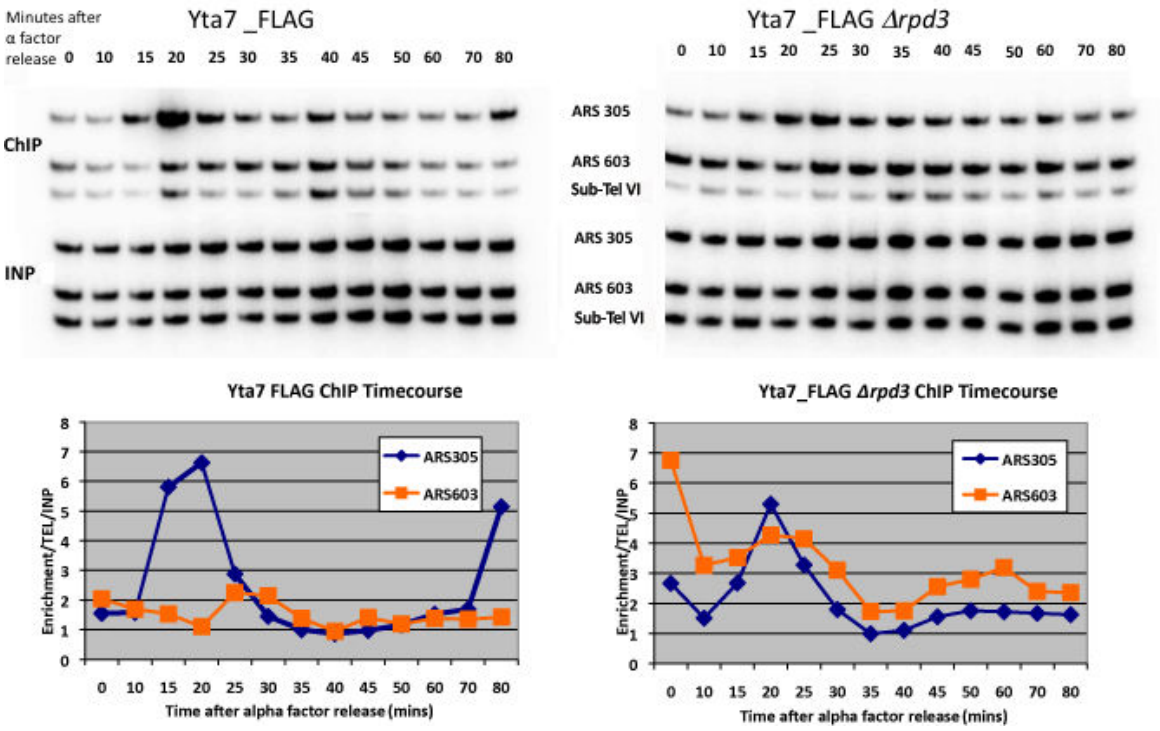

Figure 5.9: The effects of Δ*rpd3* on Yta7p binding are also repeatable at alternative origins - 1. Strains used are MVY210 (Yta7-FLAG) and MVY211 (Yta7-FLAG Δ*rpd3*). Both raw image gels and graphs produced by analysis are shown. Top half are the gels for ChIP (top) and INP (bottom) for the Yta7-FLAG (left) and Yta7-FLAG Δ*rpd3* (right) strains. Gels from left to right show each time point after alpha factor release. Gels from top to bottom show signal at ARS305, ARS603, and TEL VI. Graphs display analysed results. X axes are time after alpha factor release. Y axes are Yta7-FLAG ChIP signals at origins normalised to INP and divided by normalised TEL VI signal. Left hand side graph is Yta7-FLAG strain. Right hand side is Yta7-FLAG Δ*rpd3*. Blue line is early origin ARS305 and orange line is late origin ARS603. Yta7p shows peak binding to ARS305 at 15-20 minutes and to ARS603 at 30 minutes in MVY210 (Δ*rpd3*). Yta7p shows peak binding to ARS607 at 15 minutes, to ARS1412 at 15 minutes in MVY211, when adjusted for delayed budding.

In a final comparison it can be concluded that the profile of Yta7p binding to the alternative set of origins for both YTA7-FLAG and YTA7-FLAG Δ*rpd3* is also repeatable in the MVY104

and MVY105 strain backgrounds; Fig. 5.10. Once again in this second set of strains at this second set of origins the binding of Yta7p to the late-firing origin is both of a relatively increased level and at an advanced time point in a Δ*rpd3* strain when compared with WT Yta7-FLAG. Both ARS305 and ARS603 were bound simultaneously at the 20 minute time point in the Yta7-FLAG Δ*rpd3* strain, which corresponds to approximate S phase entry; Fig. 5.2(C). Compare Yta7p binding patterns in Fig. 5.10 with Fig. 5.9, along with the corresponding FACS analyses, to confirm once again the repeatability of this experiment.

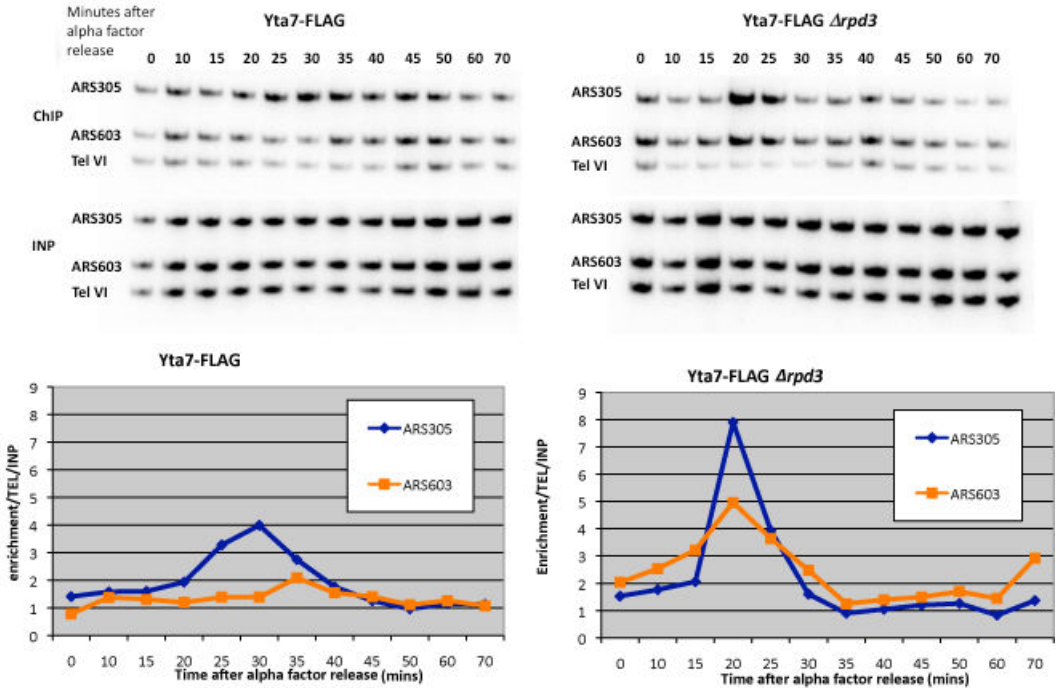

Figure 5.10: The effects of Δ*rpd3* on Yta7p binding are also repeatable at alternative origins - 2. Strains used are MVY104 (Yta7-FLAG) and MVY105 (Yta7-FLAG Δ*rpd3*). Both raw image gels and graphs produced by analysis are shown. Top half are the gels for ChIP (top) and INP (bottom) for the Yta7-FLAG (left) and Yta7-FLAG Δ*rpd3* (right) strains. Gels from left to right show each time point after alpha factor release. Gels from top to bottom show signal at ARS305, ARS603 and TEL VI. Graphs display analysed results. X axes are time after alpha factor release. Y axes are Yta7-FLAG ChIP signals at origins normalised to INP and divided by normalised TEL VI signal. Left hand side graph is Yta7-FLAG strain. Right hand side is Yta7-FLAG Δ*rpd3*. Blue line is early origin ARS305 and orange line is late origin ARS603. Yta7p shows peak binding to ARS305 at 25 minutes and to ARS603 at 30-35 minutes in MVY104, when adjusted for delayed budding. Yta7p shows peak binding to ARS305 at 20 minutes and to ARS603 at 20 minutes in MVY105.

5.3 Discussion

The above results suggest that the role of Yta7p in DNA replication could be a far more direct and varied one than simply influencing the levels of histone gene transcription. The fact that levels of Yta7p bound to origins are greatly increased at the time that it would be estimated those origins are activated is very interesting, but if it could be shown more accurately that this time of binding was really the moment of activation the results would be hugely compelling. To this end, I endeavoured to build a strain that contained a second tag of Cdc45p, which is known to bind to origins at the time that they activate [Aparicio et al., 1999]. The ultimate goal was to repeat the original ChIP time course in these strains, with simultaneous ChIP of both proteins, however it was not possible to create this strain in the Yta7-FLAG WT background (MVY104). Positive colonies were selected only for the Yta7-FLAG Δ*rpd3* Cdc45-MYC strain. Failure to produce the strain in the MVY104 background was possibly due to the problems later identified in this strain. Therefore, this experiment would have to be attempted by using alternative means. The Cdc45-MYC strain could be re-built in the MVY210 and MVY211 strain backgrounds. Alternatively one could use a second tagged protein or a good antibody, if available, raised directly to a protein that can be found at activated replication origins, for example polymerase δ. One could also use alkaline smear gels or 2D gel electrophoresis to detect replication at specific origin regions in a particular time point of the experiment. The 2D gels have the additional advantage that you can specifically monitor activation of the origin, whilst it could be argued that Cdc45p binding could also be a sign of passive replication. Using Cdc45p could also have its advantages; if the resolution of the experiment were good enough it might be possible to detect Yta7p binding just prior to, or just after, Cdc45p binding, which would indicate at which point of origin activation or replication Yta7p might act. Detecting the presence of Yta7p at regions downstream from an origin at appropriate time points after origin activation could also determine if Yta7p is, in addition, a component of the replication fork.

The ChIP data supports the hypothesis that Yta7p binds to increased histone acetylation that surrounds replication origins. The change in levels and time of Yta7p binding at late-firing origins in the Δ*rpd3* strain also supports the hypothesis. However, the results are not definitive. To further test this hypothesis it will be necessary to gain a better insight into the binding properties of Yta7p. This could be done from two separate angles. One angle would be to investigate the importance and role of the bromodomain, which will be discussed in Chapter 7. The other angle would be to understand whether Yta7p recognises the acetylation of specific histone residues, or if to simply increase histone acetylation in general is sufficient for recruitment of Yta7p. One additional experiment could be to discover if targeting of the HAT, Gcn5p, to a specific late-firing replication origin (as per [Vogelauer et al., 2002]) would be sufficient to induce increased Yta7p binding to only that origin compared to the other late firing origins. This result would confirm that it is acetylation, specifically, that is attracting Yta7p to particular replication origins. However, given that the bromodomain of Yta7p has a less conserved binding region when compared with the other bromodomain-containing proteins in *S.*

cerevisiae [Jambunathan et al., 2005], it is not certain that Yta7p, in fact, binds to acetylated histone residues. Rather, in the two published studies that have looked specifically at the modified histone preference of Yta7p it was found that not only does the bromodomain of Yta7p prefer to bind unmodified histones, but also that the bromodomain is not the only histone binding region of Yta7p [Gradolatto et al., 2008], [Gradolatto et al., 2009].

In [Gradolatto et al., 2008] a recombinant version of the Yta7p bromodomain region was tested for binding to acid extracted *T. thermophila* histones and bound H3, and to a lesser extent H2B, was identified. The bromodomain was incubated with a number of H3 peptide mimics and the strongest binding partner was found to be the unmodified version. These results are all *in vitro* and, therefore might not reflect the binding requirements of Yta7p *in vivo*. It is also possible that a full length Yta7p may be required for binding of acetylated histones and that additional *in vivo* modifications of Yta7p may be required. As stated in Section 1.9, Yta7p may be a target of both CDK1 and Rad53p [Ubersax et al., 2003], [Smolka et al., 2006]; phosphorylation of Yta7p may alter its binding specificity or activity. In a further experiment of [Gradolatto et al., 2008] Yta7-PrA bound H3 was isolated directly from cells and tested for acetylation at specific residues. The isolation led to a 41 percent peptide coverage for H3, however only H3K56ac was identified; the other residues contained zero percent acetylation. The authors suggest that Yta7p can co-exist with the H3K56ac mark, but it is not required for binding. They suggest the unmodified histone is the substrate for Yta7p, but this interpretation requires that Yta7p does not co-exist with any other acetylation mark and that it binds zero percent of modified histones. However, in [Gradolatto et al., 2009] the same authors identified 622 binding sites for Yta7-MYC across the genome. To purify zero percent acetylated histones with native Yta7p (beyond the H3K56 modification) none of these regions should contain any modification except H5K56ac. It may be necessary to look at cells that are in a specific stage in the cell cycle to identify any modifications at the different regions bound by Yta7p. As demonstrated in the ChIP experiments of this thesis, Yta7p only binds to certain replication origins in a small window of time during S phase.

In [Gradolatto et al., 2009] the authors used a Yta7-bromodomain GST fusion protein, but this time tested affinity of the fusion protein for histones from *S. cerevisiae*. Here they noted pull down of all four histone proteins but again, when tested by mass spectrometry, they observed no enrichment over input for Yta7-bromodomain bound histones for any specific modification. Histone binding in this experiment was again performed *in vitro* with a recombinant Yta7-BD. An additional finding of this report is that there is a second region of Yta7p that has affinity for histones. This will be discussed further in Chapter 7.

While it is not certain whether Yta7p has a preference for histones with post translational modifications or binds preferably to the unmodified version *in vivo*, it remains a possibility that under specific circumstances the binding of Yta7p to chromatin, including binding at replication origins, is influenced by histone acetylation. To ascertain if the binding of Yta7p, specifically to replication origins, is dependent on acetylation of certain histone residues an appropriate course of action would be to discover two things. The first discovery would be to understand

the importance of the bromodomain of Yta7p in DNA replication. The second discovery would be to identify which histone residues and which specific histone modifications are required for binding of Yta7p to origins. Through deletion of the bromodomain region I could ascertain if the bromodomain is required for the roles of Yta7p, that were identified in this thesis, in DNA replication. In addition, cellular histones could be replaced with histones, supplied on a plasmid, that were deleted for all acetylatable tail residues or that had mutations in a combination of residues. This experiment would allow systematic detection of which histone residues, if any, were important to bind Yta7p to replication origins. The above optimised ChIP conditions could be used to monitor binding of Yta7p to origins when different combinations of histones were available.

In summary, I used optimised ChIP conditions to detect Yta7p binding of replication origins in S phase. The time of binding of Yta7p to early origins co-incides with the onset of S phase, as determined by FACS analysis. The time of binding of late replication origins by Yta7p occurs approximately 10 minutes later than that at early origins and the level of Yta7p bound to late origins is much reduced. Deletion of *RPD3* results in earlier activation of "late" replication origins [Vogelauer et al., 2002] and also results in earlier recruitment of Yta7p to those same origins. The level of histone acetylation surrounding replication origins increases in a Δ*rpd3* strain [Vogelauer et al., 2002], at the same time the level of Yta7p bound to the "late-activating" origins also increases relative to the levels in a WT strain. These results were repeatable in experiments that used strains constructed via two separate methods. The fact that Yta7p binds to replication origins at approximate time of activation suggests that Yta7p plays a direct role in DNA replication , but does not allow distinction between a role for Yta7p in the replicative complex or a role for Yta7p at the replication fork. To determine this would be an important step to understanding the function of Yta7p.

Chapter 6

Yta7p has Potential Functions at Replication Origins and Forks

6.1 Introduction

One important question raised by the first FACS experiment in Fig. 3.2, which showed that Yta7p was required for the faster S phase of a Δ*rpd3* strain, is whether this requirement for Yta7p is at the replication origins or the replication forks. The WT S phase in the Δ*rpd3*Δ*yta7* strain could be explained by either an inability to fire the usually late-firing origins at an advanced time, or advanced firing followed by slowing of the replication forks leading to an extended S phase when compared to Δ*rpd3*. To address this question I looked at Cdc45-FLAG binding to replication origins in all four strains. As stated in Section 1.2.2 Cdc45p binding to origins occurs at the moment of origin activation. Binding of Cdc45p to "late-firing" origins was found to be advanced in the Δ*rpd3* strain [Vogelauer et al., 2002], which coincided with the earlier activation of those origins. If this advanced binding of Cdc45p to origins was also witnessed in a Δ*rpd3*Δ*yta7* strain then the slower S phase of this strain would not be due to reversion of the "late-firing" origins to their "normal" activation time. This result would implicate that there was a defect in replication fork movement in this strain. However, if the time of Cdc45p binding were reverted to that of WT in the double mutant, this would indicate that Yta7p is required for earlier origin activation rather than replication fork movement.

6.2 Results

Cdc45p was already FLAG tagged in the strain background that I had used for the original FACS experiment of Fig. 3.2. I therefore repeated the first timecourse FACS and in addition to the FACS and budding analysis, I also took samples for Cdc45-FLAG ChIP. The protocol was already optimised in our lab. The FACS analysis shows that the strains all completed one

cell cycle and that the faster S phase was again unique to the Δ*rpd3* strain; Fig. 6.1(A). The Budding Index (B) demonstrated that both the Δ*rpd3* and the Δ*rpd3*Δ*yta7* strains had a 5-8 minute delay to release from alpha factor which is seen as a 5 minute delay in entering S phase in the FACS. Taking this into account, I continued with the ChIP analysis.

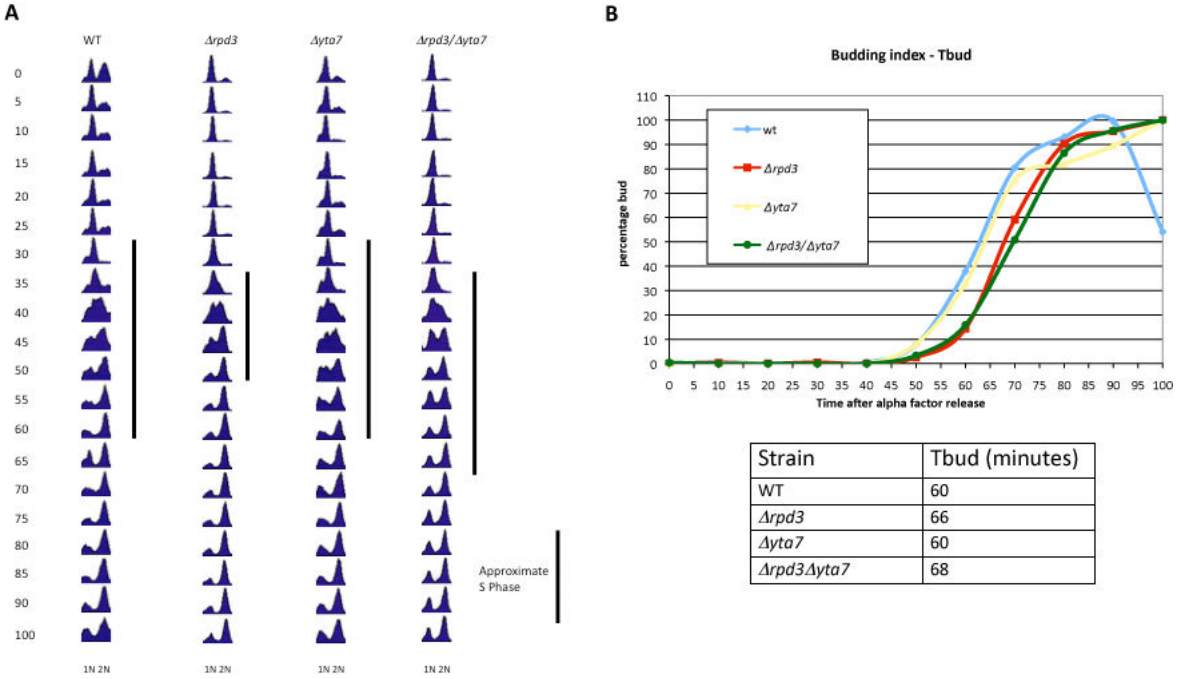

Strain	Tbud (minutes)
WT	60
Δrpd3	66
Δyta7	60
Δrpd3Δyta7	68

Figure 6.1: Cdc45-FLAG ChIP experiments. Release of the Δ*rpd3* and Δ*rpd3*Δ*yta7* strains were delayed by approximately 5-8 minutes. (A): FACS profile of synchronised G1 release of WT (MMY033) and deletion mutant strains: Δ*rpd3* (MVY51), Δ*yta7* (MVY63) and Δ*rpd3*Δ*yta7* (MVY64). Each time point indicates the minutes following alpha factor release. 1N indicates a haploid DNA content. 2N indicates the cells have replicated the DNA completely. Black bar indicates approximate S phase length in each case. S Phase length was assigned using parameters described in Fig. 3.2. Despite the delay to enter S phase of the Δ*rpd3* and Δ*rpd3*Δ*yta7* strains, all strains completed S phase in the expected time frame with only Δ*rpd3* showing a faster completion. The experiment was only completed once. (B): As per Fig. 3.3, number of buds at each indicated time point were counted in the same four strains used for the FACS analysis. Y axis represents the number of buds reached as a percentage of total buds for each strain. X axis represents time in minutes. Blue line is strain MMY033 (WT), red line is MVY51 (Δ*rpd3*), yellow line is MVY63 (Δ*yta7*) and green line is MVY64 (Δ*rpd3*Δ*yta7*). The table gives the Tbud value for each strain, that is the time at which 50 percent of the cells were budded. Tbud calculations show that 50 percent of cells were budded by 60 minutes in the WT and Δ*yta7* strains while the Δ*rpd3* and Δ*rpd3*Δ*yta7* strains only reached 50 percent between 65 and 68 minutes.

For the ChIP analysis, again both the radioactive gel image and the quantification as a line graph are shown. Once adjusted for the delay in budding, the early-firing ARS607 displays peak

Cdc45p binding at the 30 minute time point in all four strains; refer to Fig. 6.2. In contrast the late-firing ARS1412 displays advanced Cdc45p binding at 35 minutes in the Δ*rpd3* strain compared with 45 minutes in both the WT and Δ*yta7* strains. The double mutant Δ*rpd3*Δ*yta7* displays an intermediate time of binding of 35-40 minutes. This suggests that Yta7p might be required for both origin activation and replication fork progression.

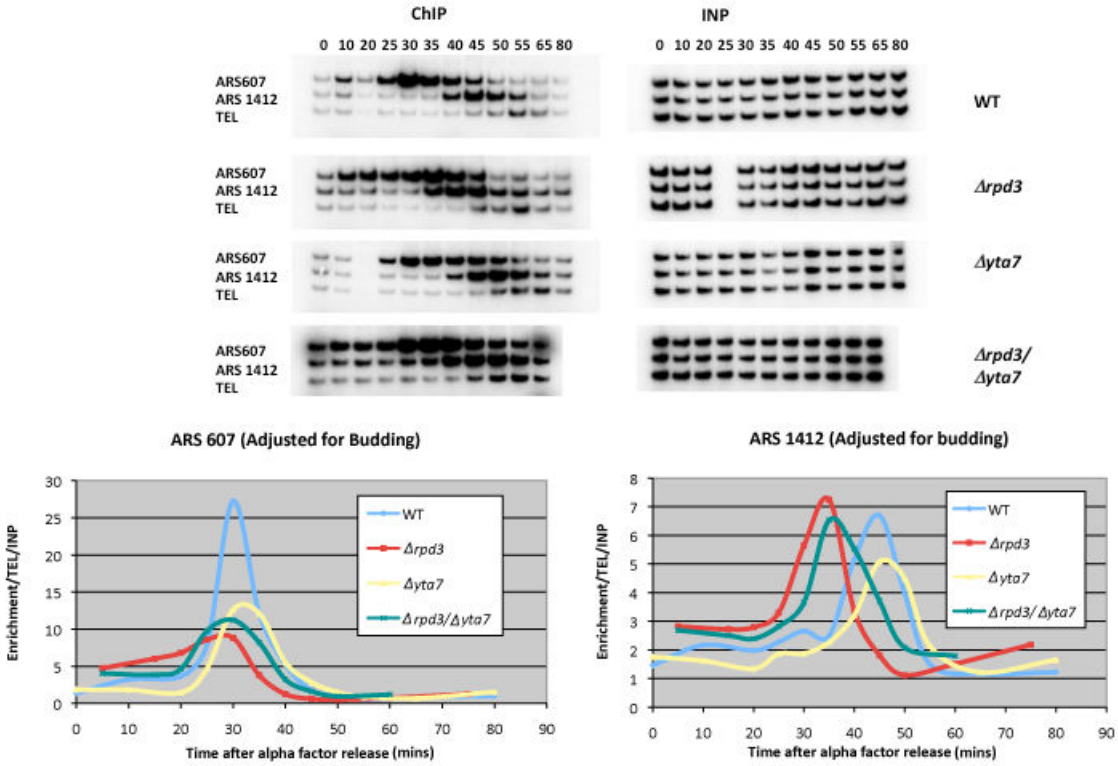

Figure 6.2: Δ*yta7* partially reverts earlier firing of "late" origins in a Δ*rpd3* strain. Strains used are MMY033 (WT), MVY51 (Δ*rpd3*), MVY63 (Δ*yta7*) and MVY64 (Δ*rpd3* Δ*yta7*). Both raw image gels and graphs produced by analysis are shown. Top half are the gels for ChIP (left) and INP (right) for all tested strains. Top gels are WT strain, second gels are Δ*rpd3*, third set of gels are for Δ*yta7* and bottom set are Δ*rpd3*Δ*yta7*. Individual gels from left to right show each time point after alpha factor release. Individual gels from top to bottom show signal at ARS607, ARS1412, and TEL VI. Graphs display analysed results. X axes are time after alpha factor release. Y axes are Cdc45-FLAG ChIP signals at origins normalised to INP and divided by normalised TEL VI signal. Left hand side graph is early-firing ARS607. Right hand side is late-firing ARS1412. All data has been adjusted to account for late release of strains containing Δ*rpd3*. Blue line is WT strain, red line is Δ*rpd3*, yellow line is Δ*yta7* and green line is Δ*rpd3*Δ*yta7*. Peak Cdc45p binding to ARS607 occurs at 30 minutes. However, the binding of Cdc45p to ARS1412 is advanced to 35 minutes in Δ*rpd3* compared with 45 minutes for WT and Δ*yta7*. Cdc45p binding displays intermediate timing for Δ*rpd3*Δ*yta7* with binding from 35-40 minutes.

To test if the same effect was true at alternative origins I repeated the ChIP analysis using primers at the ARS305 and ARS603 regions; refer to Fig. 6.3. Peak Cdc45p binding occurred at 25-30 minutes in the Δ*rpd3* strain and 30 minutes for the other strains at the early-firing ARS305. While again, at the late-firing ARS603 Cdc45p peak binding was at 30 minutes for the Δ*rpd3* strain compared to 45 minutes for the WT and Δ*yta7* strains. Once again the double mutant Δ*rpd3*Δ*yta7* displayed an intermediate time of peak Cdc45p binding of 35 minutes.

6.3 Discussion

The results included in this chapter are made of preliminary data as the experiment was only performed once. The experiment would need repeating, ideally with all four strains releasing from arrest at the same rate before being used as a conclusive result. However, the implications of this preliminary data open discussion and allow thought on the future direction of experiments to be taken. The suggestion that Yta7p might function both at replication origins and replication forks is supported by the fact that I have unmasked two roles for Yta7p. One avenue of investigation suggests that Yta7p allows a faster S phase in conditions where *RPD3* is deleted, possibly by acting on both origin activation and replication fork progression. In addition, Yta7p is found at replication origins in S phase. The other avenue of investigation suggests that Yta7p is required for a redundant function in allowing efficient recovery from S phase checkpoint activation. Whether this second role is due to a function at the replication fork is still to be determined.

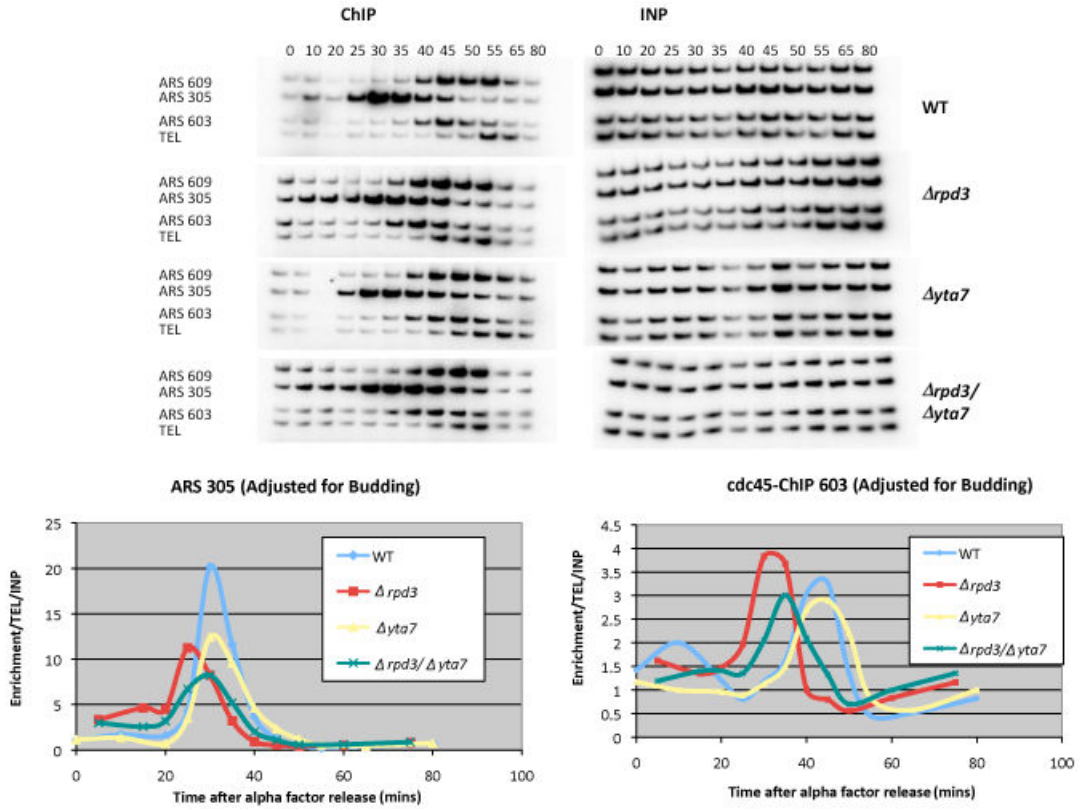

Figure 6.3: The intermediate effect of Δ*rpd3*Δ*yta7* on time of Cdc45p binding is repeatable at alternative origins. As per Fig. 6.2, strains used are MMY033 (WT), MVY51 (Δ*rpd3*), MVY63 (Δ*yta7*) and MVY64 (Δ*rpd3* Δ*yta7*). Both raw image gels and graphs produced by analysis are shown. Top half are the gels for ChIP (left) and INP (right) for all tested strains. Top gels are WT strain, second gels are Δ*rpd3*, third set of gels are for Δ*yta7* and bottom set are Δ*rpd3*Δ*yta7*. Individual gels from left to right show each time point after alpha factor release. Individual gels from top to bottom show signal at ARS609, ARS305, ARS603 and TEL VI. Graphs display analysed results. X axes are time after alpha factor release. Y axes are Cdc45-FLAG ChIP signals at origins normalised to INP and divided by normalised TEL VI signal. Left hand side graph is early-firing ARS305. Right hand side is late-firing ARS603. All data has been adjusted to account for late release of strains containing Δ*rpd3*. Blue line is WT strain, red line is Δ*rpd3*, yellow line is Δ*yta7* and green line is Δ*rpd3* Δ*yta7*. Peak binding occurs at 25-30 minutes in all strains at the early-firing ARS305, similar to the situation observed at ARS607. However as before, the late-firing origin (ARS603), displays an earlier Cdc45p enrichment at 30 minutes in a Δ*rpd3* strain compared with 45 minutes for both WT and Δ*yta7*. Δ*rpd3*Δ*yta7* displays intermediate binding at 35 minutes.

Chapter 7

The Importance of the Yta7p Bromodomain

7.1 Introduction

As discussed in Section 5.3, it is not certain whether Yta7p has a preference for histones with post translational modifications or binds preferably to the unmodified version *in vivo*. Therefore, it is possible that under specific circumstances the binding of Yta7p to chromatin, including binding at replication origins, is influenced by histone acetylation. To ascertain if the binding of Yta7p specifically to replication origins is dependent on acetylation, an efficient first line of investigation would be to determine the importance of the bromodomain of Yta7p in DNA replication.

7.2 Results

In order to investigate if the role of Yta7p in DNA replication was dependent on its ability to bind to histones via its bromodomain a *yta7*Δ*BD* strain was created. The approach taken was to order a plasmid (pBSK) that contained the *YTA7* ORF sequence with the bromodomain removed, from ATG:biosynthesis. I designed the sequence to remove 309bp, that encompassed the bromodomain region (2994bp-3303bp), based on [Tackett et al., 2005]. Then a strain which replaced most of the *YTA7* ORF with a *URA3* marker was constructed and confirmed by URA-plate selection and colony PCR. The plasmid (pBSK) was subjected to restriction digestion, which separated the *YTA7*, minus bromodomain, sequence (3941bp fragment in Fig. 7.1(A)) from the rest of the plasmid. The fragment of interest was then gel extracted, purified and transformed into the *yta7*::URA strain (MVY212). Colonies were selected by growth on 5-FOA plates and colony PCR was performed for confirmation. Positive colonies underwent a further transformation to FLAG tag Yta7p (minus bromodomain) as per previous experiments, so that

a western blot could confirm that the protein without the bromodomain was expressed to the same level as the WT protein. Refer to Fig. 7.1(B), where the *yta7*Δ*BD*-containing strains give a lower size band that is of equal intensity as the full length version, and the Pgk1p loading control is equivalent in all lanes. The selected strain was then sequenced across the *YTA7* ORF to confirm that the sequence was correct, with no introduced mutations, and that the only region removed was the required 309bp. Supplementary Fig. 9.4 gives examples of the resulting sequence for the 5′ region, the region surrounding the bromodomain deletion and the 3′ region of *YTA7*. No additional mutations were observed within the entire gene sequence. Finally a Δ*rpd3 yta7*Δ*BD* strain was created by replacing the *RPD3* ORF with the *TRP* selection marker, which once again was selected by growth on TRP- plates and confirmed by colony PCR; Fig. 7.1(C). All of this was originally performed in the MMY001 background, but, as before, the procedure in this background resulted in sickness for the *yta7*Δ*BD*-FLAG strain. Hence, the strains were re-built using the re-made WT strain, which had resulted from crossing MVY105 and MVY155 (see Table 2.1). These are the strains represented in Fig. 7.1 and Supplementary Fig. 9.4. These strains were FLAG tagged for Western blot, but the final sequenced strains used for the following experiments did not contain the FLAG tag (refer to Table 2.1).

Having confirmed that I had deleted the Yta7p bromodomain without introducing additional mutations, or affecting the protein levels, the first logical experiment was to test the requirement of the bromodomain for the ability of Yta7p to facilitate the faster S phase of the Δ*rpd3* strain. If the bromodomain recognises increased histone acetylation surrounding usually "late-firing" origins in Δ*rpd3*, then it would be expected that without the bromodomain Yta7p could not be recruited efficiently to these regions. Therefore, *yta7*Δ*BD* would have the same effect as deletion of the whole gene, that is reversion of the Δ*rpd3* S phase to WT length. The WT, Δ*rpd3*, *yta7*Δ*BD* and Δ*rpd3 yta7*Δ*BD* strains were therefore used to repeat the original timecourse FACS analysis of Fig. 3.2. A Budding Index was used to demonstrate synchronous release from alpha factor arrest and, as is evident from Fig. 7.2(B), both of the re-built strains that contained Δ*rpd3* displayed a delay in release. Cells showed 50 percent budding at approximately 47 minutes for the WT and *yta7*Δ*BD*, while the Δ*rpd3* reached 50 percent at approximately 54 minutes and the Δ*rpd3 yta7*Δ*BD* strain was delayed to 60 minutes. This again seems to be a strain dependent phenomenon as it occurred in both repeats of this experiment and previously in the Yta7-FLAG Δ*rpd3* re-built strain (MVY211); refer back to Fig. 5.1. Regardless of this all strains enter S phase and then complete DNA replication unhindered.

The FACS analysis clearly shows that the bromodomain of Yta7p is not required to allow the faster S phase of the Δ*rpd3* strain. Even with the 10 minute delay the Δ*rpd3 yta7*Δ*BD* strain still completes S phase faster than its WT counterpart. When compared, approximate length of S phase (blue bars in Fig. 7.2(A)) in the Δ*rpd3 yta7*Δ*BD* and the Δ*rpd3* strains is approximately 25 minutes, whilst both the WT and *yta7*Δ*BD* strains require 35 minutes to complete S phase.

The second question that could be addressed with these newly constructed strains was

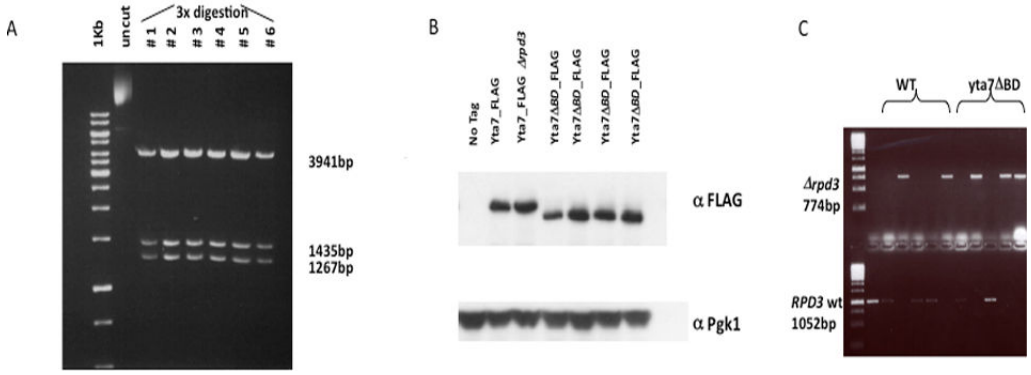

Figure 7.1: Construction of *yta7ΔBD* strains. (A): Plasmid pBSK was restriction digested and the relevant fragment was purified by gel extraction. First lane of the gel is a 1kb ladder. Second lane is the undigested plasmid. lanes 3-8 are plasmids isolated from independent colonies then restriction digested with three different enzymes. The band at 3941bp contains the *YTA7* sequence minus the bromodomain. (B): After transformation and FLAG tagging the strains were tested by western blot to confirm expression levels. Strains used are MMY001 (no tag in lane 1), MVY210 (Yta7-FLAG in lane 2), MVY211 (Yta7-FLAG Δ*rpd3* in lane 3) and four of the colonies that contain *yta7ΔBD*-FLAG to test (lanes 4-7). *yta7ΔBD* did not result in altered expression of the protein. Pgk1p is included as a loading control for each strain. (C): Final required strains were constructed by deleting *RPD3* in both WT and *yta7ΔBD* (No FLAG) backgrounds, which was confirmed by colony PCR. First lane of gel is 1kb ladder. Lanes 2-5 contain colonies in a WT (MVY109) background. Lanes 6-9 contain colonies in a *yta7ΔBD* background (MVY212). Top gel has PCR products specific for Δ*rpd3* (774bp in length), bottom gel is the PCR product produced using primers specific to the WT *RPD3* (1052bp in length).

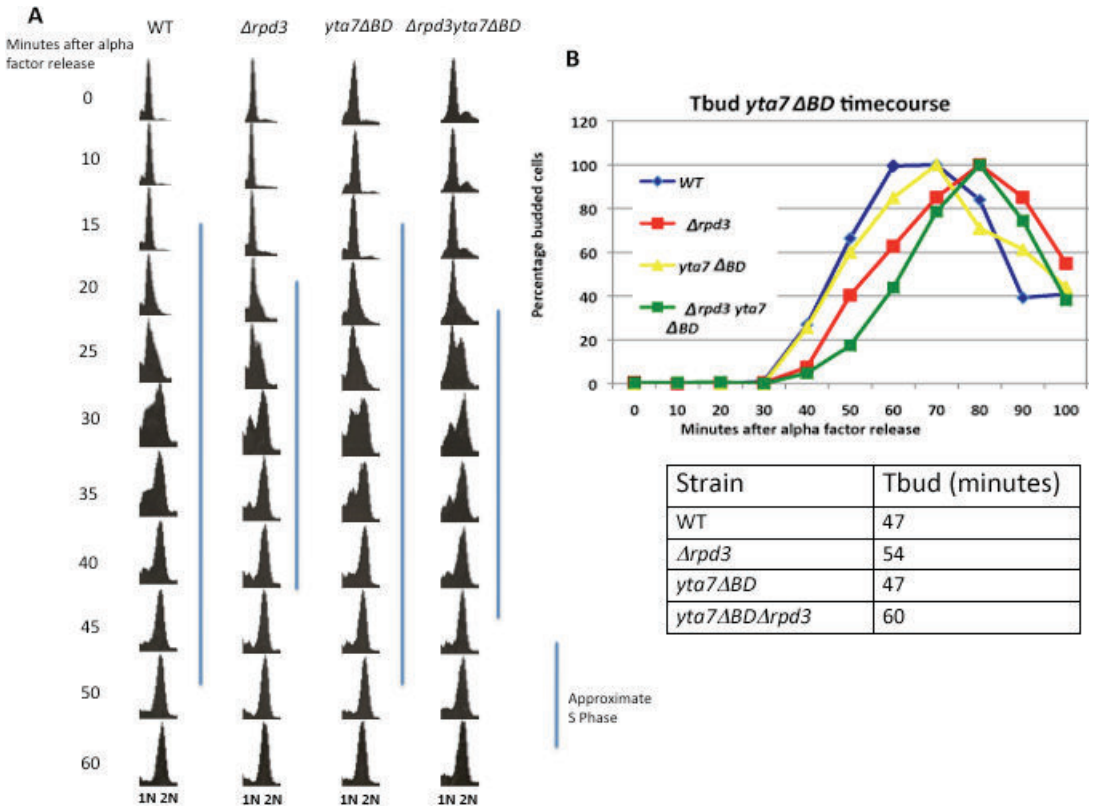

Strain	Tbud (minutes)
WT	47
Δrpd3	54
yta7ΔBD	47
yta7ΔBDΔrpd3	60

Figure 7.2: The bromodomain of Yta7p is not required for the faster S phase of a Δ*rpd3* strain. (A): FACS profile of synchronised G1 release of WT (MVY209) and deletion mutant strains: Δ*rpd3* (MVY215), *yta7*Δ*BD* (MVY213) and Δ*rpd3 yta7*Δ*BD* (MVY216). Each time point indicates the minutes following alpha factor release. 1N indicates a haploid DNA content. 2N indicates the cells have replicated the DNA completely. Blue bar indicates approximate S phase length in each case. S Phase length was assigned using parameters described in Fig. 3.2. FACS analysis shows that the approximate S phase length of a Δ*rpd3 yta7*Δ*BD* strain is the same as that for a Δ*rpd3* strain. WT and *yta7*Δ*BD* strains have the same longer S phase (refer to blue bars). (B): As per Fig. 3.3, number of buds at each indicated time point were counted in the same four strains used for the FACS analysis. Y axis represents the number of buds reached as a percentage of total buds for each strain. X axis represents time in minutes. Blue line is strain MVY209 (WT), red line is MVY215 (Δ*rpd3*), yellow line is MVY213 (*yta7*Δ*BD*) and green line is MVY216 (Δ*rpd3 yta7*Δ*BD*). The table gives the Tbud value for each strain, that is the time at which 50 percent of the cells were budded. Tbud is 47 minutes for WT and *yta7*Δ*BD*, 54 minutes for Δ*rpd3* and 60 minutes for Δ*rpd3 yta7*Δ*BD*.

whether the bromodomain was required for the S phase checkpoint function of Yta7p. An efficient way to test this was to grow the strains on 100mM HU, as before in Fig. 3.5, and assess if the double mutant Δ*rpd3 yta7*Δ*BD* is sensitive to HU, similar to the Δ*rpd3*Δ*yta7* strain. Hence, spot tests with a serial dilution of 1:10 of WT, Δ*rpd3*, *yta7*Δ*BD*, Δ*rpd3 yta7*Δ*BD* and Δ*rpd3*Δ*yta7* were performed on both YPD as a control and 100mM HU. As can be seen in Fig. 7.3, deletion of the bromodomain of Yta7p in a Δ*rpd3* strain had an intermediate effect when compared with the Δ*rpd3*Δ*yta7* strain. The double deletion mutant displayed, as before, between a 100 and 1000 times sensitivity to HU when compared to WT, whilst the bromodomain deletion in Δ*rpd3* is between 10 and 100 times more sensitive than WT. The Δ*rpd3* strain and the *yta7*Δ*BD* strain grew similarly to WT. The intermediate effect of HU on the Δ*rpd3 yta7*Δ*BD* strain is similar to that found for the *spt16-11 yta7*Δ*BD* and the *asf1*Δ*yta7*Δ*BD* strains, tested at 34°C and on 100mM HU respectively, in [Gradolatto et al., 2009]. Therefore, the bromodomain is partially required for the functions of Yta7p that overlap with these proteins.

7.3 Discussion

The results suggest that the bromodomain of Yta7p is not required for the faster S phase of a Δ*rpd3* strain. There are several potential explanations for the FACS result: the binding of Yta7p at replication origins is not regulated by histone acetylation, the bromodomain is not the only domain of Yta7p able to bind acetylated histones, Yta7p is recruited to origins by an additional protein, or recruitment of Yta7p to origins is not required for the effect on S phase length in Δ*rpd3*. The fact that the S phase phenotype of Δ*rpd3* was not affected by deletion of the bromodomain (Fig. 7.2) and neither was binding of the *HTA1-HTB1* loci [Gradolatto et al., 2009], might suggest that histone gene transcription could have an effect on this phenotype, but again this would not necessarily be the only effect given the lack of a detectable change in H3 levels in a Δ*rpd3*Δ*yta7* strain and the fact that Yta7p is physically present at replication origins under WT conditions. Each of the four possibilities posed above could be addressed and, in fact, a further experiment could use a FLAG tagged strain and the previously optimised ChIP conditions, to test if Yta7p can still bind to replication origins without its bromodomain. This would provide immediate evidence either for or against the last possibility; that Yta7p binding at origins is not required to affect S phase length when *RPD3* is deleted.

The most promising hypothesis at this point would be the second or third option; given the fact that increasing acetylation at late-firing origins leads to a large increase in Yta7p recruitment, it does appear to be relevant, contrary to the first option. The Second option is also supported by recent data also supplied in [Gradolatto et al., 2009], in which deletion of the bromodomain of Yta7p led to the loss of some activities, for example maintenance of the barrier at the *HMR* region, but did not affect others, such as binding at the *HTA1-HTB1* locus or *HTB1* mRNA levels. The authors identified a second region of Yta7p that can potentially bind the core histones, and found that binding of Yta7p is redistributed, but not abolished

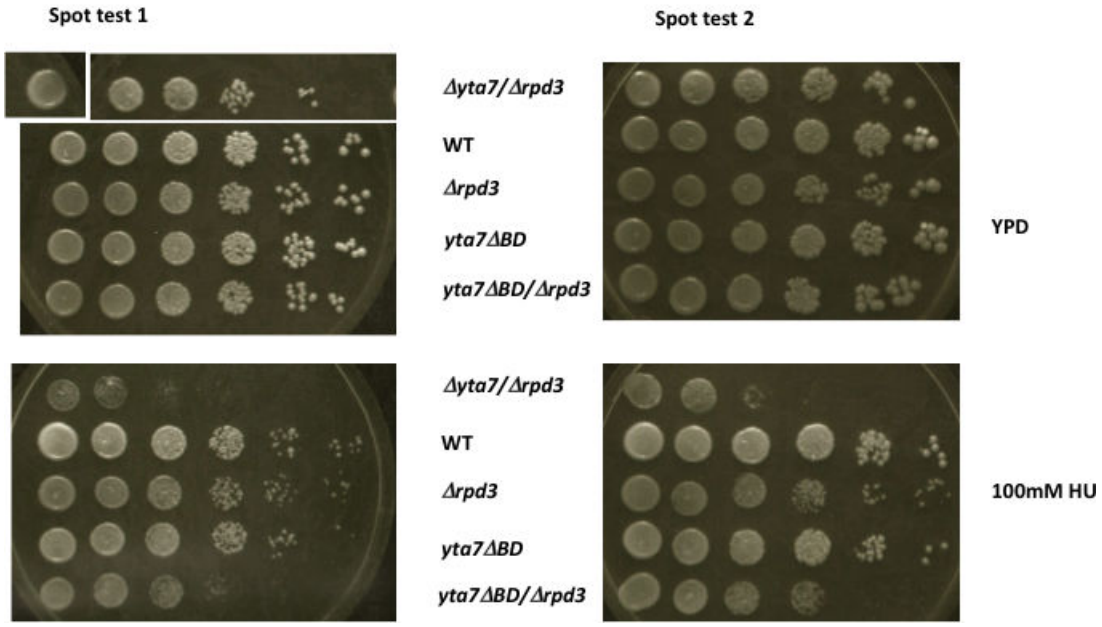

Figure 7.3: Deletion of the bromodomain of Yta7p in a Δ*rpd3* background leads to sensitivity to HU compared with WT or *yta7*Δ*BD* alone. Cultures of strains MVY64 (Δ*rpd3*Δ*yta7*), MVY209 (WT), MVY215 (Δ*rpd3*), MVY213 (*yta7*Δ*BD*) and MVY216 (Δ*rpd3* *yta7*Δ*BD*) were grown to log phase then equal concentrations of cells were spotted in a 1:10 serial dilution on either YPD or 100mM HU plates for comparison. Each lane from right to left represents a 10 fold, 100 fold, 1000 fold, 10,000 fold and 100,000 fold growth difference compared to the first lane. The experiment was repeated and both results are shown (experiment 1 is on the left and experiment 2 on the right). Top plates are YPD, bottom plates are 100mM HU. The effect on HU of the Δ*rpd3* *yta7*Δ*BD* strain is an intermediate effect when compared with the sensitivity of Δ*rpd3*Δ*yta7*.

when the bromodomain is deleted. They suggest that Yta7p binding is dependent on its acidic N terminal domain, with the bromodomain responsible for "fine tuning" the binding to specific sites. ChIP-Chip analysis showed that the bromodomain-deleted protein and the WT protein only share 104 common binding sites, with bromodomain deletion leading to 734 additional binding sites, whilst the WT had only an additional 518. The importance of DNA replication to the cell suggests that replication origin binding could be one of the functions not dependent solely on the bromodomain. At this point the experiment, described in the previous section, to test the effect of deleting/mutating the tail residues of the histones on Yta7p recruitment would determine if histone acetylation influences binding of Yta7p with or without its bromodomain.

The bromodomain FACS and HU experiments performed in this thesis give an important result, as they separate the functions of Yta7p in DNA replication and the S phase checkpoint. Different activities of this protein are required for the different processes. It is possible that in the case of the S phase checkpoint the bromodomain is required for "fine tuning" of binding to chromatin as suggested by [Gradolatto et al., 2009]. In this respect it would be important to identify if Yta7p binds at replication forks, and, specifically, if this binding is required for continued synthesis after removal of the S phase checkpoint. I began initial work to monitor if Yta7p is bound to regions as the replication fork passes, and preliminary data suggests it may, however these experiments would need to be repeated to produce better quality data and so are not included in this body of work.

The separation of function for Yta7p leads into the next major question to address. Yta7p is required to shorten the synthesis phase of the cell cycle when *RPD3* is deleted, binds at replication origins at approximate time of firing, shows synthetic lethality with proteins involved in replication, chromatin assembly and disassembly and elongation through chromatin, and is required for a redundant function in the S phase checkpoint. However, the exact function of the protein in these processes is unknown and many different experiments could be conducted to explore the possible candidates. For example, a large scale screen to identify suppressors of the Δ*rpd3*Δ*yta7* HU sensitivity phenotype could be performed. This could highlight the potential pathways that Yta7p is involved in and suggest a direction in which to proceed for further experiments to test direct function. To identify the function of Yta7p in both DNA replication and S phase checkpoint recovery would be the final goal of this project. However time constraints meant that only one course of investigation could be followed so I chose a more targeted approach. The main aim of this thesis was to test the hypothesis that Yta7p binds to replication origins in conditions of increased histone acetylation to allow earlier firing. Yta7p has been identified in a complex with the proteins Spt16p, Top2p and Sas3p. Spt16p and Top2p are known to be involved in DNA replication. Yta7p also shows synthetic defects with the FACT subunit Spt16p. Therefore, a possible function for Yta7p could be that it is responsible for recruitment of these proteins to replication origins to allow replication to begin and progress in an efficient manner. This was the premise for the final experiment.

Chapter 8

Δ*yta7* Results in Increased Recruitment of Spt16p to Replication Origins

8.1 Introduction

If Yta7p were to act to recruit proteins that are required for DNA replication to origins, then deletion of *YTA7* should lead to a reduction in recruitment of those proteins at origins. Two of the proteins that are found in a complex with Yta7p to create boundary elements have functions at the replication fork. As stated in Section 1.10, Spt16p-containing FACT is proposed to be required for chromatin disassembly and reassembly [Wittmeyer et al., 1999], whilst Top2p is required for release of torsional stress at the replication fork [Bermejo et al., 2007]. In addition, a third protein in the complex, Sas3p, has no identified role in DNA replication, and it is not known if it binds to replication origins or forks, but Sas3p is a histone acetyltransferase whose human homologue, MOZ/MORF, does have a potential role in DNA replication [Doyon et al., 2006]. Therefore, recruitment of this protein to replication origins by Yta7p is also a possibility. Hence, these three proteins were chosen to test for recruitment by Yta7p.

8.2 Results

Spt16p, Top2p and Sas3p were FLAG tagged separately in either a WT or Δ*yta7* strain and expression levels were monitored by western blot to account for any transcriptional effects of Δ*yta7* directly on the protein. As can be seen in Fig. 8.1(A) all proteins were tagged effectively and deletion of *YTA7* had no effect on the expression levels of either Spt16p or Top2p (compare

lanes 3 and 4 for Spt16p and then lanes 5 and 6 for Top2p in reference to the loading control Pgk1p). There is a slight decrease in Sas3p levels (compare lanes 7 and 8) when *YTA7* is deleted, which should be taken into account for future reference.

Since there is also a synthetic defect for *spt16-11* $\Delta yta7$ cells [Gradolatto et al., 2008], Spt16p was chosen to investigate first. Identification of Spt16p recruitment at replication origins required the optimisation of ChIP conditions for this protein. In addition, whilst image-quantification of radioactive PCR products was used previously to identify levels of bound Yta7p, the levels of alteration in Spt16p recruitment might be more subtle. This hypothesis is based on the fact that Spt16p is an essential protein and that the function of Yta7p in DNA replication has some redundancy, hence there would likely be alternative recruitment mechanisms for Spt16p. Therefore, subtle reductions in Spt16p recruitment to origins would be expected. Hence, the ChIP process was optimised for formaldehyde cross-linking and subsequent analysis by QPCR, a more quantitative detection method than radioactive PCR.

No tag and Spt16-FLAG strains were grown to log phase and samples were taken for cross-linking. Primers were designed to cover positive and negative binding regions. The highly transcribed *ASC1* ORF region was chosen as a positive control region, as FACT was originally characterised by its ability to facilitate transcriptional elongation [Orphanides et al., 1998]. A region on chromosome VIII, which had no nearby ORFs, was chosen as a negative control region. Samples were run on a Stratagene MX3500 and CT values (which represents cycle number at which an automatically and individually assigned threshold is crossed for each sample) were exported using the MxPro package. The ΔCT method was used to calculate each enrichment signal as a percentage of INP.

As per Fig. 8.1(B), Spt16p was enriched to 5.5%INP at the *ASC1* ORF compared to 0.15%INP for the No tag. Spt16p was enriched only to 0.45%INP at the chromosome VIII negative control region compared to 0.01%INP for the untagged protein. Hence, the ChIP protocol is optimised for Spt16p, but there is a slightly increased level of Spt16p identified at the negative region when compared with the untagged protein at either region (column 3 of graph in Fig. 8.1(B)). This comparatively high level of Spt16p at the negative region could be due to the high expression levels of the protein. To ensure that the positive signal for Spt16p at *ASC1* was specific to Spt16p I repeated the PCR using an Mcm2-FLAG ChIP as a negative control. Mcm2p should not bind to either region tested. Fig. 8.1(C) clearly demonstrates that the binding of Spt16p to the *ASC1* ORF is specific to this protein, for this experiment, because there is no binding of Mcm2p to the *ASC1* region (compare column 1 with column 5 where the Spt16p enrichment was again 5.5%INP, but the %INP signal for Mcm2p only reached 0.24 compared with a No tag signal of 0.19%INP).

The percentage INP calculation method was chosen in preference to a fold enrichment method, which would have given a very different binding profile. Each analysis method has advantages and disadvantages, but the only major advantage for fold enrichment is that it takes into account the enrichment of bound protein over the No tag signal for each region. This means that if one region amplifies preferentially to another for any reason it does not affect the result

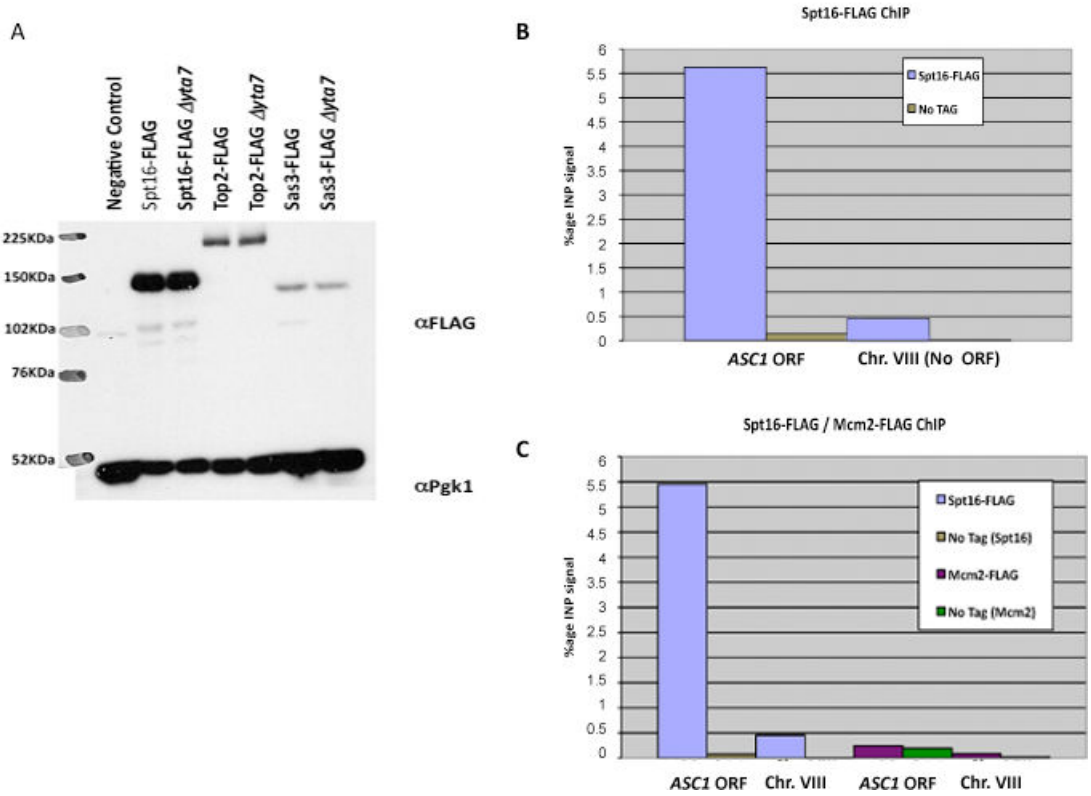

Figure 8.1: Construction of Spt16-FLAG strains and optimisation of ChIP-QPCR. (A): Western blot to show expression levels of flag tagged proteins in the presence and absence of *YTA7*. Lane 1 contains the molecular marker. Lane 2 is strain MMY001 (negative control). Lanes 3 and 4 show Spt16-FLAG in strains MVY179 (Spt16-FLAG) and MVY180 (Spt16-FLAGΔ*yta7*). Lanes 5 and 6 show Top2-FLAG in strains MVY182 (Top2-FLAG) and MVY177 (Top2-FLAGΔ*yta7*). Lanes 7 and 8 show Sas3-FLAG in strains MVY178 (Sas3-FLAG) and MVY183 (Sas3-FLAGΔ*yta7*). Pgk1p is included as a loading control for each lane. Approximate molecular weight for untagged protein, as taken from SGD, should be for Spt16p 118.5KDa, for Top2p 164KDa, for Sas3p 97.5KDa and for Pgk1p 45KDa. Deletion of *YTA7* does not affect expression of Spt16p (lanes 2 and 3). (B): QPCR analysis as a bar graph. X axis shows region of genome tested (*ASC1* ORF followed by the CHR.8 NO ORF region). Y axis is the ChIP signal as a percentage of INP signal. Blue bars are the signal for Spt16-FLAG and brown bars are the signal for the no tag strain. Strains are MVY001 (No tag) and MVY179 (Spt16-FLAG). Optimised conditions allowed detection of Spt16-FLAG at the *ASC1* ORF 5′ region, but showed minimal detection at a region of Chromosome VIII that contained no ORFs. (C): QPCR analysis as a bar graph. X axis shows region of genome tested (*ASC1* ORF followed by the CHR.8 NO ORF region). Y axis is the ChIP signal as a percentage of INP signal. Blue bars are the signal for Spt16-FLAG and brown bars are the signal for the no tag strain. Purple bars are the signal for Mcm2-FLAG and green bars are the signal for its corresponding no tag strain. Strains are MVY179 (Spt16-FLAG), MVY125 (Mcm2-FLAG) and MMY001 (both no tags). The detection of Spt16p at *ASC1* was specific to this protein as no Mcm2-FLAG was detected at either of the regions tested.

because an increase in protein enrichment would be divided by an increase in no tag signal for preferential regions. However, the % INP method normalises to INP which should account for primer efficiency and sonication efficiency at different regions. In addition each primer set was put through a qualification process and only used if it passed quality criteria; refer to Fig. 9.5 for an example. Each subsequent QPCR plate was tested using a standard curve that covered DNA dilutions in the range of the ChIP samples, except in some cases where the No tag samples were too low. These very low No tag signals are the reason why fold enrichment would overemphasise enrichment for some regions; division of a small enrichment by a no tag signal that is produced by a sub-optimal amplification would create false positive results. Therefore, an increased confidence can be taken in the % INP calculations, which allow comparison between signal levels for both protein and No tag independently for each separate region.

Thus, the ChIP conditions were optimised and the most appropriate analysis method was chosen. Therefore, a timecourse experiment to assess Spt16p recruitment levels to replication origins in the presence and absence of Yta7p could be undertaken. No Tag, Spt16-FLAG and Spt16-FLAG $\Delta yta7$ strains were synchronised with alpha factor and then released into S phase; samples for FACS, Budding Index and ChIP were taken every 10 minutes. All strains released in a synchronous manner. DNA synthesis is evident in the FACS profiles by the 30 minute time point for all three strains; Fig. 8.2(A). In addition, the Tbud occurs between 72 and 75 minutes into the experiment for each strain; Fig. 8.2(B).

The samples were analysed by QPCR using primers that covered the early-firing ARS607, the late-firing ARS1412, and the TEL VI region as a negative control. Each plate was loaded, as per the optimisation, with samples in triplicate. A standard curve was included to test the amplification and reports were generated. Standard curves were generated using a pool of INP DNA serially diluted 1:5. In addition to running a melting curve to test primer specificity, a subset of standards were run on agarose gels to visualise the amplification products and confirm the generated report. Refer to Fig. 9.6(A), where only one PCR product of the correct size (approximately 85bp) is observed for each triplicate dilution sample and there is no product in the no template control on the agarose gel. This fits with the melting curve generated for this plate shown next to the gel. Plates, also as per the optimisation, had to pass stringent quality criteria. In some cases the No Tag samples fell outside the efficiency range of the primers, but use of the %INP method for analysis will not create false positives for the affected regions. Refer to Fig. 9.6(B) where blue squares represent the standard DNA dilutions, while blue triangles represent the ChIP samples tested. Three triangles fall outside of the concentration range of the standard curve for the IP samples in Fig. 9.6(B)(ii) and these are a subset of No tag samples.

The timecourse data was plotted onto line graphs for visualisation of results. Fig. 8.3 contains the graphs generated for ARS607 (early), ARS1412 (late) and TEL VI (negative control). The No Tag strain had minimal enrichment at all regions (blue line in graphs). Recruitment of Spt16p to origins in WT conditions (red line) peaks at 0.3%INP for ARS607 and 0.2%INP for ARS1412, however in the $\Delta yta7$ background (yellow line) recruitment to ARS607 peaks with 0.8%INP and recruitment to ARS1412 peaks with 0.7%INP. This result excludes the possibility

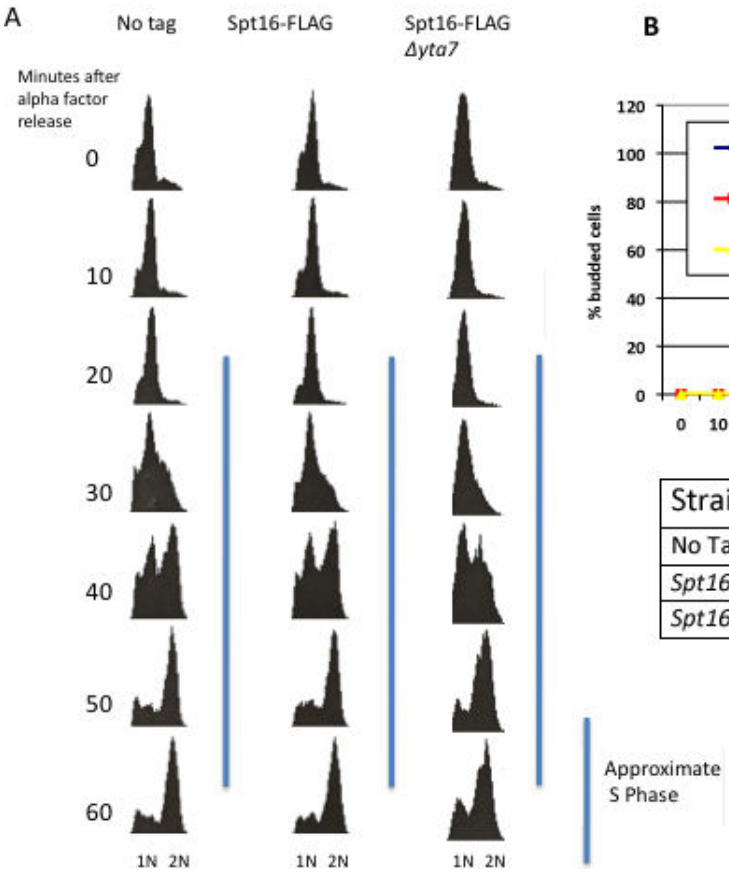

Strain	Tbud (minutes)
No Tag	75
Spt16-FLAG	75
Spt16-FLAGΔyta7	75

Figure 8.2: Spt16-FLAG time course. All strains displayed a synchronous release from alpha factor. (A): FACS analysis demonstrates that all strains had entered S phase by the 30 minute timepoint. Strains are MMY001 (No tag), MVY179 (Spt16-FLAG) and MVY180 (Spt16-FLAG$\Delta yta7$). Each time point indicates the minutes following alpha factor release. 1N indicates a haploid DNA content. 2N indicates the cells have replicated the DNA completely. Blue bar indicates approximate S phase length in each case. S Phase length was assigned using parameters described in Fig. 3.2. (B): As per Fig. 3.3, number of buds at each indicated time point were counted in the same three strains used for the FACS analysis. Y axis represents the number of buds reached as a percentage of total buds for each strain. X axis represents time in minutes. Blue line is strain MMY001 (No tag), red line is MVY179 (Spt16-FLAG) and yellow line is MVY180 (Spt16-FLAG$\Delta yta7$). The table gives the Tbud value for each strain, that is the time at which 50 percent of the cells were budded. T Bud analysis shows that 50 percent budding is reached by 75 minutes in all three strains. The experiment was performed twice and one representative result is shown.

that Yta7p is required to recruit Spt16p to replication origins. In fact, deletion of *YTA7* results in increased recruitment of Spt16p to origins. Given the synthetic interaction identified for Yta7p and Spt16p [Gradolatto et al., 2008], which implies they share a common function, this drastic increase in Spt16p recruitment to origins could reflect a need for excess levels of Spt16p at replication origins to compensate for loss of Yta7p. The related function of these two proteins would be one interesting avenue of future investigation.

The profile at TEL VI revealed no significant recruitment of Spt16p to this region in either the No Tag or Spt16-FLAG strains. There was a very slight increase at the 30 minute time point to 0.06%INP for the Spt16-FLAG strain compared with the other time points. This was also true in the Spt16-FLAG Δ*yta7* strain which did show recruitment of 0.2%INP at the 30 minute time point, but Spt16p levels are increased compared to the other strains at all time points and 0.2% is not equivalent to the recruitment levels seen at the other regions in this strain. However, an interesting observation is that peak S phase recruitment of Spt16p occurred at the same time point in all regions, a very different pattern to that observed for Yta7-FLAG. One possible reason for this simultaneous peak recruitment could be increased expression of Spt16p at the 30 minute time point of the experiment, which leads to increased detection of the protein at this time. To investigate this further I compared the cell cycle expression profile of Spt16p, available on the yeast cell cycle analysis project database[1], to my results. Peak expression on the database occurs in G1 and decreases as S phase is entered. Peak binding in my experiment was for G1 arrested cells, which coincides with peak expression. However, in my experiment there is a second peak at 30 minutes after release, which is just subsequent to the point where S phase began based on the FACS profile; refer to blue bar in Fig. 8.2(A). This would be a point in the cell cycle where expression of Spt16p would be dropping based on the cell cycle analysis data. To confirm that expression did not peak at this time in this particular experiment, samples could be taken at each time point for western blot to look at protein levels across S phase for these specific strains.

Levels of Spt16p detected at TEL VI were only approximately one quarter that of those detected at ARS1412 in both strains. In addition, the recruitment of Spt16p reached its S phase peak at 30 minutes, but there is also an increased level of Spt16p at the 20 minute time point at the earlier firing ARS607 in both strains. This increased level of Spt16p at 20 minutes is not present at ARS1412, which suggests that there is a slight differential time of recruitment to these two regions. This experiment is a lower resolution than that of the Yta7-FLAG experiment (samples were taken every 10 minutes instead of 5), therefore the time of recruitment of Spt16p could show subtle differences at origins that is not reflected by this experiment. However, the conclusion of the experiment remains that, despite no increase in general Spt16p levels in a Δ*yta7* strain, deletion of *YTA7* results in increased recruitment of Spt16p to replication origins. Further evidence to support this result could be generated if it was observed that the increased recruitment of Spt16p to origins in a Δ*yta7* strain was repeatable at alternative replication origins.

[1] `genome-www.stanford.edu/cellcycle` (June 2009)

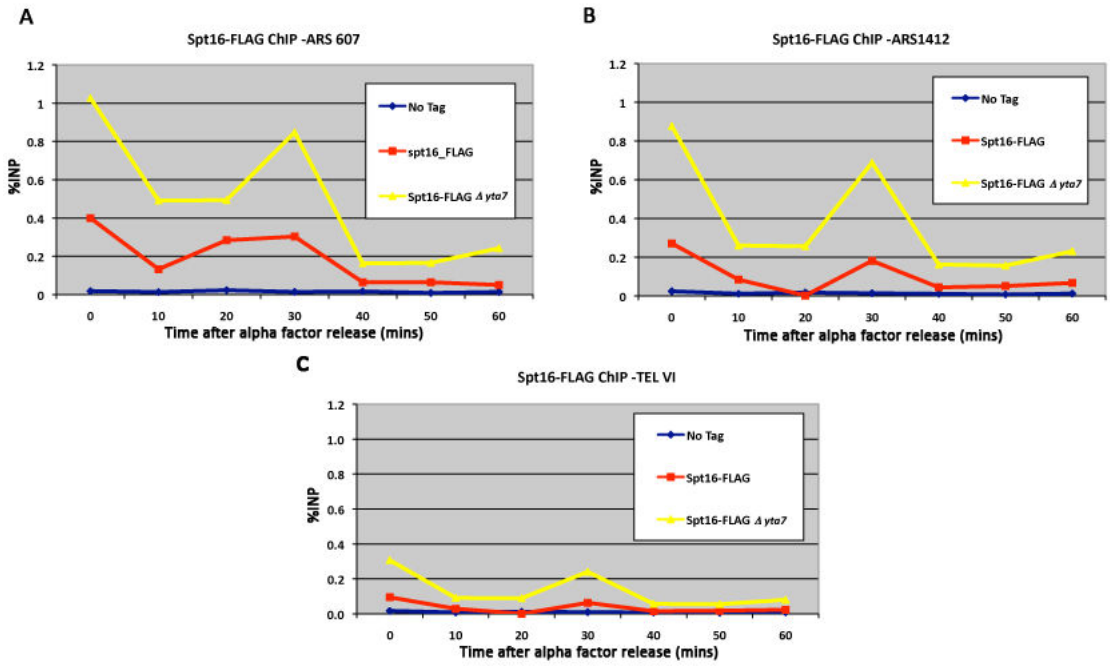

Figure 8.3: Deletion of *YTA7* results in increased recruitment of Spt16p to replication origins. QPCR results are displayed as line graphs. Strains used in this experiment are MMY001 (No tag), MVY179 (Spt16-FLAG) and MVY180 (Spt16-FLAG$\Delta yta7$). In each graph shown X axis is time after alpha factor release, Y axis is the ChIP signal as a percentage of the corresponding INP signal, blue line is for No tag, red line is Spt16-FLAG and yellow line is Spt16-FLAG$\Delta yta7$. The experiment was performed twice and one representative result is shown. (A): ChIP samples were amplified using primers in the ARS607 region to generate a time course profile for Spt16p recruitment. Levels of Spt16p identified at ARS607 increase approximately 2.5 times when Yta7p is not present. (B): ChIP samples were amplified using primers in the ARS1412 region to generate a time course profile for Spt16p recruitment. Levels of Spt16p identified at ARS1412 increase approximately 3 times when Yta7p is not present. (C): Recruitment of Spt16p to TEL VI region is minimal with only minor enrichment at 30 minutes.

8.3 Discussion

While recruitment of Spt16p to the replication origins tested is not dependent on the presence of Yta7p, it is possible that recruitment to origins of one of the other proteins of the identified boundary complex, described in Section 1.9, is dependent on Yta7p. I optimised conditions for the Sas3-FLAG ChIP and for subsequent analysis by QPCR, but there was insufficient time to test if Sas3p is recruited to replication origins and if that recruitment requires Yta7p. This is just one of the exciting possibilities that requires future investigation.

An additional promising avenue of investigation would be to determine the importance of the AAA ATPase domain of Yta7p for the DNA replication phenotypes identified, similar to the experiment involving the bromodomain. Two proteins that contain ATPase domains are Ino80p and Isw1p, which are subunits of chromatin remodeling complexes; refer to Fig. 1.10. Chromatin remodeling complexes also contain histone modification recognition domains such as bromodomains and/or PHD domains and are capable of ATP dependent remodeling of histones in the regions where they bind. According to [Clapier and Cairns, 2009] "all remodelers share five basic properties": an affinity for the nucleosome, histone modification recognition domains, an ATPase domain, domains or proteins that regulate the ATPase domain and domains or proteins for interaction with other chromatin factors. It is important to investigate if the ATPase domain of Yta7p confers some of its replication functions. Yta7p, either within the protein or within the larger identified boundary complex, is known to share all of the mentioned features except one: domains or proteins that regulate the ATPase domain. Hence, Yta7p also has the potential to be capable of chromatin remodeling.

To identify a function for Yta7p in DNA replication could be a challenging process, but use of the data provided by this thesis would aid in the creation of new hypotheses that can be tested in a step wise manner. Recent publications that contain large scale experiments [Collins et al., 2007], [Mitchell et al., 2008], [Lambert et al., 2009], [Beltrao et al., 2009] have identified many proteins that have synthetic phenotypes or physical interactions with Yta7p, some of which are summarised in Table 8.1. Identifying which of those interactions are important to the DNA replication and S phase checkpoint roles of Yta7p, through the use of both wide scale and targeted approaches, will add to our knowledge of the replication functions of Yta7p.

Interaction Partner	Nature of Interaction
SPT16 (FACT subunit)	synthetic growth defect
ASF1 (H3/H4 chaperone)	synthetic growth defect
HIR1/2 (histone transcription/deposition)	synthetic growth defect/phenotypic enhancement
EAF1/3 (NuA4 subunits)	synthetic growth defect
CSE4 (centromere specific H3 variant)	synthetic growth defect
ESA1 (essential HAT of NuA4)	synthetic growth defect
RPA (DNA replication)	phenotypic enhancement
RFC (DNA replication)	phenotypic enhancement
POB3 (FACT subunit)	phenotypic enhancement
HTA (core histone)	phenotypic enhancement
HTZ1 (histone variant)	phenotypic enhancement
SIN3 (RPD3 complex subunit)	phenotypic enhancement
SWR1 (histone exchange)	phenotypic enhancement
IES2 (INO80 subunit)	phenotypic enhancement
ARP4 (Shared INO80/NuA4/SWR1 subunit)	phenotypic enhancement
RSC6/8 (RSC chromatin remodeler)	phenotypic enhancement
ISW1 (ISWI chromatin remodeler)	phenotypic enhancement
CHD1 (SAGA/SLIK HAT subunit)	phenotypic enhancement
BMH1 (14-3-3)	phenotypic enhancement
HHF (core histone)	phenotypic suppression
HHT (core histone)	phenotypic suppression
RTT106 (histone deposition)	phenotypic suppression
ITC1 (chromatin remodeling)	phenotypic suppression
Orc1p (DNA replication)	physical interaction
Mcm2/3/4/5/7p (DNA replication)	physical interaction
RFA (DNA replication)	physical interaction
RFC (DNA replication)	physical interaction
RPA (DNA replication)	physical interaction
Top1p/2p (topoisomerase)	physical interaction
Sas3p (NuA3 HAT)	physical interaction
Nto1p (NuA3 subunit)	physical interaction
Pob3p (FACT)	physical interaction
Spt16p (FACT)	physical interaction
Htz1p (histone variant)	physical interaction
Htb2p (core histone)	physical interaction
Hta2p (core histone)	physical interaction
Npl6p (RSC subunit)	physical interaction
Rad53p	physical interaction
CDK	biochemical activity
Clb2p	biochemical activity

Table 8.1: Select interactions involving *YTA7*. Information taken from SGD (`www.yeastgenome.org`, January 2010), where relevant references can be found. Colour code: red = replication related gene, blue = suppressive phenotype.

Chapter 9

Summary, Discussion and Future Direction

DNA replication is of vital importance to the cell and the implications of deregulation of replication in humans are diseases such as cancer. To understand the exact mechanisms that are involved in DNA replication will greatly enhance our ability to identify malfunctions, and aid treatment of diseases caused by abnormal replication. In the past, the importance of histone modifications and chromatin remodeling to transcription has been highlighted. Now the importance of chromatin regulation to DNA replication is also becoming apparent and the merging of information from these two large fields is necessary.

The model organism *S. cerevisiae* offers an excellent platform for experiments to investigate the regulation of DNA replication events in a more simplified manner. A great advantage to this system is the wealth of knowledge we already have, but much remains to be discovered. This thesis aimed to utilise this informative *S. cerevisiae* system to investigate the molecular mechanisms that allow an increase in histone acetylation surrounding particular "late activating" replication origins to alter the time of firing of those origins. In the course of the investigation a bromodomain-containing protein, Yta7p, was identified through its requirement for a faster completion of S phase in conditions where *RPD3* is deleted and histone acetylation at "late" replication origins should be increased. Previously unidentified roles for Yta7p in both normal DNA replication and S phase checkpoint function were discovered and an S phase specific binding of Yta7p to replication origins was observed. Deletion of *YTA7* in a Δ*rpd3* strain partially reverted to WT the time of firing of usually "late-activating" replication origins, based on Cdc45p association with origins. The role of the bromodomain of Yta7p was investigated, in both DNA replication and the S phase checkpoint, and this revealed a separation of function for the bromodomain in the two independent roles of Yta7p. Finally, an altered level of the FACT subunit Spt16p was observed at replication origins in the absence of Yta7p.

The results of this thesis add further to our knowledge and understanding of the DNA replication, S phase checkpoint and chromatin fields. To understand the exact function of

Yta7p, in both of the discovered roles, will be an exciting new direction. The information provided by this thesis will now allow identification of previously unknown functions for Yta7p and by using the results supplied here, future experiments can be targeted to the discovery of a direct role for Yta7p in DNA replication. It is also possible that the results of this thesis have highlighted roles for Yta7p in DNA replication that are achieved via functions already identified for this protein. One such function is the ability of Yta7p, as part of a large complex, to maintain barriers that separate chromatin compartments. The concluding section of this thesis will discuss the potential functions Yta7p could have in the two identified processes and the experiments that could be performed to elucidate which of the discussed theories are correct.

9.1 The Role of Yta7p in DNA Replication

During the course of this thesis a role for Yta7p in DNA replication was identified. This role is redundant under WT conditions as deletion of the HDAC *RPD3* is required to observe replication related phenotypes. The role for Yta7p in DNA replication is indicated by its ability to allow a faster S phase, the genetic interaction of *YTA7* with the S phase DDK subunit *CDC7*, and the susceptibility of a Δ*yta7* strain to HU, all of which depend upon the absence of Rpd3p. The S phase specific binding of Yta7p to replication origins was also identified. The level of bound Yta7p increased correspondingly at normally "late-firing" origins when histone acetylation of the region, which was previously shown to advance time of firing [Vogelauer et al., 2002], is increased. The role of Yta7p in S phase length of a Δ*rpd3* strain was demonstrated to be separate to its identified role in the S phase checkpoint, as deletion of the bromodomain only affected the S phase checkpoint function. Finally, deletion of *YTA7* resulted in increased recruitment of Spt16p to replication origins.

The original hypothesis that Yta7p binds, via its bromodomain, to regions of increased histone acetylation at replication origins to cause earlier firing would now require some modification. However, the main concept is still supported by much of the information supplied. Yta7p does have an effect on DNA replication in a Δ*rpd3* strain, and is found at replication origins in S phase. Yta7p is highly enriched at primarily early-firing origins, with only a small and delayed (relative to early) enrichment at typically late origins. This high enrichment of Yta7p can also be found at "late-firing" origins only under conditions where the time of firing of those origins becomes advanced (which is the case in a Δ*rpd3* strain as shown by [Vogelauer et al., 2002]), however, the original hypothesis is still valid if the bromodomain were not the region of the protein responsible for identifying and binding the acetylated histones. This lack of requirement for the bromodomain of Yta7p to bind replication origins, as stated, is a possibility, due to the recent identification of the N terminal region of Yta7p as a second histone binding module [Gradolatto et al., 2009]. Another possibility is that Yta7p is recruited as part of a much larger complex and so can be brought to replication origins by its association with another protein. The bromodomain could stabilise the binding of the complex, but might not be required for initial recruitment, and the stabilisation may be redundant with other protein domains. In

fact bromodomains have been shown to bind peptides that contain acetylated lysine residues, but this does not have to be restricted to peptides of histone proteins and the bromodomain could be involved in other protein-protein interactions [Dhalluin et al., 1999].

Many experiments could be performed to investigate the binding properties of Yta7p and would be invaluable to test the hypothesis. A crucial experiment would be to check that, in fact, Yta7p can still bind to origins without its bromodomain. If Yta7p no longer binds, but can still have an effect on S phase, then this points immediately to a more indirect role. However, if a bromodomain-less Yta7p is still present at origins, then a direct role is indicated. Following this, if Yta7p were still bound to origins without its bromodomain then to test which modifications were required for binding, using histones mutated at specific residues, would be the next course of action. Another informative experiment would be to ChIP the regions surrounding the early and late-firing origins used in this thesis in a WT background using a well tested antibody against acetylated H3 and H4. ChIP-Chip studies to look at modifications have been done (for example [Pokholok et al., 2005]), but to my knowledge they are all in asynchronous cells. I would propose to look at the regions included in this thesis specifically at time points throughout S phase. This could be done in the same samples taken for a Yta7p ChIP experiment if the amount of sample taken for each time point was increased. If there is an increase in histone acetylation at the same time or just prior to Yta7p binding at origins under WT conditions, it would strengthen the case for histone acetylation as a recruitment device and Yta7p as an "activator" of replication origins. In addition, the experiments that would demonstrate if the time of binding of Yta7p truly coincides with origin activation would be important, as mentioned in Chapter 5. All of these experiments could potentially add to our understanding of how the temporal programme of origin firing in *S. cerevisiae* is controlled.

To identify if Yta7p is an activator of replication origins it would be important to determine if it were part of the replication complex. Yta7p could also act at the replication fork or, indeed, be involved in both origin activation and replication fork progression. In a further experiment I investigated the effect of *YTA7* deletion on time of Cdc45p binding to replication origins in a Δ*rpd3* strain; refer to Figs. 6.1, 6.2 and 6.3. As mentioned in Section 1.2.2, time of Cdc45p binding correlates with origin activation [Aparicio et al., 1999]. If Yta7p were involved in time of activation it would be expected that Cdc45p binding would be delayed in the double mutant Δ*rpd3*Δ*yta7* compared to the single Δ*rpd3*. However, if the effect on S phase in the double mutant were due to impaired fork progression the time of Cdc45p binding would still be advanced to the same time as Δ*rpd3*. The preliminary results in Chapter 6 suggest that Yta7p acts both to allow a slightly advanced firing of replication origins and to allow efficient replication fork progression, suggesting it acts at both stages of DNA replication. This experiment would require repeating and in addition, it would also be prudent to check by 2D gel electrophoresis that time of Cdc45p binding corresponded to origin activation in this particular strain.

Another experiment that was attempted in this thesis sought to determine if detection of Yta7p at active replication forks was possible. ChIP against Yta7p at discrete distances from replication origins corresponding to a particular time after origin activation still requires opti-

misation. One recent paper [Lambert et al., 2009] used a specialised mChIP process to identify complexes of Yta7p and found Orc1p, Mcm2/3/4/5/7p, RPA, RFC and RFA as interactors of Yta7p, giving additional support to my observation that Yta7p binds to replication origins and to the possibility that it also binds at forks. It is tempting to speculate that Yta7p is part of the RC as well as the replication fork machinery due to the fact that ORC does not travel with the fork, and RFC is not part of the RC. However, ORC has many functions outside of DNA replication that could explain the interaction with Yta7p, without this interaction being, necessarily, related to replication origins.

The final major question to answer would be the function of Yta7p at replication origins/forks. Regardless of what the Yta7p function is, it would have to be redundant because all of the replication phenotypes identified here were only visible when the additional Δ*rpd3* mutation was present. To determine whether this effect is due to a common function of these two proteins or if you simply have to fire more replication origins, and hence have more active replication forks at one time (which is one effect of deleting *RPD3*), to unmask the redundant function of Yta7p would be important. Again, the data in Chapter 6 would suggest that origin firing is still slightly advanced when both *RPD3* and *YTA7* are removed in comparison with a WT strain. Hence, the idea that deleting *RPD3* causes an additional stress to the cell that Yta7p is needed to cope with is plausible.

The results of the Spt16p recruitment experiment also offer insight into potential Yta7p function. Yta7p has both a physical interaction and a genetic interaction with Spt16p and the other FACT subunit Pob3p; refer to Table 8.1. The fact that Δ*yta7* leads to increased Spt16p recruitment to origins could mean either that Yta7p binding to Spt16p usually keeps it away from replication origins, perhaps by sequestering or by occupying it with another function, or that increased Spt16p is required at replication origins to cope with loss of Yta7p. Since FACT is suggested to be the H2A/H2B histone chaperone and Yta7p has genetic interactions with other histone chaperones, it is possible that the replication function of Yta7p is in histone turnover at the replication fork. As explained previously, both Yta7p and the histone chaperones can regulate histone gene transcription, but it is suggested that for Yta7p this is not dependent on the bromodomain [Gradolatto et al., 2009]. However, the synthetic growth defects of Yta7p with the histone chaperones are slightly dependent on the bromodomain, which suggests they also share an additional common function. The histone chaperones show some level of redundancy in histone turnover at replication forks. As mentioned in Section 1.5.2, in yeast the role of Caf1p can be performed by Hira when necessary.

One proposed mechanism for Yta7p to regulate histone gene transcription is through its function as a barrier protein, similar to its function at the *HMR* region. Yta7p prevents the spreading of "heterochromatin", by preventing inappropriate binding of Rtt106p at histone gene ORFs [Fillingham et al., 2009] and also prevents spreading of silencing into the region adjacent to *HMR* [Tackett et al., 2005], [Jambunathan et al., 2005]. It is therefore possible that Yta7p provides a similar function at replication origins; that is, to create a barrier that allows the region of replication origins/forks to maintain an accessible chromatin conformation. This effect could

be redundant in WT circumstances as other chromatin remodelers could counteract the spread of "heterochromatin". The genetic interactions of Yta7p also include proteins that are subunits of the RSC, ISWI and INO80 chromatin remodelers (Table 8.1). Alternatively, Yta7p could also be an active remodeler and the importance of its ATPase domain should be addressed.

A final possible function for Yta7p in DNA replication could involve its interaction with HATs. Yta7p has been identified to have a physical interaction with both Sas3p and Nto1p (subunits of NuA3); refer to Table 8.1. Since the phenotypes of Δ*yta7* are redundant with *RPD3* deletion they could share a common function. Whilst if Yta7p were involved with a HAT it would seem to have a function that opposed Rpd3p-containing complexes, I have highlighted that sometimes it is the balance between histone acetylation and deacetylation that is important for some functions. Refer back to Section 1.5 for the example of H3K56, where removal of the modification is equally important to its addition for genome stability. One possibility is that Yta7p is required to maintain the increased acetylation at "late-firing" origins in a Δ*rpd3* strain, perhaps through association with Sas3p. A ChIP experiment to compare histone acetylation levels at "late" origins in a Δ*rpd3*Δ*yta7* mutant strain with the corresponding levels in WT, Δ*rpd3* and Δ*yta7* strains would indicate if acetylation levels at origins drop in the absence of Yta7p.

All of these hypotheses will require testing, but to narrow down the possibilities a combined large scale and targeted approach could be taken. Continuing with the experiment to test if Sas3p is recruited to replication origins and if it is reduced when *YTA7* is deleted could point to, or rule out, a role involving the NuA3 HAT. A large scale screen to identify third mutations that cause synthetic sickness in the Δ*rpd3*Δ*yta7* strain (akin to the *CDC7*ts mutation) might highlight which, if any, of the above mentioned pathways are involved in the role of Yta7p in DNA replication.

When looking to Yta7p homologues in other species for clues to the function of this protein there is some recent data available. As previously stated the *C. elegans* LEX-1 protein is similar to Yta7p and LEX-1 is required for transcription in heterochromatic regions [Tseng et al., 2007]. This function of LEX-1 has similarities to Yta7p in that it appears to function as an activator of genes and the authors propose that LEX-1, together with a second protein TAM-1, functions to regulate chromatin in repetitive regions of the genome in order to promote gene activation. The proposed human homologue of *YTA7* is *ATAD2*. The protein product of *ATAD2* contains two ATPase domains and a bromodomain, identical to Yta7p. One study identified increased *ATAD2* expression as a poor prognosis marker in osteosarcoma patients [Fellenberg et al., 2007]. More recently, the realisation that *ATAD2* expression is increased in multiple tumour types lead to a study of the function of the ATAD2 protein [Ciro et al., 2009]. This study describes how decreased expression of *ATAD2* in human fibroblast cells impairs progression into S phase and results in decreased colony formation for both WT and cancerous cell lines. Binding of ATAD2 to H3 via its bromodomain was witnessed and this binding increased when histone acetylation was increased. Binding was reduced, but not abrograted when the bromodomain was subjected to specific deletions. The authors also describe how ATAD2 binds to MYC and is involved

in transcriptional activation, both via this patnership with MYC and alone. A suggestion that this transcriptional activation is involved in the poor prognosis of cancer patients with increased *ATAD2* expression was made. Increased *ATAD2* expression was identified in many different cancer types, but involvement of *ATAD2* in replication processes was not explored. This possibility of linking ATAD2 with DNA replication in humans would be an interesting area of future investigation.

9.2 The Role of Yta7p in S phase Checkpoint Recovery

This thesis has highlighted a role for Yta7p in the S phase checkpoint. The initial suggestion that Yta7p could be involved in both DNA replication and S phase checkpoint function was provided by the HU sensitivity phenotype observed in a Δ*rpd3*Δ*yta7* double mutant. The sensitivity to HU was highlighted by spot test plates and survival curves. Further investigation revealed that Yta7p and Rpd3p are not required for efficient S phase checkpoint activation, but are required for recovery after removal of the checkpoint stimulus. It remains to be investigated if this inefficient recovery is due to continued checkpoint activation, collapsed replication forks, an inability to fire subsequent replication origins, or a combination of these events. Each possibility can be tested as described in Chapter 3. As for the DNA replication phenotype, it is unclear at this point if the redundancy witnessed with *RPD3* deletion is due to a common function of these proteins. It could be checked if the "late-firing" replication origins that fire before checkpoint activation in a Δ*rpd3* strain have also already fired in a Δ*rpd3*Δ*yta7* strain arrested with HU. This could point to the effect of Δ*rpd3*Δ*yta7* being due to an increased number of replication forks and a requirement of Yta7p to stabilise them.

An additional result provided by this thesis is that the role of Yta7p in S phase checkpoint recovery is partially dependent on the presence of the bromodomain. This could be due to a misguided binding of Yta7p to chromatin, which was witnessed for some binding regions of Yta7p across the genome [Gradolatto et al., 2009]. Alternatively, the bromodomain may be required for protein-protein interactions that could be important for recruitment of Yta7p, or an interacting partner of Yta7p, to a relevant region. In addition to binding to histones, bromodomains can also preferentially bind other acetylated proteins.

It could be speculated that Yta7p might be involved in other cell cycle checkpoints. In fact, the genetic interactors of Yta7p include several subunits of the NuA4 and INO80 complexes in addition to: a SWR1 subunit, the Sin3p subunit of RPD3 containing complexes, the Bmh1p (14-3-3) protein and the histone variant Htz1p, as per Table 8.1. These complexes/proteins are all involved in the DNA damage repair pathway and were highlighted in Sections 1.6 and 1.7. The DNA repair pathway could also potentially involve Yta7p.

Many large scale screens highlight interactions between proteins, but do not always specify which proteins are involved in different pathways. In order to find relevant interactions for

the S phase checkpoint specifically, a screen to identify suppressors of the HU sensitivity in a Δ*rpd3*Δ*yta7* strain could be performed.

The fact that Yta7p is involved in recovery from S phase checkpoint activation and could potentially be involved in other checkpoints also has implications for the function of the humam ATAD2 protein. Since *ATAD2* is over expressed in many cancer types the link between ATAD2 and both DNA replication and checkpoint function could be explored.

9.3 Supplementary Data

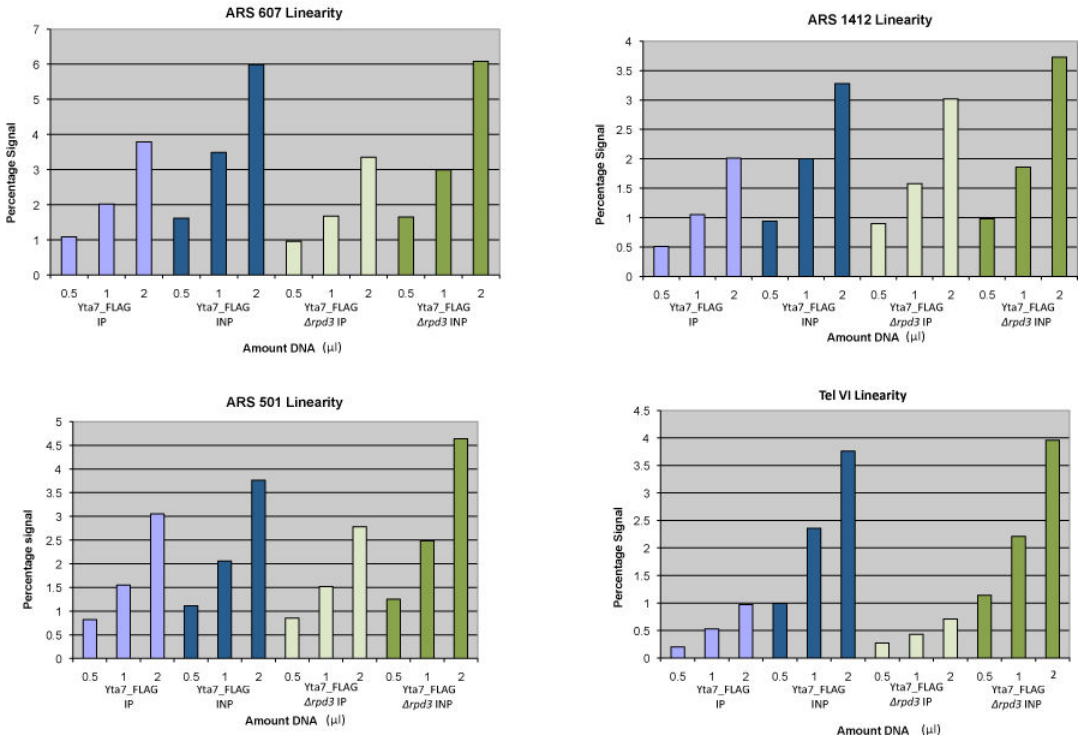

Figure 9.1: Primer set 1 for ChIP analysis is in the linear range. All primer sets were tested for linearity. Amplified products were assigned a signal intensity by Image Quant and these were plotted as bar graphs. In each graph the X axis represents each sample in sets of three ascending starting volumes (for each sample an amount of 0.5, 1 or 2 microliters of starting material were used) and the Y axis is the signal assigned to a particular sample at a particular region as a percentage of the total signals. Samples for IP and INP from both strains, Yta7-FLAG (MVY210) and Yta7-FLAG Δ*rpd3* (MVY211) were chosen. Light blue bars are the PCR products of the 0.5, 1 and 2 microliter reactions using the Yta7-FLAG ChIP sample. Dark blue bars are the same for the Yta7-FLAG INP sample. Light green bars are the Yta7-FLAG Δ*rpd3* ChIP samples and dark green bars are the Yta7-FLAG Δ*rpd3* INP samples. Top left graph displays the results for the ARS607 region. Top right graph is the ARS1412 region. Bottom left graph shows the ARS501 region. Bottom right graph is for the Tel VI region. Linear products should double in intensity when double the amount of starting DNA is used. Primer set 1 oligos (ARS607, ARS1412, ARS501 and TelVI) were in the linear range.

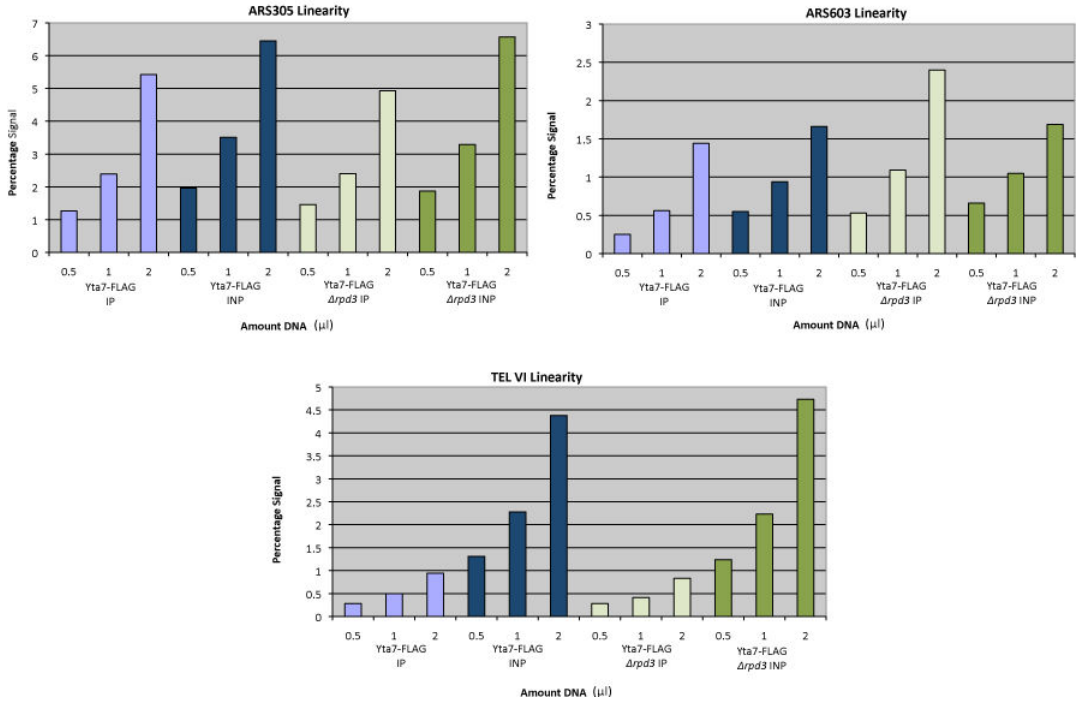

Figure 9.2: Primer set 2 for ChIP analysis is in the linear range. All primer sets were tested for linearity. Amplified products were assigned a signal intensity by Image Quant and these were plotted as bar graphs. In each graph the X axis represents each sample in sets of three ascending starting volumes (for each sample an amount of 0.5, 1 or 2 microliters of starting material were used) and the Y axis is the signal assigned to a particular sample at a particular region as a percentage of the total signals. Samples for IP and INP from both strains, Yta7-FLAG (MVY210) and Yta7-FLAG Δ*rpd3* (MVY211) were chosen. Light blue bars are the PCR products of the 0.5, 1 and 2 microliter reactions using the Yta7-FLAG ChIP sample. Dark blue bars are the same for the Yta7-FLAG INP sample. Light green bars are the Yta7-FLAG Δ*rpd3* ChIP samples and dark green bars are the Yta7-FLAG Δ*rpd3* INP samples. Top left graph displays the results for the ARS305 region. Top right graph is the ARS603 region. Bottom graph is for the Tel VI region. Linear products should double in intensity when double the amount of starting DNA is used. Primer set 2 oligos (ARS305, ARS603 and TelVI) were in the linear range.

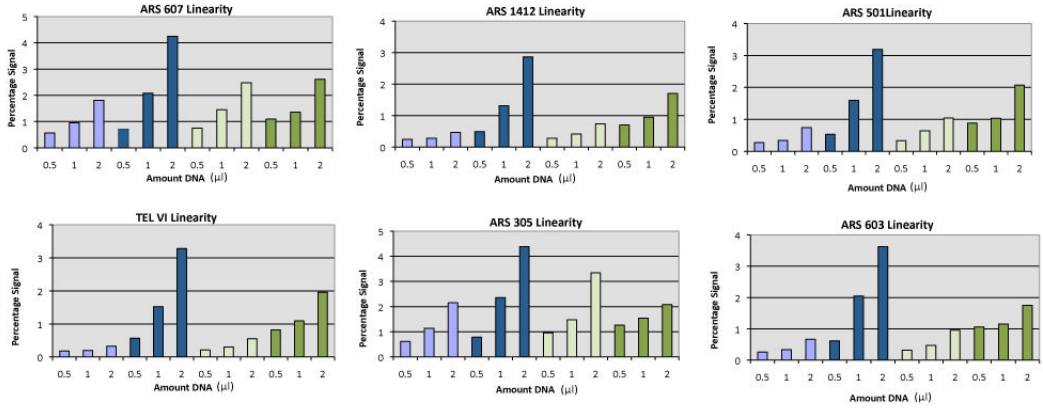

Figure 9.3: Linearity results for original ChIP samples. All primer sets were tested for linearity. Amplified products were assigned a signal intensity by Image Quant and these were plotted as bar graphs. In each graph the X axis represents each sample in sets of three ascending starting volumes (for each sample an amount of 0.5, 1 or 2 microliters of starting material were used) and the Y axis is the signal assigned to a particular sample at a particular region as a percentage of the total signals. Samples for IP and INP from both strains, Yta7-FLAG (MVY104) and Yta7-FLAG Δ*rpd3* (MVY105) were chosen. Light blue bars are the PCR products of the 0.5, 1 and 2 microliter reactions using the Yta7-FLAG ChIP sample. Dark blue bars are the same for the Yta7-FLAG INP sample. Light green bars are the Yta7-FLAG Δ*rpd3* ChIP samples and dark green bars are the Yta7-FLAG Δ*rpd3* INP samples. Top left graph displays the results for the ARS607 region. Top middle graph is the ARS1412 region. Top right graph is the ARS501 region. Bottom left graph is for the Tel VI region. Bottom middle graph shows the ARS305 region. Bottom right graph is the ARS603 region. Linear products should double in intensity when double the amount of starting DNA is used. Primers were fairly linear with a slight tendency to over amplify the lowest concentration. This is most likely due to inaccurate dilution as these primers are very linear in Figs. 9.1 and 9.2. If the slight over amplification were true this would only serve to increase No Tag or negative region signals and so any enrichment might be slightly underestimated.

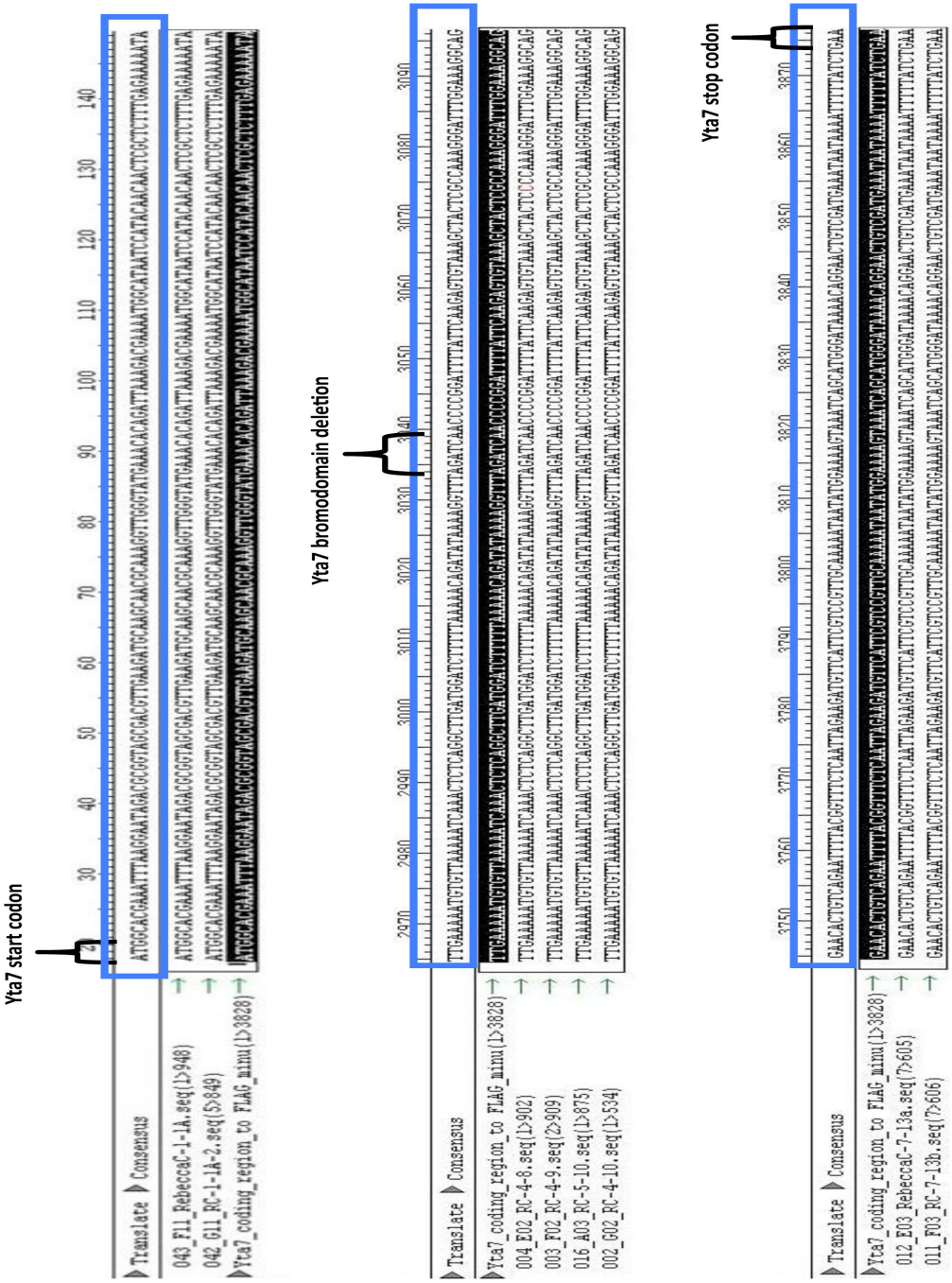

Figure 9.4: Verification of *yta7ΔBD* strains. The *yta7ΔBD* strain (MVY213) was used to sequence the *YTA7* ORF to confirm no additional mutations were added. Representative sequences are shown. Top section is the start of the *YTA7* coding region, including the start codon. Middle section includes the region surrounding the deleted bromodomain. Bottom section contains sequence for the end of the *YTA7* region up to the stop codon. Top line of each sequence section represents the consensus sequence (surrounded by blue box) that was built from all tested sequence fragments. This consensus sequence was compared with the sequence I designed in Seq Builder (highlighted in black).

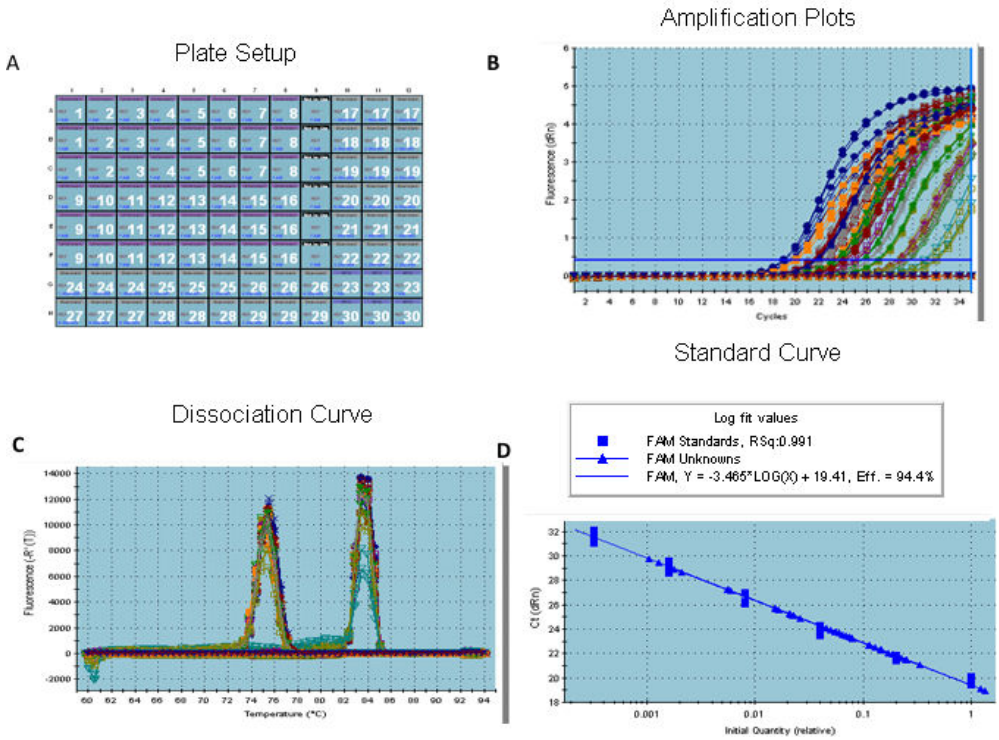

Figure 9.5: Optimisation and quality control of QPCR data. Reports generated by MXpro were used to qualify primers and validate accuracy of experiments. (A): Plate set up. Samples were run in triplicate and an averaged Ct value was produced for the three wells. No template controls were included on every plate. (B): Amplification plots were sigmoidal and a threshold was automatically assigned to each plate (blue line). X axis is cycle number, Y axis is fluorescence. Each coloured line in graph represents an individual sample. Each colour has three lines and these are the triplicate experiments. (C): A melting curve was included to detect specific binding products. X axis is temperature and Y axis is fluorescence. This report represents the optimisation experiment and so products specific to the *ASC1* region (right hand curve) and Chr. VIII region (left hand curve) were detected for each sample. (D): Ct values from triplicate samples of serially diluted INP DNA were averaged to generate a standard curve. Y axis shows the ct value and the X axis is the relative input quantity. Blue squares represent the serially diluted INP samples that were used as standards. Blue triangles represent the samples tested. The standard curve had an R Squared value of more than 0.99 and a primer efficiency score of between 90 and 100 percent in order to pass quality criteria.

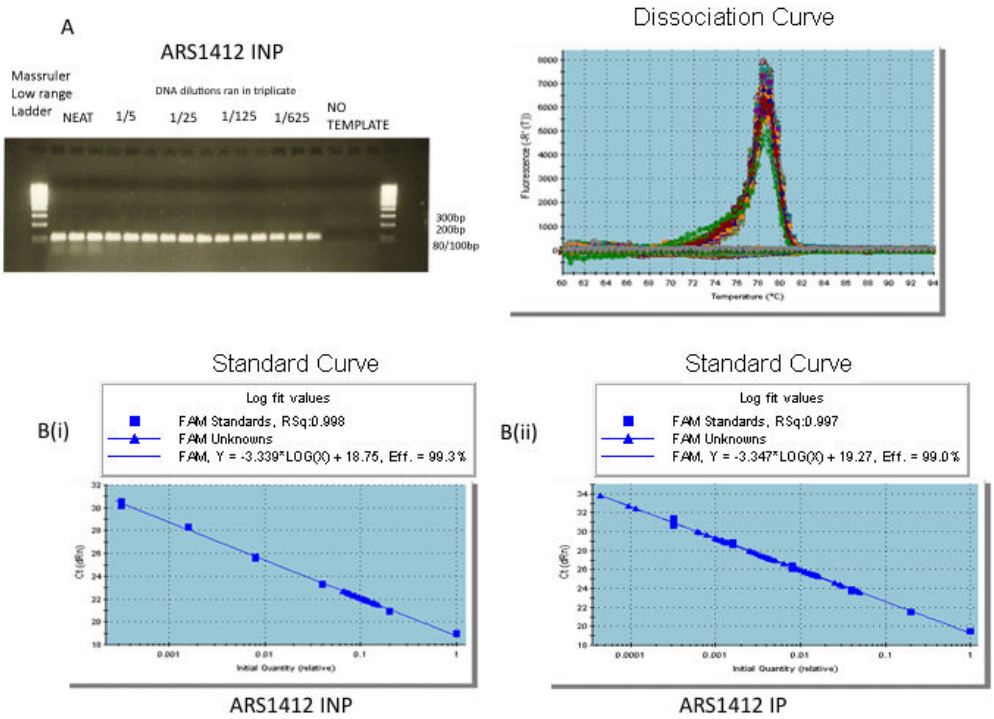

Figure 9.6: Quality control of Spt16-FLAG timecourse data. (A): A subset of PCR products were run on agarose gels to confirm data generated by melting curve analysis. This gel represents the standard curve samples of the ARS1412 INP plate, which made one specific product of the expected size and showed no amplification of the no template wells. Lane 1 is the low range ladder. Lanes 2-4 are the NEAT INP samples in triplicate. Lanes 5-7 are the same INP sample diluted 1/5 in triplicate. Lanes 8-10 are the 1/25 dilution of the INP. Lanes 11-13 are the 1/125 dilution. Lanes 14-16 are the 1/625 dilution. Lanes 17-19 are the no template controls. The accompanying melting curve is shown where the X axis is temperature and the Y axis is fluorescence. (B) Ct values from triplicate samples of serially diluted INP DNA were averaged to generate a standard curve. Y axis shows the ct value and the X axis is the relative input quantity. Blue squares represent the serially diluted INP samples that were used as standards. Blue triangles represent the samples tested. (i): All of the INP samples amplified using the ARS1412 primers (blue triangles) were within the efficiency range of the primers (regions between blue squares that represent diluted standards). (B)(ii): All IP samples (blue triangles) except a subset of the No Tag samples were also within the efficiency range.

Bibliography

[Ai and Parthun, 2004] Ai, X. and Parthun, M. R. (2004). The nuclear Hat1p/Hat2p complex: a molecular link between type B histone acetyltransferases and chromatin assembly. Mol Cell *14*, 195–205.

[Aparicio et al., 2004] Aparicio, J. G., Viggiani, C. J., Gibson, D. G. and Aparicio, O. M. (2004). The Rpd3-Sin3 histone deacetylase regulates replication timing and enables intra-S origin control in Saccharomyces cerevisiae. Mol Cell Biol *24*, 4769–80.

[Aparicio et al., 1999] Aparicio, O. M., Stout, A. M. and Bell, S. P. (1999). Differential assembly of Cdc45p and DNA polymerases at early and late origins of DNA replication. Proc Natl Acad Sci U S A *96*, 9130–5.

[Aparicio et al., 1997] Aparicio, O. M., Weinstein, D. M. and Bell, S. P. (1997). Components and dynamics of DNA replication complexes in S. cerevisiae: redistribution of MCM proteins and Cdc45p during S phase. Cell *91*, 59–69.

[Aparicio et al., 2006] Aparicio, T., Ibarra, A. and Mendez, J. (2006). Cdc45-MCM-GINS, a new power player for DNA replication. Cell Div *1*, 18.

[Azvolinsky et al., 2006] Azvolinsky, A., Dunaway, S., Torres, J. Z., Bessler, J. B. and Zakian, V. A. (2006). The S. cerevisiae Rrm3p DNA helicase moves with the replication fork and affects replication of all yeast chromosomes. Genes Dev *20*, 3104–16.

[Barrales et al., 2008] Barrales, R. R., Jimenez, J. and Ibeas, J. I. (2008). Identification of novel activation mechanisms for FLO11 regulation in Saccharomyces cerevisiae. Genetics *178*, 145–56.

[Bell and Dutta, 2002] Bell, S. P. and Dutta, A. (2002). DNA replication in eukaryotic cells. Annu Rev Biochem *71*, 333–74.

[Bell and Stillman, 1992] Bell, S. P. and Stillman, B. (1992). ATP-dependent recognition of eukaryotic origins of DNA replication by a multiprotein complex. Nature *357*, 128–34.

[Beltrao et al., 2009] Beltrao, P., Trinidad, J. C., Fiedler, D., Roguev, A., Lim, W. A., Shokat, K. M., Burlingame, A. L. and Krogan, N. J. (2009). Evolution of phosphoregulation: comparison of phosphorylation patterns across yeast species. PLoS Biol *7*, e1000134.

[Bermejo et al., 2007] Bermejo, R., Doksani, Y., Capra, T., Katou, Y. M., Tanaka, H., Shirahige, K. and Foiani, M. (2007). Top1- and Top2-mediated topological transitions at replication forks ensure fork progression and stability and prevent DNA damage checkpoint activation. Genes Dev *21*, 1921–36.

[Bianchi and Shore, 2007] Bianchi, A. and Shore, D. (2007). Early replication of short telomeres in budding yeast. Cell *128*, 1051–62.

[Biswas et al., 2008] Biswas, D., Takahata, S. and Stillman, D. J. (2008). Different genetic functions for the Rpd3(L) and Rpd3(S) complexes suggest competition between NuA4 and Rpd3(S). Mol Cell Biol *28*, 4445–58.

[Bjergbaek et al., 2005] Bjergbaek, L., Cobb, J. A., Tsai-Pflugfelder, M. and Gasser, S. M. (2005). Mechanistically distinct roles for Sgs1p in checkpoint activation and replication fork maintenance. Embo J *24*, 405–17.

[Bochman and Schwacha, 2008] Bochman, M. L. and Schwacha, A. (2008). The Mcm2-7 complex has in vitro helicase activity. Mol Cell *31*, 287–93.

[Boyer et al., 2004] Boyer, L. A., Latek, R. R. and Peterson, C. L. (2004). The SANT domain: a unique histone-tail-binding module? Nat Rev Mol Cell Biol *5*, 158–63.

[Branzei and Foiani, 2005] Branzei, D. and Foiani, M. (2005). The DNA damage response during DNA replication. Curr Opin Cell Biol *17*, 568–75.

[Branzei and Foiani, 2006] Branzei, D. and Foiani, M. (2006). The Rad53 signal transduction pathway: Replication fork stabilization, DNA repair, and adaptation. Exp Cell Res *312*, 2654–9.

[Brewer and Fangman, 1987] Brewer, B. J. and Fangman, W. L. (1987). The localization of replication origins on ARS plasmids in S. cerevisiae. Cell *51*, 463–71.

[Buhler and Gasser, 2009] Buhler, M. and Gasser, S. M. (2009). Silent chromatin at the middle and ends: lessons from yeasts. Embo J *28*, 2149–61.

[Burgers, 1998] Burgers, P. M. (1998). Eukaryotic DNA polymerases in DNA replication and DNA repair. Chromosoma *107*, 218–27.

[Burgers, 2009] Burgers, P. M. (2009). Polymerase dynamics at the eukaryotic DNA replication fork. J Biol Chem *284*, 4041–5.

[Carrozza et al., 2005] Carrozza, M. J., Li, B., Florens, L., Suganuma, T., Swanson, S. K., Lee, K. K., Shia, W. J., Anderson, S., Yates, J., Washburn, M. P. and Workman, J. L. (2005). Histone H3 methylation by Set2 directs deacetylation of coding regions by Rpd3S to suppress spurious intragenic transcription. Cell *123*, 581–92.

[Celic et al., 2006] Celic, I., Masumoto, H., Griffith, W. P., Meluh, P., Cotter, R. J., Boeke, J. D. and Verreault, A. (2006). The sirtuins hst3 and Hst4p preserve genome integrity by controlling histone h3 lysine 56 deacetylation. Curr Biol *16*, 1280–9.

[Celic et al., 2008] Celic, I., Verreault, A. and Boeke, J. D. (2008). Histone H3 K56 hyperacetylation perturbs replisomes and causes DNA damage. Genetics *179*, 1769–84.

[Ciro et al., 2009] Ciro, M., Prosperini, E., Quarto, M., Grazini, U., Walfridsson, J., McBlane, F., Nucifero, P., Pacchiana, G., Capra, M., Christensen, J. and Helin, K. (2009). ATAD2 is a novel cofactor for MYC, overexpressed and amplified in aggressive tumors. Cancer Res *69*, 8491–8.

[Clapier and Cairns, 2009] Clapier, C. R. and Cairns, B. R. (2009). The biology of chromatin remodeling complexes. Annu Rev Biochem *78*, 273–304.

[Clarke et al., 1999] Clarke, A. S., Lowell, J. E., Jacobson, S. J. and Pillus, L. (1999). Esa1p is an essential histone acetyltransferase required for cell cycle progression. Mol Cell Biol *19*, 2515–26.

[Cobb et al., 2003] Cobb, J. A., Bjergbaek, L., Shimada, K., Frei, C. and Gasser, S. M. (2003). DNA polymerase stabilization at stalled replication forks requires Mec1 and the RecQ helicase Sgs1. Embo J *22*, 4325–36.

[Collins et al., 2002] Collins, N., Poot, R. A., Kukimoto, I., Garcia-Jimenez, C., Dellaire, G. and Varga-Weisz, P. D. (2002). An ACF1-ISWI chromatin-remodeling complex is required for DNA replication through heterochromatin. Nat Genet *32*, 627–32.

[Collins et al., 2007] Collins, S. R., Miller, K. M., Maas, N. L., Roguev, A., Fillingham, J., Chu, C. S., Schuldiner, M., Gebbia, M., Recht, J., Shales, M., Ding, H., Xu, H., Han, J., Ingvarsdottir, K., Cheng, B., Andrews, B., Boone, C., Berger, S. L., Hieter, P., Zhang, Z., Brown, G. W., Ingles, C. J., Emili, A., Allis, C. D., Toczyski, D. P., Weissman, J. S., Greenblatt, J. F. and Krogan, N. J. (2007). Functional dissection of protein complexes involved in yeast chromosome biology using a genetic interaction map. Nature *446*, 806–10.

[Corpet and Almouzni, 2009] Corpet, A. and Almouzni, G. (2009). Making copies of chromatin: the challenge of nucleosomal organization and epigenetic information. Trends Cell Biol *19*, 29–41.

[Cosgrove et al., 2002] Cosgrove, A. J., Nieduszynski, C. A. and Donaldson, A. D. (2002). Ku complex controls the replication time of DNA in telomere regions. Genes Dev *16*, 2485–90.

[Cross, 1995] Cross, F. R. (1995). Starting the cell cycle: what's the point? Curr Opin Cell Biol *7*, 790–7.

[DePamphilis, 2003] DePamphilis, M. L. (2003). The 'ORC cycle': a novel pathway for regulating eukaryotic DNA replication. Gene *310*, 1–15.

[Dhalluin et al., 1999] Dhalluin, C., Carlson, J. E., Zeng, L., He, C., Aggarwal, A. K. and Zhou, M. M. (1999). Structure and ligand of a histone acetyltransferase bromodomain. Nature *399*, 491–6.

[Diffley, 2004] Diffley, J. F. (2004). Regulation of early events in chromosome replication. Curr Biol *14*, R778–86.

[Dionne and Wellinger, 1998] Dionne, I. and Wellinger, R. J. (1998). Processing of telomeric DNA ends requires the passage of a replication fork. Nucleic Acids Res *26*, 5365–71.

[Dohrmann et al., 1999] Dohrmann, P. R., Oshiro, G., Tecklenburg, M. and Sclafani, R. A. (1999). RAD53 regulates DBF4 independently of checkpoint function in Saccharomyces cerevisiae. Genetics *151*, 965–77.

[Dohrmann and Sclafani, 2006] Dohrmann, P. R. and Sclafani, R. A. (2006). Novel role for checkpoint Rad53 protein kinase in the initiation of chromosomal DNA replication in Saccharomyces cerevisiae. Genetics *174*, 87–99.

[Donaldson and Blow, 1999] Donaldson, A. D. and Blow, J. J. (1999). The regulation of replication origin activation. Curr Opin Genet Dev *9*, 62–8.

[Donaldson et al., 1998] Donaldson, A. D., Raghuraman, M. K., Friedman, K. L., Cross, F. R., Brewer, B. J. and Fangman, W. L. (1998). CLB5-dependent activation of late replication origins in S-cerevisiae. Molecular Cell *2*, 173–182.

[Downs et al., 2004] Downs, J. A., Allard, S., Jobin-Robitaille, O., Javaheri, A., Auger, A., Bouchard, N., Kron, S. J., Jackson, S. P. and Cote, J. (2004). Binding of chromatin-modifying activities to phosphorylated histone H2A at DNA damage sites. Mol Cell *16*, 979–90.

[Doyon et al., 2006] Doyon, Y., Cayrou, C., Ullah, M., Landry, A. J., Cote, V., Selleck, W., Lane, W. S., Tan, S., Yang, X. J. and Cote, J. (2006). ING tumor suppressor proteins are critical regulators of chromatin acetylation required for genome expression and perpetuation. Mol Cell *21*, 51–64.

[Driscoll et al., 2007] Driscoll, R., Hudson, A. and Jackson, S. P. (2007). Yeast Rtt109 promotes genome stability by acetylating histone H3 on lysine 56. Science *315*, 649–52.

[Duncker and Brown, 2003] Duncker, B. P. and Brown, G. W. (2003). Cdc7 kinases (DDKs) and checkpoint responses: lessons from two yeasts. Mutat Res *532*, 21–7.

[Duncker et al., 2002] Duncker, B. P., Shimada, K., Tsai-Pflugfelder, M., Pasero, P. and Gasser, S. M. (2002). An N-terminal domain of Dbf4p mediates interaction with both origin recognition complex (ORC) and Rad53p and can deregulate late origin firing. Proc Natl Acad Sci U S A *99*, 16087–92.

[Early et al., 2004] Early, A., Drury, L. S. and Diffley, J. F. (2004). Mechanisms involved in regulating DNA replication origins during the cell cycle and in response to DNA damage. Philos Trans R Soc Lond B Biol Sci *359*, 31–8.

[Fangman and Brewer, 1991] Fangman, W. L. and Brewer, B. J. (1991). Activation of replication origins within yeast chromosomes. Annu Rev Cell Biol *7*, 375–402.

[Fellenberg et al., 2007] Fellenberg, J., Bernd, L., Delling, G., Witte, D. and Zahlten-Hinguranage, A. (2007). Prognostic significance of drug-regulated genes in high-grade osteosarcoma. Mod Pathol *20*, 1085–94.

[Ferguson and Fangman, 1992] Ferguson, B. M. and Fangman, W. L. (1992). A position effect on the time of replication origin activation in yeast. Cell *68*, 333–9.

[Fillingham et al., 2009] Fillingham, J., Kainth, P., Lambert, J. P., van Bakel, H., Tsui, K., Pena-Castillo, L., Nislow, C., Figeys, D., Hughes, T. R., Greenblatt, J. and Andrews, B. J. (2009). Two-color cell array screen reveals interdependent roles for histone chaperones and a chromatin boundary regulator in histone gene repression. Mol Cell *35*, 340–51.

[Formosa et al., 2002] Formosa, T., Ruone, S., Adams, M. D., Olsen, A. E., Eriksson, P., Yu, Y., Rhoades, A. R., Kaufman, P. D. and Stillman, D. J. (2002). Defects in SPT16 or POB3 (yFACT) in Saccharomyces cerevisiae cause dependence on the Hir/Hpc pathway: polymerase passage may degrade chromatin structure. Genetics *162*, 1557–71.

[Friedman et al., 1996] Friedman, K. L., Diller, J. D., Ferguson, B. M., Nyland, S. V., Brewer, B. J. and Fangman, W. L. (1996). Multiple determinants controlling activation of yeast replication origins late in S phase. Genes Dev *10*, 1595–607.

[Gambus et al., 2006] Gambus, A., Jones, R. C., Sanchez-Diaz, A., Kanemaki, M., van Deursen, F., Edmondson, R. D. and Labib, K. (2006). GINS maintains association of Cdc45 with MCM in replisome progression complexes at eukaryotic DNA replication forks. Nat Cell Biol *8*, 358–66.

[Ge et al., 2007] Ge, X. Q., Jackson, D. A. and Blow, J. J. (2007). Dormant origins licensed by excess Mcm2-7 are required for human cells to survive replicative stress. Genes Dev *21*, 3331–41.

[Gietz and Woods, 2002] Gietz, R. D. and Woods, R. A. (2002). Transformation of yeast by lithium acetate/single-stranded carrier DNA/polyethylene glycol method. Methods Enzymol *350*, 87–96.

[Goldstein and McCusker, 1999] Goldstein, A. L. and McCusker, J. H. (1999). Three new dominant drug resistance cassettes for gene disruption in Saccharomyces cerevisiae. Yeast *15*, 1541–53.

[Goldstein et al., 1999] Goldstein, A. L., Pan, X. and McCusker, J. H. (1999). Heterologous URA3MX cassettes for gene replacement in Saccharomyces cerevisiae. Yeast *15*, 507–11.

[Gradolatto et al., 2008] Gradolatto, A., Rogers, R. S., Lavender, H., Taverna, S. D., Allis, C. D., Aitchison, J. D. and Tackett, A. J. (2008). Saccharomyces cerevisiae Yta7 regulates histone gene expression. Genetics *179*, 291–304.

[Gradolatto et al., 2009] Gradolatto, A., Smart, S. K., Byrum, S., Blair, L. P., Rogers, R. S., Kolar, E. A., Lavender, H., Larson, S. K., Aitchison, J. D., Taverna, S. D. and Tackett, A. J. (2009). A noncanonical bromodomain in the AAA ATPase protein Yta7 directs chromosomal positioning and barrier chromatin activity. Mol Cell Biol *29*, 4604–11.

[Groth et al., 2007] Groth, A., Corpet, A., Cook, A. J., Roche, D., Bartek, J., Lukas, J. and Almouzni, G. (2007). Regulation of replication fork progression through histone supply and demand. Science *318*, 1928–31.

[Gunjan et al., 2005] Gunjan, A., Paik, J. and Verreault, A. (2005). Regulation of histone synthesis and nucleosome assembly. Biochimie *87*, 625–35.

[Gunjan and Verreault, 2003] Gunjan, A. and Verreault, A. (2003). A Rad53 kinase-dependent surveillance mechanism that regulates histone protein levels in S. cerevisiae. Cell *115*, 537–49.

[Han et al., 2007a] Han, J., Zhou, H., Horazdovsky, B., Zhang, K., Xu, R. M. and Zhang, Z. (2007a). Rtt109 acetylates histone H3 lysine 56 and functions in DNA replication. Science *315*, 653–5.

[Han et al., 2007b] Han, J., Zhou, H., Li, Z., Xu, R. M. and Zhang, Z. (2007b). Acetylation of lysine 56 of histone H3 catalyzed by RTT109 and regulated by ASF1 is required for replisome integrity. J Biol Chem *282*, 28587–96.

[Hartwell and Weinert, 1989] Hartwell, L. H. and Weinert, T. A. (1989). Checkpoints: controls that ensure the order of cell cycle events. Science *246*, 629–34.

[Harvey and Newport, 2003] Harvey, K. J. and Newport, J. (2003). Metazoan origin selection: origin recognition complex chromatin binding is regulated by CDC6 recruitment and ATP hydrolysis. J Biol Chem *278*, 48524–8.

[Hassan et al., 2002] Hassan, A. H., Prochasson, P., Neely, K. E., Galasinski, S. C., Chandy, M., Carrozza, M. J. and Workman, J. L. (2002). Function and selectivity of bromodomains in anchoring chromatin-modifying complexes to promoter nucleosomes. Cell *111*, 369–79.

[Hereford et al., 1981] Hereford, L. M., Osley, M. A., Ludwig, T. R., n. and McLaughlin, C. S. (1981). Cell-cycle regulation of yeast histone mRNA. Cell *24*, 367–75.

[Hiraga et al., 2008] Hiraga, S., Botsios, S. and Donaldson, A. D. (2008). Histone H3 lysine 56 acetylation by Rtt109 is crucial for chromosome positioning. J Cell Biol *183*, 641–51.

[Ho et al., 2002] Ho, Y., Gruhler, A., Heilbut, A., Bader, G. D., Moore, L., Adams, S. L., Millar, A., Taylor, P., Bennett, K., Boutilier, K., Yang, L., Wolting, C., Donaldson, I., Schandorff, S., Shewnarane, J., Vo, M., Taggart, J., Goudreault, M., Muskat, B., Alfarano, C., Dewar, D., Lin, Z., Michalickova, K., Willems, A. R., Sassi, H., Nielsen, P. A., Rasmussen, K. J., Andersen, J. R., Johansen, L. E., Hansen, L. H., Jespersen, H., Podtelejnikov, A., Nielsen, E., Crawford, J., Poulsen, V., Sorensen, B. D., Matthiesen, J., Hendrickson, R. C.,

Gleeson, F., Pawson, T., Moran, M. F., Durocher, D., Mann, M., Hogue, C. W., Figeys, D. and Tyers, M. (2002). Systematic identification of protein complexes in Saccharomyces cerevisiae by mass spectrometry. Nature *415*, 180–3.

[Hodgson et al., 2007] Hodgson, B., Calzada, A. and Labib, K. (2007). Mrc1 and Tof1 regulate DNA replication forks in different ways during normal S phase. Mol Biol Cell *18*, 3894–902.

[Homesley et al., 2000] Homesley, L., Lei, M., Kawasaki, Y., Sawyer, S., Christensen, T. and Tye, B. K. (2000). Mcm10 and the MCM2-7 complex interact to initiate DNA synthesis and to release replication factors from origins. Genes Dev *14*, 913–26.

[Huberman et al., 1987] Huberman, J. A., Spotila, L. D., Nawotka, K. A., el Assouli, S. M. and Davis, L. R. (1987). The in vivo replication origin of the yeast 2 microns plasmid. Cell *51*, 473–81.

[Iida and Araki, 2004] Iida, T. and Araki, H. (2004). Noncompetitive counteractions of DNA polymerase epsilon and ISW2/yCHRAC for epigenetic inheritance of telomere position effect in Saccharomyces cerevisiae. Mol Cell Biol *24*, 217–27.

[Iizuka et al., 2006] Iizuka, M., Matsui, T., Takisawa, H. and Smith, M. M. (2006). Regulation of replication licensing by acetyltransferase Hbo1. Mol Cell Biol *26*, 1098–108.

[Im et al., 2009] Im, J. S., Ki, S. H., Farina, A., Jung, D. S., Hurwitz, J. and Lee, J. K. (2009). Assembly of the Cdc45-Mcm2-7-GINS complex in human cells requires the Ctf4/And-1, RecQL4, and Mcm10 proteins. Proc Natl Acad Sci U S A *106*, 15628–32.

[Jacobson et al., 2000] Jacobson, R. H., Ladurner, A. G., King, D. S. and Tjian, R. (2000). Structure and function of a human TAFII250 double bromodomain module. Science *288*, 1422–5.

[Jambunathan et al., 2005] Jambunathan, N., Martinez, A. W., Robert, E. C., Agochukwu, N. B., Ibos, M. E., Dugas, S. L. and Donze, D. (2005). Multiple bromodomain genes are involved in restricting the spread of heterochromatic silencing at the Saccharomyces cerevisiae HMR-tRNA boundary. Genetics *171*, 913–22.

[John et al., 2000] John, S., Howe, L., Tafrov, S. T., Grant, P. A., Sternglanz, R. and Workman, J. L. (2000). The something about silencing protein, Sas3, is the catalytic subunit of NuA3, a yTAF(II)30-containing HAT complex that interacts with the Spt16 subunit of the yeast CP (Cdc68/Pob3)-FACT complex. Genes Dev *14*, 1196–208.

[Kamimura et al., 2001] Kamimura, Y., Tak, Y. S., Sugino, A. and Araki, H. (2001). Sld3, which interacts with Cdc45 (Sld4), functions for chromosomal DNA replication in Saccharomyces cerevisiae. Embo J *20*, 2097–107.

[Kan et al., 2008] Kan, J., Zou, L., Zhang, J., Wu, R., Wang, Z. and Liang, C. (2008). Origin recognition complex (ORC) mediates histone 3 lysine 4 methylation through cooperation with Spp1 in Saccharomyces cerevisiae. J Biol Chem *283*, 33803–7.

[Kanter et al., 2008] Kanter, D. M., Bruck, I. and Kaplan, D. L. (2008). Mcm subunits can assemble into two different active unwinding complexes. J Biol Chem *283*, 31172–82.

[Kasten et al., 2004] Kasten, M., Szerlong, H., Erdjument-Bromage, H., Tempst, P., Werner, M. and Cairns, B. R. (2004). Tandem bromodomains in the chromatin remodeler RSC recognize acetylated histone H3 Lys14. Embo J *23*, 1348–59.

[Katou et al., 2003] Katou, Y., Kanoh, Y., Bando, M., Noguchi, H., Tanaka, H., Ashikari, T., Sugimoto, K. and Shirahige, K. (2003). S-phase checkpoint proteins Tof1 and Mrc1 form a stable replication-pausing complex. Nature *424*, 1078–83.

[Kemp et al., 2005] Kemp, M. G., Ghosh, M., Liu, G. and Leffak, M. (2005). The histone deacetylase inhibitor trichostatin A alters the pattern of DNA replication origin activity in human cells. Nucleic Acids Res *33*, 325–36.

[Kim et al., 2003] Kim, J. M., Yamada, M. and Masai, H. (2003). Functions of mammalian Cdc7 kinase in initiation/monitoring of DNA replication and development. Mutat Res *532*, 29–40.

[Knott et al., 2009] Knott, S. R., Viggiani, C. J., Tavare, S. and Aparicio, O. M. (2009). Genome-wide replication profiles indicate an expansive role for Rpd3L in regulating replication initiation timing or efficiency, and reveal genomic loci of Rpd3 function in Saccharomyces cerevisiae. Genes Dev *23*, 1077–90.

[Kuo and Allis, 1998] Kuo, M. H. and Allis, C. D. (1998). Roles of histone acetyltransferases and deacetylases in gene regulation. Bioessays *20*, 615–26.

[Kurdistani and Grunstein, 2003a] Kurdistani, S. K. and Grunstein, M. (2003a). Histone acetylation and deacetylation in yeast. Nat Rev Mol Cell Biol *4*, 276–84.

[Kurdistani and Grunstein, 2003b] Kurdistani, S. K. and Grunstein, M. (2003b). In vivo protein-protein and protein-DNA crosslinking for genomewide binding microarray. Methods *31*, 90–5.

[Labib and Gambus, 2007] Labib, K. and Gambus, A. (2007). A key role for the GINS complex at DNA replication forks. Trends Cell Biol *17*, 271–8.

[Labib and Hodgson, 2007] Labib, K. and Hodgson, B. (2007). Replication fork barriers: pausing for a break or stalling for time? EMBO Rep *8*, 346–53.

[Laman et al., 1995] Laman, H., Balderes, D. and Shore, D. (1995). Disturbance of normal cell cycle progression enhances the establishment of transcriptional silencing in Saccharomyces cerevisiae. Mol Cell Biol *15*, 3608–17.

[Lambert et al., 2009] Lambert, J. P., Mitchell, L., Rudner, A., Baetz, K. and Figeys, D. (2009). A novel proteomics approach for the discovery of chromatin-associated protein networks. Mol Cell Proteomics *8*, 870–82.

[Laroche et al., 1998] Laroche, T., Martin, S. G., Gotta, M., Gorham, H. C., Pryde, F. E., Louis, E. J. and Gasser, S. M. (1998). Mutation of yeast Ku genes disrupts the subnuclear organization of telomeres. Curr Biol *8*, 653–6.

[Lee and Workman, 2007] Lee, K. K. and Workman, J. L. (2007). Histone acetyltransferase complexes: one size doesn't fit all. Nat Rev Mol Cell Biol *8*, 284–95.

[Lei et al., 1997] Lei, M., Kawasaki, Y., Young, M. R., Kihara, M., Sugino, A. and Tye, B. K. (1997). Mcm2 is a target of regulation by Cdc7-Dbf4 during the initiation of DNA synthesis. Genes Dev *11*, 3365–74.

[Lew and Reed, 1993] Lew, D. J. and Reed, S. I. (1993). Morphogenesis in the yeast cell cycle: regulation by Cdc28 and cyclins. J Cell Biol *120*, 1305–20.

[Li et al., 2007] Li, B., Gogol, M., Carey, M., Lee, D., Seidel, C. and Workman, J. L. (2007). Combined action of PHD and chromo domains directs the Rpd3S HDAC to transcribed chromatin. Science *316*, 1050–4.

[Li et al., 2005] Li, J., Santoro, R., Koberna, K. and Grummt, I. (2005). The chromatin remodeling complex NoRC controls replication timing of rRNA genes. Embo J *24*, 120–7.

[Li and Kelly, 1984] Li, J. J. and Kelly, T. J. (1984). Simian virus 40 DNA replication in vitro. Proc Natl Acad Sci U S A *81*, 6973–7.

[Lipford and Bell, 2001] Lipford, J. R. and Bell, S. P. (2001). Nucleosomes positioned by ORC facilitate the initiation of DNA replication. Mol Cell *7*, 21–30.

[Longhese et al., 2003] Longhese, M. P., Clerici, M. and Lucchini, G. (2003). The S-phase checkpoint and its regulation in Saccharomyces cerevisiae. Mutat Res *532*, 41–58.

[Longtine et al., 1998] Longtine, M. S., McKenzie, A., r., Demarini, D. J., Shah, N. G., Wach, A., Brachat, A., Philippsen, P. and Pringle, J. R. (1998). Additional modules for versatile and economical PCR-based gene deletion and modification in Saccharomyces cerevisiae. Yeast *14*, 953–61.

[Lottersberger et al., 2007] Lottersberger, F., Panza, A., Lucchini, G. and Longhese, M. P. (2007). Functional and physical interactions between yeast 14-3-3 proteins, acetyltransferases, and deacetylases in response to DNA replication perturbations. Mol Cell Biol *27*, 3266–81.

[Lu et al., 2009] Lu, P. Y., Levesque, N. and Kobor, M. S. (2009). NuA4 and SWR1-C: two chromatin-modifying complexes with overlapping functions and components. Biochem Cell Biol *87*, 799–815.

[Ma et al., 1998] Ma, X. J., Wu, J., Altheim, B. A., Schultz, M. C. and Grunstein, M. (1998). Deposition-related sites K5/K12 in histone H4 are not required for nucleosome deposition in yeast. Proc Natl Acad Sci U S A *95*, 6693–8.

[Makovets et al., 2004] Makovets, S., Herskowitz, I. and Blackburn, E. H. (2004). Anatomy and dynamics of DNA replication fork movement in yeast telomeric regions. Mol Cell Biol *24*, 4019–31.

[Masumoto et al., 2005] Masumoto, H., Hawke, D., Kobayashi, R. and Verreault, A. (2005). A role for cell-cycle-regulated histone H3 lysine 56 acetylation in the DNA damage response. Nature *436*, 294–8.

[Masumoto et al., 2002] Masumoto, H., Muramatsu, S., Kamimura, Y. and Araki, H. (2002). S-Cdk-dependent phosphorylation of Sld2 essential for chromosomal DNA replication in budding yeast. Nature *415*, 651–5.

[Masumoto et al., 2000] Masumoto, H., Sugino, A. and Araki, H. (2000). Dpb11 controls the association between DNA polymerases alpha and epsilon and the autonomously replicating sequence region of budding yeast. Mol Cell Biol *20*, 2809–17.

[Matangkasombut and Buratowski, 2003] Matangkasombut, O. and Buratowski, S. (2003). Different sensitivities of bromodomain factors 1 and 2 to histone H4 acetylation. Mol Cell *11*, 353–63.

[McCune et al., 2008] McCune, H. J., Danielson, L. S., Alvino, G. M., Collingwood, D., Delrow, J. J., Fangman, W. L., Brewer, B. J. and Raghuraman, M. K. (2008). The temporal program of chromosome replication: genomewide replication in clb5Delta Saccharomyces cerevisiae. Genetics *180*, 1833–47.

[McGarry and Kirschner, 1998] McGarry, T. J. and Kirschner, M. W. (1998). Geminin, an inhibitor of DNA replication, is degraded during mitosis. Cell *93*, 1043–53.

[Messer, 1987] Messer, W. (1987). Initiation of DNA replication in Escherichia coli. J Bacteriol *169*, 3395–9.

[Micialkiewicz and Chelstowska, 2008] Micialkiewicz, A. and Chelstowska, A. (2008). The essential function of Swc4p - a protein shared by two chromatin-modifying complexes of the yeast Saccharomyces cerevisiae - resides within its N-terminal part. Acta Biochim Pol *55*, 603–12.

[Mimura et al., 2004] Mimura, S., Seki, T., Tanaka, S. and Diffley, J. F. (2004). Phosphorylation-dependent binding of mitotic cyclins to Cdc6 contributes to DNA replication control. Nature *431*, 1118–23.

[Miotto and Struhl, 2010] Miotto, B. and Struhl, K. (2010). HBO1 histone acetylase activity is essential for DNA replication licensing and inhibited by Geminin. Mol Cell *37*, 57–66.

[Mitchell et al., 2008] Mitchell, L., Lambert, J. P., Gerdes, M., Al-Madhoun, A. S., Skerjanc, I. S., Figeys, D. and Baetz, K. (2008). Functional dissection of the NuA4 histone acetyltransferase reveals its role as a genetic hub and that Eaf1 is essential for complex integrity. Mol Cell Biol *28*, 2244–56.

[Morrison et al., 2004] Morrison, A. J., Highland, J., Krogan, N. J., Arbel-Eden, A., Greenblatt, J. F., Haber, J. E. and Shen, X. (2004). INO80 and gamma-H2AX interaction links ATP-dependent chromatin remodeling to DNA damage repair. Cell *119*, 767–75.

[Mousson et al., 2007] Mousson, F., Ochsenbein, F. and Mann, C. (2007). The histone chaperone Asf1 at the crossroads of chromatin and DNA checkpoint pathways. Chromosoma *116*, 79–93.

[Nedelcheva et al., 2005] Nedelcheva, M. N., Roguev, A., Dolapchiev, L. B., Shevchenko, A., Taskov, H. B., Stewart, A. F. and Stoynov, S. S. (2005). Uncoupling of unwinding from DNA synthesis implies regulation of MCM helicase by Tof1/Mrc1/Csm3 checkpoint complex. J Mol Biol *347*, 509–21.

[Nguyen et al., 2001] Nguyen, V. Q., Co, C. and Li, J. J. (2001). Cyclin-dependent kinases prevent DNA re-replication through multiple mechanisms. Nature *411*, 1068–73.

[Nieduszynski et al., 2007] Nieduszynski, C. A., Hiraga, S., Ak, P., Benham, C. J. and Donaldson, A. D. (2007). OriDB: a DNA replication origin database. Nucleic Acids Res *35*, D40–6.

[Nieduszynski et al., 2006] Nieduszynski, C. A., Knox, Y. and Donaldson, A. D. (2006). Genome-wide identification of replication origins in yeast by comparative genomics. Genes Dev *20*, 1874–9.

[Orphanides et al., 1998] Orphanides, G., LeRoy, G., Chang, C. H., Luse, D. S. and Reinberg, D. (1998). FACT, a factor that facilitates transcript elongation through nucleosomes. Cell *92*, 105–16.

[Owen et al., 2000] Owen, D. J., Ornaghi, P., Yang, J. C., Lowe, N., Evans, P. R., Ballario, P., Neuhaus, D., Filetici, P. and Travers, A. A. (2000). The structural basis for the recognition of acetylated histone H4 by the bromodomain of histone acetyltransferase gcn5p. Embo J *19*, 6141–9.

[Papamichos-Chronakis and Peterson, 2008] Papamichos-Chronakis, M. and Peterson, C. L. (2008). The Ino80 chromatin-remodeling enzyme regulates replisome function and stability. Nat Struct Mol Biol *15*, 338–45.

[Pappas et al., 2004] Pappas, D. L., J., Frisch, R. and Weinreich, M. (2004). The NAD(+)-dependent Sir2p histone deacetylase is a negative regulator of chromosomal DNA replication. Genes Dev *18*, 769–81.

[Parsons et al., 2004] Parsons, A. B., Brost, R. L., Ding, H., Li, Z., Zhang, C., Sheikh, B., Brown, G. W., Kane, P. M., Hughes, T. R. and Boone, C. (2004). Integration of chemical-genetic and genetic interaction data links bioactive compounds to cellular target pathways. Nat Biotechnol *22*, 62–9.

[Parthun et al., 1996] Parthun, M. R., Widom, J. and Gottschling, D. E. (1996). The major cytoplasmic histone acetyltransferase in yeast: links to chromatin replication and histone metabolism. Cell *87*, 85–94.

[Pokholok et al., 2005] Pokholok, D. K., Harbison, C. T., Levine, S., Cole, M., Hannett, N. M., Lee, T. I., Bell, G. W., Walker, K., Rolfe, P. A., Herbolsheimer, E., Zeitlinger, J., Lewitter, F., Gifford, D. K. and Young, R. A. (2005). Genome-wide map of nucleosome acetylation and methylation in yeast. Cell *122*, 517–527.

[Poot et al., 2005] Poot, R. A., Bozhenok, L., van den Berg, D. L., Hawkes, N. and Varga-Weisz, P. D. (2005). Chromatin remodeling by WSTF-ISWI at the replication site: opening a window of opportunity for epigenetic inheritance? Cell Cycle *4*, 543–6.

[Probst et al., 2009] Probst, A. V., Dunleavy, E. and Almouzni, G. (2009). Epigenetic inheritance during the cell cycle. Nat Rev Mol Cell Biol *10*, 192–206.

[Pryde et al., 2009] Pryde, F., Jain, D., Kerr, A., Curley, R., Mariotti, F. R. and Vogelauer, M. (2009). H3 k36 methylation helps determine the timing of cdc45 association with replication origins. PLoS One *4*, e5882.

[Raghuraman et al., 2001] Raghuraman, M. K., Winzeler, E. A., Collingwood, D., Hunt, S., Wodicka, L., Conway, A., Lockhart, D. J., Davis, R. W., Brewer, B. J. and Fangman, W. L. (2001). Replication dynamics of the yeast genome. Science *294*, 115–121.

[Rao et al., 2005] Rao, B., Shibata, Y., Strahl, B. D. and Lieb, J. D. (2005). Dimethylation of histone H3 at lysine 36 demarcates regulatory and nonregulatory chromatin genome-wide. Mol Cell Biol *25*, 9447–59.

[Ray-Gallet et al., 2002] Ray-Gallet, D., Quivy, J. P., Scamps, C., Martini, E. M., Lipinski, M. and Almouzni, G. (2002). HIRA is critical for a nucleosome assembly pathway independent of DNA synthesis. Mol Cell *9*, 1091–100.

[Rhind, 2006] Rhind, N. (2006). DNA replication timing: random thoughts about origin firing. Nat Cell Biol *8*, 1313–6.

[Ricke and Bielinsky, 2004] Ricke, R. M. and Bielinsky, A. K. (2004). Mcm10 regulates the stability and chromatin association of DNA polymerase-alpha. Mol Cell *16*, 173–85.

[Rowley et al., 1991] Rowley, A., Singer, R. A. and Johnston, G. C. (1991). CDC68, a yeast gene that affects regulation of cell proliferation and transcription, encodes a protein with a highly acidic carboxyl terminus. Mol Cell Biol *11*, 5718–26.

[Santamaria et al., 2000] Santamaria, D., Viguera, E., Martinez-Robles, M. L., Hyrien, O., Hernandez, P., Krimer, D. B. and Schvartzman, J. B. (2000). Bi-directional replication and random termination. Nucleic Acids Res *28*, 2099–107.

[Santocanale and Diffley, 1996] Santocanale, C. and Diffley, J. F. (1996). ORC- and Cdc6-dependent complexes at active and inactive chromosomal replication origins in Saccharomyces cerevisiae. Embo J *15*, 6671–9.

[Schlesinger and Formosa, 2000] Schlesinger, M. B. and Formosa, T. (2000). POB3 is required for both transcription and replication in the yeast Saccharomyces cerevisiae. Genetics *155*, 1593–606.

[Schulze et al., 2009] Schulze, J. M., Wang, A. Y. and Kobor, M. S. (2009). YEATS domain proteins: a diverse family with many links to chromatin modification and transcription. Biochem Cell Biol *87*, 65–75.

[Schwob et al., 1994] Schwob, E., Bohm, T., Mendenhall, M. D. and Nasmyth, K. (1994). The B-type cyclin kinase inhibitor p40SIC1 controls the G1 to S transition in S. cerevisiae. Cell *79*, 233–44.

[Scott and Plon, 2003] Scott, K. L. and Plon, S. E. (2003). Loss of Sin3/Rpd3 histone deacetylase restores the DNA damage response in checkpoint-deficient strains of Saccharomyces cerevisiae. Mol Cell Biol *23*, 4522–31.

[Seki et al., 2006] Seki, T., Akita, M., Kamimura, Y., Muramatsu, S., Araki, H. and Sugino, A. (2006). GINS is a DNA polymerase epsilon accessory factor during chromosomal DNA replication in budding yeast. J Biol Chem *281*, 21422–32.

[Shahbazian and Grunstein, 2007] Shahbazian, M. D. and Grunstein, M. (2007). Functions of site-specific histone acetylation and deacetylation. Annu Rev Biochem *76*, 75–100.

[Shi et al., 2006] Shi, X., Hong, T., Walter, K. L., Ewalt, M., Michishita, E., Hung, T., Carney, D., Pena, P., Lan, F., Kaadige, M. R., Lacoste, N., Cayrou, C., Davrazou, F., Saha, A., Cairns, B. R., Ayer, D. E., Kutateladze, T. G., Shi, Y., Cote, J., Chua, K. F. and Gozani, O. (2006). ING2 PHD domain links histone H3 lysine 4 methylation to active gene repression. Nature *442*, 96–9.

[Shibahara and Stillman, 1999] Shibahara, K. and Stillman, B. (1999). Replication-dependent marking of DNA by PCNA facilitates CAF-1-coupled inheritance of chromatin. Cell *96*, 575–85.

[Shimada et al., 2008] Shimada, K., Oma, Y., Schleker, T., Kugou, K., Ohta, K., Harata, M. and Gasser, S. M. (2008). Ino80 chromatin remodeling complex promotes recovery of stalled replication forks. Curr Biol *18*, 566–75.

[Simpson, 1990] Simpson, R. T. (1990). Nucleosome positioning can affect the function of a cis-acting DNA element in vivo. Nature *343*, 387–9.

[Smolka et al., 2005] Smolka, M. B., Albuquerque, C. P., Chen, S. H., Schmidt, K. H., Wei, X. X., Kolodner, R. D. and Zhou, H. (2005). Dynamic changes in protein-protein interaction and protein phosphorylation probed with amine-reactive isotope tag. Mol Cell Proteomics *4*, 1358–69.

[Smolka et al., 2006] Smolka, M. B., Chen, S. H., Maddox, P. S., Enserink, J. M., Albuquerque, C. P., Wei, X. X., Desai, A., Kolodner, R. D. and Zhou, H. (2006). An FHA domain-mediated protein interaction network of Rad53 reveals its role in polarized cell growth. J Cell Biol *175*, 743–53.

[Stevenson and Gottschling, 1996] Stevenson, J. and Gottschling, D. (1996). The late firing of telomere-proximal origins of replications is SIR-dependent. Molecular Biology of the Cell *7*, 2967–2967.

[Stevenson and Gottschling, 1999] Stevenson, J. B. and Gottschling, D. E. (1999). Telomeric chromatin modulates replication timing near chromosome ends. Genes Dev *13*, 146–151.

[Stinchcomb et al., 1979] Stinchcomb, D. T., Struhl, K. and Davis, R. W. (1979). Isolation and characterisation of a yeast chromosomal replicator. Nature *282*, 39–43.

[Strahl and Allis, 2000] Strahl, B. D. and Allis, C. D. (2000). The language of covalent histone modifications. Nature *403*, 41–5.

[Sun et al., 1996] Sun, Z., Fay, D. S., Marini, F., Foiani, M. and Stern, D. F. (1996). Spk1/Rad53 is regulated by Mec1-dependent protein phosphorylation in DNA replication and damage checkpoint pathways. Genes Dev *10*, 395–406.

[Sun and Hampsey, 1999] Sun, Z. W. and Hampsey, M. (1999). A general requirement for the Sin3-Rpd3 histone deacetylase complex in regulating silencing in Saccharomyces cerevisiae. Genetics *152*, 921–32.

[Suter et al., 2007] Suter, B., Pogoutse, O., Guo, X., Krogan, N., Lewis, P., Greenblatt, J. F., Rine, J. and Emili, A. (2007). Association with the origin recognition complex suggests a novel role for histone acetyltransferase Hat1p/Hat2p. BMC Biol *5*, 38.

[Szyjka et al., 2005] Szyjka, S. J., Viggiani, C. J. and Aparicio, O. M. (2005). Mrc1 is required for normal progression of replication forks throughout chromatin in S. cerevisiae. Mol Cell *19*, 691–7.

[Tackett et al., 2005] Tackett, A. J., Dilworth, D. J., Davey, M. J., O'Donnell, M., Aitchison, J. D., Rout, M. P. and Chait, B. T. (2005). Proteomic and genomic characterization of chromatin complexes at a boundary. J Cell Biol *169*, 35–47.

[Takayama et al., 2003] Takayama, Y., Kamimura, Y., Okawa, M., Muramatsu, S., Sugino, A. and Araki, H. (2003). GINS, a novel multiprotein complex required for chromosomal DNA replication in budding yeast. Genes Dev *17*, 1153–65.

[Takeda and Dutta, 2005] Takeda, D. Y. and Dutta, A. (2005). DNA replication and progression through S phase. Oncogene *24*, 2827–43.

[Tan et al., 2006] Tan, B. C., Chien, C. T., Hirose, S. and Lee, S. C. (2006). Functional cooperation between FACT and MCM helicase facilitates initiation of chromatin DNA replication. Embo J *25*, 3975–85.

[Tanaka and Diffley, 2002] Tanaka, S. and Diffley, J. F. (2002). Interdependent nuclear accumulation of budding yeast Cdt1 and Mcm2-7 during G1 phase. Nat Cell Biol *4*, 198–207.

[Toone et al., 1997] Toone, W. M., Aerne, B. L., Morgan, B. A. and Johnston, L. H. (1997). Getting started: regulating the initiation of DNA replication in yeast. Annu Rev Microbiol *51*, 125–49.

[Toueille and Hubscher, 2004] Toueille, M. and Hubscher, U. (2004). Regulation of the DNA replication fork: a way to fight genomic instability. Chromosoma *113*, 113–25.

[Tourriere and Pasero, 2007] Tourriere, H. and Pasero, P. (2007). Maintenance of fork integrity at damaged DNA and natural pause sites. DNA Repair (Amst) *6*, 900–13.

[Tourriere et al., 2005] Tourriere, H., Versini, G., Cordon-Preciado, V., Alabert, C. and Pasero, P. (2005). Mrc1 and Tof1 promote replication fork progression and recovery independently of Rad53. Mol Cell *19*, 699–706.

[Tseng et al., 2007] Tseng, R. J., Armstrong, K. R., Wang, X. and Chamberlin, H. M. (2007). The bromodomain protein LEX-1 acts with TAM-1 to modulate gene expression in C. elegans. Mol Genet Genomics *278*, 507–18.

[Tye, 1999] Tye, B. K. (1999). MCM proteins in DNA replication. Annu Rev Biochem *68*, 649–86.

[Ubersax et al., 2003] Ubersax, J. A., Woodbury, E. L., Quang, P. N., Paraz, M., Blethrow, J. D., Shah, K., Shokat, K. M. and Morgan, D. O. (2003). Targets of the cyclin-dependent kinase Cdk1. Nature *425*, 859–64.

[Ullah et al., 2008] Ullah, M., Pelletier, N., Xiao, L., Zhao, S. P., Wang, K., Degerny, C., Tahmasebi, S., Cayrou, C., Doyon, Y., Goh, S. L., Champagne, N., Cote, J. and Yang, X. J. (2008). Molecular architecture of quartet MOZ/MORF histone acetyltransferase complexes. Mol Cell Biol *28*, 6828–43.

[Utley et al., 2005] Utley, R. T., Lacoste, N., Jobin-Robitaille, O., Allard, S. and Cote, J. (2005). Regulation of NuA4 histone acetyltransferase activity in transcription and DNA repair by phosphorylation of histone H4. Mol Cell Biol *25*, 8179–90.

[van Attikum et al., 2007] van Attikum, H., Fritsch, O. and Gasser, S. M. (2007). Distinct roles for SWR1 and INO80 chromatin remodeling complexes at chromosomal double-strand breaks. Embo J *26*, 4113–25.

[van Brabant et al., 2001] van Brabant, A. J., Buchanan, C. D., Charboneau, E., Fangman, W. L. and Brewer, B. J. (2001). An origin-deficient yeast artificial chromosome triggers a cell cycle checkpoint. Mol Cell *7*, 705–13.

[Verreault, 2000] Verreault, A. (2000). De novo nucleosome assembly: new pieces in an old puzzle. Genes Dev *14*, 1430–8.

[Vincent et al., 2008] Vincent, J. A., Kwong, T. J. and Tsukiyama, T. (2008). ATP-dependent chromatin remodeling shapes the DNA replication landscape. Nat Struct Mol Biol *15*, 477–84.

[Vogelauer et al., 2002] Vogelauer, M., Rubbi, L., Lucas, I., Brewer, B. J. and Grunstein, M. (2002). Histone acetylation regulates the time of replication origin firing. Molecular Cell *10*, 1223–1233.

[Vogelauer et al., 2000] Vogelauer, M., Wu, J. S., Suka, N. and Grunstein, M. (2000). Global histone acetylation and deacetylation in yeast. Nature *408*, 495–498.

[Waga and Stillman, 1994] Waga, S. and Stillman, B. (1994). Anatomy of a DNA replication fork revealed by reconstitution of SV40 DNA replication in vitro. Nature *369*, 207–12.

[Waga and Stillman, 1998] Waga, S. and Stillman, B. (1998). The DNA replication fork in eukaryotic cells. Annu Rev Biochem *67*, 721–51.

[Wang, 1996] Wang, J. C. (1996). DNA topoisomerases. Annu Rev Biochem *65*, 635–92.

[Warren et al., 2009] Warren, E. M., Huang, H., Fanning, E., Chazin, W. J. and Eichman, B. F. (2009). Physical interactions between Mcm10, DNA, and DNA polymerase alpha. J Biol Chem *284*, 24662–72.

[Weinert and Hartwell, 1988] Weinert, T. A. and Hartwell, L. H. (1988). The RAD9 gene controls the cell cycle response to DNA damage in Saccharomyces cerevisiae. Science *241*, 317–22.

[Weinreich et al., 2004] Weinreich, M., Palacios DeBeer, M. A. and Fox, C. A. (2004). The activities of eukaryotic replication origins in chromatin. Biochim Biophys Acta *1677*, 142–57.

[Weitao et al., 2003] Weitao, T., Budd, M. and Campbell, J. L. (2003). Evidence that yeast SGS1, DNA2, SRS2, and FOB1 interact to maintain rDNA stability. Mutat Res *532*, 157–72.

[Wittmeyer et al., 1999] Wittmeyer, J., Joss, L. and Formosa, T. (1999). Spt16 and Pob3 of Saccharomyces cerevisiae form an essential, abundant heterodimer that is nuclear, chromatin-associated, and copurifies with DNA polymerase alpha. Biochemistry *38*, 8961–71.

[Woodfine et al., 2004] Woodfine, K., Fiegler, H., Beare, D. M., Collins, J. E., McCann, O. T., Young, B. D., Debernardi, S., Mott, R., Dunham, I. and Carter, N. P. (2004). Replication timing of the human genome. Hum Mol Genet *13*, 191–202.

[Wyrick et al., 2001] Wyrick, J. J., Aparicio, J. G., Chen, T., Barnett, J. D., Jennings, E. G., Young, R. A., Bell, S. P. and Aparicio, O. M. (2001). Genome-wide distribution of ORC and MCM proteins in S. cerevisiae: high-resolution mapping of replication origins. Science *294*, 2357–60.

[Xu et al., 2008] Xu, C., Cui, G., Botuyan, M. V. and Mer, G. (2008). Structural basis for the recognition of methylated histone H3K36 by the Eaf3 subunit of histone deacetylase complex Rpd3S. Structure *16*, 1740–50.

[Xu et al., 2005] Xu, F., Zhang, K. and Grunstein, M. (2005). Acetylation in histone H3 globular domain regulates gene expression in yeast. Cell *121*, 375–85.

[Xu et al., 1990] Xu, H. X., Johnson, L. and Grunstein, M. (1990). Coding and noncoding sequences at the 3' end of yeast histone H2B mRNA confer cell cycle regulation. Mol Cell Biol *10*, 2687–94.

[Yabuki et al., 2002] Yabuki, N., Terashima, H. and Kitada, K. (2002). Mapping of early firing origins on a replication profile of budding yeast. Genes Cells *7*, 781–9.

[Zappulla et al., 2002] Zappulla, D. C., Sternglanz, R. and Leatherwood, J. (2002). Control of replication timing by a transcriptional silencer. Curr Biol *12*, 869–75.

[Zegerman and Diffley, 2007] Zegerman, P. and Diffley, J. F. (2007). Phosphorylation of Sld2 and Sld3 by cyclin-dependent kinases promotes DNA replication in budding yeast. Nature *445*, 281–5.

[Zhou et al., 2005] Zhou, J., Chau, C., Deng, Z., Stedman, W. and Lieberman, P. M. (2005). Epigenetic control of replication origins. Cell Cycle *4*, 889–92.

[Zink, 2006] Zink, D. (2006). The temporal program of DNA replication: new insights into old questions. Chromosoma *115*, 273–87.

[Zou and Stillman, 2000] Zou, L. and Stillman, B. (2000). Assembly of a complex containing Cdc45p, replication protein A, and Mcm2p at replication origins controlled by S-phase cyclin-dependent kinases and Cdc7p-Dbf4p kinase. Molecular and Cellular Biology *20*, 3086–3096.